Fall 2022

The Synthesis and Characterization of Pb(II) Cyanoximates

Patricia McDaniel
Missouri State University, Patricia220@live.missouristate.edu

THE SYNTHESIS AND CHARACTERIZATION OF Pb(II) CYANOXIMATES

A Master's Thesis

Presented to

The Graduate College of

Missouri State University

In Partial Fulfillment

Of the Requirements for the Degree

Master of Science, Chemistry

By

Patricia McDaniel

December 2022

THE SYNTHESIS AND CHARACTERIZATION OF Pb(II) CYANOXIMATES

Chemistry Department

Missouri State University, December 2022

Master of Science

Patricia McDaniel

ABSTRACT

A new series of Pb(II) cyanoximates were synthesized and characterized by elemental analysis (C, H, N, S), IR spectroscopy, thermal analysis, and X-ray crystallography. The goal was to synthesize compounds with a PbL_2 (L= selected known chelating cyanoximes) composition for use as potential new non-linear optical (NLO) materials, specifically second harmonic generators (SHG), which must belong to non-centrosymmetric space groups. A desktop procedure using Pb^{2+} is chosen due to its typically active $6s^2$ lone pair of electrons, which are known to distort central polyhedra. A 1:2 ratio of Pb(II) to ligand were used to synthesize bulk products and grow crystals for structural determination. Bulk product resulted with 3 compounds with the desired PbL_2 structure but unable to confirm non-centrosymmetric space group due to lack of single crystals for XRD analysis. Thus, crystal growth using a variety of methods became the main objective, although this proved difficult due to hydrolysis occurring on both the lead and ligand sides. Lead hydrolysis appears to dominate, as those fragments are present in most crystal structures. Overall, 30 promising crystals were analyzed resulting with six different lead/ ligand determined structures. The H(2PCO) ligand was the most successful system with three different structures. Crystal data revealed dimeric structure of $Pb\{(H2PCO)(2PCO)_2 \cdot H_2O\}$ with one $2PCO^-$ anion in cis-syn orientation, which has never been seen before with this ligand, forming 6-member ring in chelation while acting as a μ-2 bridge. The only structure determined exclusively containing lead/ligand was $Pb\{(H2PCO)_2(2PCO)_2\}$and the only compound without active lone pair of electrons. Other structures determined were $Pb_3(2PCO)_4(NO_3)_2$, $Pb_3(OH)(NO_3)(DCO)_4$, $Pb_4(OH)_3(NO_3)_2(PiPCO)_3(H_2O)$, and one hydrolysis product from H(ECO) reaction, $K_2[Pb_3(AACO)_4(H_2O)]_2$. The Pb(II) lead centers in crystal growth had high coordination with multiple lead centers, ligands acting as bridges, and invasion of spectator ions resulting in much more complex structures than desired, all belonging to centrosymmetric space groups. Unexpected results showed three products have properties of high-energy compounds, which violently decompose with release of significant heat and kinetic energy. Compared to known high-energy compounds these have high potential for use as heat-triggered actuators.

KEYWORDS: lead(II) compounds, synthesis cyanoximes, X-ray analysis, crystal growth, hydrolysis reactions, high-energy compounds, thermal analysis

THE SYNTHESIS AND CHARACTERIZATION OF Pb(II) CYANOXIMATES

By

Patricia McDaniel

A Master's Thesis
Submitted to the Graduate College
Of Missouri State University
In Partial Fulfillment of the Requirements
For the Degree of Master of Science, Chemistry

December 2022

Approved:

Nikolay N. Gerasimchuk, Ph.D., Thesis Committee Chair

Amitava Choudhury, Ph.D., Committee Member

Natasha M. DeVore, Ph.D., Committee Member

Gary A. Meints, Ph.D., Committee Member

Fei Wang, Ph.D., Committee Member

Julie Masterson, Ph.D., Dean of the Graduate College

ACKNOWLEDGEMENTS

I would like to thank Dr. Gerasimchuk for the incredible amount of time, energy, and patience invested in me throughout my graduate program. You have been a passionate mentor, patient research advisor, and cheerleader during this long journey.

I would like to thank my committee members for their time and expertise invested in my research project.

I am very grateful for the timely practical help with collecting, free of charge, data sets during our in-house diffractometer break down from Dr. Jeanette Krause (University of Cincinnati, OH) and Prof. Alen Oliver (Notre Dame University, IN). Not only data collection, but also structures solutions and refinement was done by Dr. Alex Filatov (University of Chicago, IL) and Dr. Sergey Lindeman (Marquette University, WI). It was a valuable contribution to my work during limited access to our research facilities due to COVID-19 lockdown. Because of their kind help my work did not stop.

I would also like to thank the Missouri State University Graduate College and the Chemistry Department for research funding.

A sincere thank you to Linda Allen, Chemistry Department faculty, and the Electronics Support Services (Mike Murphy and Craig Baird) for being available to help with large and small tasks, even when it wasn't in your job description.

I would like to dedicate this thesis to my kids, Ryan and Connor. You guys spent almost as much time in Temple Hall as I did! To my parents, Roger and Patricia Jarman, without you guys this would not have been accomplished. Thank you for the unending encouragement and support. This was accomplished as a family, not an individual, and should have all our names attached.

TABLE OF CONTENTS

LIST OF TABLES

LIST OF FIGURES

I. INTRODUCTION

During the last three decades a considerable research effort was dedicated to a new class of small molecules of organic ligands—cyanoximes—that have a general formula NC-C(=NOH)-***R***. The **R** is an electron-withdrawing group such as cyano-, amide/thioamide, keto-, ester, aryl and heterocyclic fragments. Presence of the CN-group makes cyanoximes about 10,000 times more acidic and better ligands than other known conventional monoximes and dioximes. These simple low molecular weight molecules represent a series of new excellent ampolydentate ligands [1] for coordination and organometallic chemistry.

A new series of new Pb(II) cyanoximates were synthesized and characterized in this study. Bivalent lead complexes are anticipated to have interesting and unpredictable geometry because of the presence of the stereoactive $6s^2$ lone electron pair that can distort coordination polyhedron of the central metal atom. Such distortion can lead to non-centrosymmetric crystal structures resulting in interesting optical and electrophysical properties. Efforts to grow single crystals in the series are essential as they are used to study the precise geometric atomic connectivity and spatial arrangement through X-ray diffraction analysis. Acentric crystals, for example, can exhibit non-linear optical behaviour, such as the second harmonic generation effect (SHG). This phenomenon is important for the design of new materials for photonic applications and many other advanced technologies in optics.

There is only one known Pb(II) cyanoximate structure [2]. It crystallizes in a centrosymmetric space group but based on literature data surrounding other metals and chelating cyanoximes, architecture for thermally stable and non-centrosymmetric space groups is believed to be a high possibility.

II. LITERATURE REVIEW

II.1 Coordination Compounds

Coordination compounds are composed of a metal atom (or ion) and one or more ligands binding to it. A ligand can be an atom, ion, or molecule that forms a coordinate bond and attaches itself to the metal center. Coordinate bonds represent donor/acceptor type and are formed as the ligand(s) donate both of their electrons to the central atom as opposed to the formation of other bonds, such as a covalent bond, which is formed as two entities each donates a single electron for the union. The donation of an electron pair in a compound is the definition of a Lewis base, therefore the interactions in coordination compounds is essentially acid-base chemistry. Most often the ligand is the electron rich or electron donor entity in the complex, also known as the Lewis base (nucleophile), and the metal atom or ion is usually the Lewis acid (electrophile), or the electron acceptor [3-4]. Some common examples of ligands are neutral ligands such as water (H_2O) and ammonia (NH_3), anionic ligands such as chloride (Cl^-) and hydroxide (OH^-), and least common are cationic ligands such as nitrosonium (NO^+) [5].

These compounds (or often called complexes) are defined by their coordination number and their coordination geometry. The coordination number (CN) is the number of bonds that are found around the central metal atom. Typically, there are 2-9 ligands that will bind to the metal center via a coordinate bond. However, some ligands have more than one atom that can function as an electron pair donor. When this happens, both atoms can bind to the same metal center, forming a ring (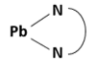), and creates two adjacent bonds on the central atom. This is called a chelate ring which means "having pincer-like claws" and can be referred to as being *bidentate* [6]. Some ligands that possess multiple donor atoms are not capable of bonding simultaneously

due to steric or electronic reasons. Multiatomic ligands that can donate electron pairs to a metal center (one coordinate bond) using either donor atom in their structure are known as ambidentate ligands. Thiocyanate (SCN^-) is an example of an ambidentate ligand as it can coordinate through the sulfur atom or the oxygen atom, [7] or both forming bridges of different complexity. These ambidentate ligands received attention due to the formation of linkage isomerism. Depending upon the linkage between the ligands and the metal center(s), coordination compounds can be found as small molecules packed into a unit cell or long polymeric chains.

The total number of coordination sites occupied around the central atom will determine the geometrical arrangement of the molecule. This central atom (or ion) and the atoms that are directly coordinated form the coordination polyhedron. The polyhedron displays molecular/electron geometry and may be distorted depending upon the sterics and electronics of the ligands. Also, presence of lone pairs may facilitate distortion of coordination polyhedron. This is documented for Sb(III) [8], Sn(II) [9], and Tl(I) [10] complexes. It is known that the geometry and symmetry elements in a crystal structure--which may be studied by single crystal x-ray diffraction--will govern the physical properties of the compound. Understanding the chemistry of the ligands and metallic center allows for an educated prediction as to how they will likely coordinate together thus producing the desired geometrical and symmetrical elements in a crystal. With this knowledge it is possible to synthesize products that possess a desired physical property (magnetism, conductivity, optical properties) due to the intrinsic nature of the crystal lattice.

II.2 Applications of Coordination Compounds

Coordination compounds are found everywhere, and the applications are extensive and diverse. These compounds are found as naturally occurring molecules or found extensively as synthetic materials. Many applications are based on their interesting chemical properties. They can be found as naturally occurring coordination compounds such as hemoglobin (containing iron), Vitamin B12 (containing cobalt), and chlorophyll (containing magnesium) are found supporting the very foundation of life through biological processes. Additional uses can be found for critical medicinal and industrial purposes. Examples include cisplatin, a platinum-based cancer treatment drug, while industrially they are used as dyes (copper phthalocyanine—blue dye containing copper), complexing agents for ore extraction (cyanide ion used to extract gold from ore), and catalysis (Wilkinson's Catalyst, a rhodium centered complex used in the hydrogenation of alkenes) to name a few (Figure 1). Other applications can be based on the compound's physical properties such as magnetism, conductivity, and optical properties. Some of the more unusual, yet useful physical properties, stem from unusual coordination geometry and symmetry in the crystal lattice.

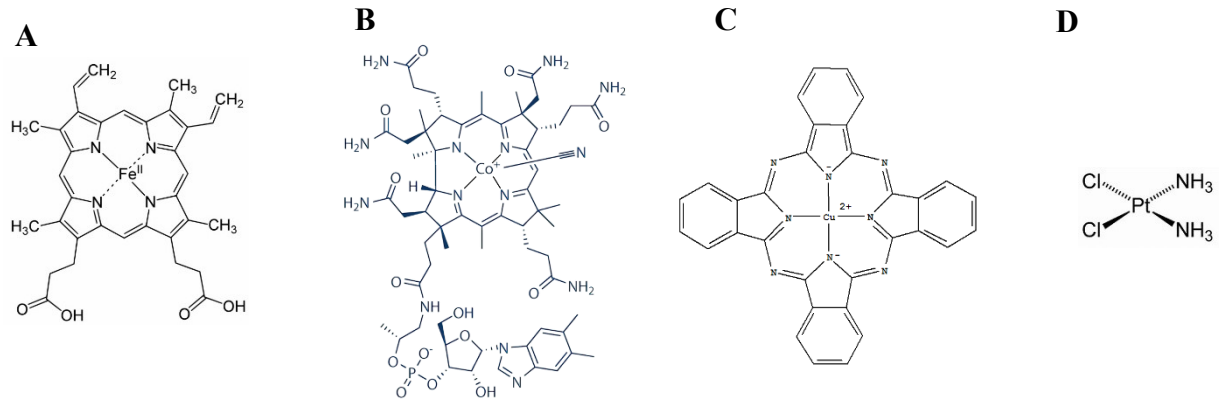

Figure 1. Examples of useful coordination compounds. **A** - Iron centered hemoglobin; **B** - Cobalt centered Vitamin B12; **C** – Copper centered copper phthalocyanine (blue dye); **D** - Platinum centered cisplatin

II.3 Optical Responses of Coordination Compounds

Combining two practical purposes for studying coordination chemistry, creating unusual coordination geometry and utilizing interesting and unusual physical properties, guides this study towards a useful application in the field of optics. Optics is a branch of physics that studies the behavior of the electromagnetic radiation spectrum and its interactions with matter. This very broad field includes the transmission, absorption, and deflection of radiation including visible light (VIS), infrared radiation (IR), and ultraviolet radiation (UV).

Transmission (T) is defined and calculated as a ratio of the intensity of light that passes through an object (I) over the intensity of incident light (I_o) that is introduced to the matter, being a lens, material, or crystal (Figure 2). The amount of transmission of light is based on the properties of the matter and is generally recorded as a percentage: $T = \frac{I}{Io}$ or $\% T = 100 \frac{I}{Io}$

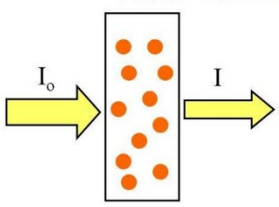

Figure 2. Transmittance example showing light introduction (Io) to a sample and the intensity of light leaving the sample.

The interaction of light with matter can also be recorded as absorption (A). Absorption measures the amount of incident light that is absorbed by the matter as opposed to being transmitted through, reflected, or refracted by the object. Transmission and absorption are mathematically related through a logarithmic relationship: $A = \log \frac{1}{T}$ or $A = \log \frac{Io}{I}$. The

absorbance value can be found by using a spectrophotometer or calorimeter which measures the intensity of light that passes through the sample.

Most solutions follow Beer's Law which states that as the concentration increases the absorbance increases proportionally: $\frac{Io}{I} = \varepsilon lc$

where $\frac{Io}{I}$ = absorbance, ε = the molar extinction coefficient, l = length of the sample, and c = the concentration of the sample in molarity. Samples that follow Beer's Law show a linear optical response (also known as an ideal linear response). Meaning, when the concentration of a sample is plotted against the absorbance at a specified wavelength, the data points should be connected with a regression line. Not as common, a sample may have a non-linear optical response. These Non-Beer's Law materials DO NOT form a straight line when a plot is made under the conditions previously mentioned. Non-linear responses will have either a positive or negative deviation in this relationship creating an upward or downward arc in the plot (Figure 3).

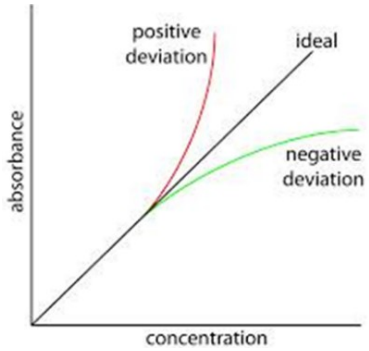

Figure 3. Linear (or ideal) optical response (black line) which follows Beer's Law while the red and green lines show two different non-linear optical responses.

Beer's Law, as presented above, is generally associated for use in solution chemistry, however a comparison of the same type of behavior is found in the attenuation of light traveling

through a material. Thus, both positive and negative deviations are important practical application of such materials. Optical limitation is important property of transparent compounds and materials widely used in different areas of modern technology.

II.4 Non-Linear Optics

More specifically, non-linear optics (NLO) is the branch of optics that describes the behavior of light in non-linear media, that is, media in which the polarization density responds non-linearly to the electric field of the light. This definition describes the positive deviation (upward arc) and negative deviation (downward arc) from Figure 3. The non-linear relationship between absorbance and concentration results from frequency mixing (sum or difference) when light interacts with a medium (Figure 4) [11]. The difference or decrease of frequency results in an optical limiting effect. A common application for this type of material is for eyeglass lenses that turn dark in the sun. The opposite effect is frequency doubling, which is known as Second Harmonic Generation (SHG).

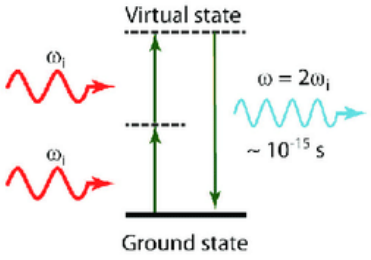

Figure 4. Second Harmonic Generation showing two photons combining to produce one higher energy photon as the wavelengths phase match.

Second harmonic generation was first demonstrated on a single crystal by Peter Franken, A. E. Hill, C. W. Peters, and G. Weinreich at the University of Michigan, Ann Arbor, in 1961.

The demonstration was made possible by the invention of the laser, which created the required high intensity coherent light. They focused a ruby laser with a wavelength of 694 nm into a quartz sample. They sent the output light through a spectrometer which indicated the production of light at 347 nm [12]. The formulation of SHG was initially described by N. Bloembergen and P. S. Pershan at Harvard in 1962 [13-14].

II.5 Applications of SHG and Non-Linear Optical Materials

Inorganic optical technology is in massive production for industrial customers in photonics, which is the technology of generating and harnessing light and other forms of radiant energy whose quantum unit is the photon. Some vital uses of photonics are lasers, optical switches, high density optical storage media, fiber optics and optical communication technology, information technology, homeland security, and many others. Depending upon the application, the required NLO material can be utilized as a thin film deposited on a surface or it may require an optical grade crystal $<$ 1 mm in diameter or an optical grade crystal as large as one meter per face.

Because of the high demand for NLO and SHG materials necessary for these technological advances the search for new materials must continue. Research shows that no "all around best" NLO material exists. A material well-suited to one application might be a poor candidate for a different set of operating conditions. Very few materials find application as a second harmonic generating material because of the extensive requirements for an optical-grade crystal. Not only must the crystal exhibit a strong SHG output, but other essential qualities based on their chemical and mechanical stability are imperative. Criteria includes electrooptic coefficients, low dielectric dispersion coefficients, ultrafast response times, thermal conductivity,

and a high damage threshold to give them a high figure of merit [15]. There are many crystals that exhibit SHG character but are not able to withstand the physics of the frequency conversion introduced laser intensity and heat exchange involved which damages the crystal's surface, induce uncontrollable changes in the crystal's properties, or destroy the crystal itself. Synthesizing a crystal with these properties is a sizeable task but it must also be grown to an adequate size while being a uniform single crystal [16]. Finally, the material must be optically transparent to the incident and generated radiation and relatively stable to about 150° C.

A schematic showing the phenomenon of SHG registration can be seen in Figure 5. This setup uses an yttrium aluminum garnet (YAG) laser which emits NIR light at 1064 nm which is invisible to the human eye. The laser beam is directed through meticulously placed mirrors and optical lenses onto the crystalline sample. As the beam travels through a non-linear crystal, polarization of the photons occurs. Two photons that are traveling through the medium undergo phase matching and frequency doubling where two photons merge their energy into one photon. The combined energy doubles the wavelength, and the light exits the sample as a visible green light emitted at 532 nm—twice the frequency of the original beam. The optical setup is made with the help of short band-pass-filters in such way that only photons with $\lambda = 532$ are detected.

Two examples of widely used NLO and SHG materials are potassium titanyl phosphate ($KTiOPO_4$, also known as KTP), and lithium niobate ($LiNbO_3$, also known as LN) –both being inorganic coordination compounds. The KTP has been characterized by x-ray crystallography showing "chains of TiO_6 octahedra [Ti(IV)], which are linked at two corners, and the chains are separated by PO_4 tetrahedra [17]. There are two chains per unit cell, and the chain direction alternates between long and short Ti–O bonds along these chains, which result in a net *z*-directed polarization and are the major contributor to KTP's large nonlinear-optic and electro-optic

coefficients" [18]. Large crystals can be grown by hydrothermal and flux techniques, which require high pressure and an extremely high temperature, taking two weeks to two months depending on the size required. The KTP is a non-centrosymmetric crystal with an orthorhombic lattice in space group $Pna2_1$. Applications include frequency-doubling solid-state lasers which can be used in laser pointers or laser surgery, practical as an optical waveguide, and used as modulators, diodes, and semiconductors. The LN has also been characterized by x-ray crystallography and shows chains of octahedra NbO_6 and octahedra LiO_6 linked at the corners through the oxide ion [19]. Suitable crystals can be grown through hydrothermal and flux techniques as well as the Czochralski Method melt-growth technique [20]. Again, these methods require high temperatures and pressure for production. The LN is also a non-centrosymmetric crystal with a trigonal lattice in space group R3c used for similar applications with the added benefit that it is also a ferroelectric material [21].

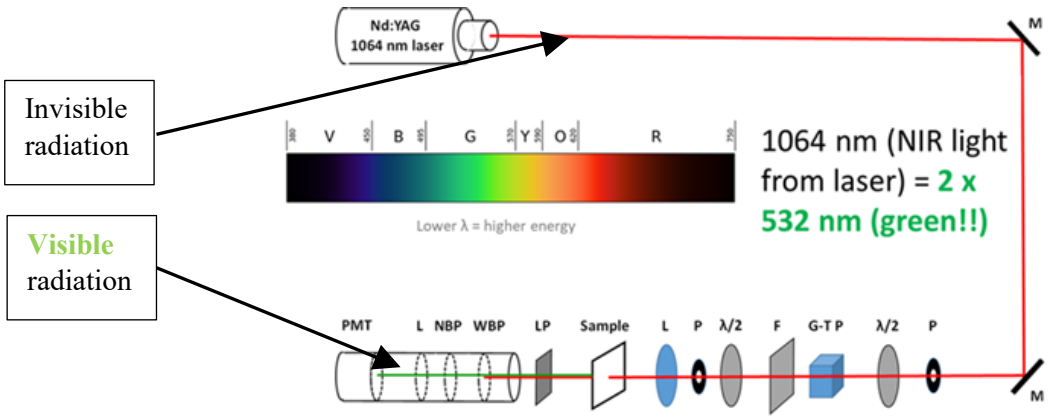

Figure 5. Second Harmonic Generation optical test following the invisible NIR light through mirrors and lenses. If the sample is a SHG crystal, results will show a visible green light due to the frequency doubling.

II.6 Unusual Geometry in Crystal Structures

Atomic composition and the molecular geometries are taught in basic chemistry curriculum. This core concept is critical to understand and unravel because the physical properties possessed by every compound, crystal, or material are dependent upon their makeup. If one atom is changed in a molecule the polarity and geometrical arrangement might be very highly altered resulting in a very different function/application compared to the original. The purpose of this study is to investigate new materials that might display the SHG phenomenon. It is well known in the optics community that materials must be acentric to have a NLO response [15, 22]. In crystallographic terms, a compound must be non-centrosymmetric therefore lacking a center of symmetry (*i*) symmetry operation. Crystals that possess a center of symmetry, also known as an inversion center, are termed centrosymmetric and will not display any non-linear optical behavior. A center of symmetry operation is present when every atom is able to move through the center of the molecule to a position opposite the original position and the identical distance from the central point as where it started (Figure 6).

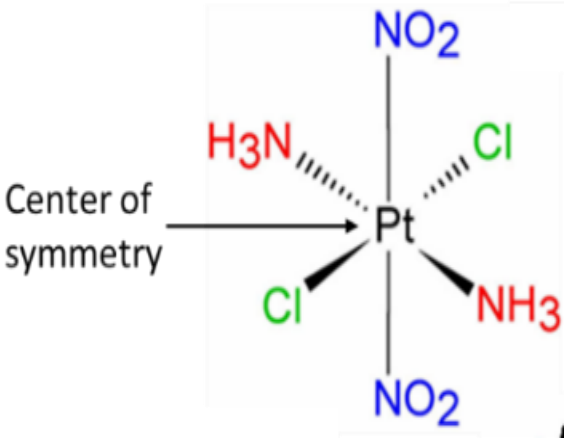

Figure 6. Center of symmetry (*i*) operation showing how each point moves through the center of the molecule identical distance and opposite of the original position.

According to a CSD database search approximately 25% of all structures are non-centrosymmetric [23]. This may appear to be a large number but most of these compounds will not exhibit a large SHG output or meet the stringent requirements discussed earlier to be a viable option for optical applications. As technology continues to advance the search for new NLO crystals is of great importance. If metal-based coordination compounds can be made with a non-centric crystal structure then they can be a good candidate for NLO applications because they are generally much more thermally stable than pure organic compounds, more energy efficient to prepare, able to be deposited as thin films from solutions, and easier to handle when compared to minerals that need to be of optical quality. Non-centrosymmetric unit cell of KTP can be seen in Figure 7.

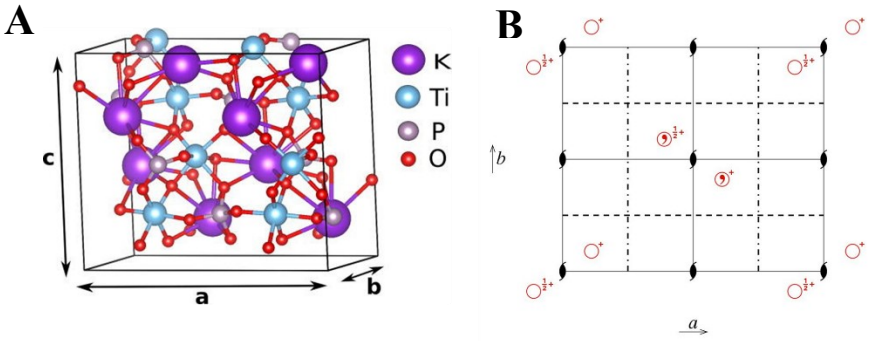

Figure 7. KTP unit cell. **A -** figure adapted from Ghoohestani et al. [24]; **B -** Symmetry operations in KTP crystal (Space group #33) showing no inversion centers which would be indicated by a small open circle.

II.7 Cyanoximes: Small Organic Ligands

Over the last 30 years considerable research has gone into finding practical uses for small organic ligands known as cyanoximes. They are a type of molecular "Lego" used to create small to complex compounds when combined with various metal ions. Cyanoximes represent a new subclass of oximes. An oxime has a general formula of RR'C=NOH, where R is an organic

sidechain and R' may be a hydrogen atom, forming an aldoxime, or another organic group which will form a ketoxime. To build the cyanoximes, one of the R- groups in an oxime will be replaced with a *cyano* group (-CN) giving the general formula NC-C(=NOH)-R, where R is an electron-withdrawing group. The presence of the –CN group significantly increases the acidity from 100-1,000,000 times compared to a common oxime [25] resulting in pKa values ranging from 3.9 – 7.4. This makes the molecule a better ligand because it can be easily deprotonated upon addition of a base to these compounds in solution. The anionic species formed will more readily act as a nucleophile (base) towards metal cations. As of now there are over 40 cyanoximes known (Figure 8) with more than 250 crystal structures of coordination compounds reported. There are different types of cyanoximes such as monoximes, dioximes, and trioximes and they may be aliphatic or aromatic molecules all which contribute to different sizes, sterics, multiple functionalities, and applications. In fact, these compounds represent a unique and diverse library of metal binding small molecules. Cyanoximes are excellent ligands for coordination chemistry because they are so versatile, display a variety of binding modes, and have interesting stereochemistry.

As ampolydentate ligands these small molecules can be very versatile. One form of coordination will be favored by one metal while a different metal will attract an alternative donor site of a ligand [26]. This can partly be explained through the Hard and Soft Acids and Bases (HSAB) theory. This classifies acids and bases on their polarizability; low polarized ions are considered *hard* while highly polarized ions are considered *soft*. Hard acids prefer to bind with hard bases while soft acids prefer to bind with soft bases. Interactions between two hard species or two soft species produce more stable compounds [3].

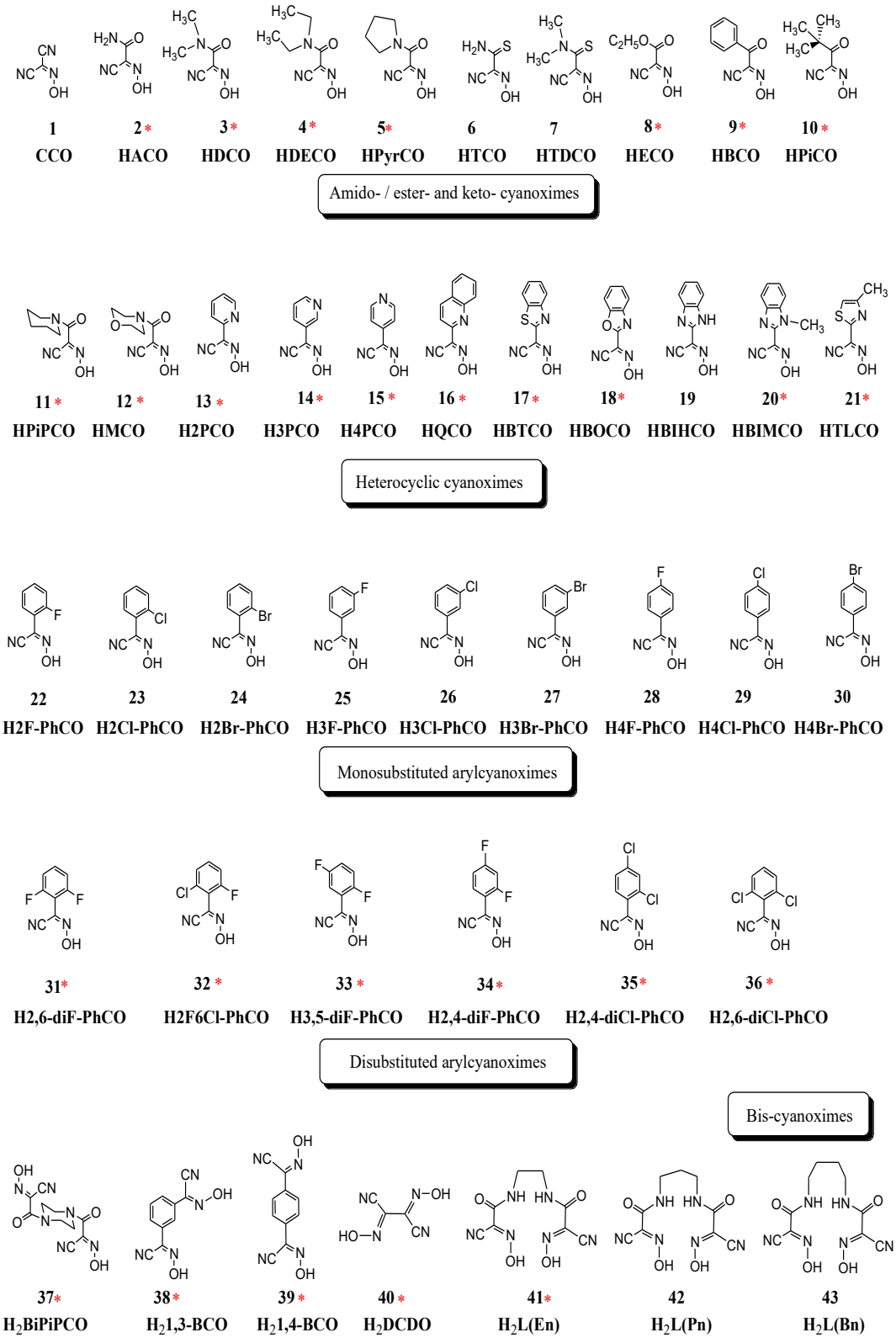

Figure 8. List of known and studied cyanoximes. Asterisk signifies known crystallographic data.

Ampolydentate ligands can act as a monodentate, bidentate, polydentate ligands or act as a chelator. Cyanoximes can coordinate to a metal center via the oxygen or nitrogen atom of the nitroso group, coordinate via an atom from the R-group, form one or more bridges in a compound, and they may act as a chelator. Cyanoximes acting as a chelator will form rings, also known as metallocycles, through the nitrogen or oxygen atom of the oxime group and another available donor atom (N, O, S) that is available in the R-group [1]. Figure 9 shows the versatility of these ligands and their potential coordination sites [27]. Chelating ligands are desirable for a few reasons. When rings are formed, especially a five or six membered ring, ***more stable*** compounds are generally formed. This can be explained through thermodynamic parameters such as a relative change of enthalpy and entropy and is known as the chelate effect [28]. There is much data showing cyanoximes act as good chelators with transition metals with some examples found in Co^{3+} [29], Ni^{2+}[30, 31], $Cu^{2=}$ [31,32], Pd^{2+} [33], and Pt^{2+} [33,34].

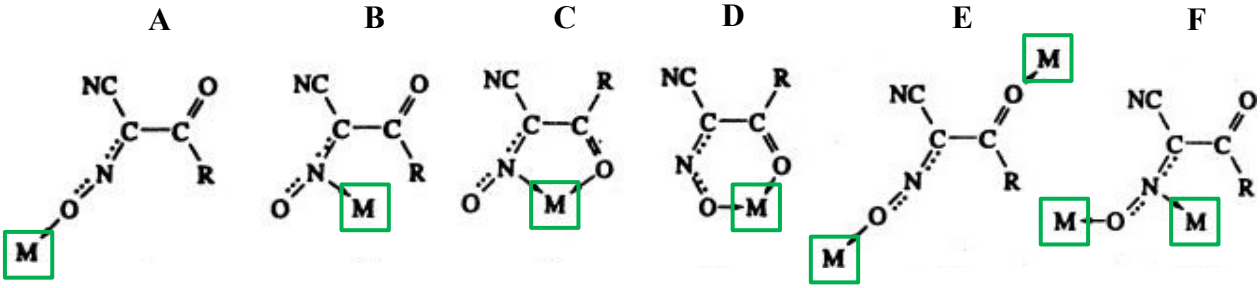

Figure 9. Multiple coordination sites for cyanoxime ligands showing capabilities for: **A** - monodentate coordination; **B** – Monodentate coordination; **C** – 5-ring chelator; **D** – 6-ring chelator; **E** – Bridge; **F** – Bidentate coordination where M represents a metal center.

Cyanoximes and their metal complexes demonstrate a rich stereochemistry and exist as four main principal geometrical isomers such as cis /trans (with respect to the oxime C=N bond orientation relative to the size/heteroatom ranking) and syn /anti (with respect to the oxime N-

OH fragment orientation relative to the CN-group) (See Figure 10) [25]. For these reasons, cyanoxime complexes have the potential for interesting and unusual geometry therefore making it difficult to predict the stereochemistry of a final crystal structure. Thus, investigations of stereochemistry of cyanoximes-based complexes is fully justified.

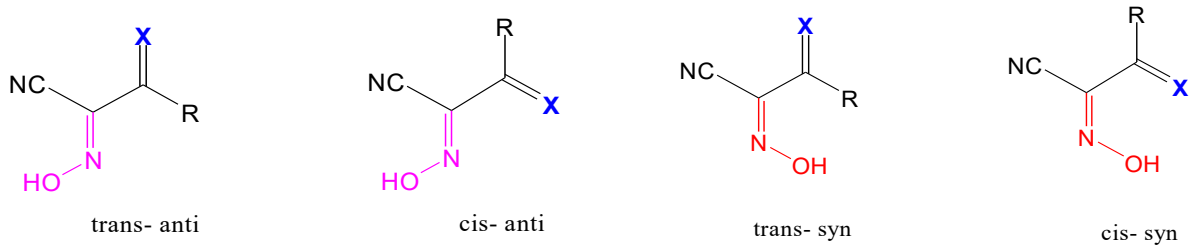

Figure 10. Four possible geometrical isomers for a typical monocyanoxime.

Literature shows that protonated cyanoximes, their salts, and coordination compounds possess quite unusual molecular geometry and can be found crystallizing in centrosymmetric and non-centrosymmetric space groups. The centricity of a complex does not appear to be dependent on the centricity of the uncoordinated ligand and no visible pattern is present. For example, a ligand in a non-centrosymmetric space group, when coordinated with a metal, can form a complex in a centrosymmetric space group. Examples can be found in Table 1.

Table 1. Uncoordinated ligands and their space groups upon crystallization vs. their complex compounds and space groups.

Ligand	**Ligand Space Group**	**Complex**	**Complex Space Group**
Cs(ACO)	$Pbn2_1$ (Non-symmetric)	Pb(ACO)	Pnam (Centrosymmetric)
H(2PCO)	$P2_1/c$ (Centrosymmetric)	Tl(2PCO)	$P2_1/c$ (Centrosymmetric)
H(3F-PhCO)	$P2_1/c$ (Centrosymmetric)	Tl(3F-PhCO)	$Pna2_1$ (Non-centrosymmetric)

II.8 Element of Choice: Lead

After consideration of potential metals for this study, lead was chosen for multiple reasons. The most noteworthy reason is that bivalent lead exhibits a distinctive presence of an active lone pair of electrons ($6s^2$) in a significant number of coordination compounds. An electron lone pair is defined as two electrons, paired together, which sit on a central atom but are not bonded with any atoms. There are two types of geometry that can be defined around a central atom: electron and molecular geometry. Electron geometry is determined by both the electron pairs and the bonds present in a molecule compared to the molecular geometry which is determined only by the number of bonds around the central atom. The molecular geometry and the electron geometry can be the same or different in a compound and will dictate the stereochemistry. If there are more electron groups than bonding groups, then a lone pair or pairs of electrons are present. There are two categories of lone pairs: stereoactive and non-stereoactive. Stereoactive electrons are found around a central atom and occupy the same space where a bond would be expected. In a crystallographic analysis, stereoactive electrons would be "viewed" as an empty space around the central atom. Non-stereoactive electrons, also known as delocalized electrons, exhibit no obvious sign or open space of their presence around the central atom. The charge has been more evenly distributed around the central atom. Stereoactive electrons are as critical in determining the geometry of a molecule as bonded atoms. The lone electron pair behave much like bonded atoms in regard to the amount of space they occupy. Since the electrons remain closer in proximity to the central atom, they have more repulsion power towards the other bonded atoms. This may slightly or significantly affect the expected molecular geometry around the central atom by distorting the central polyhedron through repulsion as they "push" the other atoms further away. This will alter the bonding angles and

bonding distances. This phenomenon plays an important role in the stereochemistry both in non-metal and metallic elements. Ammonia, (NH_3), is a common example of a molecule with a stereoactive lone pair. In this molecule there are 3 bonded atoms and an unbonded electron pair. According to the VSEPR Theory, four bonding groups have a tetrahedral electron geometry with an expected bond angle of 109.5° around the central atom. However, since one of the electron groups is an unbonded electron group this will change the molecular geometry to trigonal pyramidal. This also effects the bond angles and will be less than the 109.5°. Thus, distortion can be seen in ammonia where the bond angles are 107°. In lead compounds this phenomenon has been identified as holodirectional and hemidirectional coordination [35]. As seen in Figure 11, the holodirectional coordination shows the evenly distributed coordination sites around the central atom while the bond lengths and bond angles are fairly similar to one another. In the hemidirectional diagram the presence of the active lone pair can be found in the cleft at the top of the central atom (identified by the arrow). The elongated and shortened arrows represent longer bonds adjacent to the electrons and shorter bonds further away thus showing the distortion in the molecular geometry from the stereoactive lone pair.

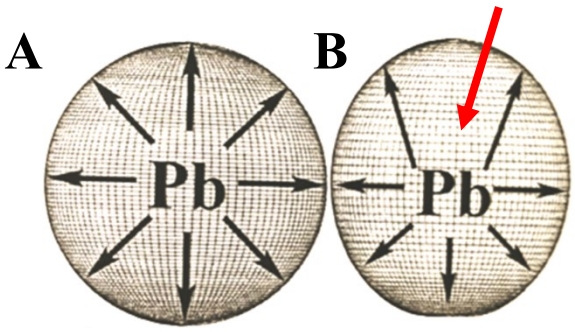

Figure 11. Coordination around lead center showing holodirectional and hemidirectional coordination [35]. **A -** Holodirectional shows non-active lone pair of electrons with evenly distributed bonds. **B -** Hemidirectional coordination with stereoactive lone pairs showing distorted polyhedron, varying bond lengths, and bond angles. Location of active lone pair identified by the red arrow.

There are other metals that exhibit a lone pair of electrons that were considered for the project, however Pb^{2+} is most suitable for bench top lab work as it is air stable, unlike Sn^{2+} and Sb^{3+}, which generally require an air-free protective environment during synthesis. Other metals considered for study were Tl^{1+} and Hg^{1+} but they were eliminated due to their high toxicity. The toxicity of lead was considered but using gloves during preparation provides adequate protection. In addition, most Pb^{2+} complexes form higher degree ionic bonds, so it is not easily absorbed into the skin. Bismuth (III), another heavy metal, was seriously considered but has a high propensity to hydrolysis. Bivalent lead was carefully chosen and has the additional quality of being inexpensive and readily available.

Literature searching resulted in one lead and cyanoxime compound, $Pb(ACO)_2 \cdot H_2O$ that is known today [2]. This complex has one Pb^{2+} metal center, two ACO^- anions, one water molecule, and an active lone pair of electrons. This was an inspiration to continue working with lead and other oximates that are known chelators. Even though this compound crystallized out in the centrosymmetric space group Pnam the possibility of non-centrosymmetric crystals is highly possible. In May 2022 a detailed search in the Cambridge Crystallographic Data Center (CCDC) was conducted looking for other bivalent lead complexes with similar chelating donor atoms. With over 1.1 million entries in the database only 577 Pb-complexes were found, and only 111 entries (about 20%) were non-centrosymmetric. Of these structures, about 75% have a stereoactive lone pair of electrons. Some of these structures have more than one crystallographically different lead ions in their ASU with most of them having stereoactive lone pairs. However, six complexes have mixed activity, meaning that one or more lead ions in the ASU has a stereoactive lone pair and the other ion(s) are non-stereoactive. The tables below show the CCDC reference code, space group, and indication if a lone pair of electrons is present

in known non-centrosymmetric compounds. Four coordination combination chelating fragments were each searched for 5- and 6-membered rings: lead with two nitrogen atoms (Pb-N-N), lead with two oxygen atoms (Pb-O-O), lead with one nitrogen and one oxygen atom (Pb-N-O), and lead with one nitrogen atom and one sulfur atom (Pb-N-S) as displayed in Figure 12. The search for the Pb-N-N fragment was the most common pattern found with 257 hits however only 58 of these (23%) are non-centrosymmetric. Results are shown in Table 2. There were 162 total hits with the Pb-O-O coordination pattern with 28 of those (17%) being acentric and can be seen in Table 3. Tables 4 and 5 show the results for coordination fragments of Pb-N-O and Pb-N-S. Total hits were 145 with 21 acentric compounds (15%) and 21 hits with 4 non-centrosymmetric complexes (19%) respectively. This reflects the uniqueness of acentric coordination compounds that can be found with bivalent lead and anticipation for useful NLO materials.

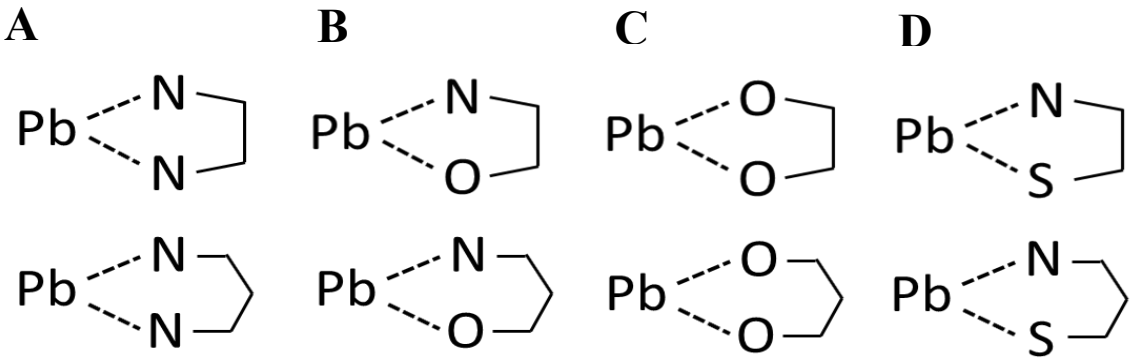

Figure 12. Structural motifs used in CCDC database search. **A** – Pb-N-N in a 5- and 6-membered ring; **B** – Pb-N-O in a 5- and 6-membered ring; **C** – Pb-O-O in a 5- and 6-membered ring; **D** – Pb-N-S in a 5- and 6-membered ring.

Table 2. Non-centrosymmetric coordination compounds with **Pb-N-N** chelation pattern with their space group and if it possesses a stereoactive lone pair of electrons

Reference Code	Space Group	Space Group #	Lone Pair?	Reference Code	Space Group	Space Group #	Lone Pair?
AGEZOD	$Pca2_1$	29	Y	OSAKID	$P2_1$	4	Y
BIZREJ	$P2_12_12_1$	19	N	OSOMEQ	$Pna2_1$	33	Y
BIZRIN	$P3_{1c}$	159	Y	PIVPUF	$Pna2_1$	33	N
BUTXIY	$Pmn2_1$	31	N	POCMUQ	P1	1	Y
FENZOO	$P2_12_12_1$	19	Y	PUQMUL	$P2_12_12_1$	19	N
FEVTIK	P1	1	Y	PUQNAS	$P2_12_12_1$	19	N
FUTZAW	$P2_12_12_1$	19	Y	QADQIY	$Pmn2_1$	31	Y
GEVWUZ	$P2_12_12_1$	19	Pb1-Y	QIDKOD	$P2_12_12_1$	19	Y
			Pb2-N	RAQFIY	$P2_12_12_1$	19	Y
GOPYEP	$P22_12_1$	18	Y	RAQFOE	$P2_12_12_1$	19	Y
HILFEO	$Pmn2_1$	31	N	RAQGEV	$P2_1$	4	Y
HILGAL	$P2_1$	4	Pb1 - Y	RAQJUO	$P2_1$	4	Y
HIXCUN	P31	144	Y	RAQHIA	$Pb2_1a$	29	Y
HOXQOB	Fdd2	43	Y	RAQKEZ	$P2_12_12_1$	19	Y
HUZFEP	$P2_12_12_1$	19	Y	RAQKID	$P2_12_12_1$	19	Y
IBEPUB	Pc	7	Y	RATCUM	$Pna2_1$	33	Y
IDAVAL	$P2_12_12_1$	19	Y	RAXRAJ	$P4_1$	76	Y
IKEWAW	$P2_12_12_1$	19	Y	RUDGAZ	$Pca2_1$	29	Y
KIKJAR	Cc	9	Y	RUTXOT	$Pna2_1$	33	Y
LATDIW	$P2_12_12_1$	19	Y	SEFYEI	$P2_1$	4	Y
LATDOC	$P2_12_12_1$	19	Y	SELNIH	$P2_1$	4	Y
LATDUI	$P2_12_12_1$	19	Y	SIJFEZ	Pc	7	Y
LATFAQ	$P2_12_12_1$	19	Y	TAGNAT	$P2_12_12_1$	19	Y
LUHNOR	Fdd2	43	Y	VOLVUO	I-4	79	Y
MALQUN	Cc	9	Y	WAKCUG	Pc	7	Y
MEHSOI	Fdd2	43	Y	WIPKAJ	Fdd2	43	N
NAYMOQ	Cc	9	Y	XACTEP	Cc	9	Y
NUXYAH	$Pna2_1$	33	Y	ZAGSIN	P1	1	Y
OSAJUO	$P2_1$	4	Y	ZOMVEE	Fdd2	43	Y
OSAKAV	Pc	7	Y	**TOTAL**	**58**	**May 2022**	

Table 3. Non-centrosymmetric coordination compounds with **Pb-O-O** chelation pattern with their space group and if it possesses a stereoactive lone pair of electrons.

Reference Code	Space Group	Space Group #	Lone Pair?	Reference Code	Space Group	Space Group #	Lone Pair?
AHIJOQ	$P2_12_12_1$	19	Y	QELTUX	Pc	7	**Pb1-Y**
BEWHEQ	$P2_1$	4	Y				**Pb2-N**
CUKZEN	$P2_12_12_1$	19	N	QOCHEW	$P2_12_12_1$	19	Y
EMUDOF	$Pna2_1$	33	N	RABLAH	Cc	9	N
FIBZOH	$Pca2_1$	29	N	RERVOB	$Pmn2_1$	31	Y
GOHWOS	$P2_12_12_1$	19	N	TEQPUB	Cc	9	Y
KUJCOH	$P2_1$	4	N	TEVZIF	$P2_1$	4	**Pb1-**
LAJCEG	Cc	9	Y				**Pb16-Y**
LEBKOS	$Pna2_1$	33	N	TEVZOL	$P2_12_12_1$	19	**Pb1-**
MIFSIE	Cc	9	N				**Pb14-Y**
NETVIR	$P2_12_12_1$	19	Y	UTAFIG	$P2_12_12_1$	19	Y
PAXKEH	$P2_12_12_1$	19	**Pb1-Y**	VELGOJ	$P2_12_12_1$	19	Y
			Pb2-Y	VERDOM	$P6_3$	173	N
POFYUG	Pc	7	Y	VOGPUC	$Pc2_1b$	29	Y
POJGOK	$P2_1$	4	Y	YULDEO	Cc	9	N
QACJUA	Fdd2	43	N	ZZZWCW	$P3_222_1$	154	Y
				TOTAL	**28**	**May 2022**	

Table 4. Non-centrosymmetric coordination compounds with **Pb-N-O** chelation pattern with their space group and if it possesses a stereoactive lone pair of electrons.

Reference Code	Space Group	Space Group #	Lone Pair?	Reference Code	Space Group	Space Group #	Lone Pair?
BOHNES	C2	5	Y	ODEWEA	C2	5	Y
DPENPB01	$P2_1$	4	Y	PEDLOZ	$P6_5$	170	**Pb1-Y**
EMUDOF	$Pna2_1$	33	N				**Pb2-Y**
FICQAJ	P3m1	156	Y				**Pb3-N**
FIFWAT	$P4_12_12$	92	Y	QELTUX	Pc	7	N
IBEPUB	Pc	7	Y	RIRRUG	C2	5	Y
IKEWAW	$P2_12_12_1$	19	Y	RUTXOT	$Pna2_1$	33	Y
KUJCOH	$P2_1$	4	Y	VELGOJ	$P2_12_12_1$	19	Y
LATDIW	$P2_12_12_1$	19	Y	VOGPUC	$Pc2_1b$	**29**	Y
LATDOC	$P2_12_12_1$	19	Y	YEFTUY	$Pna2_1$	**33**	**Pb1-Y**
LATDUI	$P2_12_12_1$	19	Y				**Pb2-N**
LATFAQ	$P2_12_12_1$	19	Y				**Pb3-Y**
LORLAF	$P6_3$	173	Y				**Pb4-Y**
				Total	**21**	**May 2022**	

Table 5. Non-centrosymmetric coordination compounds with **Pb-N-S** chelation pattern with their space group and if it possesses a stereoactive lone pair of electrons.

Reference Code	Space Group	Space Group #	Lone Pair?	Reference Code	Space Group	Space Group #	Lone Pair?
DPENPB01	$P2_1$	4	Y	NUFQEL	$P2_12_12_1$	19	Y
GEVWUZ	$P2_12_12_1$	19	**Pb1-N**	WAKCUG	P_c	7	Y
			Pb2-Y	**TOTAL**	**4**	**May**	**2020**

III. RESEARCH GOALS

The main goal of this project is to synthesize a series of new Pb(II) cyanoximates containing chelating cyanoxime ligands. With only one known precedent, $Pb(ACO)_2 \cdot H_2O$, nothing is known about how Pb(II) will react with these small ligands. Ten various chelating ligands were chosen from a library of 48 cyanoximes. These ligands represent a variety of steric and electronic effects that will allow exploration of previously unknown coordination chemistry of lead compounds and determine their crystal structures (Figure 13). Synthesized bivalent lead complexes were anticipated to have interesting and unpredictable geometry because of the presence of the stereoactive $6s^2$ lone electron pair that can distort coordination polyhedron of the central metal atom. Such distortion typically leads to non-centrosymmetric structures. Compounds were planned to make as bulk product, but crystal growth is a crucial part of the project and becomes the prime objective as single crystals are necessary for XRD analysis. An exhaustive approach is made as multiple techniques are employed trying to achieve growth of the desired products. Samples are characterized using elemental analysis, spectroscopic methods, thermal analysis, and X-ray crystallography. An in-depth study of the refinement data reveals the molecular makeup and geometry of the asymmetric unit (ASU) along with crucial information on the packing of the unit cells. The symmetry operations associated with (or not found) the assigned space groups (specifically looking for the lack of an inversion center) will designate if the crystal is centrosymmetric or non-centrosymmetric. Acentric structures display interesting properties and can exhibit non-linear optical behaviour, such as the second harmonic generation effect (SHG). This phenomenon is important for the design of new materials for photonics application therefore any non-centrosymmetric materials discovered will be further tested (off-site) as potential candidates for SHG materials.

The second part of this project was to make thermal stability evaluation of the obtained compounds. Our compounds have ionic bonding between lead and nitrogen, similar to lead azide [$Pb(N_3)_2$] and $Pb(OCN)_2$ fulminate, which are known high energy compounds. Both are used as primers in detonators to set explosives. This portion of the study will not only document the stability of the complexes but investigate their potential as high energy compounds.

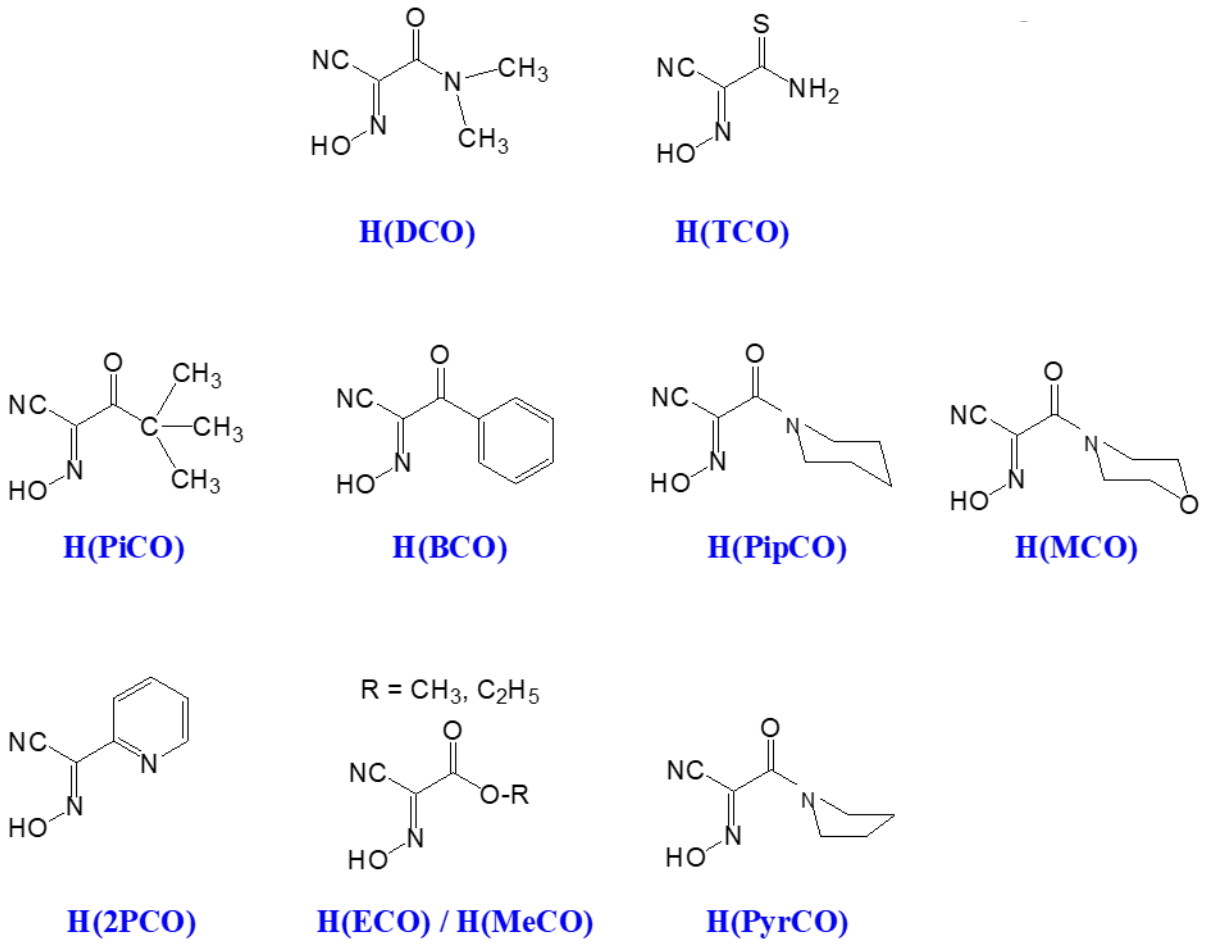

Figure 13. Ten ligands chosen for study with Pb(II) ion.

IV. EXPERIMENTAL

IV.1 Reagents and Solvents.

Two cyanoxime ligands, H(PiPCO), and H(PyrCO), were synthesized for this study. The other ligands were available in the NNG laboratory, having been synthesized in bulk previously by other research group members. The only exception is the H(ECO) which is commercially available and obtained from Aldrich. We keep in the lab a stockpile (or a "bank") of numerous oximes for a variety of projects that are currently in the progress of being developed in Dr. Gerasimchuk's research lab. The ligands available in the lab bank for my study are H(2PCO) made by Abraham Opalade, H(BCO) made by Mark Whitted, H(TCO) made by NNG to avoid graduate students' exposure to stench or toxic chemical compounds but was purified by myself prior to use, H(PiPCO) by Jessica Ratcliff, H(MeCO) by Zsolt Ferenz, H(PiCO) by Mark Whitted, H(BCO) made by Stephanie Dannon, H(DCO) made by Mark Whitted and purified by myself, and H(MCO) made by Kevin Pinks, Manuel Myer, and myself.

Other materials used for synthesis, purification, crystallization, and characterization procedures were obtained from various commercial vendors. The 1-cyanoacetylpyrrolidine, key precursor for H(PyrCO), was made by Danielle Klaus. Compounds such as methyl cyanoacetate, pyrrolidine, piperidine, tetramethylammonium hydroxide (TMA) solution 25 wt. % in methanol, propionitrile, chloroform, potassium carbonate all from Sigma-Aldrich. Acetonitrile, ethyl acetate, hexane, ether, anhydrous ethyl ether, propanol, methanol, sulfuric acid, acetone, toluene, and nitric acid, hydrochloric acid, potassium hydroxide, and Norite® are from Fisher. Lead oxide, lead acetate, dimethylformamide, and celite are from ACROS Organics while lead nitrate analytical reagent and sodium metal are from Mallinckrodt.

Potassium carbonate (Anhydrous), granular, purified from Spectrum Chemical Mfg. Corp, sodium hydroxide from VWR International, iron (II) sulfate heptahydrate from Alfa Aesar, anhydrous sodium sulfate from Baker, sodium silicate (granular) from Frey Scientific Co., and sodium nitrite from Environmental Sampling Supplies. Deuterated dichloromethane for NMR analysis are from Cambridge Isotope Laboratories, Inc.

IV.2. Materials and Methods.

Identification of compounds were carried out by thin-layer chromatography (TLC) on silica gel plates (Merk) using a UV-fluorescent lamp (254 nm) as an indicator. Organic mobile phases varied in composition between polar and non-polar components. Elemental analyses on C, H, N (and S with thioamide-based compounds) content were conducted by Atlantic Microlabs, Inc. (Norcross, Georgia). All melting points or quick decomposition checks were obtained using a Digi-Melt MPA160 made by Stanford Research Systems in open capillary tubes. An Aldrich hot oil bath with a digital Omega Engineering thermocouple is used for a few attempts at crystal growth using technique of sealed ampoules in a steel bomb. Brian Grindstaff, machinist at MSU, fabricated this device to place the sealed ampoule in during an attempt using the thermal solid state crystal growth procedure.

IV.3 Instrumentation

IV.3.1 Vibrational Spectroscopy. The IR-spectra for all ligands and Pb(II) cyanoximates were obtained on a Bruker Platinum-ATR spectrophotometer. All spectra were set at 64 scans with a range of 400-4000 cm^{-1} at resolution of 4 cm^{-1}. An atmospheric compensation and baseline correction were applied.

IV.3.2 Thermogravimetric Analysis/Differential Scanning Calorimetry. All thermal analyses were conducted on a SDC Q600 simultaneous TGA/DSC made by TA Instruments. Scans were recorded in a protected nitrogen environment with flow rate of 100 mL/min. Oven ramps ranged from 5°- 20° /minute within a temperature range of 30° to 1000° C. Heat flow and weight of sample are both recorded until sample's complete decomposition. Analysis of thermal behavior data was carried out using the TA Universal Analysis software package.

IV.3.3 X-Ray Crystallographic Analysis. Suitable crystals generated from a variety of methods from all systems were sorted, collected, and stored for analysis on glass microscope slides in non-drying Paraton immersion oil for microscopy. Of the 9 crystal structures reported in the discussion, 6 were studied and refined on the Bruker APEX-2 diffractometer, equipped with a DDC area detector, here at MSU. Crystals were mounted in the MiTeGen plastic loops or cryoLoop and then placed to the copper pin positioned on the goniometer head. The data sets were measured at low temperatures. The intensity data were collected in ω scan mode, using the Mo tube (Kα radiation; λ = 0.71073 Å) with a highly oriented graphite monochromator. The intensities were integrated from four series of 364 exposures each, covering 0.5° in ω at 10 to 60 seconds of exposure time, with the total data collection set being a sphere. Unfortunately, during this part of my project our diffractometer was not operational at times. Thus, we received kind and free of charge help from other crystallographers. Data for Pb{(H2PCO)(2PCO)$_2$ · H_2O} was collected by Dr. Jeanette Krause at the University of Cincinnati. Intensity data were collected at 150K on a Bruker APEX-II CCD diffractometer using Mo Kα radiation, λ=0.71073Å (TRIUMPH curved-graphite monochromator). The data frames were processed using the program SAINT. The data were corrected for decay, Lorentz and polarization effects as well as absorption and beam corrections (numerical). Experimental data for

$Pb_4(OH)_3(NO_3)_2(PiPCO)_3(H_2O)$ was collected by Dr. Sergey Lindeman at Marquette University and data for $Pb_3(OH)(NO_3)(DCO)_4$ was conducted by Dr. Alex Filatov from the University of Chicago. As said, these crystallographers from other US institutions of higher education kindly helped when our instrument was down. These scientists used their diffractometers with optimized pre-set best strategies to collect the "full sphere of reflections". Some data sets had Cu-radiation (Dr. S. Lindeman; Marquette University, WI), while other have Mo-radiation sources (Dr. A. Filatov; University of Chicago, IL and Dr. J. Krause; University of Cincinnati, OH). All models, pictures, and projections of crystal data were accomplished using the ORTEP 3v.2 and Mercury 4.2 software packages.

IV.4 Synthesis of Cyanoximes

General considerations. Preparations of H(PyrCO) [36] and H(PiPCO) [33] are known and have been previously published so details of synthesis will be omitted. The synthetic route for synthesizing cyanoximes is represented by a general three-step procedure (Figure 14). Here it is shown using H(PipCO) as an example but was used for H(PyrCO) as well with only one initial reactant being different. Precursors for the synthesis of H(PiPCO) are methyl cyanoacetate [$NC–CH_2–C(O)OCH_3$] and piperidine. Piperidine is replaced with pyrrolidine for the synthesis of H(PyrCO). All chemicals and precursors were purchased from Sigma Aldrich chemical company and were used without additional purification. Procedure was slightly altered as Step 1 was carried out in an ice bath with argon gas bubbling through the mixture during synthesis. The gaseous methyl nitrite in step 3 was prepared in situ during the nitrosation reaction and details can be found in published patent [37]. Oximes were collected, dried, and weighed then added to the cyanoxime bank in the lab.

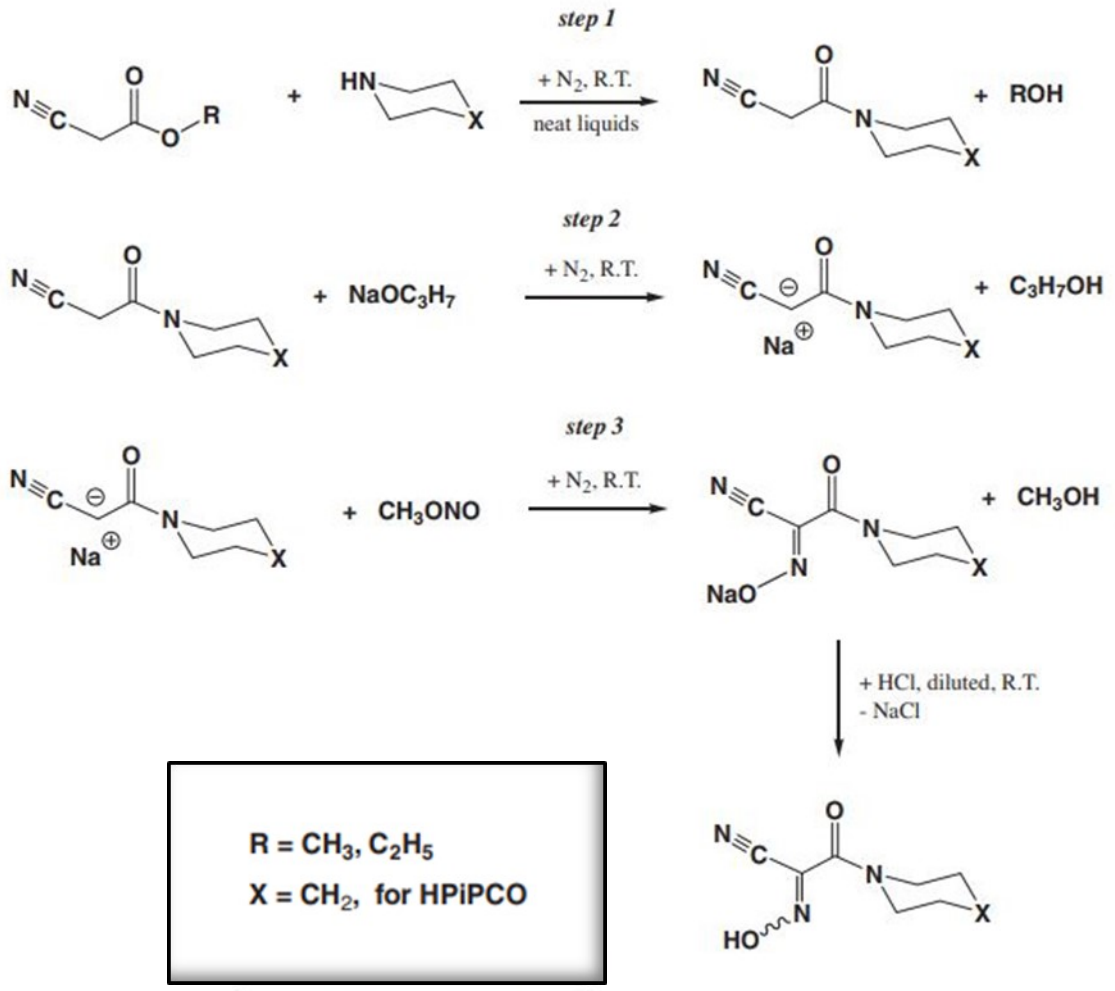

Figure 14. The synthetic route for synthesizing cyanoximes is represented by a general three-step procedure. H(PipCO) shown here as an example, but this process was also used for H(PyrCO).

IV.4.1 Synthesis of H(PyrCO). Beginning reactants are 3.83 mL of methyl cyanoacetate (density = 1.123 g/mol) and 3.92 mL pyrrolidine (density=0.866 g/cm^3). Step 1 was conducted three times with same volume of reactants and had total yield of 11.222 g of 1-cyanoacetylpyrrolidine. Two small vials of the same compound had been previously made by Danielle Klaus, so it was combined with previous yield for a total of 15.791 g for reactant in Step 2. Procedure appeared to be unsuccessful as no product precipitated out. Solution instead had

three layers: dark orange oily layer, yellow emulsion, and clear orange aqueous layer. Each layer was tested via TLC plate against a H(PyrCO) standard and showed desired product was present along with a contaminant. An exhaustive extraction using brine of all layers did produce final light-yellow product from aqueous layer and a mustard yellow product from oily layer. Total yield was 1.821 g. TLC plates were run with a 2:1 ethyl acetate: hexane mobile phase against a standard to confirm product. Dr. Gerasimchuk recorded the ^{1}H and ^{13}C NMR spectra, compared it to a known standard, which confirmed product of H(PyrCO). Multiple small batches of this compound were synthesized and then after purity check combined instead of one large batch.

IV.4.2 Synthesis of H(PiPCO). Three batches of 1-cyanoacetylpiperidine were synthesized in Step 1 before proceeding to Step 2 (Figure 14). Each trial began with 3.48mL of methyl cyanoacetate (density=1.123 g/mL) and 4.28 mL of piperidine (density=0.862 g/mL). Yields were 1.957 g, 2.230 g, and 1.768 g respectively. Continuing with Step 2 of the synthesis, two trials were completed to final product of H(PiPCO). First trial started with 2.649 g of 1-cyanoacetylpiperidine. Smooth synthesis yielded 2.078 g of protonated cyanoxime with confirmation through TLC by matching R_f value to standard. Mobile phase was a 9:1 ratio of ethyl alcohol: chloroform. An additional "quick oxime test" indicated the presence of an oxime. A tiny amount of compound, water, and baking soda can be added to a small test tube and dissolved. When a few crystals of $FeSO_4$ are added a color change to dark purple/blue indicates the presence of the cyanoxime. This is highly sensitive colorimetric test on cyanoximes that has been developed in the past [38]. The second trial began with 3.810 g of 1-cyanoacetylpiperidine resulting with 2.906 g of H(PiPCO). Confirmation of product is made through three avenues: a "quick oxime test" with a dark purple result; TLC plate which is run with ligand against a

standard of ligand with 9:1 mobile phase of ethyl alcohol: chloroform with matching R_f values; and melting point of 155.5°-158.8° C matches published value of 159° C.

IV.5 Synthesis of Pb(II) Cyanoximates

IV.5.1 Benchtop Synthesis of PbL_2. All ten ligands were reacted with Pb(II) cations coming from different salts (nitrate and acetate) in anticipation of being one Pb(II) metal center and two chelating ligands with the possibility of water molecules. This generalized two-step reaction can be seen in Figure 15 where HL represents the protonated ligand and PbL represents the lead and ligand complex. Step 1 deprotonates the ligand in aqueous solution with a 1: 1 ratio with one of the many base choices we used such as potassium hydroxide, sodium hydroxide, potassium carbonate, and tetramethylammonium hydroxide in attempt to develop the best route and yield of a target complex. Step 2 is the coordination of the metal ion to the ligands and has the stoichiometry of two ligands for one lead. Figure 16 shows the reaction with the **anticipated** geometrical structure for the coordination compounds using the H(2PCO) ligand as an example. Each reaction consists of a ligand combined with one of the bases in a small beaker, dissolved in minimal water (starting with 10mL), heated in a water bath (on a hot plate), and sonicated,

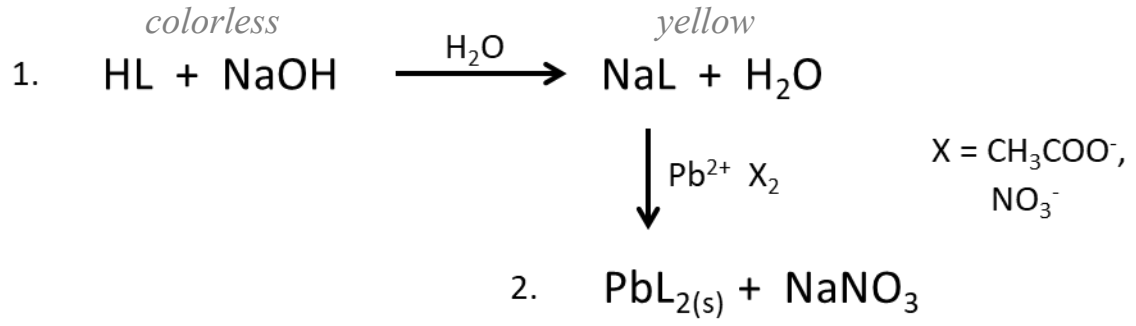

Figure 15. The generalized two-step reaction for synthesis of lead (II) cyanoximates. Step 1 shows the deprotonation of ligand (HL) and Step 2 immediately follows with the reaction of making desired PbL_2.

adding water as needed in increments of 5 mL until ligand is dissolved appearing as a clear yellow aqueous solution. In another vessel, we dissolve the lead nitrate in 5 mL of water making sure the solution stays clear. A stir bar is placed into the beaker and the aqueous lead solution is slowly added dropwise into the heated beaker (about 1 drop every 2-3 seconds). We continued to stir the reaction mixture for a few minutes after all lead has been added, then removed from heat and allowed to set for a couple of days (Figure 17). When the precipitate was observed, it was filtered off using gravity filtration with filter paper. The precipitate was washed with small amounts of water then allowed to air dry. Final product was packed into a vial. Also, we sifted through the product under microscope and whenever possible retrieved suitable crystals for crystallographic study. The filtrate was left for the crystal growth. A total of 17 reactions were conducted using this procedure and were carried out at ambient conditions on the desktop. The complete series of Pb(II) cyanoximates can be seen in Figure 18 and Table 6 shows the reaction number, reactants, and the total amount of water for the reactions.

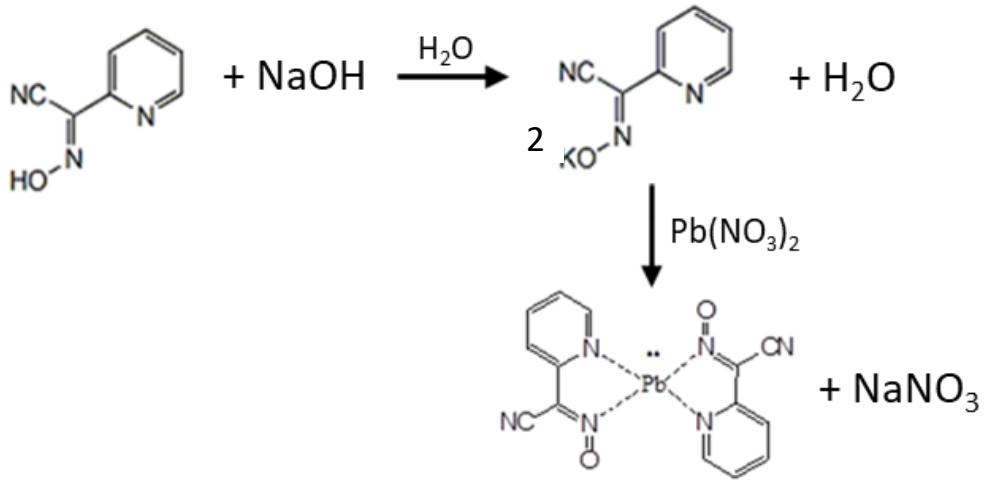

Figure 16. The 2-step reaction for synthesis of lead cyanoximates with the H(2PCO) ligand showing the anticipated geometrical structure of product.

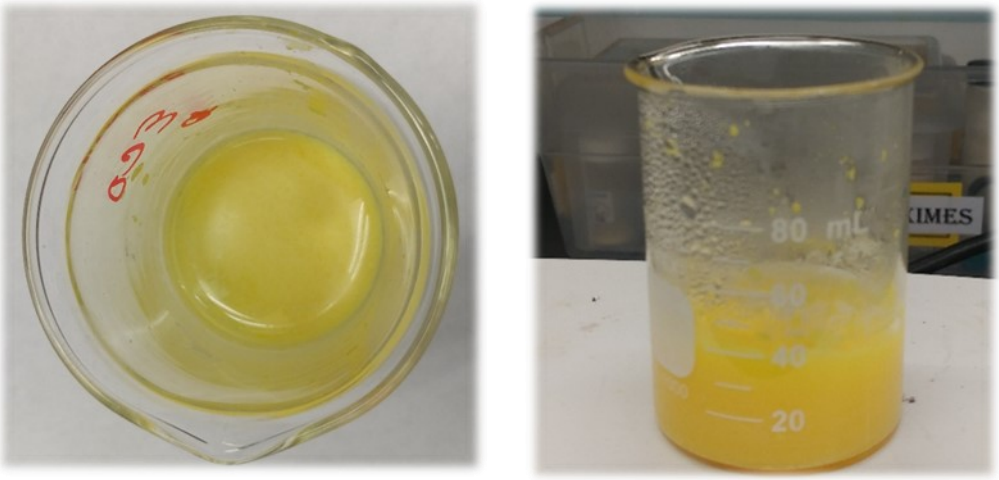

Figure 17. Benchtop synthesis of "Pb(ECO)".

Figure 18. Complete series of Pb(II) cyanoximates as prepared on the benchtop using simple "$2L^- + Pb^{2+} \longrightarrow$ product" approach.

Table 6. Reactants for the synthesis of Pb(II) cyanoximates. (* indicates concentration either in molarity (mol/L) or density (g/cm^3).

Rxn	Ligand	(g)	Base	Amt.	Concentration*	Pb(NO3)2 (g)	H2O (mL)
1-1	H(2PCO)	0.2993	K2CO3	0.1408 g	*	0.4059	30
2-1	H(2PCO)	0.3787	KOH	1.89 mL	1.079	0.3386	25
2-2	H(2PCO)	0.3008	KOH	1.89 mL	1.079	0.3386	45
3-1	H(BCO)	0.2635	KOH	1.40 mL	1.079	0.2521	35
3-2	H(BCO)	0.1556	TMA	0.375 mL	d = 0.866	0.1483	25
4-1	H(ECO)	0.3001	K_2CO_3	0.1465 g	*	0.3406	35
4-2	H(ECO)	0.3015	K_2CO_3	0.1473 g	*	0.3519	10
5-1	H(MeCO)	0.3011	K_2CO_3	0.1626 g	*	0.3896	24
5-2	H(MeCO)	0.3008	K_2CO_3	0.1626 g	*	0.3893	23
6-1	H(TCO)	0.5000	KOH	3.590 mL	1.079	0.6411	10
7-1	H(PipCO)	0.3001	KOH	4.64 mL	0.3569	0.2744	25
7-2	H(PipCO)	0.2042	KOH	1.130 mL	1.00	0.1878	35
8-1	H(PiCO)	0.2465	KOH	1.60 mL	1.00	0.2657	17
9-1	H(DCO)	0.2950	KOH	2.090 mL	1.00	0.3461	15
10-1	H(PyrCO)	0.1750	TMA	0.4406 mL	d = 0.866	0.1733	8
11-1	H(MCO)	0.3008	KOH	1.64 mL	1.00	0.2712	8
12-1	H(MCO)	0.1935	NaOH	2.105 mL	0.502	0.1749	n/a

IV.5.2 Schlenk Line Synthesis of PbL_2. The sulfur containing cyanoxime ligand H(TCO) appeared to be unstable in an open-air synthesis. The PbL_2 is attempted under a protected environment using available in the lab Schlenk line. In general, sulfur based cyanoximes, HTCO and others, are not very stable in air and have to be purified before synthesis. Two reactions are conducted with H(TCO). At first let's describe the procedure of making pure ligand. **Purification process of H(TCO)**: We placed impure olive green colored HTCO (that had partially decomposed after exposure to air and light) in flask, added 150 mL ether, and swirled until dissolved then added charcoal powder. Prepared a celite packed filter by using a course frit glass filter and pack until half full of celite and place on a 250 mL vacuum flask. The solution of H(TCO) was warmed with a heat gun until boiling. Content was poured over celite. The flask was rinsed with small amount of ether and poured over filter. The clear orange filtrate was transferred to a pear flask where the solvent was stripped off under vacuum with a rotary evaporator which made a bright-yellow solid. Purified H(TCO) represented a lemon-yellow precipitate.

IV.5.2.1 Synthesis of $Pb(TCO)_2$ Reaction 13-1. The synthesis started with 0.388 g HTCO in a pear bottom flask from the purification process. Twenty mL of anhydrous ethanol was added to flask to dissolve the ligand and transferred the solution to reaction vessel. Next, 1.275 mL of tetramethylammonium hydroxide was added to same reaction vessel to deprotonate the H(TCO) ligand. Then dissolved 0.5735 g of lead acetate trihydrate in 10 mL of water and added to reaction vessel-2 for use on the Schlenk line. The glassware setup was vacuumed and then filled with argon. Under protected environment the two vessels were positioned together in such way that the contents were mixed together. Immediately a mustard yellow precipitate was formed. It was anaerobically transferred to a vacuum filter and dried.

IV.5.2.2 Synthesis of $Pb(TCO)_2$ Reaction 14-1. The second trial followed the same procedure as 13-1. We started with 0.14 g of purified H(TCO), 485 µL of $NMe_4^+OH^-$ base, and 0.19 g of $Pb(NO_3)_2$. A Schlenk glass filter was used under argon environment to filter the precipitate. Product was collected as a yellow cake. (Figure 19) The filter tube was filled with argon and sealed until further analysis can be conducted. The dark yellow orange filtrate solution in the Schlenk flask was filled with argon, sealed with a stopper, then placed in a 4° refrigerator to see if any crystals will grow.

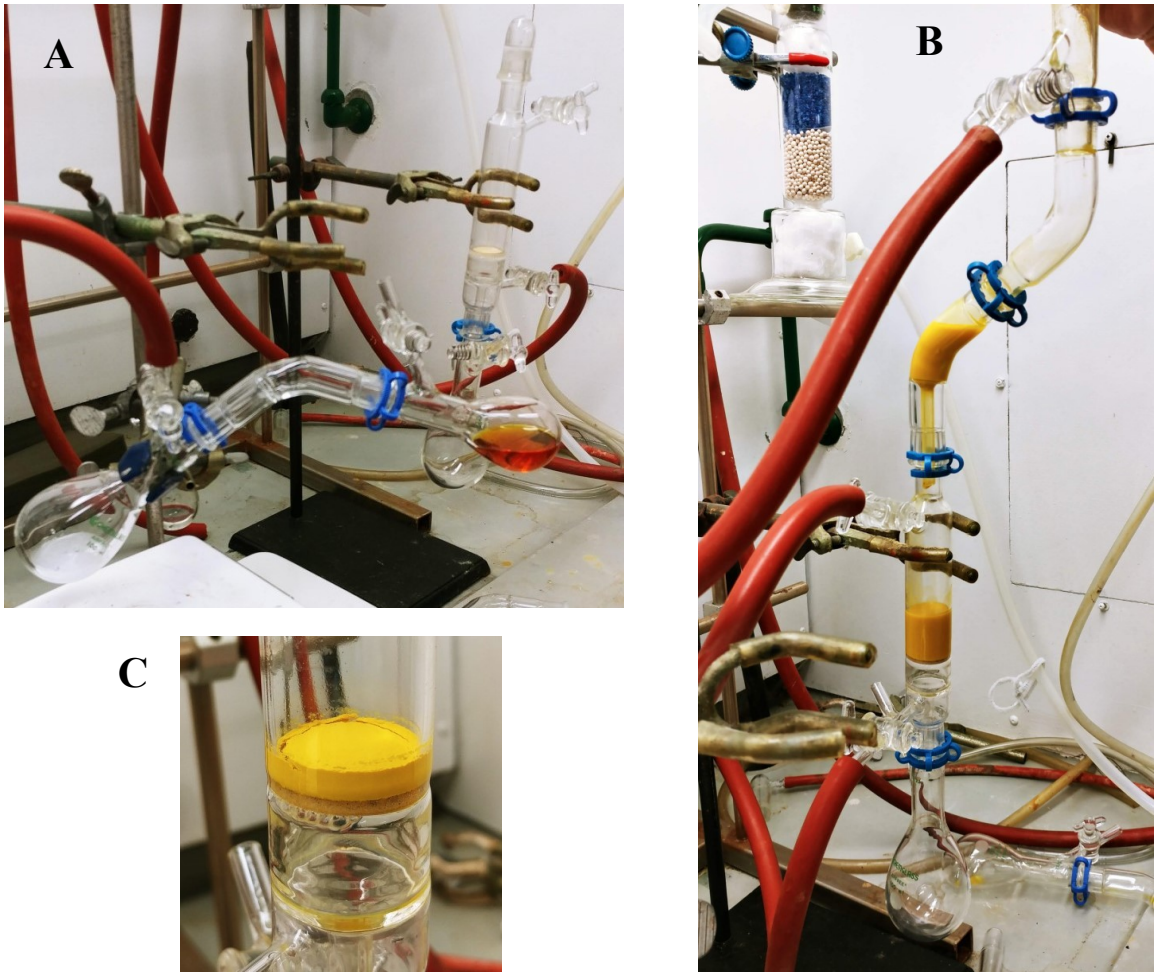

Figure 19. Schlenk line synthesis of $Pb(TCO)_2$; **A -** Set up showing reactants in flask under protected environment prior to mixing; **B -** $Pb(TCO)_2$ product being filtered; **C -** Final product.

IV.6 Crystal Growth of Pb(II) Cyanoximates

Crystal growth and determination of crystal structures are essential for this study. The growth of suitable for the XRD analysis crystals proved to be a great challenge. We undertook an extensive exploration through multiple attempts and variety of procedures in effort to grow quality crystals. Several methods will be presented below.

IV.6.1. Crystal Growth from PbL_2 Synthesis Filtrate. The filtrates from the 17 reactions listed in Table 6 (plus Reaction 14-1) were collected and preserved in polypropylene tubes (Figure 20-D). The tubes were left open for water evaporation and placed to be undisturbed in a dark cabinet. Once the water evaporated off the tubes they were carefully searched for any suitable crystals. For that purpose, all contents were delicately scraped off and examined under a microscope looking for any crystalline material (Figure 20-E).

IV.6.2 Crystal Growth of PbL_2 in Narrow Tubes. During synthesis small diameter, ~ 5 mm Pyrex tubes were made in attempt to grow PbL_2 crystals using direct reaction between components. In this method two soluble reactants with different densities were layered so that the liquid/liquid boundary is distinct. Narrow tubes are preferred because it is easier to build the layers when the boundary area is a small surface (Figure 17-A). Allowed to sit undisturbed, slow diffusion occurs slowing down the process of the reaction therefore increasing the chances for a single crystal. At the point of contact a precipitate of the PbL_2 forms a plug. (Figure 20-B). Allowed to sit undisturbed, slow diffusion occurs slowing down the process of the reaction therefore increasing the chances for a single crystal.

Using blowtorch 23 tubes of ~12" in length were made. Stock solutions were prepared: $Pb(NO_3)_2$ –0.302 M made with 10.010 g in a 100.0 mL volumetric flask; $Pb(C_2H_3O_2)$ –0.26 M made with 10.00 g in 100.0 mL volumetric flask and tetramethylammonium hydroxide (TMA),

[$N(CH_3)_4OH$ solution 25% weight in methanol (density – 0.866 g/mL)] was obtained from the lab stock. Tubes were loaded with either a 1:2 ratio of lead to ligand or a 1:4 ratio. Ligands were weighed out, dissolved in 1 mL of acetonitrile (CH_3CN), then base added. The aqueous lead stock solution was carefully added first to the bottom of the tube with a long-tipped dropper avoiding any solution getting on the inner sides inside the tube. Next, the organic layer is gently layered on top of the aqueous lead careful not to disturb or "break" the surface of the aqueous lead layer when added. Mini cork stoppers were used to plug the tubes and were sealed with paraffin. Tubes were placed in a 4° refrigerator and left undisturbed for crystals to grow for a long period of time periodically being checked on a weekly basis. Crystals developed in some tubes as quickly as 48 hours. To retrieve crystals, tubes had to be cut open near the plug. Most crystals were harvested from the precipitate, formed in the plug area, but others were found growing on the interior walls of the tubes in various diffusion areas, both in the aqueous and organic layers. Table 7 shows the reactants used in each tube for this crystal growth method.

IV.6.3 Crystal Growth of PbL_2 in Gel U-tubes. This method utilizes technique developed by Henisch [39]. Thus, individual gel U-tubes were made in attempt to grow PbL_2 crystals in gel. In this method two soluble reactants are allowed to diffuse through a gel made of silicic acid where they react and form an insoluble or relatively less soluble crystalline product. Glass tubing, with an inner diameter approximately 7 mm, was obtained from the inorganic synthesis CHM 432 lab and cut in approximately 8-inch lengths. Using the glass blowing station, both ends of the tubing were fire-polished and carefully bent into a U-shape making sure to not seal off the tubes on the curves. In total, ten tubes were made. Then starting solutions of 0.3020 M $Pb(NO_3)_2$ and 1.0 M NaOH were obtained from pre-made lab stock. About 2 g of sodium silicate and 12 mL of water were added in a small beaker and completely dissolved. This

Table 7. Reactants for the crystal growth of PbL_2 in narrow tubes.

Tube #	Ligand	Ratio	Ligand (g)	Lead Source	Lead (mL)	TM A (µL)
1	H(2PCO)	1:2	0.0889	$Pb(NO_3)_2$	1.0	255
2	H(2PCO)	1:4	0.1778	$Pb(NO_3)_2$	1.0	510
3	H(PiCO)	1:2	0.0935	$Pb(NO_3)_2$	1.0	255
5	H(ECO)	1:2	0.0858	$Pb(NO_3)_2$	1.0	255
6	H(ECO)	1:4	0.1719	$Pb(NO_3)_2$	1.0	510
7	H(MeCO)	1:2	0.0773	$Pb(NO_3)_2$	1.0	255
8	H(MeCO)	1:4	0.1552	$Pb(NO_3)_2$	1.0	510
9	H(BCO)	1:2	0.1052	$Pb(NO_3)_2$	1.0	255
10	H(BCO)	1:4	0.2104	$Pb(NO_3)_2$	1.0	510
11	H(PyrCO)	1:2	0.1010	$Pb(NO_3)_2$	1.0	255
13	H(DCO)	1:2	0.0852	$Pb(NO_3)_2$	1.0	510
14	H(DCO)	1:4	0.1704	$Pb(NO_3)_2$	1.0	510
15	H(MCO)	1:2	0.1106	$Pb(NO_3)_2$	1.0	255
16	H(MCO)	1:4	0.2212	$Pb(NO_3)_2$	1.0	510
17	H(PiPCO)	1:2	0.1094	$Pb(NO_3)_2$	1.0	255
18	H(PiPCO)	1:4	0.2188	$Pb(NO_3)_2$	1.0	510
19	H(MeCO)	1:2	0.0675	$Pb(C_2H_3O_2)_2$	1.0	255
20	H(ECO)	1:2	0.0749	$Pb(C_2H_3O_2)_2$	1.0	255
21	H(BCO)	1:2	0.0918	$Pb(C_2H_3O_2)_2$	1.0	255
22	H(PiPCO)	1:2	0.0955	$Pb(C_2H_3O_2)_2$	1.0	255
23	H(PYRCO)	1:2	0.0881	$Pb(C_2H_3O_2)_2$	1.0	255
24	H(DCO)	1:2	0.0744	$Pb(C_2H_3O_2)_2$	1.0	255
25	H(2PCO)	1:2	0.0776	$Pb(C_2H_3O_2)_2$	1.0	255

resulted in a pH around 12 as tested with universal pH paper strips. The solution must be acidified to gel therefore a solution of 1:5 concentrated HCl to water was added dropwise until signs of thickening appear. A plastic pipette was used to fill the U-tubes across the bottom and about 1 inch up both sides. Additional HCl solution was added drop by drop on each side of the tube and stirred with a thin glass stir rod to completely solidify the gel and to obtain the desired

pH for each side. One side of the tube is basic, pH about 8 and more gelatinous, and carries the deprotonated ligand while the other side of the tube is acidic, pH about 4 and more aqueous, and loaded with the lead nitrate solution. The pH levels are approximate and are tested, again, with universal pH paper strips. The ligand, 1mL of water, and the base was added to a beaker and stirred until dissolved then added gently to the top of the basic side of the U-tube. The stock solution of lead was gently added to the acidic side of the tube. The amount for each reactant is listed in Table 8. Both ends of the tube were corked and parafilm placed over the top to seal then carefully placed where they would not be disturbed for crystal growth (Figures 20-F and 20-G). Periodic inspection showed that some crystals have grown in the gel. Retrieval of crystals is more challenging in this medium. U-Tubes had to be cut and the gel placed on a large paper filter. Literally digging through amorphous gel material with a thin molybdenum needle allowed retrieval of some crystals used in the XRD studies.

Table 8. Reactants for the crystal growth of PbL_2 in gel U- tubes.

Tube #	Ligand	Ligand (mg)	NaOH (µL)	$Pb(NO_3)_2$ (µL)	Ligand pH	Lead pH
1	H(2PCO)	53.00	720	298	8	4
2	H(2PCO)	44.32	610	250	8	2
3	H(MCO)	31.84	350	145	9	5
4	H(2PCO)	51.15	0	300	8	3
5	H(PiPCO)	47.25	700	220	9	2
6	H(BCO)	39.61	460	190	8	5
7	H(DCO)	43.62	615	260	8	5
8	H(PyrCO)	46.35	555	230	9	6
9	H(PiPCO)	44.11	570	240	8	5
10	H(ECO)	50.60	710	295	8	6

IV.6.4 Crystal Growth of PbL_2 in Vapor Diffusion Tubes. Vapor diffusion tubes were set up for six trials. This procedure involves the diffusion of the vapor of a volatile solvent, in which the compound is not soluble, into the solvent containing the sample to be crystallized. As the more volatile solvent diffuses into the sample it decreases the overall solubility forcing the compound out of solution as crystalline product. This system consists of a test tube placed inside a larger sealed vial. Four of the ligand solutions are prepared with products from the desktop syntheses that had C, H, N analysis confirming the product of PbL_2. About 40 mg of the product was dissolved in 1 mL of dimethylformamide (DMF), dissolved completely, and run through a small glass wool plug filter to remove any residue. This was transferred to the small interior test tube. The more volatile solvent is added in outer tube and is filled with enough solvent so that when the smaller test tube is gently lowered into it that the solvent will be about halfway up on the interior test tube. The other two interior test tubes are filled with filtrate from Reaction 9-1, a reaction of making $Pb(DCO)_2$. Once the small test tube is gently placed inside, the larger tube is tightly capped, sealed with a layer of parafilm, and placed in a 4° refrigerator and left for crystal growth (Figure 20-C). Reactants for the vapor diffusion tubes can be seen in Table 9.

Table 9. Reactants for crystal growth of PbL_2 in vapor diffusion tubes.

Tube #	Complex	Source	Solvent	Outer Solvent
1	Pb(TCO)	Rxn 6-1	DMF	Ether
2	Pb(2PCO)	Rxn 2-2	DMF	Ether
3	Pb(PiCO)	Rxn 8-1	DMF	Ether
4	Pb(PiPCO)	Rxn 7-2	DMF	Ether
5	Pb(DCO)	Rxn 9-1 F	Water	Acetone
6	Pb(DCO)	Rxn 9-1 F	Water	Acetonitrile

IV.6.5 Solid State Crystal Growth in the DSC/TGA Instrument. Solid state reactions are simple reactions to perform and are considered "clean" as they do not involve any other chemical compounds that can be used in a product's crystal structure. However, it is not as easy for reactions to occur because they are heterophase having two solids interacting. The heat source used for these reactions came from the DSC/TGA instrument as the temperature can be raised to the desired temperature and kept for a long time using protective atmosphere of Ar flow. When heat is turned off the reaction vessel (crucible) is able to cool down at a slow pace which is conducive to crystal growth. A ratio between lead oxide and ligand was 1:4. Lead oxide and H(2PCO) were weighed out and ground together until very fine in a mortar and pestle. Reactants were placed in alumina crucible for analysis on DSC/TGA instrument, purged with Ar gas and heated. Trial two used PbO and H(DCO) ligand for the reactants. Each trial was heated at a ramp of 10º/ minute and waited for 20 minutes at maximum temperature. The H(2PCO) trial was heated to 150º C and the H(DCO) trial had a max temperature of 130º C. (Figure 21-F and 21-G)

IV.6.6 Solid State Crystal Growth in Ampoules in Oil. Three attempts were made at growing PbL_2 crystals via solid state crystal growth. Two procedure used lead oxide (PbO) and H(DCO) ligand. An agate mortar and pestle were used to crush and thoroughly combine the two reactants via mixing. Sample was placed in a glass ampoule and onto a Schlenk Line where all air was removed from the reaction tube by vacuum and flushed with argon gas. Then under vacuum a propane torch was used to seal the ampoule. (Figure 21) Then ampoule was placed in the lead sheath and in the hot oil bath where the temperature was raised for about 24 hours then allowed to cool to room temperature before checking for crystalline material. The third ampoule was prepared the same way but with a few modifications being the reactants were dissolved in 3

mL of propionitrile and prior to sealing this ampoule, liquid nitrogen was used to solidify the contents. This was necessary as the flash point of propionitrile is 6° C so would be an explosion hazard without freezing. Details of the reactants can be found in Table10.

Table 10. Reactants for crystal growth of PbL_2 with Solid State Crystal Growth Ampoules in hot oil bath.

Trial	H(DCO) (g)	PbO (g)	Temp (°C)	Time (hours)
4-1	0.276	0.1082	150	24
4-2	0.276	0.1088	130	20
4-3	0.276	0.1087	120	21.5

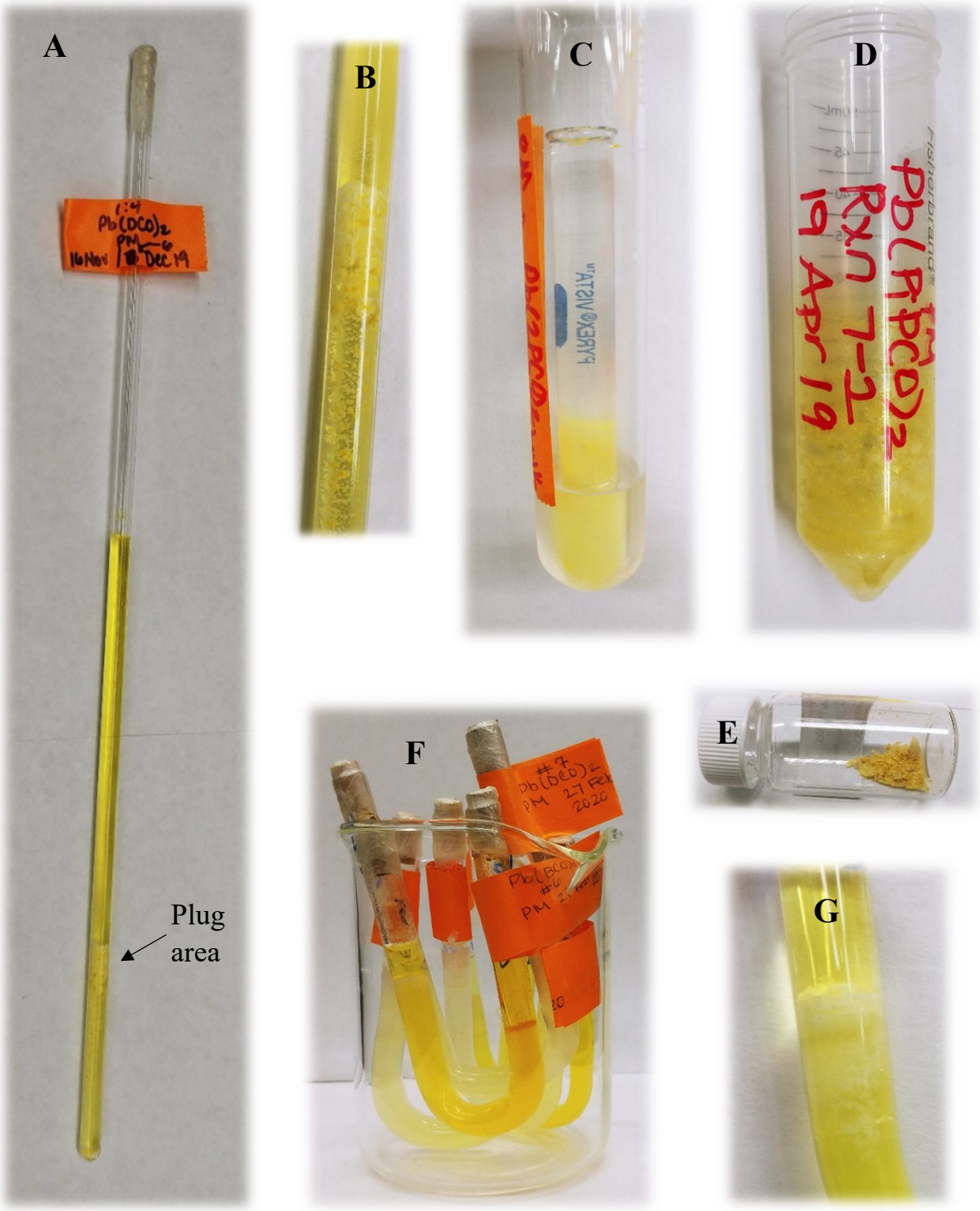

Figure 20. Methods used for crystal growth of lead (II) cyanoximates. **A -** Narrow tube; **B -** Narrow tube plug; **C -** Vapor diffusion; **D –** Slow filtrate Evaporation; **E –** Product collected from filtrate evaporation; **F -** Gel U-tubes; **G -** Crystal growth in gel.

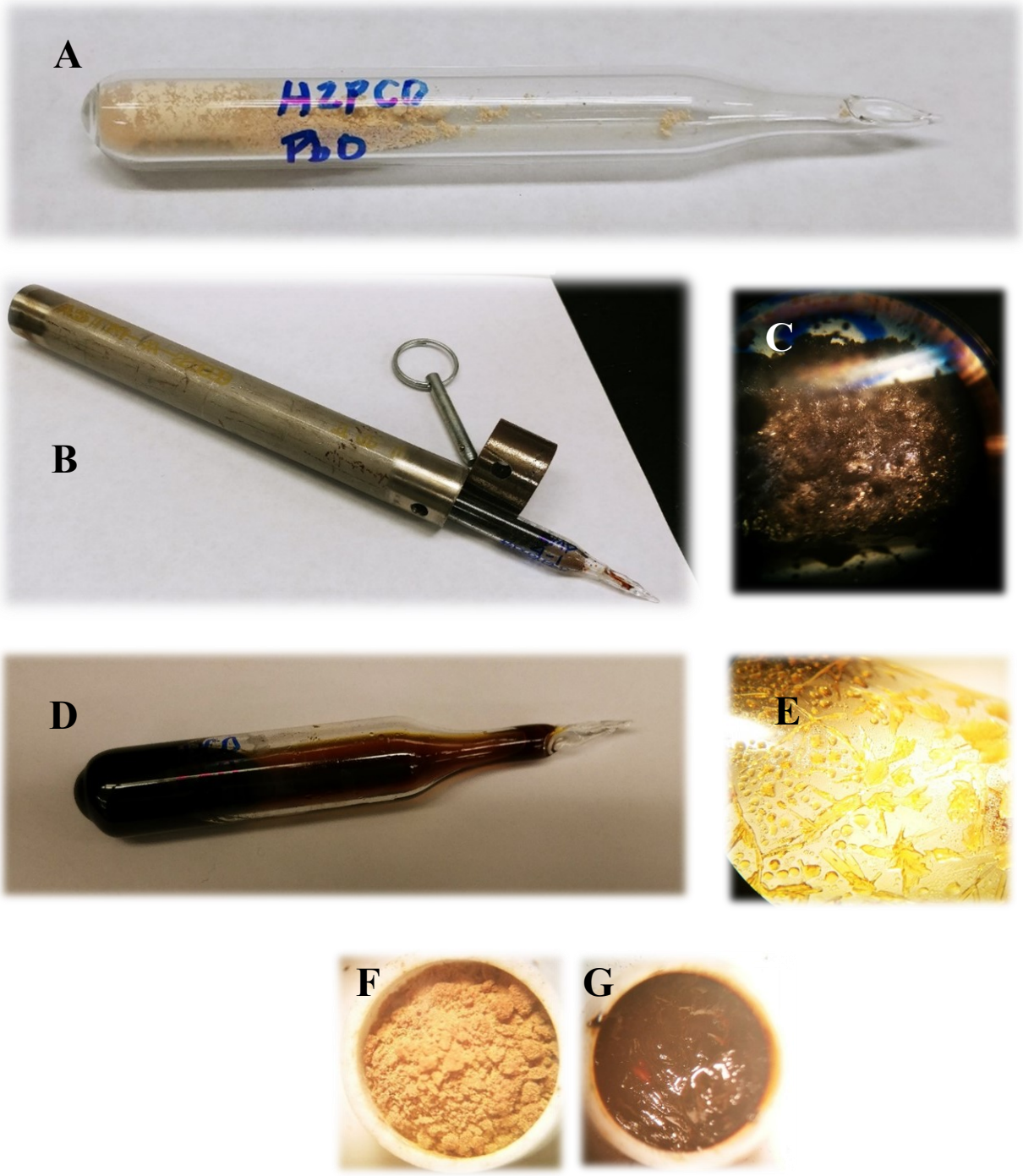

Figure 21. Solid state crystal growth. **A -** Prepared ampoule loaded with PbO and H2PCO; **B -** Ampoule in lead safety sheath; **C -** Charred results from hot oil procedure; **D -** Results from hot oil procedure in solvent; **E –** Mushy crystalline-like product from hot oil procedure in solvent; **F –** Crucible with PbO and H2PCO after DSC/TGA heating to 150° C; **G –** Crucible with PbO and H(DCO) after DSC/TGA heating to 130° C.

V. RESULTS AND DISCUSSION

The task at the beginning of this project was to synthesize a series of lead(II) cyanoximates using $Pb(NO_3)_2$ and the ten chosen ligands that are able to form chelates. The initial approach seemed clear with a very straight forward path to the finale. The journey would begin with the preparation of a bulk product for each PbL_2 compounds, simply made on the benchtop in the lab, followed by characterization with a C, H, N, (S) elemental analysis, thermal analysis, and vibrational spectroscopy. Filtrates from the reactions would produce necessary crystals for the XRD analysis. Ultimately, we would dissolve our bulk PbL_2 in low polarity solvent and grow crystals from that setup. Crystal structure results would be reviewed and reported—expecting similar results to the one known lead (II) cyanoximates—but a more winding road was on the horizon.

V.1 Benchtop Synthesis of PbL_2

Nineteen trials were completed using the desktop procedure in efforts to synthesize new PbL_2 compounds using ten different chelating cyanoximate ligands, formulas of which are shown in Figure 13, and lead (II) ion sources. The PbL_2 bulk product procedure, as discussed in the experimental section, resulted with 12%-84% yield in 17 trials and 1 trial with 0% yield as it resulted in no useable product (Reaction 3-1 with HBCO) due to contaminated ligand. Attempts were made to maximize the yield, so some trials were replicated using slight modifications to the procedure, such as a change in the base used for deprotonation of the ligand or a change of the temperature reaction vessels. All products were powder-like with a hue of yellow to yellow orange with one exception, the Pb(TCO) products, which initially were yellowish but quickly

turned very dark olive green. The precipitates were examined and the most homogeneous PbL_2 sample for each ligand were sent out for C, H, N, (S) elemental analysis. Theoretical values for the elemental percentages were based on a projected product containing one lead atom and two ligands. Four of the 11 samples (two samples of $Pb(TCO)_2$ were analyzed due to assumed decomposition of samples) were within parameters indicating that the products were our targeted PbL_2 compounds; $Pb(2PCO)_2$, $Pb(PiCO)_2$, $Pb(TCO)_2$ from Reaction 6-1 and $Pb(TCO)_2$ from Reaction 14-1. These four systems, identified by the green data points, were calculated to be within ± 3% of theoretical value (Table 11). Further studies were conducted to see if there were any water molecules in these crystal structures like the $Pb(ACO)_2 \cdot H_2O$ compound, the only known lead (II) cyanoximate, [2] and will be discussed next.

V.1.1 $Pb(2PCO)_2$. The elemental analysis supports the structure of one lead and two ligands with the theoretical (actual) data of presented in Table 11. In addition, a DSC/TGA analysis was conducted on the $Pb(2PCO)_2$ compound, and it did not show any evidence for water leaving the system. After being heated to 1000° C a small amount of charred carbon (or lead) product remained in the crucible. Before and after photos of the actual compound can be seen in Figure 22. IR spectroscopy further confirms the PbL_2 structure through the presence of key

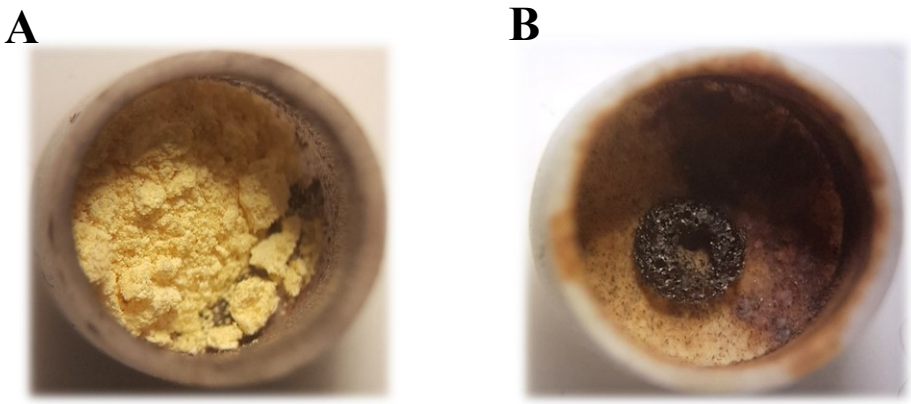

Figure 22. Crucible containing bulk product from synthesis of Pb(2PCO)2. **A -** Before DSC-TGA analysis; **B -** After DSC-TGA analysis.

bonding groups for the compound as reported: ν(C-H) 3088 cm^{-1}, ν(C≡N) 2221 cm^{-1}, ν($C=N_{py}$) 1588 cm^{-1}, ν($C=N_{ox}$) 1461 cm^{-1}, ν(N-O) 1022 cm^{-1} and no sign of O-H bonding around 3400 cm^{-1} was present. Multiple crystals were harvested in systems with Pb^{2+} and $2PCO^{-}$ for reactants but no crystal structures were identified to match the elemental analysis data. We are confident that the desired product PbL_2 was synthesized in bulk therefore this emphasized the complexities involved in growing the desired single crystals with lead. This will be discussed further in the section on hydrolysis of lead (II) cations.

V.1.2 $Pb(PiCO)_2 \cdot 3\ H_2O$. The elemental analysis supports the structure of one lead, two ligands, and three water molecules with the theoretical (actual) data as shown in Table 11. The DSC/TGA analysis was conducted, and it supports three water molecules leaving in a two-step process. One molecule leaves the system at 138° C with a weight loss of 2.22% and the last two are lost at 175° C with a total weight loss of 10.85% compared to the theoretical value of 9.53%. The thermal scan was conducted to 800° C leaving about 34% weight in the crucible. Observation of crucible after TG experiment showed small amount of black residue remaining to be the final product of elemental lead at 37% amount. Regardless of final appearance, based on its weight, the compound decomposed mostly to elemental lead. The IR spectroscopy confirms the presence of key bonding groups for the compound $PbL_2 \cdot 3\ H_2O$ as reported: ν(O-H) 3320, ν(C-H) 2974 cm^{-1}, ν(C≡N) 2212 cm^{-1}, ν(C=O) 1644, ν($C=N_{ox}$) 1368 cm^{-1}, ν(N-O) 962 cm^{-}. No single crystals were harvested with this composition despite numerous attempts.

V.1.3 $Pb(TCO)_2 \cdot 2\ H_2O$. The dark yellow complex from Reaction 6-1, which was synthesized on the desktop, turned out to contain two water molecules in its structure. Confirmation through a thermal analysis strongly indicated the presence of two water molecules

Table 11. Results from the desktop synthesis of lead (II) cyanoximates with elemental analysis results included. Green data indicates a match of either a PbL_2 compound or a crystal (*) reported in this study.

Rxn	Ligand	% Yield	Product Description	C, H, N (S) Theoretical	C, H, N (S) Actual	C, H, N (S) Difference
1-1	H(2PCO)	79	sunshine yellow powder	*	*	*
2-1	H(2PCO)	84	canary yellow fine powder	*	*	*
2-2	H(2PCO)	80	canary yellow powder	33.67, 1.61, 16.83	34.34,1.74, 17.18	+0.67, +0.13, +0.35
ST	H(2PCO) Ac	n/a	canary yellow precipitate	33.67, 1.61, 16.83	24.96, 2.20, 10.66	-8.71, -0.59, +6.17
5-1	H(MeCO)	36	yellowish-orange powder	20.83, 1.31, 12.14	15.48, 1.52, 10.68	-5.35, +0.21, -1.45
5-2	H(MeCO)	45	orangish-yellow powder	*	*	*
4-1	H(ECO)	12	lt yellow powder	*	*	*
4-2	H(ECO)*	41	yellow powder	19.05, 2.00, 14.44	18.49, 1.57, 8.42	+0.32, +0.03, +1.68
8-1	H(PiCO)	47	dark yellow ppt	29.63, 4.23,9.88	30.01, 3.45, 9.66	+0.38, -0.78, -0.22
3-1	H(BCO)	0	dark red sticky substance, tiny yellow ppt	*	*	*
3-2	H(BCO)	29	dark yellow powder	39.06, 1.82, 10.13	33.28, 1.89, 8.12	-5.78, +0.05, -2.02
7-1	H(PipCO)	32	yellow powder	*	*	*
7-2	H(PipCO)	28	yellow powder	33.86, 3.52, 14.80	29.76, 3.22, 12.61	+4.1, +0.3, +2.19
10-1	H(PyrCO)	9	dark yellow powder	31.17, 3.00, 15.57	25.03, 2.86, 12.36	-6.14, -0.14, -3.21
9-1	H(DCO)*	36	lemon yellow v. fine looks like paper	17.30, 0.18, 10.09	19.37, 1.97, 12.76	+1.19, +1.39, +1.67
11-1	H(MCO)	58	light yellow powder	29.41, 2.83, 14.71	23.82, 2.41, 11.83	-5.59, -0.42, -2.88
12-1	H(MCO)	19	mustard yellow powder	*	*	*
6-1	H(TCO)	71	olive green stuck to paper oxidized fast	14.44, 1.62, 16.84, 12.85	14.80, 1.48, 16.76, 12.88	+0.36, -0.14, -0.08, +0.03
13-1	H(TCO) Ac Schlenk	69	brownish-green mud	*	*	*
14-1	H(TCO) NO_3 Schlenk	35	dk yellow-orange quick to greenish black	15.55, 0.87, 18.13,13.84	16.51,1.56,17.15, 12.96	+0.96, +0.69, -0.98, -0.88

as a 7.38% weight loss occurs at 153° C compared to the theoretical weight of 7.00%. The DSC/TGA scan revealed a significant exothermic effect at around 165° C accompanied with a drastic decrease in sample weight. This type of behavior is characteristic for high energy compounds (HE) and this particular compound will be investigated more in depth for such qualities later in this study. The sample was heated to 800° C leaving about 47% of its original weight compared to 41.5% being lead. Sample after the analysis appeared to be charred metal as seen in Figure 23. The elemental analysis (Table 11) supports the formula with the two water molecules. The IR spectroscopy validates the presence of key bonding groups for the compound as reported: ν(O-H) 3400, ν(C-H) 2922 cm^{-1}, ν(C≡N) 2215 cm^{-1}, ρ(NH_2) 1590, ν(C=N_{ox}) 1462 cm^{-1}, ν(C-N-O) 1147 cm^{-}, ν(C=S) 840 consistent with the $PbL_2 \cdot 2\ H_2O$ structure. No crystalline products were collected, or crystal structure determined for this compound.

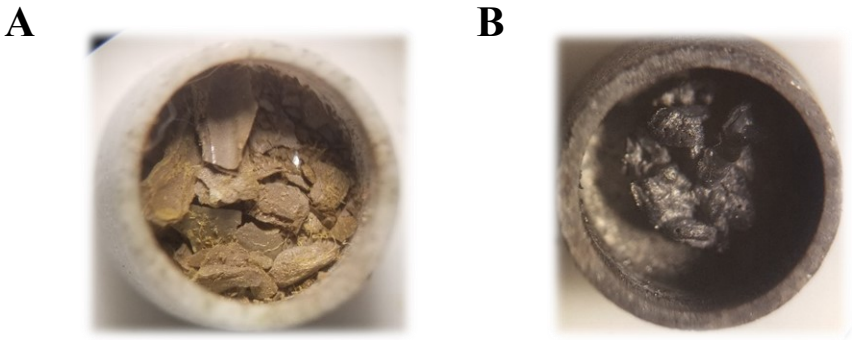

Figure 23. DSC-TGA analysis of $Pb(TCO)_2 \cdot 2\ H_2O$ product from Reaction 6-1. **A -** Before analysis; **B -** After analysis.

V.1.4 $Pb(TCO)_2 \cdot 3\ H_2O$. The complex from Reaction 14-1, which was synthesized anaerobically on a Schlenk line, resulted having three water molecules in its structure. A thermal analysis supports the presence of three water molecules by a two-step burn off process. Two molecules leave the system at 84° C with 8.55% weight loss (calculated loss is 7.0%) and the last

water molecule burning off at 151° C for a total of 10.87% weight loss (calculated loss is 10.4%). Thermal decomposition results were similar in appearance to Reaction 6-1 along with similar highly exothermic peak around 168° C which will be discussed further in the DSC-TGA analysis. The elemental analysis in Table 11 is calculated for a PbL_2 product and falls within parameters, however other data supports account for three water molecules in this compound. Results here show calculation with three water molecules for theoretical (actual) results of: C: 13.93% (16.51%), H: 1.95% (1.56%), N: 16.26% (17.15%), S: 12.41% (12.96%) which are still well within the parameters and supports a match, but the differences are a little more than the results without the water. The results of the thermal analysis strongly suggest water so final composition will include the water presence. IR spectroscopy further supports the presence of key bonding groups for the compound as reported: ν(O-H) 3400, ν(C-H) 2965 cm^{-1}, ν(C≡N) 2218 cm^{-1}, ρ(NH_2) 1624, ν(C=N_{ox}) 1462 cm^{-1}, ν(C-N-O) 1149 cm^{-}, ν(C=S) 875 for the $PbL_2 \cdot 3\ H_2O$ structure. No suitable for the X-ray analysis crystals were grown.

Decomposition appears to occur in the complexes with Pb^{2+} and the TCO^{-} anion rather quickly as the color darkens from a yellow gray to a very dark olive green over just a few days if compound is stored not under a protected environment, such as air-free and in a dark area.

V.2 Elemental Analysis

An elemental analysis (C, H, N) was conducted on 12 compounds from the series. In summary, four of the compounds matched the experimental values within ± 3% of the theoretical value, based on an expected PbL_2 product. These compounds are $Pb(2PCO)_2$, $Pb(PiCO)_2$, $Pb(TCO)_2$ from Reaction 6-1 and $Pb(TCO)_2$ from Reaction 14-1, and their preparation was already discussed in detail.

V.2.1 Pb(DCO)$_2$. The supposed "Pb(DCO)$_2$" compound did not match the analysis based on the PbL$_2$ formula. However, its analytical data did match to the crystal structure, Pb$_3$(OH)(NO$_3$)(DCO)$_4$, which was determined and is reported in the crystal analysis section. Thus, elemental composition is supported by the recalculated values seen in Table 11.

V.2.2 Pb(ECO)$_2$. The supposed "Pb(ECO)$_2$" compound did not match the elemental analysis data for PbL$_2$ composition, but the reported crystal data for the Pb-ECO system {K$_2$[Pb$_3$(AACO)$_4$(H$_2$O)]$_2$} does agree within the ±3% parameters. The recalculated theoretical (actual)(difference) elemental composition percentages are: C: 17.30%(18.49%)(+1.19%), H: 0.18%(1.57%)(+1.39%), N: 10.09%(8.42%)(-1.67%).

V.2.3 Pb(MeCO)$_2$. The expected for "Pb(MeCO)$_2$" elemental analysis composition did not match the PbL$_2$ formula. The Pb-MeCO system was checked to see if it had the same product as the Pb(ECO) product (explanation for hydrolysis of R-group is explained in the crystal data section) but was found not to match. A literature search on Ni^{2+} and H(MeCO) system reports multiple products to be found within that system [40]. Starting with those products, attempts were made to hypothesize a molecular formula. Utilizing the Chem Draw program to facilitate calculations, a probable product matched closely to the elemental analysis. Proposed structure for this system is K$_2$[Pb(AACO)$_2$](H$_2$O) and can be supported by theoretical (actual)(difference) elemental calculations of: C: 15.35%(15.48%)(-0.13%), H: 0.38%(1.52%)(-1.14%), N: 10.05%(10.68%)(-0.63%). The $AACO^{-2}$ is a dianion of hydrolyzed $MeCO^-$ and ECO^- cyanoximes. Hydrolysis reaction and structure can be seen in the Crystal Data section on page 78.

V.2.4 Pb(PiPCO)$_2$ and Pb(2PCO)$_2$ Reactions with Pb(C$_2$H$_3$O$_2$)$_2$ in Narrow Tube. Neither the Pb(PiPCO)$_2$ or the Pb(2PCO)$_2$ with acetate systems had an elemental analysis that

matched the PbL_2 formula. Although these ligand systems each produced single crystals, elemental analyses from the bulk powdery products did not match the composition of the crystal structure.

V.2.5 $Pb(BCO)_2$, $Pb(PyrCO)_2$, and $Pb(MCO)_2$. Obtained solids in these three systems did not match up to their expected PbL_2 composition. The crystals grown in these systems had no diffraction during an XRD analysis so no usable data could be collected. The possibility of $PbL_2 \cdot 4\ H_2O$ molecular formula was considered as the elemental analyses would support the composition. However, the thermal analysis shows no indication of water presence in the system. Neither IR-spectroscopic data have bands that would indicate O-H vibrations. Therefore, there are no hypothetical structures to present as the experimental data does not support them.

V.3 Crystal Growth of PbL_2

It was very important to grow single crystals for the crystal structure determination for these three systems to verify their compositions. In addition, we were still pursuing a structural investigation of the Pb^{2+} with other ligand systems regardless of the elemental analyses results. Studies of $Pb(ACO)_2$ in the past showed that recrystallization of the filtrate from the bulk synthesis produced useable crystals; therefore, filtrate recrystallization tubes were made for all 18 trials following the procedure in the experimental section. The products isolated were mostly light-yellow precipitates, yellow crystalline-like specimens, or clear crystalline-like specimens. Three different crystalline yellow specimens were found. The most attention was paid to yellow-colored crystals as they certainly contained deprotonated cyanoxime anions. Plates from

$Pb(PiPCO)_2$ and the $Pb(PiCO)_2$ system and a block shape crystal from the $Pb(MCO)_2$ system were tried on the diffractometer but did not produce any usable data.

The next approach used in attempt for quality crystals was crystal growth in the narrow tubes. Those were made using blowtorch and Pyrex tubes. Twenty-three tubes were set for crystal growth with starting material with either a 1:2 ratio or a 1:4 ratio of lead (II) ions to cyanoxime ligands. This proved to be the most successful procedure for growing and retrieving suitable crystals as every lead (II) cyanoximate that is characterized in this study were collected from a narrow tube. Crystals were harvested from the interior walls in both the aqueous layer and organic layer, but the most productive place was in the plug area. Two of the systems (ECO^- and $PiPCO^-$) produced suitable crystals from both the 1:2 and 1:4 systems and an XRD analysis determined that both systems produced the same crystals having the same unit cell. The systems containing Pb^{2+} and $2PCO^-$ anions produced five different complexes that were crystallographically characterized. Two came from the 1:2 system (also the 1:4 system) with the nitrate anion [$Pb_3(2PCO)_4(NO_3)_2$ and $Pb\{(H2PCO)_2(2PCO)_2\}$] and one from the 1:2 acetate system $\{Pb[(H2PCO)(2PCO)_2 \cdot H_2O\}$. Two different clear crystals (one block and one prism) were also retrieved from the Pb-nitrate systems. Both were found to be a form of commonly known hydroxo-nitrate $Pb(OH)NO_3$ hydrates and were dismissed as a side product. However, it should be noticed that the same compound was found and identified (through XRD analysis) in five different narrow tube systems: H(PiPCO), H(BCO), H(MCO), H(2PCO), and H(PyrCO). That means that $Pb(OH)NO_3$ is a common hydrolysis product in aqueous solutions regardless of the cyanoxime used. Overall, 16 crystals retrieved from narrow tubes were analyzed. Many of them were repeat structures since we have a total of 8 different crystal structures, 6 of which are

characterized and reported here as lead cyanoximates, and two side products have been identified before.

Without suitable crystals for several ligand systems the quest continued with vapor diffusion method for crystal growth and the use of the gel U-tubes. Six vapor diffusion tubes were prepared as explained in the experimental discussion yet after weeks and even months no retrievable crystals were observed so these systems were abandoned. Thus, for the lead (II) complexes this technique was considered to be unsuccessful. Ten gel U-shaped tubes were prepared as explained in the experimental section before. As stated earlier, one downside this technique is the difficulty to harvest grown crystals. Crystalline material could be seen in many of the tubes but were mostly destroyed when trying the remove them out of the wet silica gel on a filter paper. The gel, when exposed to air and fast drying, would create difficult conditions for removing the crystalline material without causing crystal damage. Regardless of these hardships there were two crystals isolated for XRD analysis. A clear plate from the $Pb(BCO)_2$ system produced a different side product that wasn't previously observed, Pb(OH)Cl, the result from a hydrolysis process. The chlorine atom originated from the hydrochloric acid that was used to acidify the gel during preparation. Overall, the U-tubes were a nice way to grow crystals but was not a productive crystal growing system for this study and did not provide any new insight into lead (II) cyanoximates. Some of the crystals that were harvested and analyzed can be seen in Figures 24-27.

In general, crystal growth in aqueous solutions proved to be a challenging task with Pb(II). It is known that lead typically coordinates with 3 or 4 atoms forming short bond lengths, but also can add four or five more donor atoms from other entities through longer contacts. The formula we were looking for—PbL_2—used throughout was based on this concept hoping that

two cyanoxime anions would form 4 bonds with metal center as seen before in the case of Pb(ACO)2 structure [2], and only one water molecule also bound to Pb(II). Many crystal growing techniques utilize organic solvents such as DMF, CH_3CN, picolines, pyridine, and others but these solvents were not used because they are known to be non-innocent, meaning they are able to bind to the lead centers causing "foreign" and unwanted molecules in the crystal structure. This would have defeated the purpose of trying to get compounds of "PbL_2" composition and would have led to mixed ligand complexes with high coordination numbers, which were not wanted in this study.

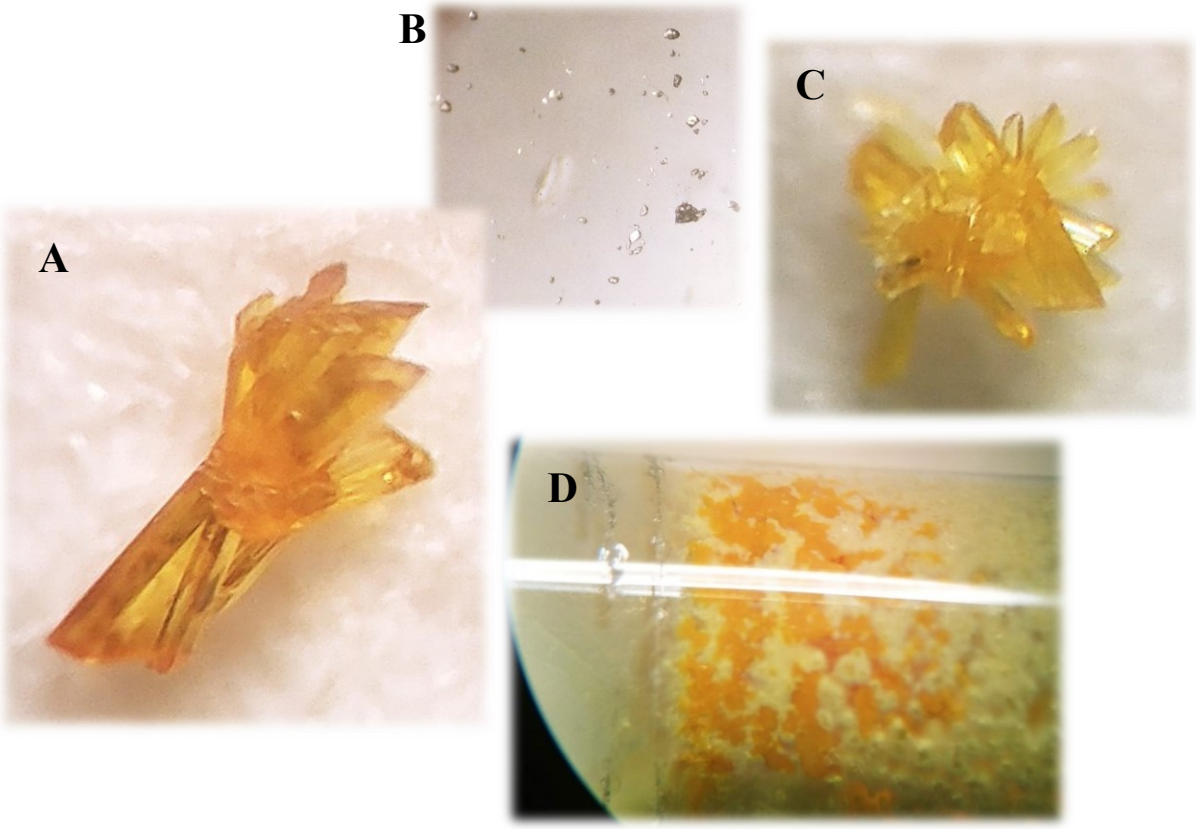

Figure 24. Crystals retrieved from the Pb^{2+} and $2PCO^-$ in narrow tubes.
A – $Pb[(H2PCO)_2(2PCO)_2]$; **B –** $Pb(OH)NO_3$; **C –** $Pb_3(2PCO)_4(NO_3)_2$; **D –** Crystals growing and lodged in the plug with molecular formula $Pb\{(H2PCO)(2PCO)_2 \cdot H_2O\}$.

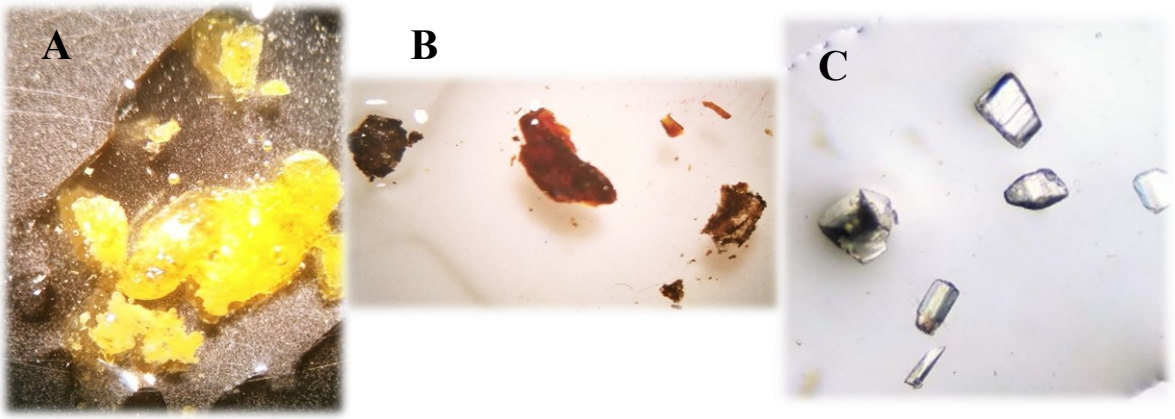

Figure 25. Crystals retrieved from various systems. **A –** $Pb(MCO)_2$ filtrate; **B –** $Pb(TCO)_2$ narrow tube; **C –** Pb(BCO) U-tube.

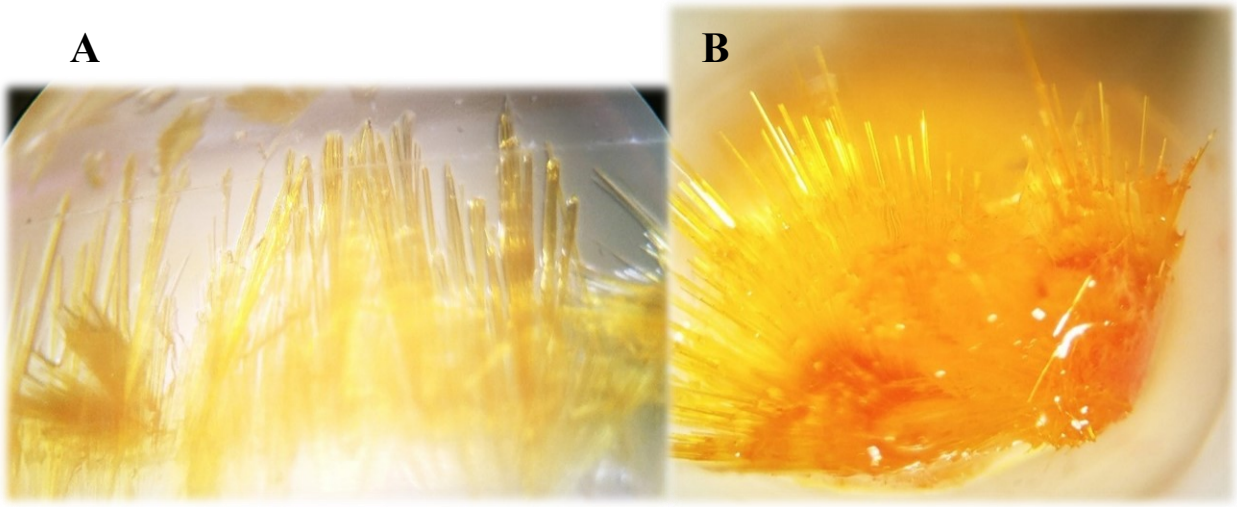

Figure 26. Crystals retrieved from the Pb^{2+} and DCO^- skinny tubes. Composition is $Pb_3(OH)(NO_3(DCO)_4$. **A –** Needles growing on the interior wall of tube; **B –** Sunburst-like needles after being removed from tube.

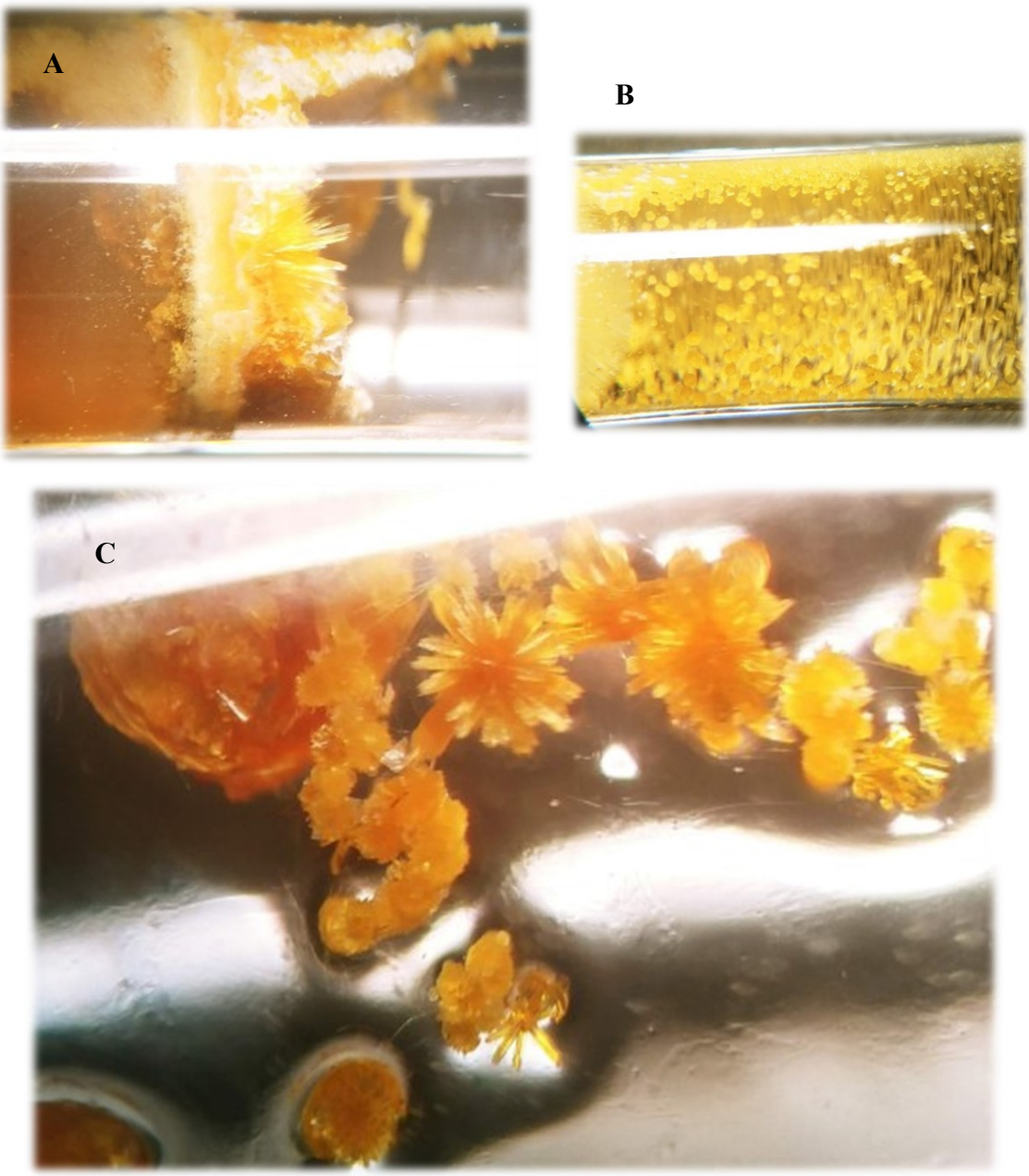

Figure 27. Crystals growing inside the 1:2 $Pb(PiPCO)_2$ mixture in the narrow tube. **A-** Needles and small blocks growing on the plug; **B -** Yellow blocks growing on the interior of the tube; **C -** Dark yellow plates growing on the interior side of the skinny tube with the composition of $Pb_4(OH)_3(NO_3)_2(PiPCO)_3(H_2O)$.

V.4 Attempts of Solid State Crystal Growth

V.4.1 Reaction in DSC/TGA Instrument. Two attempts were made with this method, one using H(2PCO) and the other using H(DCO) with PbO under Ar gas protection, and neither system were successful in obtaining suitable crystals. The rationale for this trial was to use an oxide of lead and weak acid, cyanoxime, in order to make clean neutralization reaction. Both PbO and the ligand were thoroughly mixed in agate mortar and loaded into the crucible. Both produced very dark and glassy amorphous solids in the crucible. Suspicious of the stability of the ligand, an analysis of the H(2PCO) ligand in a Digi-Melt was conducted to determine an appropriate temperature for the system. Observations showed the ligand quickly darkened followed by black precipitate in a reddish-black liquid in the capillary tube well before the documented melting point, 218° C. It became evident that the ligands were decomposing before they had a chance to react with the PbO. Therefore, we can conclude that heating these solids is not a suitable method for these compounds.

V.4.2 Reaction in Ampoules in Oil. These trials were being conducted alongside the reactions in the DSC-TGA instrument under Ar blanket. The same results were obtained—no suitable crystals or useable material. Ampoule 4-1, after removing from the hot oil bath, had product with a charcoal-like material. Examination under the scope revealed a few clear needle-like crystals which were assumed to be ligand. Ampoule 4-2 had a black carbon precipitate with a metallic glean at the bottom of the ampoule. At the top there were mustard colored needle-like growths, but it was obvious they were not crystalline. Ampoule 4-3, which had the ligand and lead oxide dissolved in the propionitrile solvent, resulted with a dark reddish-brown solution with black flecks floating in solution. The same conclusion was drawn, as in the other solid state crystal growth procedure, heating is not a suitable method for crystal growth.

V.5 Analysis of Single Crystals by X-ray Diffraction

In total, this study has identified and characterized six new lead (II) cyanoximates. Crystal structures of thiocyanoacetamide, $NC\text{-}CH_2\text{-}C(S)NH_2$, which we called (Pre-TCO), protonated thioamide cyanoxime (HTCO), and its salt Cs(TCO) have been studied and documented as well. Crystal analyses of these compounds can be found in Appendix A and the final checkCIF reports can be found in Appendix B. Six of the structures were refined in the MSU XRD lab where Dr. Gerasimchuk patiently taught me the basic principles of crystallography. Data collection for the other three structures was kindly performed by other crystallographers, Dr. Sergey Lindeman (Marquette University), Dr. Alex Filatov (University of Chicago), and by Dr. Jeanette Krause (University of Cincinnati) while our instrument was not operational due to breakdowns and cryosystem failure.

V.5.1 Crystal Structure of $Pb_3(OH)(NO_3)(DCO)_4$. The $[Pb_3(OH)(NO_3)(DCO)_4]$ complex crystallized as vivid yellow needles (Figure 28) in a triclinic system and P-1 space group. The crystal and refinement data are presented in Table 12.

Figure 28. Yellow crystals retrieved from the $Pb_3(OH)(NO_3)(DCO)_4$ system.

This compound has a framework which extends down the *a*-axis. The ASU contains three Pb(II) ion centers, all of which have a different environment, and four DCO ligands. The ORTEP representation is shown with atomic labeling (Figure 29) along with a molecular view identifying the ligands' numbering scheme and how the four cyanoxime anions are coordinated to the metal atoms. (Figure 30).

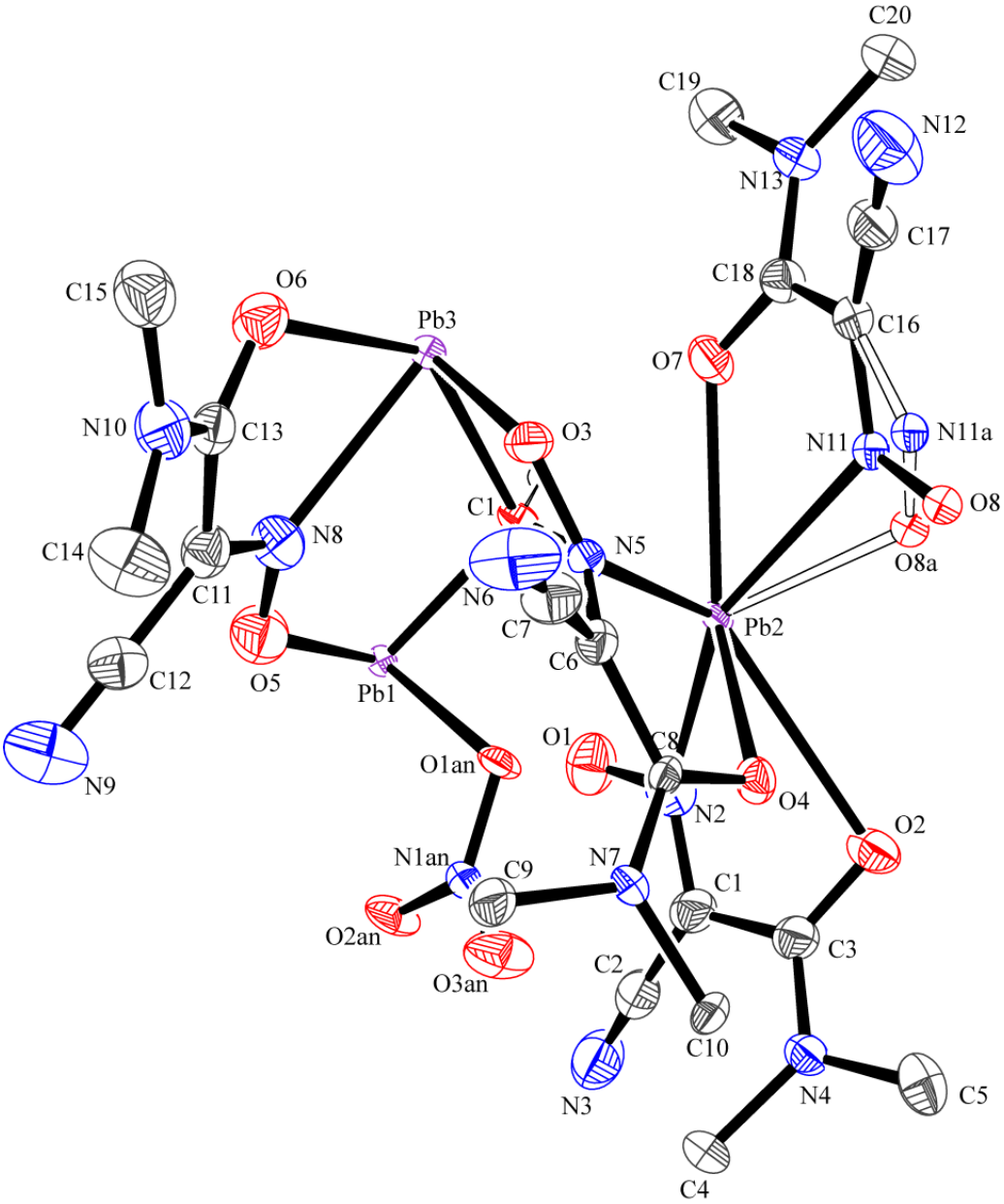

Figure 29. Molecular view of $Pb_3(OH)(NO_3)(DCO)_4$ in ORTEP representation showing atomic numbering scheme for the ASU.

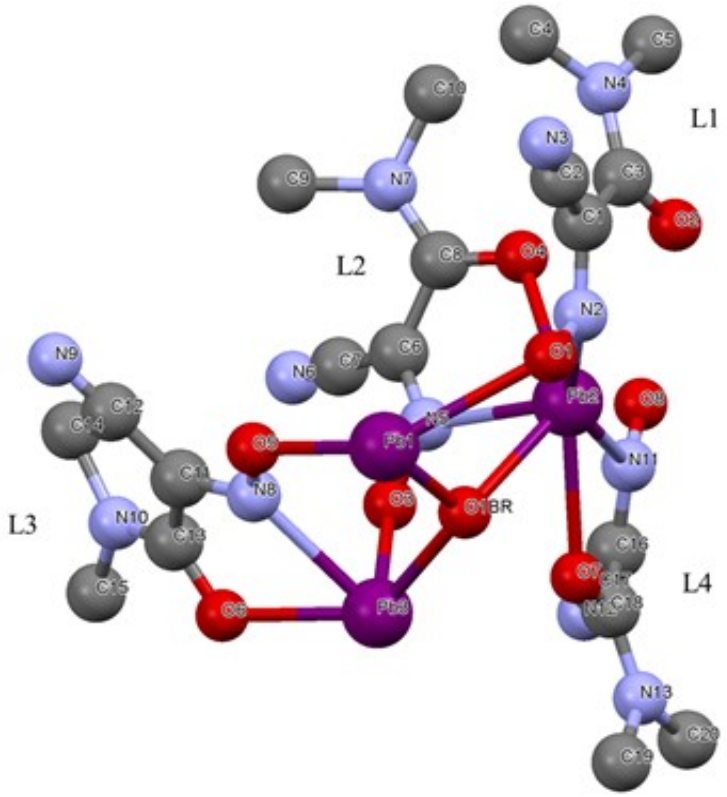

Figure 30. Molecular view of the compound showing ligands numbering. The nitrate anions and H-atoms have been omitted for clarity.

The main interest for us is the cyanoxime group. A comparison of the cyanoxime ligands in this compound was examined by analyzing the bond lengths and their planarity. The N-O bond

lengths ranged from 1.254 Å to 1.307 Å which indicates a sp(2) hybridized bond. The C-N bonds ranged from 1.328 Å to 1.366 Å which is representative of a longer bond. Thus, since the N-O bonds are shorter than the C-N bonds all four anionic ligands exhibit nitroso character.

The planarity analysis showed a general trend for L1, L3 and L4. Each ligand was mostly planar, and a mean plane was established through atoms of the -CN and -NO groups. Another mean plane could be easily viewed through the dimethyl amide group. The dihedral angles between these two planes for each ligand are 32.65º, 29.95º, and 37.74º respectively. The same

angle for L2 is significantly different. Both the amide and the dimethyl amino groups are not planar, as in the other three ligands, and has a dihedral angle of 18º between those two functional groups. In order to compare L2 to the other ligands, the cyanoxime plane was measured against the dimethyl amino group, which is 51.16º, which is much larger than that for the other three ligands.

All four of the DCO^- ligands form chelate rings via the nitrogen of the nitroso group and the oxygen atom from the dimethyl amide group. However, an interesting difference was found in L4 where the crystallographic data revealed co-crystallization of two different isomers: cis-anti and cis-syn (Figure 31). The cis-anti isomer forms PbNO five-membered ring, while cis-syn has PbO_2 in a six-membered chelation ring. This difference is only found in the Pb2 environment.

This coordination compound has three lead atoms in the ASU and each one has a different environment. The Pb1 has skewed square antiprismatic molecular geometry, a coordination number of 8, and has an active electron lone pair (Figure 32A). This lead center is interesting as it has no chelating ligands. All eight coordinating O-atoms are from eight different entities. These eight O-atoms are: L1 contributes twice with the nitroso group 2x (O1), the L2 contributes one amide atom (O4), the L3 is present by the nitroso (O5), with the L4 by the nitroso in cis-anti form (O8), two oxygen atoms from the nitrate anion (O1AN) and (O2AN), and a bridging oxygen from the OH group (O1BR) (Figure 32A). An active electron lone pair can be envisioned on the Pb1 center between O1-O1-O4-O2AN as evidenced by longer bond lengths between these oxygen atoms and metal center (2.730 Å to 2.928 Å) than the remaining oxygen atoms (2.323 Å to 2.691 Å). The larger angles recorded around these same coordinating oxygen

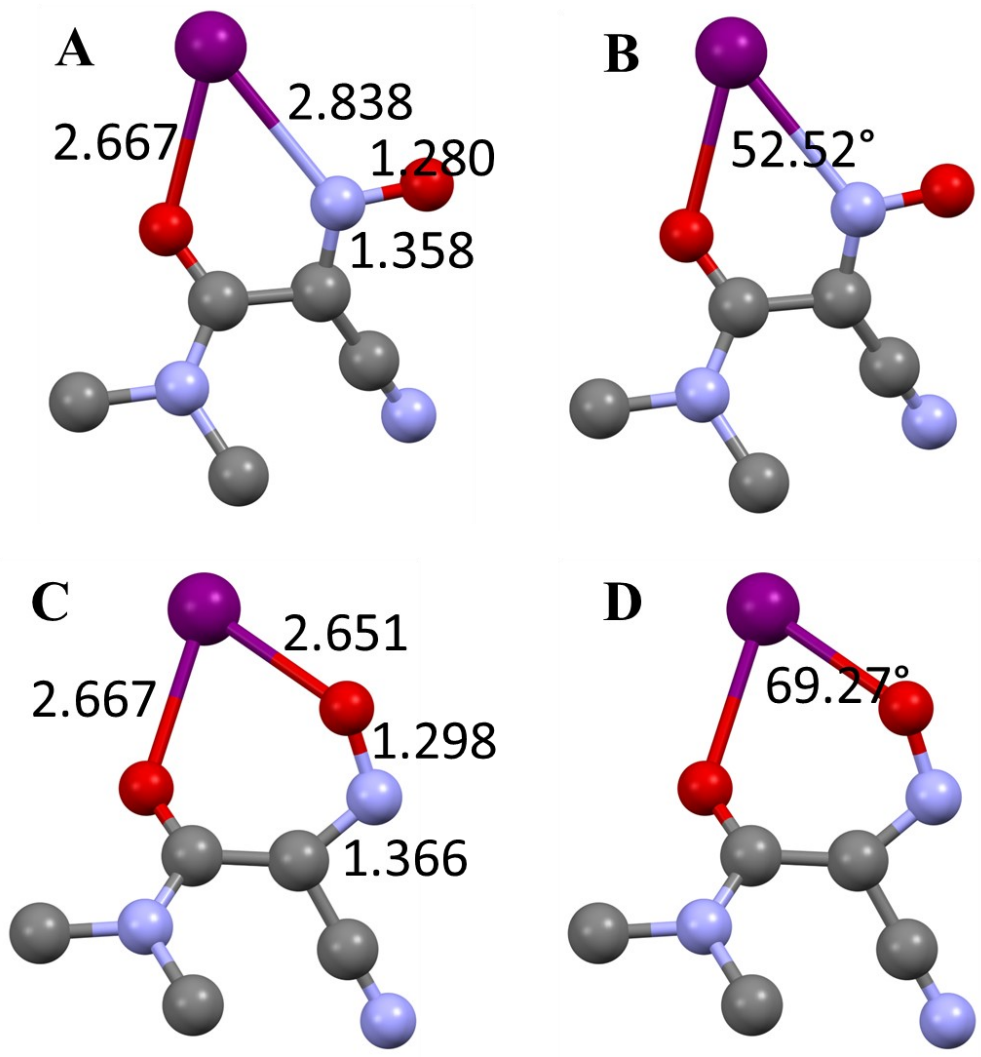

Figure 31. Molecular structures showing differences of two diastereomers of $Pb_3(OH)(NO_3)(DCO)_4$ structure at Pb2. **A** and **B** show bond lengths and bond angles, respectively, for the cis-anti form while **C** and **D** show bond lengths and bond angles, respectively, for the cis-syn form.

atoms and lead are also indicative of the presence of an active lone pair with large angles ∠O1-Pb1-O4 = 139.41º and ∠O1-Pb1-O2AN = 138.25º because of the electron repulsion.

A coordination number of eight is also found on Pb2 and has skewed square antiprismatic geometry with clearly inferred place for an active $6s^2$ lone pair. The lead atom is coordinated with an oxygen atom from the nitrate anion (O1AN), and oxygen atom from the bridging

hydroxy group (O1BR), and three chelating cyanoxime ligands. The L1 coordinates through O2 and N2, while L2 coordinates through O4 and N5 atoms (Figure 5C and 5D). As indicated earlier, Pb2 has two coordinated diastereomers of L4: cis-anti and cis-syn (Figure 30). The cis-anti diastereomer coordinates through O7 and N11 atoms and the cis-syn coordinates through O7 and O8A atoms. The "biting angles" of L1 and L2 are 76.21º and 63.09º respectively. In the cis-anti isomer, the nitrogen atom from the nitroso group and the oxygen atom from the dimethyl amide (same form as the other ligands) coordinates with the lead (II) and forms a five-membered ring with a "bite angle" of 52.52º. The cis-syn isomer, which possesses more nitroso character, based on the N-O bond length, forms a six-membered chelating ring between the oxygen atom of the nitroso group and the oxygen atom of the dimethyl amide group and has a "bite angle" of 69.27º (Figure 31). The $6s^2$ lone pair can be visualized in an open cleft between O2-N11-O4-N2. This opening can be seen in the bond angles ∠O2-Pb2-O4 of 138.83º and ∠N11-Pb2-N2 of 157.47º.

The third lead(II) atom in this compound has a skewed square pyramidal shape with a coordination number of five along with an active lone pair of electrons. The Pb3 is coordinated with one oxygen from the bridging hydroxy group (OBR), one oxygen (O3) from the nitroso-group in L2 and one oxygen atom (O8) from the nitroso group in L4 (Figure 32B). There is one "biting angle" of 62.76º with the oxygen atom from the amide (O6) and the nitrogen atom from the nitroso group from L3. The $6s^2$ lone pair can be found in an axial position on the lead above the equatorial atoms, O3-O6-O8-O1BR. With this type of geometry, we would expect to find the four equatorial atoms at a 90º angle from the axial atom (N8). The angles between the axial atoms and the equatorial nitrogen atom (N8) range from 62.76º - 78.43º, which reflects ionic

character of bonding in this complex. The three lead centers can be seen and compared together as displayed in Figure 32.

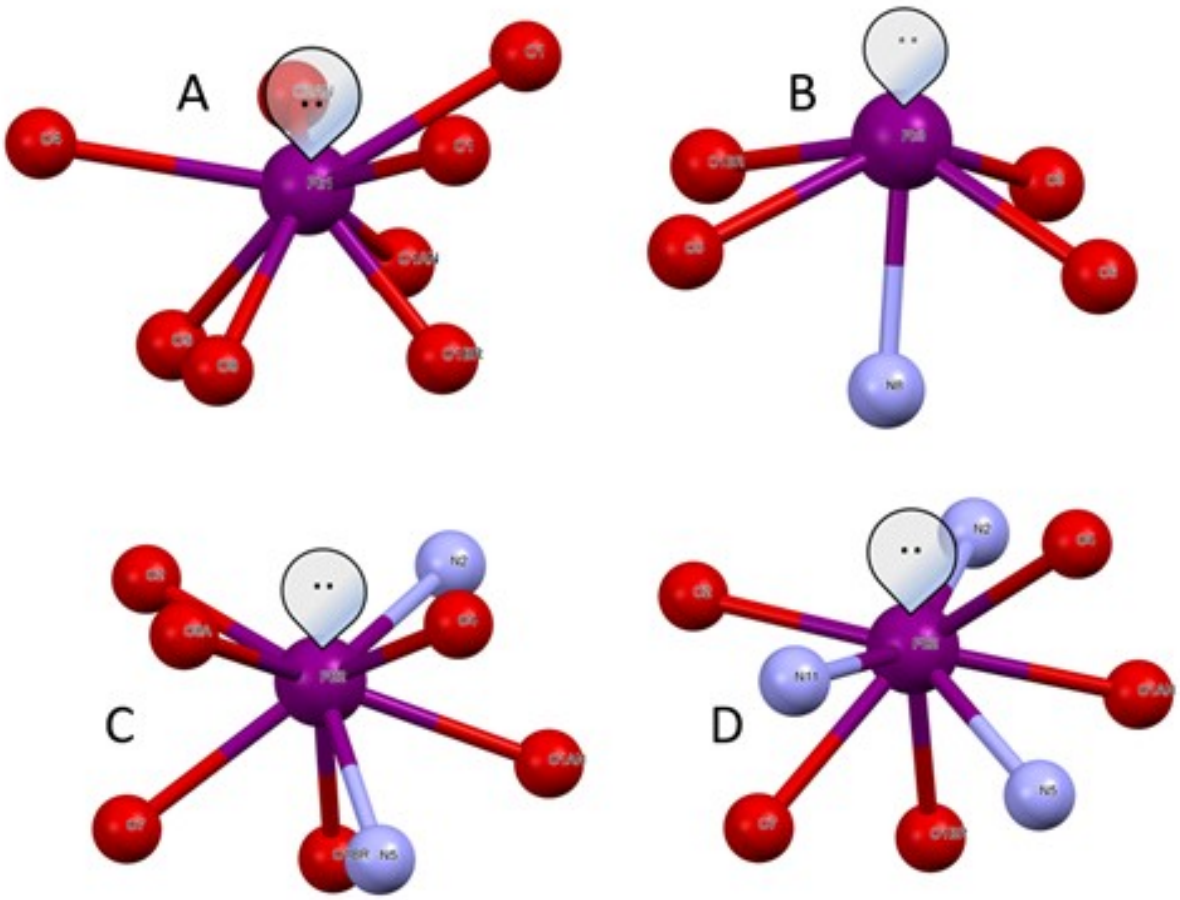

Figure 32. The lead centers comparison in the structure of $Pb_3(OH)(NO_3)(DCO)_4$: **A -** Pb1; **B -** Pb3; **C -** Pb2 cis-anti; **D -** Pb2 cis-syn.

An overall view of the metal atoms connectivity in the structure shows there are three different nitroso groups (one each from L1, L2 and L3) along with two bridging groups, a nitrate anion and μ^3-hydroxl group, that connects the three Pb centers. Metals environment also contains five different metallocycles: one 4-membered ring (Pb1-O1AN-Pb2-O1BR) and four 5-

membered rings [(Pb3-N8-O5-Pb1-O1BR), (Pb3-O1BR-Pb2-N5-O3), (Pb1-O1BR-Pb2-N2-O1), (Pb1-O1AN-Pb2-N2-O1)] (Figure 33).

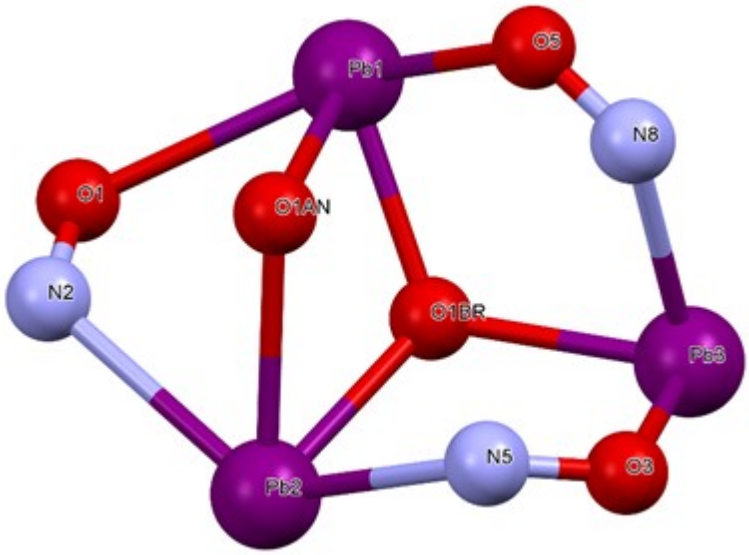

Figure 33. The connectivity of the three Pb(II) ions in the compound $Pb_3(OH)(NO_4)(DCO)_4$ showing formation of metallocycles.

Table 12. Crystal data and refinement of $Pb_3(OH)(NO_3)(DCO)_4$

Parameter	**$Pb_3(OH)(NO_3)(DCO)_4$**
Formula	$C_{20}H_{25}N_{13}O_{12}Pb_3$
F.W., g/mol	1261.1
Temperature	100(2)
Wavelength, Å	0.71073
Crystal System	Triclinic
Space Group	P-1
Unit Cell, Å/ ?	a = 7.9470(4) α = 92.001(2) b = 13.8353(7) β = 92.280(2) c = 14.6259(8) γ = 100.625(2)
Cell Volume, $Å^3$	1577.82(14)
Z	2
D (Calc), g/cm^3	2.654
Abs. μ (mm^{-1})	16.046
F(000)	1156
Cryst. Size, mm	0.010 x 0.060 x 0.280
θ Range, ?	2.76 to 29.66
Index Ranges	h: -11 to 8 k: -19 to 19 l: -20 to 20
Reflections Total	24702
Independent Refl.	8775 [R(int) = 0.0624]
Completeness, %	98.4
Absorption Method	Numerical
$T_{max.}$ / $T_{min.}$	0.8560 / 0.0940
D / R / P**	8775 / 302 / 451
GOF on F^2	1.032
Final R indices	I>2σ(I); R1 = 0.0439, wR2 = 0.0737
R Indices (all data)	all data R1 = 0.0798, wR2 = 0.0737
Largest Peak/Hole, e^- ($Å^3$)	2.627 / -2.212
Volume Taken, $Å^3$ (%)	1093.9 (69.3)
Dimensionality	1D

*-Refinement Method Full-matric least-sq. on F^2; **-listing of Data, Restraints and Parameters

V.5.2 Crystal Structure of $Pb_4(OH)_3(NO_3)_2(PiPCO)_3(H_2O)$. Suitable for x-ray analysis crystal was retrieved as a nice yellow block from a system with 1:4 ratio of ingredients. Complex crystallized in a monoclinic centrosymmetric system in $P2_{1/c}$ space group. The crystal and refinement data are displayed in Table 13. The final refinement contains some unmodeled electron density which is accounted for by disordered water molecules with less than 1 site occupied factor as the crystals were grown from an aqueous solution. It was determined to be a tetra-lead complex. Thus, the ASU is a tetranuclear lead (II) "cubane" type complex containing three deprotonated ligands (PiPCO), three hydroxyl groups, two nitrate anions and one water molecule. It should be noted that during the refinement process the three hydrogen atoms on the hydroxyl groups were objectively found on the electron density map while the other hydrogen atoms on organic PiPCO groups were attached. The ORTEP representation of the ASU is shown in Figure 34 while Figure 35 shows the connectivity and labels of the individual ligands in the structure.

An analysis of the principal fragments in this compound shows rather complex structure. All three of the $PiPCO^-$ anions act as chelating ligands via the oxygen atom from the amide group and the nitrogen atom from the oxime group bonding to one of the Pb(II) centers. The piperidine rings in all three coordinated ligands are in chair conformation. The *cyano* groups all remained linear and the "biting" angles of the three chelating ligands were similar at 56.43°, 60.87°and 59.97° respectively for **L1**, **L2** and **L3**. The cyanoxime anions have non-planar core. The values of the dihedral angles between the cyanoxime group and the amide group in the individual ligands are 29.66°, 43.91° and 37.93°. The **L1** possesses oxime character as the N-O bond (1.316 Å) is slightly longer than the C-N bond (1.314 Å). This anion chelates onto the Pb2 via the N1 and O2 atoms while the O2 atom also forms a bridge to Pb1 (Figures 34, 35). The O1

Table 13. Crystal data and refinement of $Pb_4(OH)_3(NO_3)_2(PiPCO)_3(H_2O)$.

Parameter	**$Pb_4(OH)_3(NO_3)_2(PiPCO)_3(H_2O)$**
Formula	$C_{24}H_{35}N_{11}O_{16}Pb_4$
F.W., g/mol	1562.39
Temperature	100(2)
Wavelength, Å	1.54184
Crystal System	Monoclinic
Space Group	P 1 21/c 1
Unit Cell, Å/ º	a = 16.2866(2) α = 90 b = 14.9728(2) β = 90.8176(13) c = 15.7834(2) γ = 90
Cell Volume, $Å^3$	3848.48(10)
Z	4
D (Calc), g/cm^3	2.697
Abs. μ (mm^{-1})	34.107
F(000)	2848
Cryst. Size, mm	n/a
θ Range, º	4.01 to 70.57
Index Ranges	h: -19 to 19 k: -16 to 18 l: -19 to 19
Reflections Total	35310
Independent Refl.	7291 [R(int) = 0.0599]
Completeness, %	98.8
Absorption Method	Multi-Scan
T_{max}. And T_{min}.	n/a
D / R / P**	7291 / 0 / 516
GOF on F^2	1.06
Final R values [I>2σ(I)]	R1 = 0.0447, wR2 = 0.1095
R Indices (all data)	R1 = 0.0490, wR2 = 0.1131
Largest Peak/Hole, e- $Å^3$	5.533 / -1.294***
Volume Taken, $Å^3$ (%)	2259.7 (66.5)
Dimensionality	2D

*Refinement Method Full-matric least-sq. on F2 ; **listing of Data, Restraints and Parameters

***Contains some random amounts of unaccounted and unmodeled electron density (water molecules)

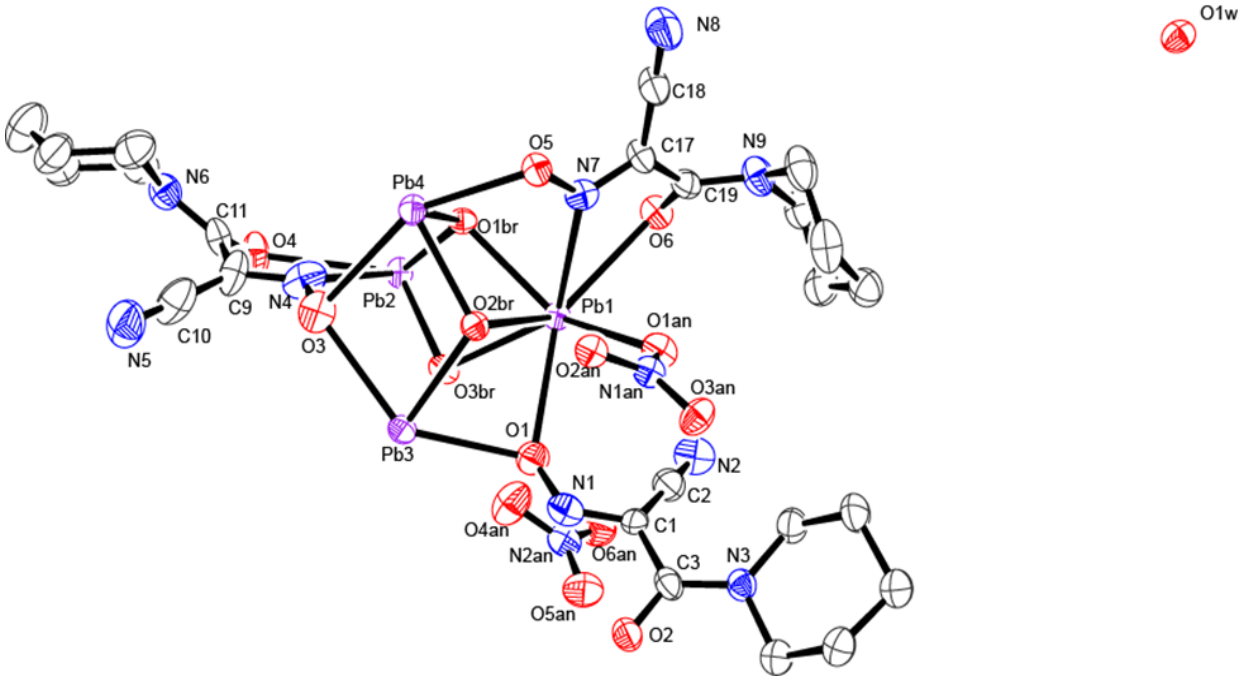

Figure 34. ASU of $Pb_4(OH)_3(NO_3)_2(PiPCO)_3(H_2O)$ showing atomic labeling and random water molecule. (H-atoms on oxygen could not be localized!)

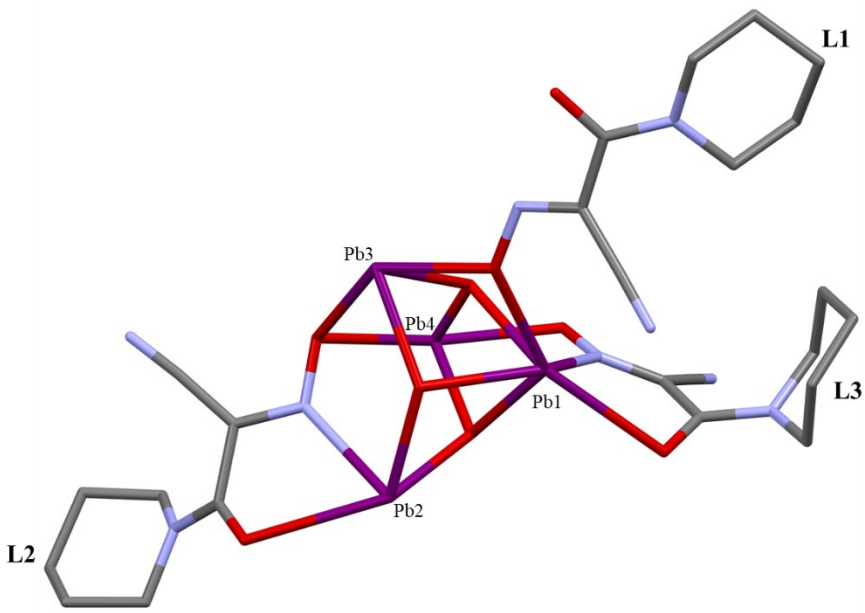

Figure 35. Capped stick representation of $Pb_4(OH)_3(NO_3)_2(PiPCO)_3(H_2O)$ showing the labeling and connectivity of the individual ligands to the lead centers in the ASU.

atom from the oxime group forms a μ^2-bridge with Pb1 and Pb3. The **L2** is in *nitroso* form, having a N-O bond length of 1.285 Å and C-N bond length of 1.370 Å, and acts as a chelator onto Pb2 as well. Here, the O3 atom (from the nitroso group) acts as a μ^2-bridge with Pb3 and Pb4. The last ligand, **L3**, is in oxime form with bond lengths very closely resembling **L1**. It acts as a chelator on Pb1 while the O5 atom from the amide group act as a μ^2- bridge between Pb2 and Pb4.

There are four different Pb(II) ions in this compound. The Pb1 has a coordination number of eight with a composition of its coordination polyhedron being $\{PbN_1O_7\}$. The geometry around this metal center is a distorted (compressed) cube and has an active $6s^2$ lone pair. Moreover, Pb1 has 5 short bonds ranging from 2.377 Å to 2.679 Å and 3 longer bonds (2.760 Å to 2.862 Å). The Pb1 has one chelating ligand (**L3**), three bridging hydroxyl groups, one bridging nitrate group, and two additional oxygen atoms from two separate L1 ligands, O1 from the oxime group and O2 from the amide group. The lone pair can be found in the cleft between O1an-O6-O2-O1. Evidence of this is due to the distortion of the polyhedron and the longer Pb-N, O bond lengths of nearby atoms. The Pb2 ion has a coordination number 7 with a composition of its polyhedron being $\{PbN_2O_5\}$. This metal center has also an active $6s^2$ lone pair. It can be found in the cleft between N1-O4-O5-O2, displaying capped trigonal prismatic geometry. It has two chelating ligands (**L1** and **L2**), an oxygen atom bond via the amide from **L3** and two other oxygen atoms from a bridging nitrate ion. The Pb3 also has a CN7 however there are no chelating ligands and has a composition of $\{PbO_7\}$. Two of the oxygen atoms are from the oxime/nitroso groups; one (O1) from **L1** and the other (O3) from **L3**. The other coordinated oxygen atoms are from a bridging nitrate anion (O2an and O3an), two bridging hydroxyl groups (O2br and O3br) and a water molecule (O1w). The stereoactive lone pair of

electrons can be easily located by the distorted pentagonal bipyramidal geometry and found in the cleft between O1w-O3-O3an-O3br. Lead center Pb4 has a CN=5 with a composition of it s coordination polyhedron being $\{PbO_5\}$. The Pb4 also has a stereoactive $6s^2$ lone pair, which can be observed in the cleft between O2br-O3-O4an-O5 and evidenced by the distorted square pyramidal geometry. The O3 atom is from the nitroso group found on **L2** and the O5 atom is from the oxime on **L3**. Two to the other oxygen atoms are from the bridging hydroxyl group and the O4 atom is from the nitrate anion. All four Pb(II) coordination centers and inferred positions of the active lone pair of electrons can be seen in Figure 36.

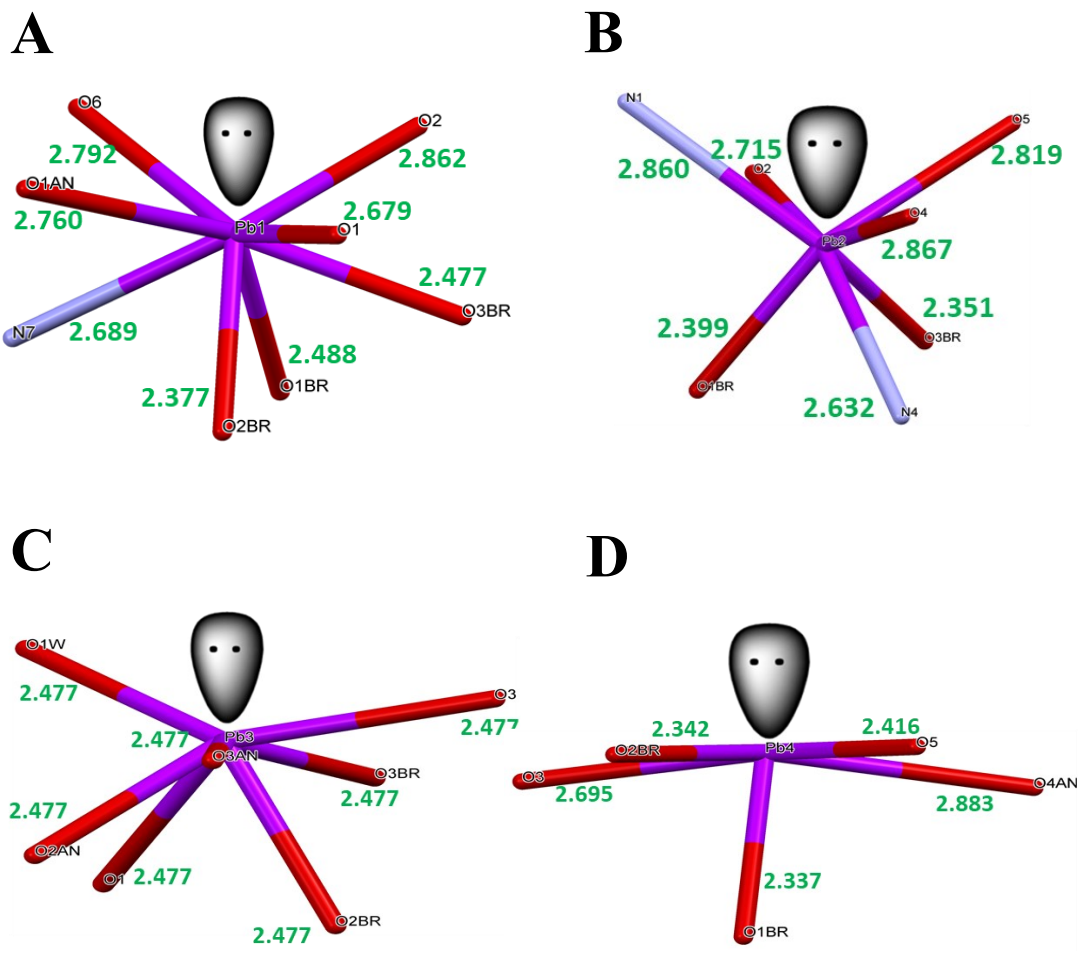

Figure 36. Lead centers of $Pb_4(OH)_3(NO_3)_2(PiPCO)_3(H_2O)$ showing atomic placement, bond lengths in Å, and the stereoactive lone pair location around each central Pb(II) ions . **A** – Pb1, **B** – Pb2, **C** – Pb3, **D** – Pb4.

An overall view of the metal atoms connectivity in the structure shows that there is a nitroso group (from **L2**) along with two bridging nitrate anions that connects the four Pb(II) centers in the coordination polyhedron appearing as a distorted "cubane" arrangement. Metal centers environments also contains six different metallocycles: four 4-membered rings [(Pb1-O1br-Pb4-O2br), (Pb1 O2br-Pb3-O3br), (Pb1-O1br-Pb2-O3br) and (Pb3-O3-Pb4-O2br)] and two 5-membered rings [(Pb2-O3br-Pb3-O3-N4) and (Pb2-O1br-Pb4-O3-N4)] as seen in Figure 37.

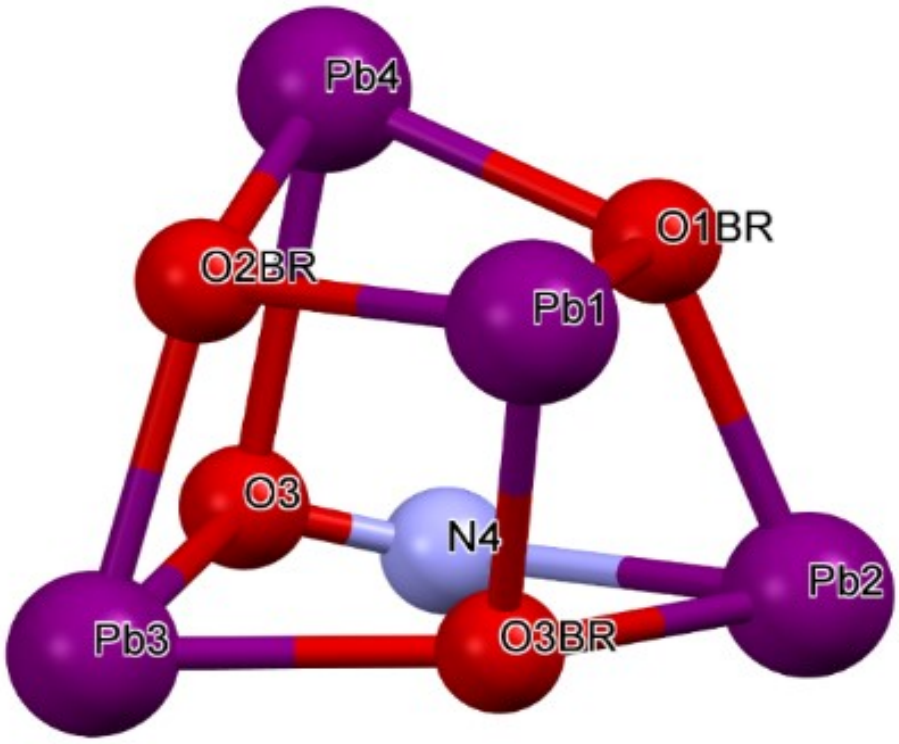

Figure 37. The connectivity in the $Pb_4(OH)_3(NO_3)_2(PiPCO)_3(H_2O)$ compound showing the four Pb(II) ions and the formation of metallocycles.

The crystal packing of this compound represents 2D-polymer that extends down the *b*-axis in one dimension and along its *c*-axis in second dimension as seen in Figure 38. Van der Waals interactions are responsible for holding these puckered sheets together to form the crystal lattice.

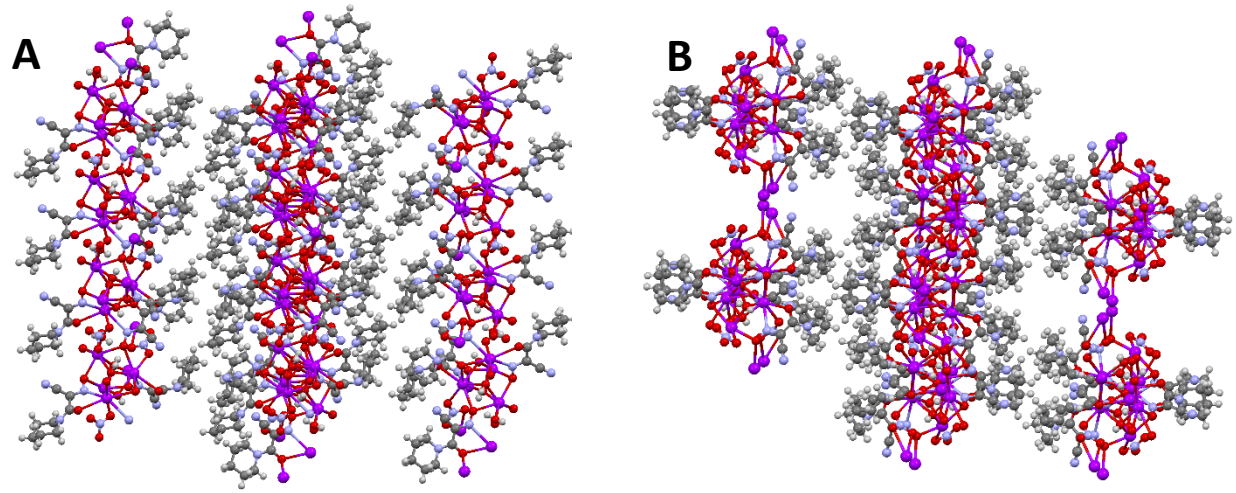

Figure 38. Crystal packing of $Pb_4(OH)_3(NO_3)_2(PiPCO)_3(H_2O)$. **A** – View down the *b*-axis; **B** – View down the *c*-axis.

V.5.3 Crystal Structure of $K_2[Pb_3(AACO)_4(H_2O)]_2$. The $K_2[Pb_3(AACO)_4(H_2O)]_2$ complex crystallized as transparent yellow blocks in a tetragonal crystal system and P4/mnc space group. The ORTEP representation of the ASU of this structure is shown with atomic labeling in Figure 39. This is a high symmetry space group; and in the unit cell there are 27 inversion centers, three mirror planes, 10 gliding planes, 13 two-fold axes, 12 two-fold screw axes and five four-fold screw axes (Figure 40). The ASU of this complex contains two non-equivalent Pb(II) ions, one $AACO^{2-}$ ligand and one potassium counter cation. There was found some residual electron density in the unit cell that could not be modeled in any other entity except disordered water molecule. Thus, it was assigned as an oxygen atom (O1w) occluded

water molecules in the structure since the preparation took place in an aqueous environment. The individual H-atoms could not be located due to the nearby presence of several heavy atoms (Pb and K). This compound forms a centrosymmetric 2D framework that extends along the *a*-axis and the *c*-axis. The crystal and refinement data are presented in Table14.

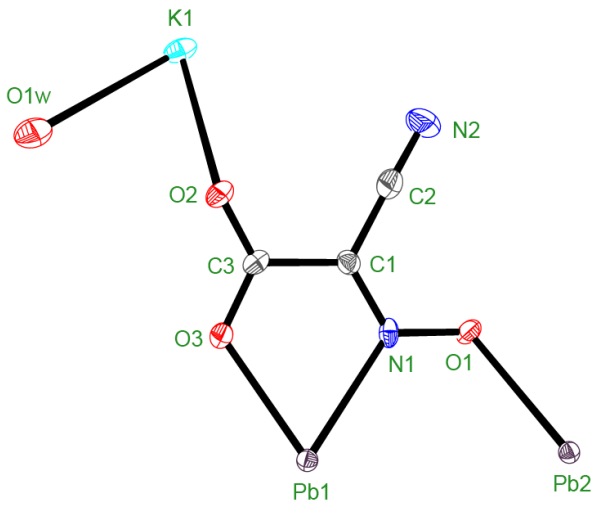

Figure 39. ORTEP representation of the ASU of $K_2[Pb_3(AACO)_4(H_2O)]_2$ showing the atomic numbering scheme with 50% thermal ellipsoids parameters.

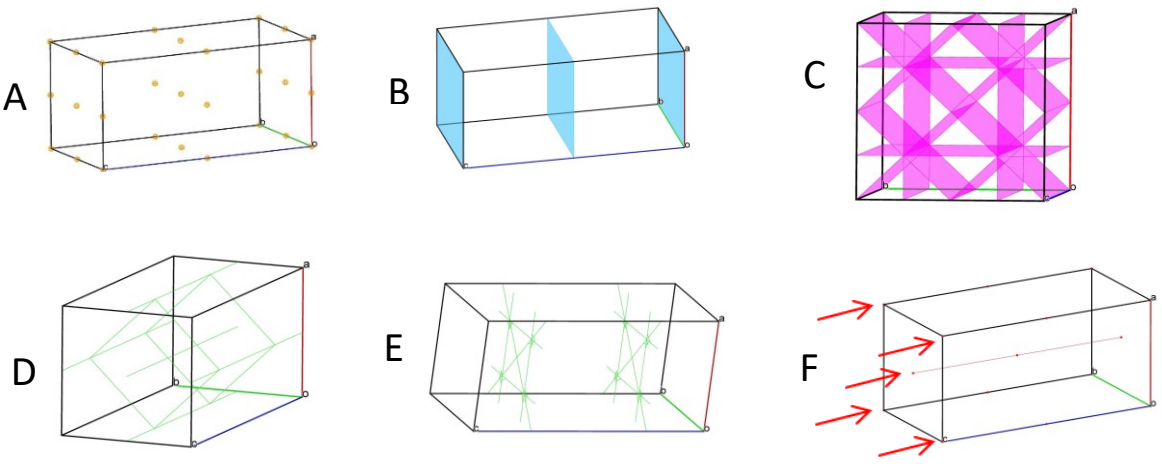

Figure 40. Dissection of symmetry elements for $K_2[Pb_3(AACO)_4(H_2O)]_2$. **A** - 27 inversion centers; **B** – 3 mirror planes; **C** – 10 gliding planes; **D** – 13 two-fold axes; **E** – 12 two-fold screw axes; **F** – 5 four-fold screw axes.

Table 14. Crystal data and refinement of $K_2[Pb_3(AACO)_4(H_2O)]_2$

Parameter	**$K_2Pb_3(AACO)_4 \cdot H_2O$**
Formula	$C_{24}K_4N_{16}O_{24.5}Pb_6$
F.W., g/mol	2304.57
Temperature	120
Wavelength, Å	0.71073
Crystal System	Tetragonal
Space Group	P4/mnc
Unit Cell, Å/ º	a = 10.7097(15) α = 90 b = 10.7097(15) β = 90 c = 21.490(3) γ = 90
Cell Volume, $Å^3$	2464.9(6)
Z	2
D (Calc), g/cm^3	3.1048
Abs. μ (mm^{-1})	20.857
F(000)	2007.6
Cryst. Size, mm	0.140 x 0.115 x 0.107
θ Range, º	3.8 to 52.66
Index Ranges	h: -13 to 13; k: -13 to 13; l: -26 to 26
Reflections Total	23259
Independent Refl.	1300 [R(int) = 0.0561
Completeness, %	100
Absorption Method	Numerical
T_{max}. And T_{min}.	0.7454 / 0.5450
D / R / P**	1300 / 0 / 90
GOF on F^2	1.002
Final R values [I>2σ(I)]	I>2σ(I); R1 = 0.0220, wR2 = 0.0523
R Indices (all data)	all data; R1 = 0.0282, wR2 = 0.0555
Largest Peak/Hole, e- $Å^3$	4.36 / -1.35
Volume Taken, $Å^3$ (%)	1873.7 (76.0)
Dimensionality	2D

*Refinement Method Full-matric least-sq. on F2 ; **listing of Data, Restraints and Parameters

The anion in this compound is a product of unintended hydrolysis of the ester group (OEt) in the HECO cyanoxime in the presence of KOH and Pb^{2+} ion. The formation of the $AACO^{2-}$ cyanoxime can be seen in Figure 41 and has been observed in past work with preparations of Pd^{2+} [33], Pt^{2+} [33], Cu^{2+} [40], and Ni^{2+} [40] complexes. After multiple attempts to combine Pb^{2+} with HECO and MeCO, (OMe), three different crystals from three different systems resulted with this hydrolyzed product. The $AACO^{2-}$ anion in this compound acts a chelator on Pb1 and as a bridging ligand to Pb2 ion in the ASU. The "biting" angle is 67.08º and is formed through the oxime N1 atom and the O3 atom from the hydrolyzed ester group. The NO^{-} group exhibits oxime character as the C1-N1 bond length is 1.299 Å and the N1-O1 bond length is 1.317 Å. The *cyano* group has a typical bond length of 1.146 Å between atoms C2-N2 and remains linear with angle C1-C2-N2 of 178.57º.

The unit cell structure is complex as the heavy atoms occupy multiple special positions. The potassium atoms occupy special positions in mirror planes and axes while the lead atoms occupy positions in gliding planes, inversion centers and multiple axes as well leading to a complex structure.

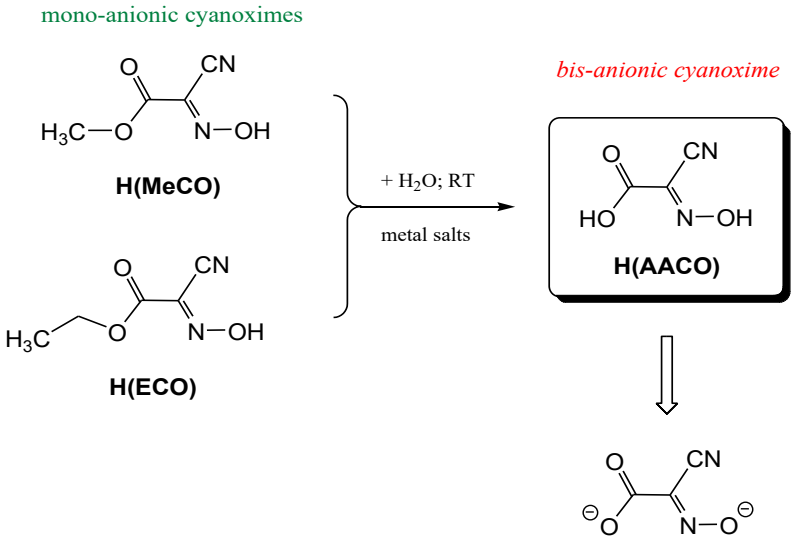

Figure 41. Formation of $AACO^{2-}$ via hydrolysis of the ester fragment.

The ASU has two different Pb^{2+} environments and both appear to have a stereoactive $6s^2$ lone pair of electrons. The Pb1 atom has two $AACO^{2-}$ anions, each chelating via the N1 and O3 atoms (biting angle of 67.08º). The Pb1-N1 bond length is 2.468 Å which is very close in distance to the Pb1-O3 bond length of 2.402 Å. There are two additional $AACO^{2-}$ ligands coordinating to Pb1 via the oxime oxygen atoms (O1) which have a bond length of 2.692 Å thus giving an overall coordination number of six. Viewing the geometry around this lead center it is easy to place the electron pair in a cleft above the Pb1 between the O1_1 and O1_2 as seen in Figure 42. (The numbering scheme with the underscored numbers identifies the two separate $AACO^{-2}$ anions from neighboring units). The angles between O1_1-Pb1-O1_2 and O3–Pb1–O3_3 are 168.54º and 137.66º respectively. Interestingly, the O1 and the O3 atoms both act as μ^2-bridges between Pb1 and Pb2 which are fundamental to the connectivity of the crystal lattice. There are eight of these bridging oxygen atoms coordinating to the Pb2 center (CN8) representing eight different $AACO^{2-}$ anions. Four are via the oxime oxygen atom (O1) and four coordinating via the ester oxygen atom (O3). The molecular geometry around Pb2 is a compressed Thompson's cube [3]. The four O3 atoms form one face of the cube and the four O1 atoms form a face opposite. The Pb2-O1 bond lengths are 2.567 Å and the Pb2-O3 bond lengths are 2.697 Å. In the cleft above the Pb2 and between the four O3 atoms is where the location of the lone pair of electrons. This assumption is made due to the elongated Pb2-O3 bond lengths and the "squished" shape of the cube (Figure 43).

The potassium ion plays a significant role in the elegant crystal packing of this compound. Two of the O2 atoms seen in contact with the potassium ion in the packed unit cell have a longer bond length than what is seen in the ASU (2.656 Å). This longer connection is 2.763 Å which is longer than an ionic interaction but much shorter than the Van der Waals radius which signifies

very strong intermolecular interactions. The K1-N2 bond length is 2.914 Å which offers significant stabilizing electrostatic connections for the unit cell as well (Figure 44).

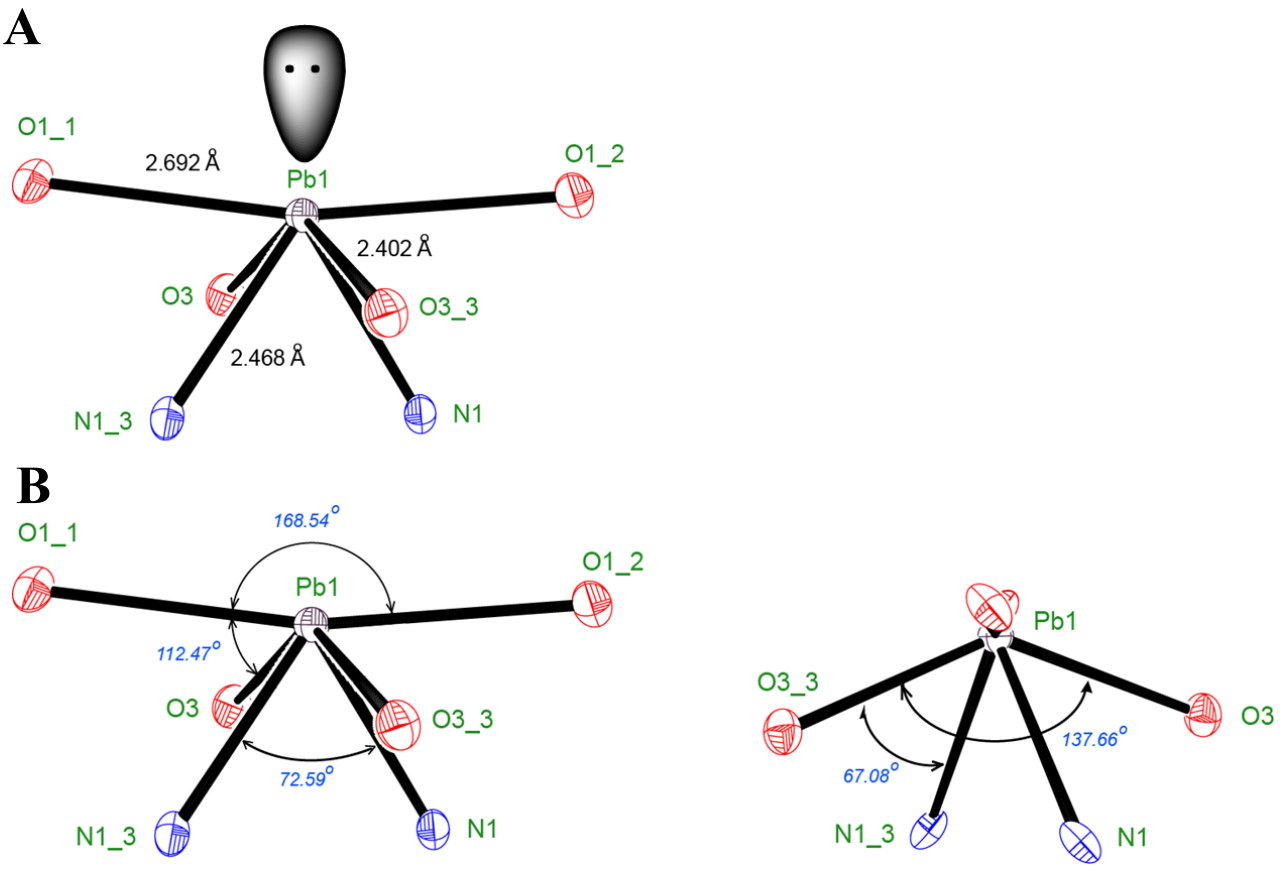

Figure 42. Details of the geometry of the $K_2[Pb_3(AACO)_4(H_2O)]_2$ complex at the Pb1 center. **A –** Bond lengths; **B –** Bond angles (orientation rotated by 180°).

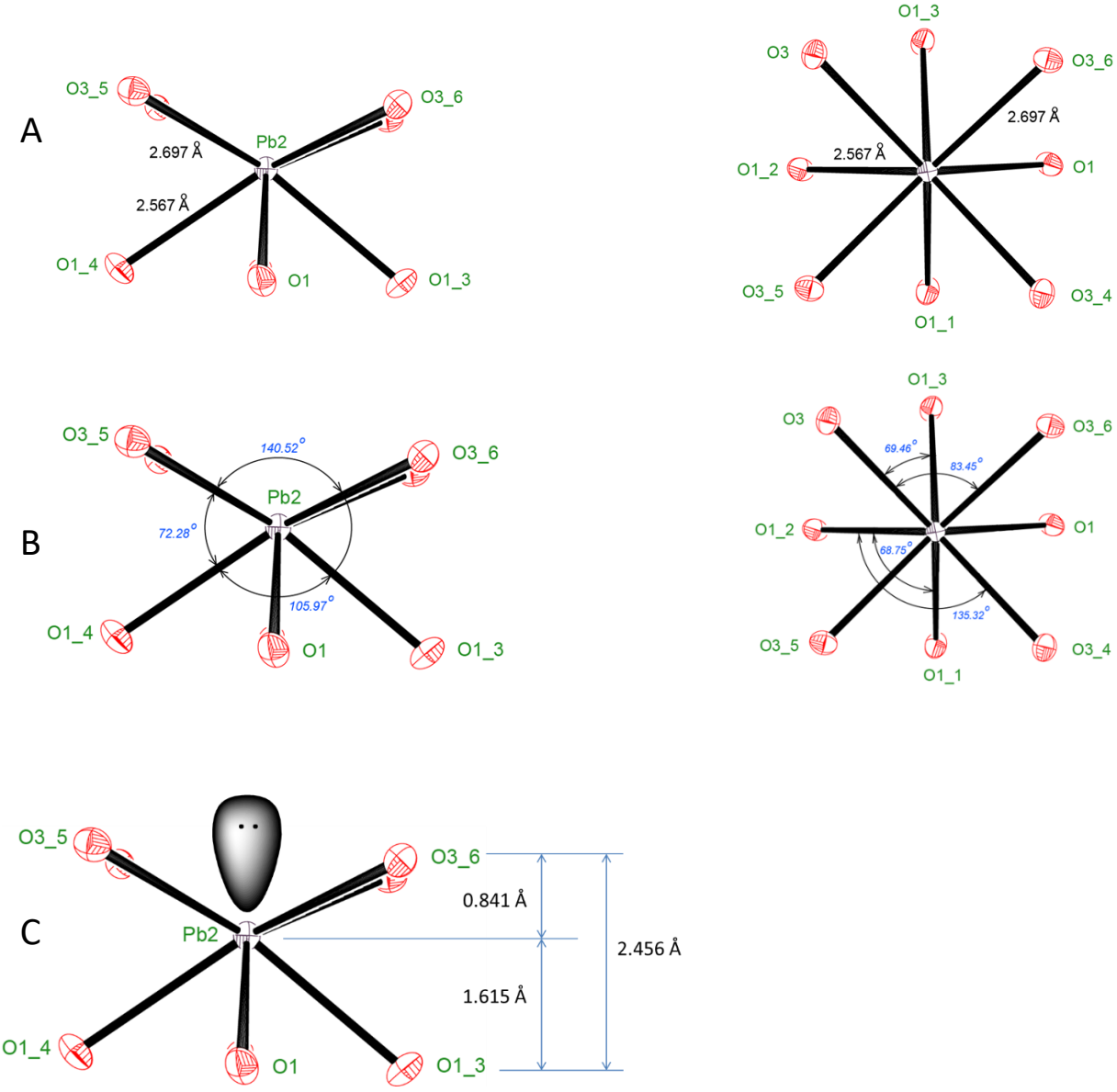

Figure 43. Details of the geometry of the $K_2[Pb_3(AACO)_4(H_2O)]_2$ complex at the Pb2 center. **A –** Bond lengths; **B –** Bond angles; **C –** Placement of the lone electron pair.

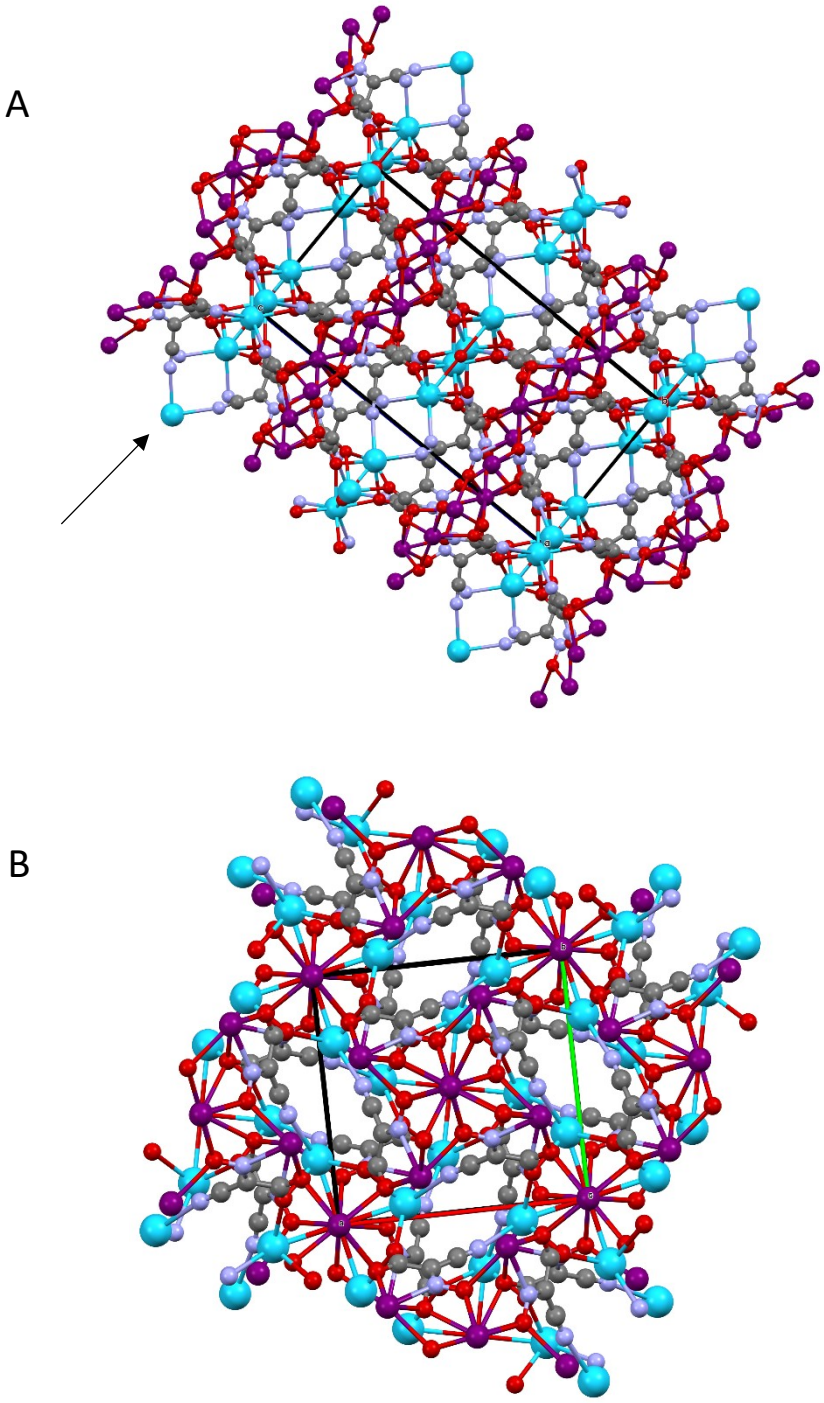

Figure 44. Crystal packing of the $K_2[Pb_3(AACO)_4(H_2O)]_2$ compound showing the heavy atoms occupying special positions in the unit cell as identified by arrow. **A –** view looking down the a-axis; **B –** View looking down the c-axis.

V.5.4 Crystal Structure of $Pb_3(2PCO)_4(NO_3)_2$. In the system containing Pb^{2+}, NO_3^- and $2PCO^-$ anions, three crystalline products were observed. These were $[Pb(2PCO)_2\{H(2PCO)_2\}]$, $[Pb_3(2PCO)_4(NO_3)_2]$, and $[Pb_4(OH)_4\{(NO_3)_2\}_4]$. The $[Pb_3(2PCO)_4(NO_3)_2]$ complex crystallized out as a small, transparent, and light yellow-colorless plate-like specimen in a triclinic system and centrosymmetric P-1 space group. Another specimen, albeit different looking, was a nice yellow prism that yielded the same unit cell at 100K and 270K and therefore was not fully characterized. The ASU of $Pb_3(2PCO)_4(NO_3)_2$ represents a trinuclear lead (II) complex with four chelating cyanoxime ligands and NO_3^- anions bound to lead. It forms a centrosymmetric lattice with a framework that extends down the *a*-axis. Bridging anions of $2PCO^-$ connect two units of the complex in a large centrosymmetric hexa-lead building block of the framework. The ORTEP representation of the ASU is shown with atomic labeling (Figure 45) along with a color-coded model to more easily visualize the placement of the ligands around the metal centers (Figure 46). Additionally, a molecular view of the formed dimer identifying the ligands' numbering scheme, and how the cyanoxime anions are coordinated to the metal centers, is presented in Figure 47. The crystal and refinement data are displayed in Table 15.

Selected bond lengths for principal fragments in this structure are found in Table 16 and Table 17. The analysis of the four $2PCO^-$ anions showed that every ligand performs both chelating and bridging functions. The chelation occurs via the nitrogen atom of the NO^- group and the nitrogen atom from the pyridyl group. The chelating "biting angles" are 62.78º, 62.09º, 62.29º and 63.27º for L1-L4 respectively. Two of the ligands (L2 and L4) are in *oxime* form and two are in *nitroso* form (L1 and L3) (Table 16). The bond lengths between the C-N and the N-O in the cyanoxime for L3 were very similar, however we suggest its nitroso-character on the grounds of shorter N-O bond which is in a good agreement with yellow color of studied

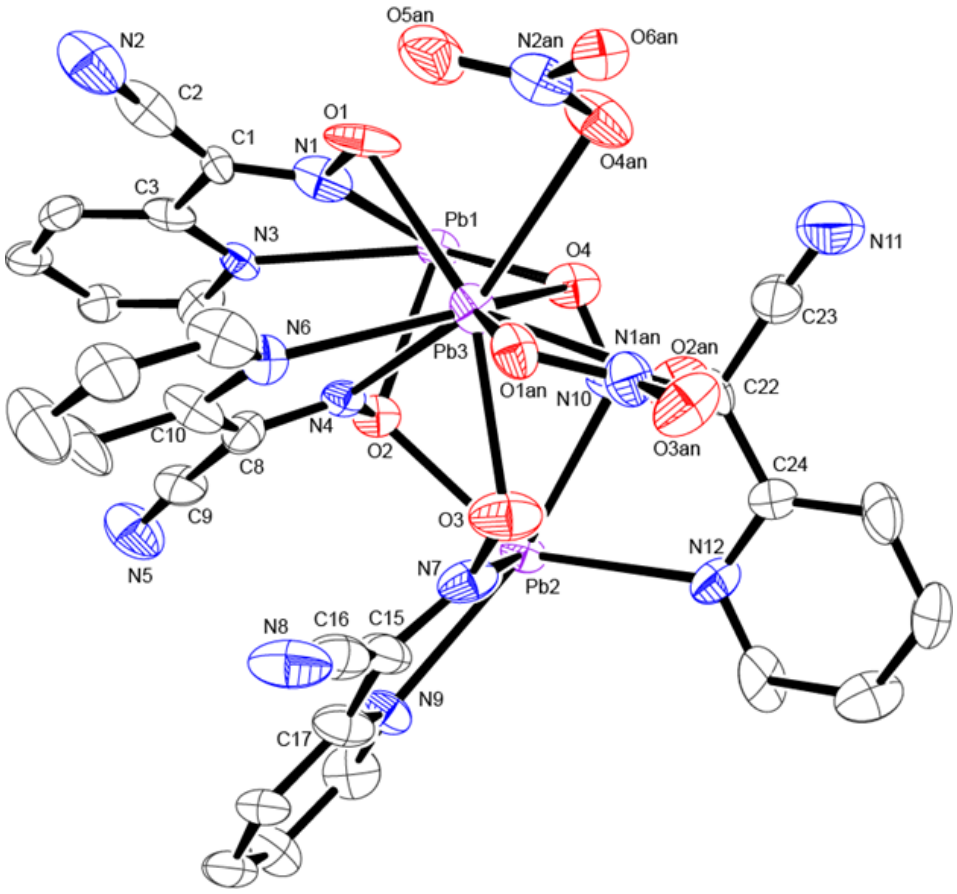

Figure 45. ORTEP representation of the ASU of $Pb_3(2PCO)_4(NO_3)_2$ showing the atomic numbering scheme with 50% thermal ellipsoids parameters.

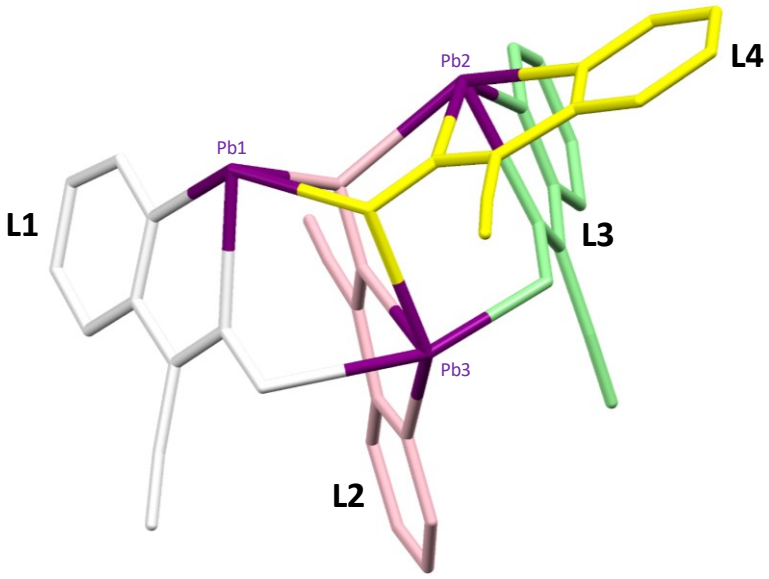

Figure 46. Atomic cap sticks representation of the ASU in the structure of complex $Pb_3(2PCO)_4(NO_3)_2$. Only lead (II) centers and $2PCO^-$ ligands are identified and color coded for visual clarity while nitrate anions and hydrogen atoms have been omitted for clarity.

Table 15. Crystal data and refinement of $Pb_3(2PCO)(NO_3)_2$

Parameter	**$Pb_3(2PCO)_4(NO_3)_2$**
Formula	$C_{14}H_8N_7O_5Pb_{1.5}$
F.W., g/mol	665.06
Temperature	100(2)
Wavelength, Å	0.71073
Crystal System	Triclinic
Space Group	P-1
Unit Cell, Å/ ?	a = 9.3579(13) α = 99.849(2) b = 14.038(2) β = 101.511(2) c = 14.627(2) γ = 107.829
Cell Volume, $Å^3$	1736.0(4)
Z	4
D (Calc), g/cm^3	2.545
Abs. μ (mm^{-1})	14.588
F(000)	1216
Cryst. Size, mm	n/a
θ Range, ?	1.57 to 26.38
Index Ranges	h: -11 to 11 k: -17 to 17 l: -18 to 18
Reflections Total	20680
Independent Refl.	7099 [R(int) = 0.0889]
Completeness, %	99.8
Absorption Method	Multi-scan
$T_{max.}$ / $T_{min.}$	0.7450 / 0.5150
D / R / P**	7099 / 0 / 496
GOF on F^2	0.966
Final R indices	I>2σ(I); R1 = 0.0497, wR2 = 0.1007
R Indices (all data)	all data R1 = 0.0935, wR2 = 0.1210
Largest Peak/Hole, e^- ($Å^3$)	4.239 / -2.226
Volume Taken, $Å^3$ (%)	1190.3 (68.6)
Dimensionality	1D

*-Refinement Method Full-matric least-sq. on F^2; **-listing of Data, Restraints and Parameters

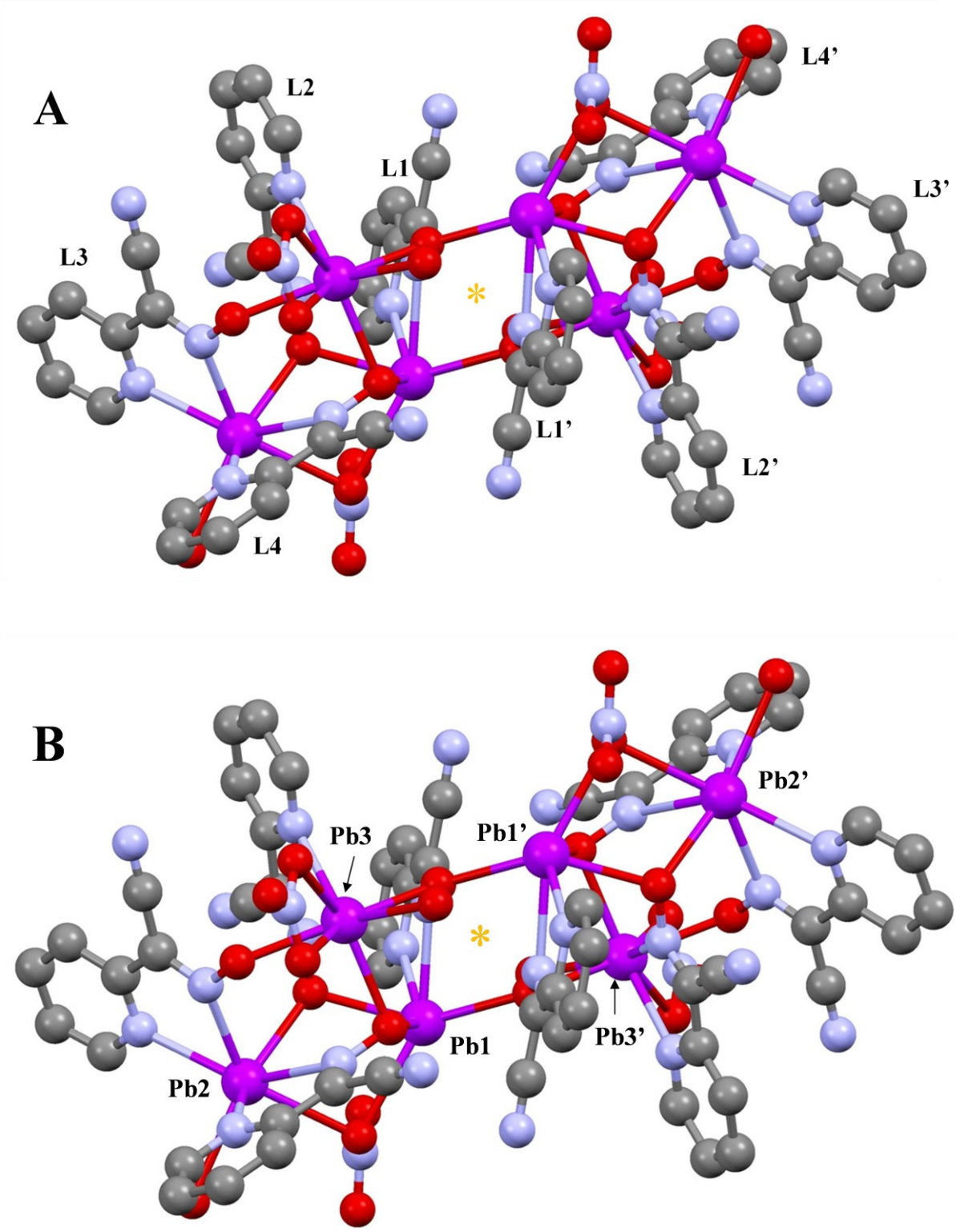

Figure 47. Two ASU joined into a centrosymmetric dimer. H-atoms are omitted for clarity. Asterisk shows inversion center in this structure. **A -** labeling scheme for oxime ligands; **B -** labeling scheme for metal centers with primes (‘) indicating symmetry related moieties.

Table 16. Selected bond lengths and angles for the oxime fragments in the $2PCO^-$ anions in $Pb_3(2PCO)_4(NO_3)_2$.

Ligand	Bond	(Å)	"Biting" Angle	(°)
L1	N1-O1	1.299	N1-Pb1-N3	62.78
	C1-N1	1.308		
L2	N4-O2	1.344	N4-Pb3-N6	62.09
	C8-N4	1.308		
L3	N10-O3	1.283	N7-Pb2-N9	62.29
	C15-N10	1.347		
L4	N7-O4	1.324	N10-Pb2-N12	63.27
	C22-N7	1.318		

Table 17. Selected bond lengths and angles for the *cyano* fragments in the $2PCO^-$ anions in $Pb_3(2PCO)_4(NO_3)_2$.

Ligand	Bond	(Å)	Angle	(°)
L1	C2-N2	1.125	C1-C2-N2	174.88
L2	C9-N5	1.155	C8-C9-N5	176.19
L3	C16-N8	1.156	C15-C16-N8	174.61
L4	C23-N11	1.135	C22-C2N11	176.19

complexes. The latter is a clear indication of the nitroso-, not oxime- character of the anion since coordinated oximes are normally colorless. (41) As earlier stated, the NO-group in all four ligands perform as a bridging group connecting the three metal atoms in the structure. In addition, the O-atoms in L1 and L3 (which are in the *nitroso* form) perform as a μ^1-bridge between metal atoms while the O-atoms in L2 and L4 (which are in the oxime form) perform as

a μ^2-bridge and are fundamental to the connectivity of the crystal lattice. The individual ligands appear planar but have a slight dihedral angle between the heterocycle and the cyanoxime group. The ligands with oxime character (L2 and L4) have the smallest angles which are 3.78º and 0.59º respectively. The ligands with nitroso character (L1 and L3) have slightly higher angles at 5.38º and 4.04º. The cyano groups are linear with the C – C – N angles being between 174.19º - 176.19º and the C-N bond lengths ranging from 1.125 Å to 1.156 Å which are typical organic nitrile bond lengths.

All three of the lead atoms present in this compound have different environments and different coordination numbers making this structure quite complex and interesting at the same time (Figure 48). Additionally, two of the lead ions have a clearly inferred place for an active $6s^2$ lone pair of electrons while the third lead center does not. An analysis of each metal center shows that Pb1 has a coordination number of six with a composition of its polyhedron being $PbN_2O_4\{O_2\}$. The L1 has an interesting function being bound to this metal center. It has the typical "biting angle" on the metal center (Pb1) via N1 and N3, but the oxygen atom from the nitroso group (O1) forms a μ^1-bridge from one ASU to Pb1 in a neighboring unit thus forming the dimeric compound (Figure 49). The O2 and O4 (oxime) atoms on the Pb1 metal center come from the μ^2-bridge from L2 and L4 with bond lengths of 2.463 Å and 2.492 Å respectively. The O6AN_2 atom (Figure 48-1A) comes from one of the bridging nitrate anions and it occupies an axial position within the distorted octahedral shape around this lead (II) ion. The N3, O2, O4 and O1 take the equatorial positions around the central metal atom, leaving the N1 atom in the other axial position. Analyzing the bond angles, it is facile to locate the $6s^2$ lone pair of electrons in the cleft between atoms O6AN_2 - N3 - O1 as depicted in Figure 48-1B. In this same part of the structure, two long electrostatic contacts can be identified from the O5AN_2 atom (2.975 Å)

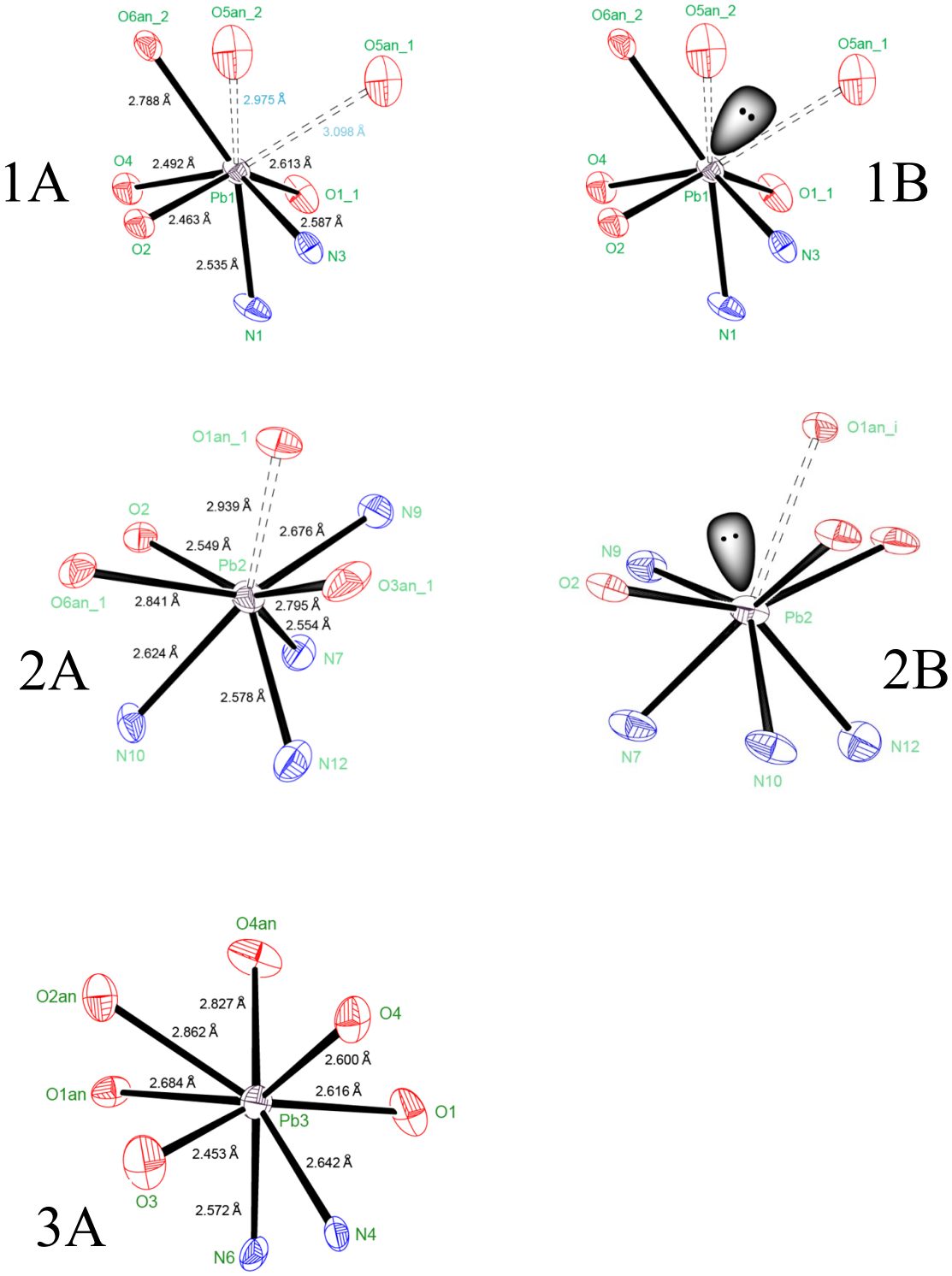

Figure 48. ORTEP representation at 50% ellipsoid of the bond lengths and location of the active 6s2 lone electron pair at the three lead centers in Pb3(2PCO)4(NO3)2. **1 A/B –** Pb1 with two long electrostatic connections represented with dashed lines. **2A/B –** Pb2 with one long electrostatic connection represented with dashed line. **3A –** Pb3

and O5AN_1 atom (3.098 Å) to the metal center Pb1. These atoms come from two different bridging nitrate anions as indicated by the underscore numbers in their labels. Overall, this lead center has a coordination number of eight when these electrostatic connections are included. The Pb2 has an active lone pair, a coordination number 7 and has a long contact with a bridging nitrate anion (O1AN) making its environment as PbN4O3{O}. This long contact and suggested place for the $6s^2$ lone electron pair can be found on the lead (II) ion in the cleft between the O3AN – N9 – O2 – O6AN atoms (Figure 48-2B). Its presence is more evident here on the Pb2 than on Pb1 atoms. This lead center has a classical hemidirectional central atom. The coordinating to metal atoms can easily be divided into two groups: short bond lengths (2.549 Å to 2.676 Å) and long bond lengths (2.795 Å to 2.939 Å). The angles between these long bonds (142.8º to 149.25º) are also greater as the electron repulsion distorts the geometrical prism with base 4 and skewed face 3 atoms. Amongst the shorter bonds, L3 and L4 are found chelating to Pb2 with "biting angles" of 62.29º and 63.27º respectively. The last lead (II) center in this compound, Pb3, has a coordination number of eight and no active $6s^2$ lone pair of electrons. The shape around the metal center is a distorted Thompson cube of PbN_2O_6 composition with base 4 and skewed face 4 atoms. There is only one chelating ligand, L2, with a "biting angle" of 62.09º (Figure 48-3A). Three of the coordinating atoms are oxygen atoms from the nitroso/oxime group from L1, L3 and L4 with bond lengths of 2.616 Å, 2.453 Å and 2.600 Å therefore all four of the $2PCO^-$ anions are coordinated on Pb3. The three remaining coordinating oxygen atoms are from the bridging nitrate anions where O1AN and O2AN are located on the same nitrate anion while O4AN is from the second nitrate anion.

In summary, the $2PCO^-$ anions act in described here complex as bridging the three lead (II) ions together (Figure 50). It should be noted that in transition metal complexes the $2PCO^-$ anion

does not act normally as bridging ligand [42]. All four ligands are present in the connectivity via the -NO^- functional group. The two nitrate anions in this unit cell act as tridentate bridges and have different bridging connectivities in the structure. The N1AN centered anion acts as a chelator on Pb3 and has a single contact to Pb2 atom. The N2AN centered anion bridges O4AN to Pb3 while O6AN is a μ^{-2} bridge between Pb2 and Pb1. The later bridge forms a four membered rhombohedron metallocycle (Pb2-O2-Pb1-O6AN) in this structure. Three additional metallocycles are: 2 – five-membered puckered rings (Pb2-O6AN-Pb1-O4-N10) and (Pb3-O1-N1-Pb1-O4), and 1 – six-membered puckered ring (Pb2-N7-O3-Pb3-O4-N10). Where the N1AN plays a key role in the connectivity of the lead ions, the O5AN atom from the N2AN nitrate anion has a distance of 2.532 Å to H7, which is shorter than the van-der-Waals radius, offering a stabilizing electrostatic contact to L1. There are multiple other intermolecular forces and hydrogen bonding responsible for the packing of this crystal lattice (Figure 51).

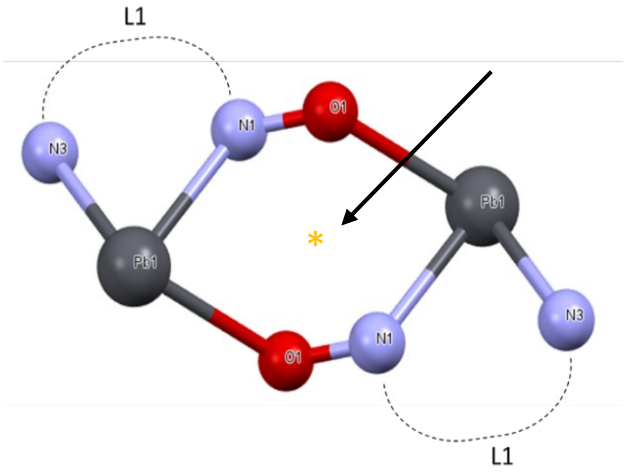

Figure 49. Pruned view of the dimeric center showing the bridging oxygen atoms from two ligands (L1). Inversion center of symmetry can be found in the center of the 6-membered metallocycle at the asterisk (*) and is highlighted by arrow.

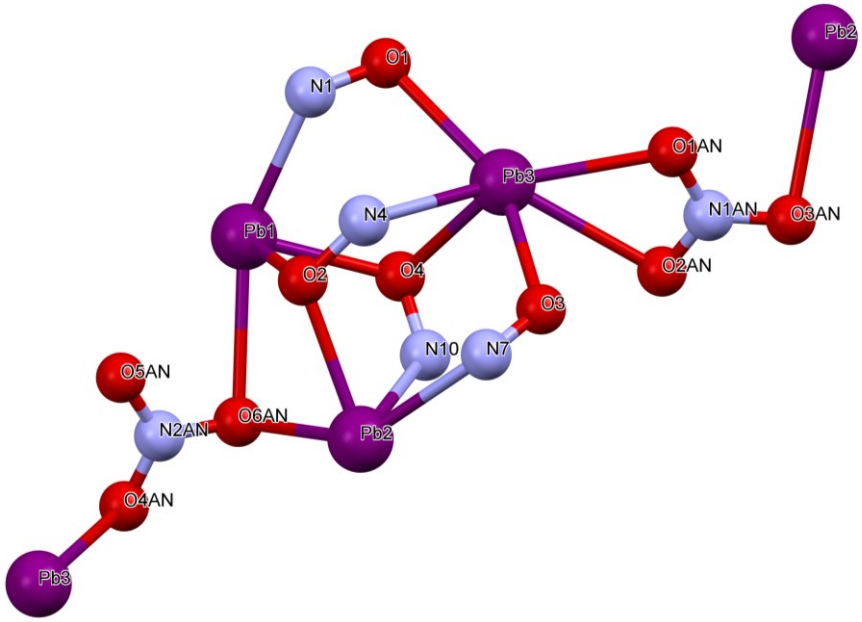

Figure 50. Molecular connectivity of metal centers showing the role of the oxime/nitroso groups the nitrate anions in assembly of the Pb-framework.

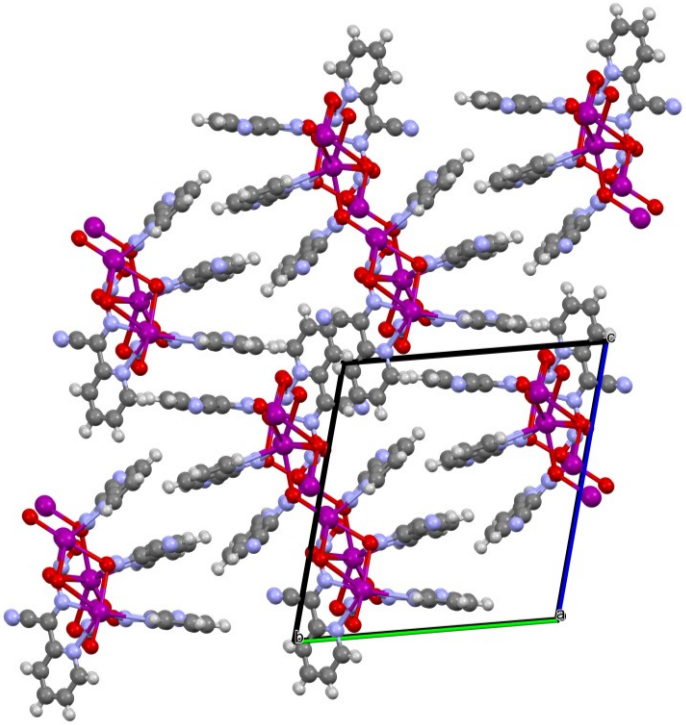

Figure 51. Crystal packing of $Pb_3(2PCO)_4(NO_3)_2$ showing extension down the *a*-axis.

V.5.5. Crystal Structure of Pb{(H2PCO)(2PCO)$_2$ · H2O}. This compound crystallized out of a lead acetate and ligand (H2PCO) mixture in a mini tube. Crystals grew as a clear light yellow rod-shaped crystal in a monoclinic system and a centrosymmetric P 2_1/n space group. The ASU is a mononuclear lead (II) complex containing one protonated ligand (H2PCO), two deprotonated ligands $(2PCO)^-$ and one water molecule. The overall building block for this framework is a dimer which is created as one of the $2PCO^-$ anions acts as a bridge connecting two asymmetric units of the complex into a centrosymmetric di-lead building block. The ORTEP representation of the ASU is shown with atomic labeling in Figure 52 while Figure 53 shows the dimer connectivity with the individual ligands labeled. The actual formula of this compound is $Pb_4C_{84}H_{52}N_{36}O_{14.29}$ as opposed to the reported unit formula of $PbC_{21}H_{13}N_9O_3$. The O1w and O2w oxygen atoms, which come from disordered water molecules, have site occupancies of 0.36 and 0.25 which is significant and must be accounted for. The H-atoms of those water molecules could not be found or attached to hosting O-atoms due to a very large electron density of 2Pb centers versus 4H atoms. This discrepancy can be justified as the oxygen atoms are in close proximity to a 2-fold rotation axis. Because of this, they were assigned as non-stoichiometric moisture (H_2O). Both O-atoms form an adduct to one of the 2PCO rings in the structure, presumably through H-bonding, and can be viewed in a void, shaped like a channel, extending in the *b*-direction of the unit cell. This water was trapped internally during crystal formation as this reaction took place in an aqueous environment. Once more, the hydrogen atoms of the water could not be found since they are of a disordered nature. The crystal and refinement data are displayed in Table 18.

An analysis of the three principal fragments in this compound shows an interesting structure of this complex. All of the $2PCO^-$ anions act as chelators on the Pb(II) center yet each

one slightly varies in chelation or whether the ligand is in its protonated or deprotonated form (Figure 54). One of the fragments in this structure has never been seen in it's said orientation and will be introduced here. The first ligand (L1) is considered to be in the *nitroso-* form. The N1-O1 bond length is 1.300 Å and the length between N1-C1 is 1.332 Å. The **L1** "bites" the Pb1 atom with an angle of 61.18º via the nitrogen atom from the *nitroso-* group and the nitrogen atom from the *pyridyl* group forming a five-membered ring. (Figure 54) The anion is in a typical cis-

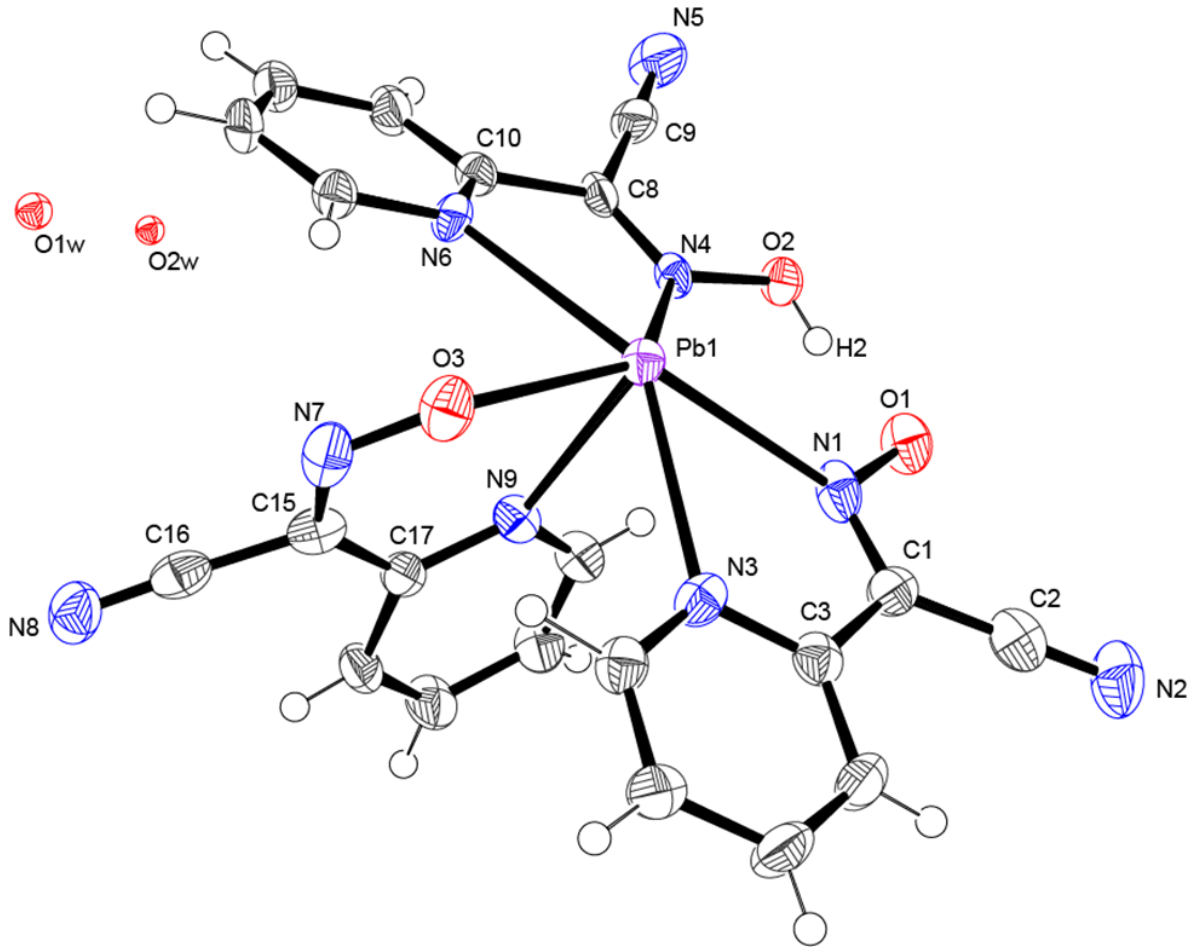

Figure 52. ORTEP representation of the ASU of Pb{(H2PCO)(2PCO)$_2$ · H2O} showing the atomic numbering scheme with 50% thermal ellipsoids parameters. There are two water molecules with partial occupancies shown as O1w and O2w.

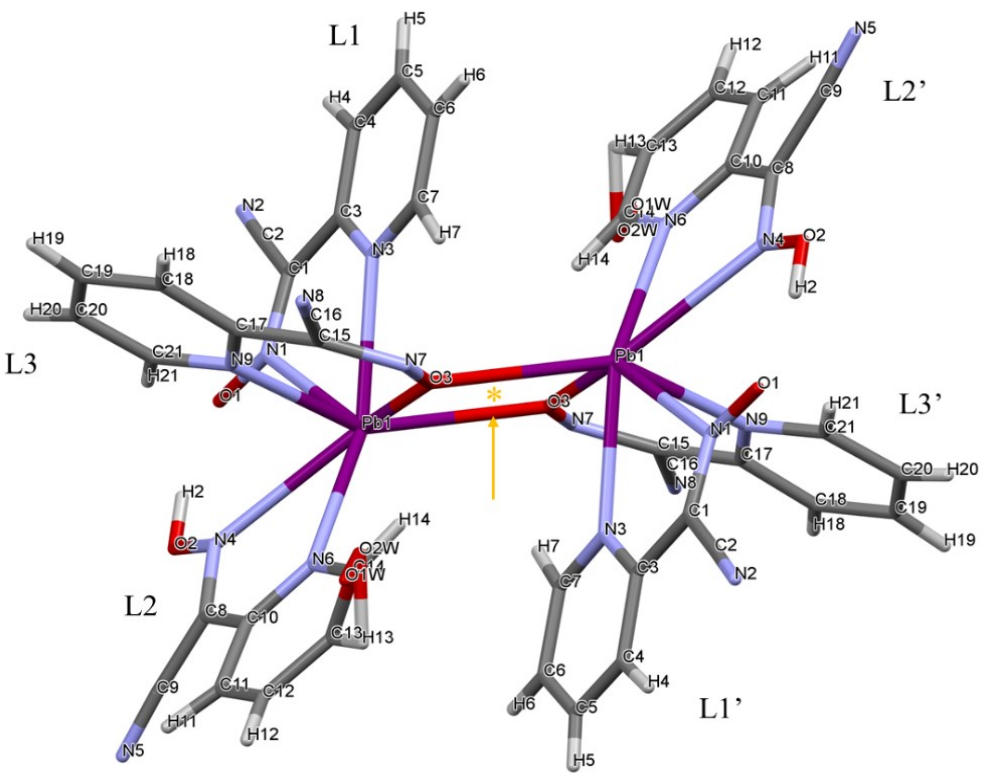

Figure 53. Capped sticks view of the dimer in Pb{(H2PCO)(2PCO)$_2$ · H2O} showing atomic labeling, ligand assignment and the inversion center, highlighted with the orange asterisk and arrow.

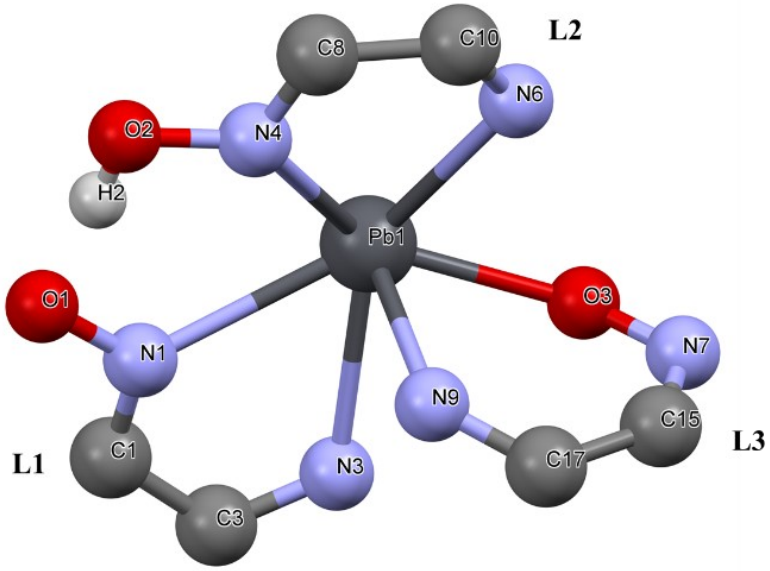

Figure 54. Metal center of Pb{(H2PCO)(2PCO)$_2$ · H2O} with pruned ligands showing the connectivity and variances of the individual ligands.

anti-configuration for this ligand. The *cyano* group has triple bond lengths and is linear in agreement with published data. The **L2** is in a protonated *oxime* form with bond lengths of N4-O2 being 1.358 Å and N4-C8 of 1.294 Å. This anion is also in the cis-anti conformation and forms a 5-membered ring (same as L1) with the Pb1 having a "biting angle" of 58.58º. The *CN*-group has typical for organic nitrile bond lengths and angles. The third ligand, **L3**, is where some interesting differences occur. The **L3** is in the *nitroso* form with bond lengths of 1.297 Å and 1.329 Å for the N7-O3 and N7-C15 respectively. This fragment is in the cis-syn orientation which has never been seen before with the $2PCO^-$ ligand. With the cis-syn orientation the "biting angle" of this anion is 74.70º. This angle is larger than the angle found in the previous two fragments (L1 and L2) which are in the cis-anti orientation. In this orientation the **L3** acts as a chelator to the Pb1 metal center via the oxygen atom (O3) from the *nitroso* group and the nitrogen atom (N9) from the *pyridyl* group forming a six-membered ring. Although this connectivity has not been reported previously using the $2PCO^-$ anion, the same trend of the larger "biting angle" with the cis-syn orientation was reported earlier in this study with Pb(II) and DCO and other cyanoximes with Ag^+ [25] and Zn^{2+} [40]. The planarities of the three ligands were compared. The dihedral angle between the plane containing the lead atom and the chelating atoms was measured against the plane containing the *cyano* group which revealed the cis-syn ligand **(L3)** had a smaller dihedral angle than the cis-anti ligands (**L1** and **L2**) with angles being 12.02º vs. 21.60º and 18.63º respectively. Another interesting function exclusive of **L3** is the role it plays in forming the building block for this compound. The same oxygen atom (O3) that is part of the chelation action on Pb1 also acts as a μ^2-bridge which connects this ligand to a second unit cell's metal center (Pb1') therefore linking both ASU into the dimer.

The sole Pb(II) ion in this compound has a coordination number of seven with a composition of $\{PbN_5O_2\}$. The geometry around this metal center is distorted pentagonal bipyramid and has a stereoactive pair of $6s^2$ electrons. The repulsion of these electrons are the cause for the distorted geometry and varying bond lengths of connected atoms. The hemidirectional bond lengths around the metal center range from 2.363 Å to 2.840 Å (Figure 55). Analyzing the equatorial atoms attached to the lead center provides more information about the skewed geometry. An expected bond angle between the axial and equatorial atoms is 90º in this type of geometry when there are no lone pairs of electrons. However, in this compound the angles are distorted towards one of the axial atoms (N9) with angles ranging between 74º and 82º. This distortion reveals the location of the $6s^2$ lone electron pair in the cleft above the Pb1 between the N4-N6-O3' atoms as seen in Figure 55-D. (The prime (') on the O3 atom represents the O3 from the neighboring bridging ligand).

The packing of this molecular compound is dependent upon intramolecular and intermolecular interactions. Thus, there is H-bonding between the hydrogen atom (H2) from **L2** and the oxygen atom (O1) from the nitroso group from **L1** which gives stability within the ASU of the structure. (Figure 56-A) Another interesting intramolecular bond is between N7-H14 and O3-H14. The hydrogen bond length is 2.413 Å and 2.448 Å respectively with angles C14-H14-N7 and C14-H14-O3 being 139.09º and 134.84º respectively. This hydrogen atom (H14) is sitting securely between the two atoms, almost equidistant, like a snug fitting puzzle piece. Within the dimer, and between the unit cells, there are multiple other electrostatic and π-π stacking interactions responsible for the crystal packing in the lattice. A final look down the *b*-axis in Figure 56-B shows a very ordered lattice of the dimer. This view aides as a visual

understanding of the water that was trapped in the channel-shaped void during crystallization as shown by arrows in this figure.

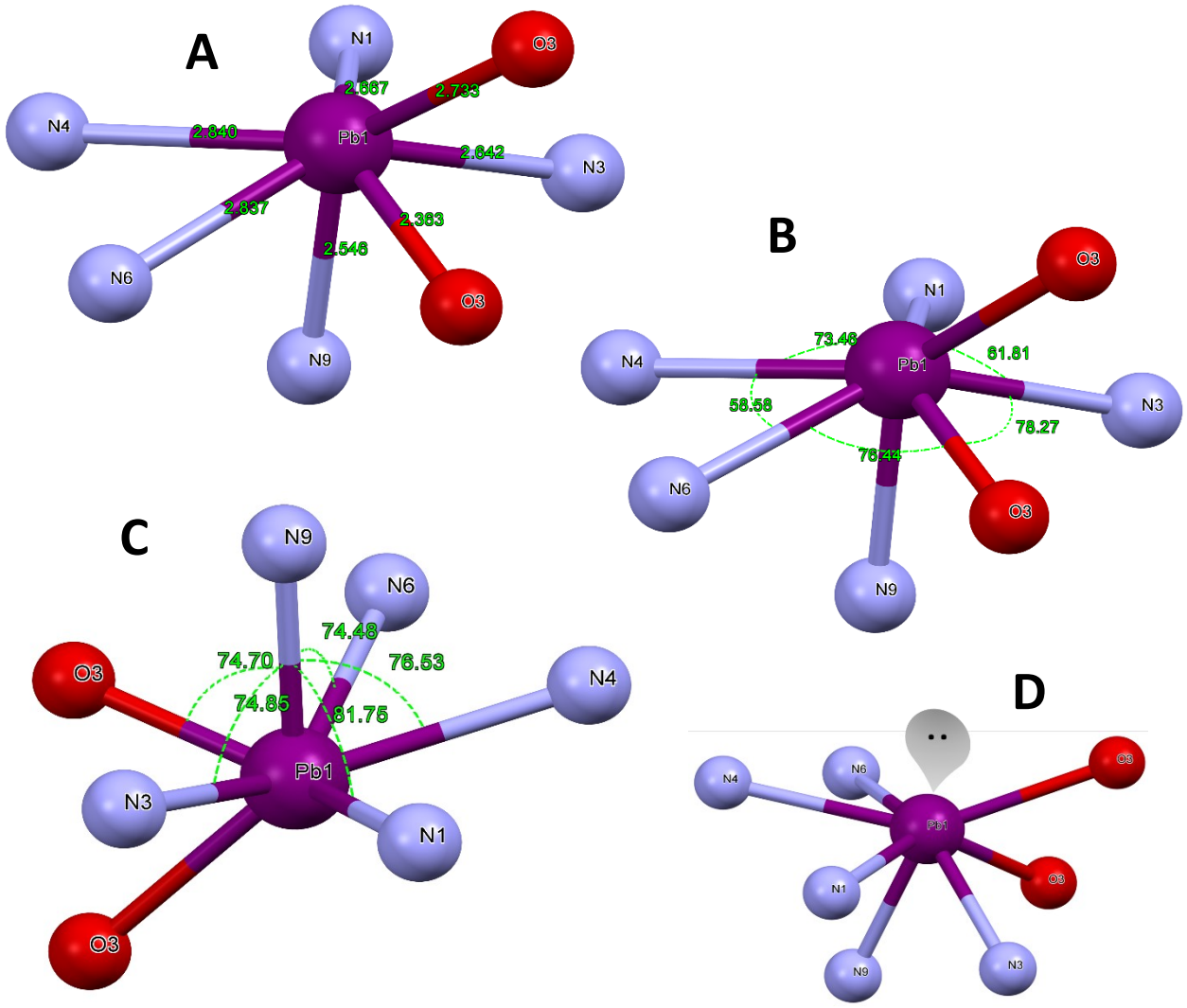

Figure 55. Pb1 metal center of Pb{(H2PCO)(2PCO)$_2$ · H2O}. **A -** Bond lengths; **B -** Equatorial bond angles; **C -** Axial to equatorial bond angles; **D -** location of the 6s^2 lone electron pair.

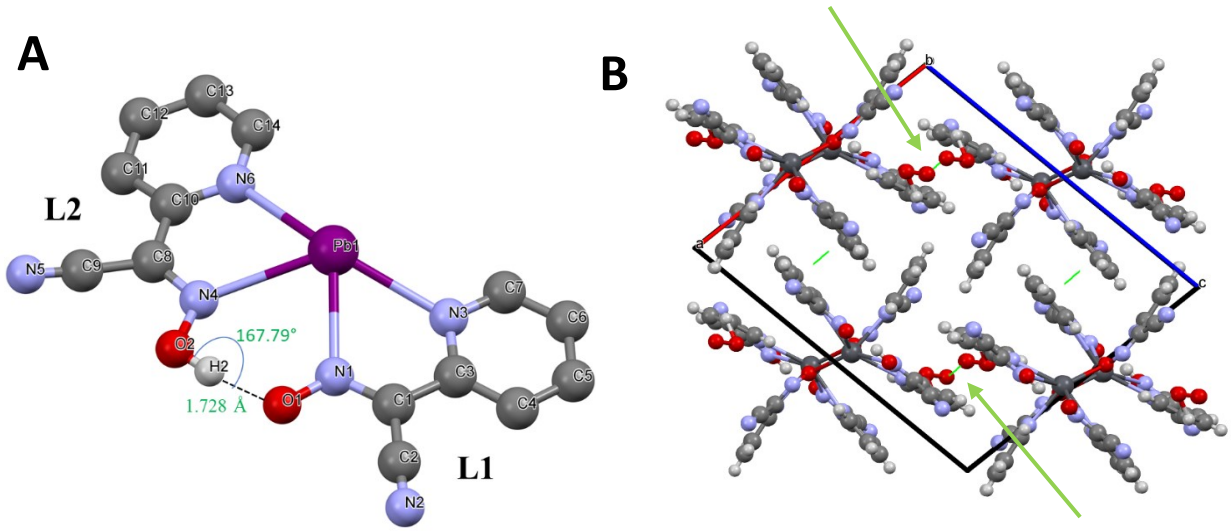

Figure 56. Crystal packing of the Pb{(H2PCO)(2PCO)$_2$ · H2O} compound. **A –** Intermolecular hydrogen bonding stabilizing the ASU; **B -** viewed down the b-axis showing the trapped water molecules in a void channel near a 2-fold rotational axis as indicated by the green arrows.

Table 18. Crystal data and refinement of Pb{(H2PCO)(2PCO)$_2$ · H_2O}.

Parameter	**Pb{(H2PCO)(2PCO)2 • H20}**
Formula	C21H13N9O4Pb
F.W., g/mol	662.59
Temperature	150(2)
Wavelength, Å	0.71073
Crystal System	Monoclinic
Space Group	P 1 21/n 1
Unit Cell, Å/ º	a = 14.1677(8) α = 90 b = 9.2091(5) β = 101.861(2) c = 16.9054(9) γ = 90
Cell Volume, Å3	2158.6(2)
Z	4
D (Calc), g/cm3	2.039
Abs. μ (mm-1)	7.867
F(000)	1264
Cryst. Size, mm	0.033 x 0.073 x 0.119
θ Range, º	1.71 to 25.00
Index Ranges	h: -16 to 16 k: -10 to 10 l: -20 to 20
Reflections Total	56701
Independent Refl.	3788 [R(int) = 0.0532]
Completeness, %	100
Absorption Method	Numerical
Tmax. And Tmin.	0.7810 / 0.4540
D / R / P**	3788 / 0 / 366
GOF on F2	1.123
Final R values [I>2σ(I)]	R1 = 0.0285, wR2 = 0.0547
R Indices (all data)	R1 = 0.0353, wR2 = 0.0569
Largest Peak/Hole, e- Å3	1.364 / -1.316
Volume Taken, Å3 (%)	1478.9 (68.5)
Dimensionality	Molecular

*-Refinement Method Full-matric least-sq. on F2 ; **-listing of Data, Restraints and Parameters

V.5.6 Crystal Structure of Pb{(H2PCO)$_2$(2PCO)$_2$}. An x-ray analysis suitable crystal was retrieved as a nice yellow block mini tube system with 1:2 ratio of starting materials. Compound crystallized in monoclinic C2/c space group. This group has multiple inversion centers, 2-fold proper rotation axes, and 2-fold screw axes is centrosymmetric. The crystal and refinement data can be found in Table 19.

The ASU in this elegant structure contains two crystallographically different Pb^{2+} ions, three protonated H2PCO ligands, and three deprotonated $2PCO^-$ anions. There are 2 different moieties in this structure. The one with Pb1 center contains two protonated and two deprotonated anions. During the refinement process it appeared that there was a charge imbalance at Pb2 center as two additional H-atoms were placed in the compound reflecting four protonated H2PCO ligands and two deprotonated $2PCO^-$ anions in the ASU. Further study revealed that one of the Pb^{2+} ions (Pb2) is occupying a special position on a 2-fold rotation axis. Because of this peculiarity it is not possible to have H-atoms attached to the oxime group fully occupied on the site. Therefore, to balance the charge the H-atoms and the anions possess 0.5 SOF (site occupancy) as well as their "master" Pb2 center. To clarify that, all connectivity of cyanoxime to the Pb2 center must be examined. That is, four molecules of $2PCO^-$ now have -2 charge which translates into -1 for one pair, symmetry related. In turn, it must be that half of the time the H-atom attached to one 2PCO moiety, and half of the time on the other 2PCO group. So, -0.5 charge on each pair (x2) will bring us to -1 which balances the charge of +1 from the Pb^{2+} center which also falls under the 0.5 SOF, as stated earlier. An ORTEP views of the ASUs can be seen in Figure 57.

This compound was the only one in the series that exclusively contained lead and the desired ligand. Without water of crystallization or spectator anions the eight ligand fragments in

Table 19. Crystal and refinement data for Pb{(H2PCO)$_2$(2PCO)$_2$}.

Parameter	**Pb$_3${(H2PCO)$_6$(2PCO)$_6$}**
Formula	$C_{84}H_{54}N_{36}O_{12}Pb_3$
F.W., g/mol	2381.2
Temperature	120(2)
Wavelength, Å	0.71073
Crystal System	Monoclinic
Space Group	C 1 2/c 1
Unit Cell, Å/ º	*a* = 24.284(5) α = 90 *b* = 9.2688(19) β = 106.587(3) *c* = 38.955(8) γ = 90
Cell Volume, Å^3	8403.(3)
Z	4
D (Calc), g/cm^3	1.882
Abs. μ (mm^{-1})	6.083
F(000)	4608
Cryst. Size, mm	n/a
θ Range, º	1.75 to 30.31
Index Ranges	h: -34 to 31 k: 0 to 13 l: 0 to 54
Reflections Total	5996
Independent Refl.	
Completeness, %	47.5
Absorption Method	
T_{max}. And T_{min}.	
D / R / P**	5996 / 412 / 617
GOF on F^2	1.034
Final R values [I>2σ(I)]	R1 = 0.0790, wR2 = 0.1158
R Indices (all data)	R1 = 0.1825, wR2 = 0.1320
Largest Peak/Hole, e- Å^3	1.539 / -1.095
Volume Taken, Å^3 (%)	5742.9 (68.3)
Dimensionality	Molecular

*Refinement Method Full-matric least-sq. on F2 ; **listing of Data, Restraints and Parameters

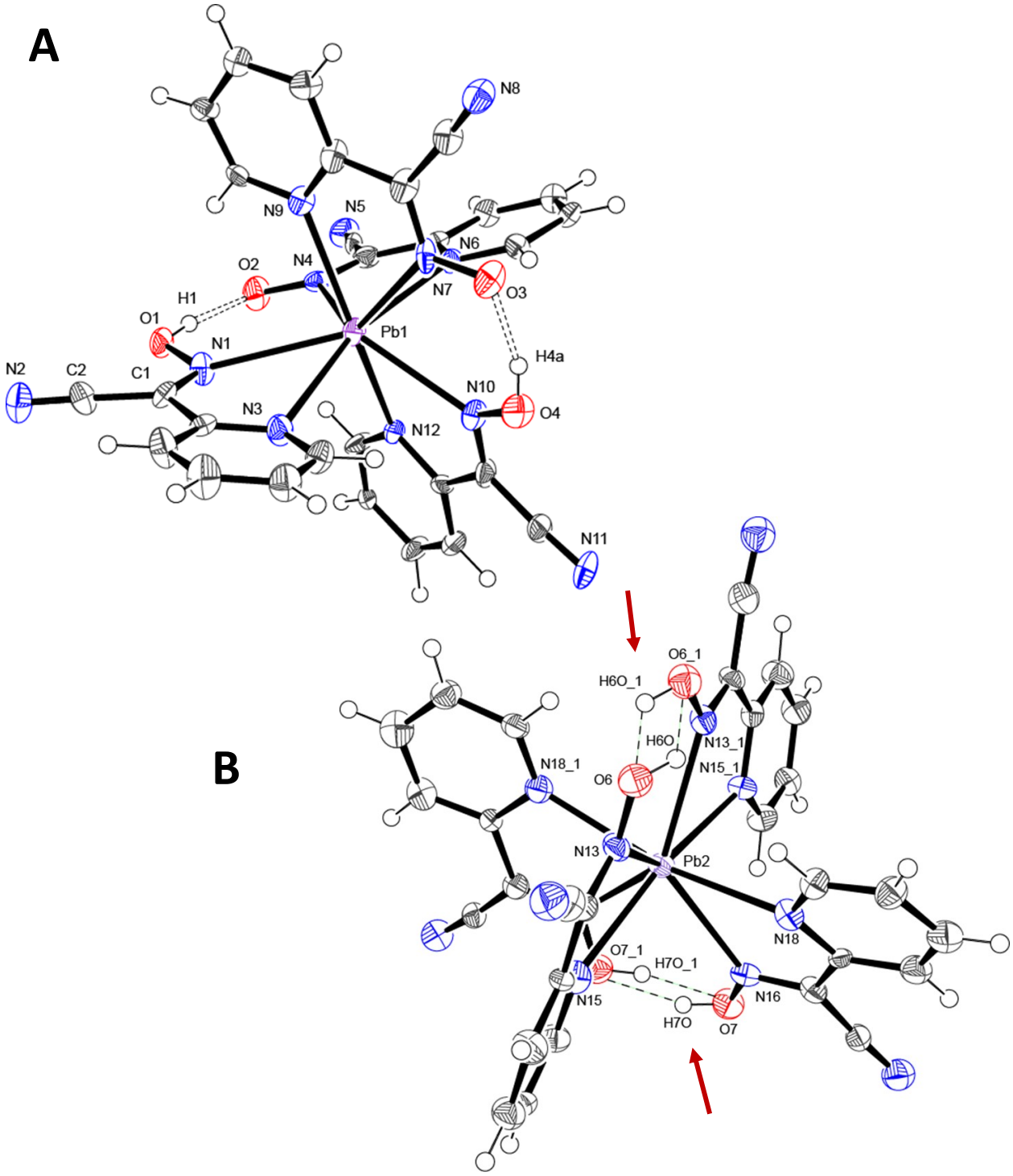

Figure 57. **A** - Molecular structure of complex at Pb1 center in ORTEP representation showing principal atoms numbering. **B** - Molecular structure of Pb2 center in ORTEP representation showing numbering of principal atoms. Positions indicated as _1 has symmetry code: -x, y, ½ - z. H-atoms H6 and H7 (shown by arrows) have 0.5 occupancy and in connection with H6_1 and H7_1 which brings total occupancy of hydrogen to 1.

the ASU it was found that they are very similar to one another. Every ligand regardless of being protonated or not acts as a chelator to a Pb(II) center via the nitrogen atom from the oxime group and the nitrogen atom from the pyridyl group. The "bite" angles were somewhat similar ranging from 56.63° to 64.30°. The *cyano*- groups remained linear in all the ligands and the overall planarity of the attached fragments remained fairly flat. The dihedral angles between the pyridyl group and the chelating N-Pb-N planes were small, ranging between 5.75° and 15.44°, with one exception being 24.26° found on **L1** (N1-Pb1-N3). This larger dihedral angle on **L1** corresponds to the smallest "biting angle" (56.63°) among the ligands. Additionally, all six of the oxime fragments in the ASU display oxime characteristics as the N-O bonds are longer than the C-N bonds. The only exception is **L2** where the two bond lengths are identical at 1.308 Å. An interesting note is that **L2** is one of the deprotonated ligands on Pb1; **L3** is deprotonated on the same metal center and has bond lengths that are very similar as well, at the same time **L1** and **L4** have a significantly longer N-O bond. The ligands on the Pb2 center seem to follow the same trend as the C-N and N-O bond lengths in the oxime fragment are very close to one another. As stated earlier, **L5** and **L6** on Pb2 are deprotonated half of the time which may contribute to the much more similar bond lengths. See Tables 20 and 21 for selected bond lengths and angles. Both metal centers in the structure have a coordination number of eight with a composition of $\{PbN_8\}$ and neither appears to have an active $6s^2$ lone pair of electrons. Additionally, they both have a distorted cubic geometry. The differences in the two can be seen in the bond lengths surrounding the central atoms and the "bite" angles of the ligands. Thus, Pb1 has eight coordinating nitrogen atoms from four chelating 2PCO ligands: six with bond lengths ranging from 2.554 Å to 2.694 Å and two longer bonds (2.850 Å and 2.886 Å). The Pb2, again, has much more similar bond lengths ranging from 2.683 Å to 2.716 Å. (Figure 58)

Table 20. Selected bond lengths and angles for the oxime fragments in the $2PCO^-$ anion in $Pb\{(H2PCO)_2(2PCO)_2\}$.

Ligand	Bond	(Å)	"Biting" angle	(°)
L1	C1-N1	1.278	N1-Pb1-N3	56.63
	N1-O1	1.368		
L2	C8-N4	1.308	N4-Pb1-N6	64.3
	N4-O2	1.308		
L3	C15-N7	1.307	N7-Pb1-N9	61.98
	N7-O3	1.322		
L4	C22-N10	1.294	N10-Pb1-N12	60.94
	N10-O4	1.354		
L5	C29-N13	1.300	N13-Pb2-N15	60.45
	N13-O6	1.343		
L6	C36-N16	1.302	N16-Pb2-N18	60.25
	N16-O7	1.337		

Table 21. Selected bond lengths and angles for the *cyano* group in the $2PCO^-$ anion in $Pb\{(H2PCO)_2(2PCO)_2\}$.

Ligand	Bond	(Å)	Angle	(°)
L1	C2-N2	1.152	C1-C2-N2	176.56
L2	C9-N5	1.130	C8-C9-N5	177.71
L3	C16-N8	1.139	C15-C16-N8	176.52
L4	C23-N11	1.140	C22-C23-N11	176.29
L5	C30-N14	1.144	C29-C30-N14	175.89
L6	C37-N17	1.150	C36-C37-N17	174.99

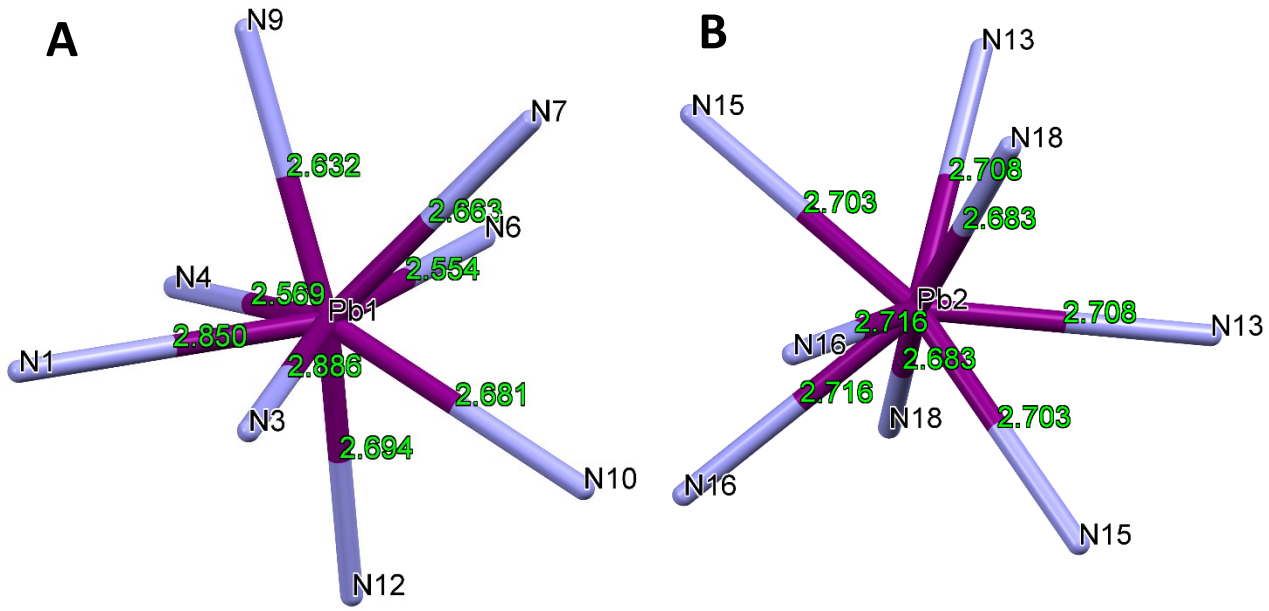

Figure 58. Lead center for Pb{(H2PCO)$_2$(2PCO)$_2$} moiety in capped sticks representation showing atom connectivity and bond lengths. **A –** for Pb1. **B –** for Pb2

This molecular compound is beautifully packed and resembles kaleidoscope pieces when viewed down the *b*-axis (Figure 59). Intramolecular hydrogen bonding inside each Pb1 and Pb2 complexes helps in formation of Pb(HL)$_2$L$_2$ units while Van der Waals interactions are responsible for packing of this compound in the crystal lattice.

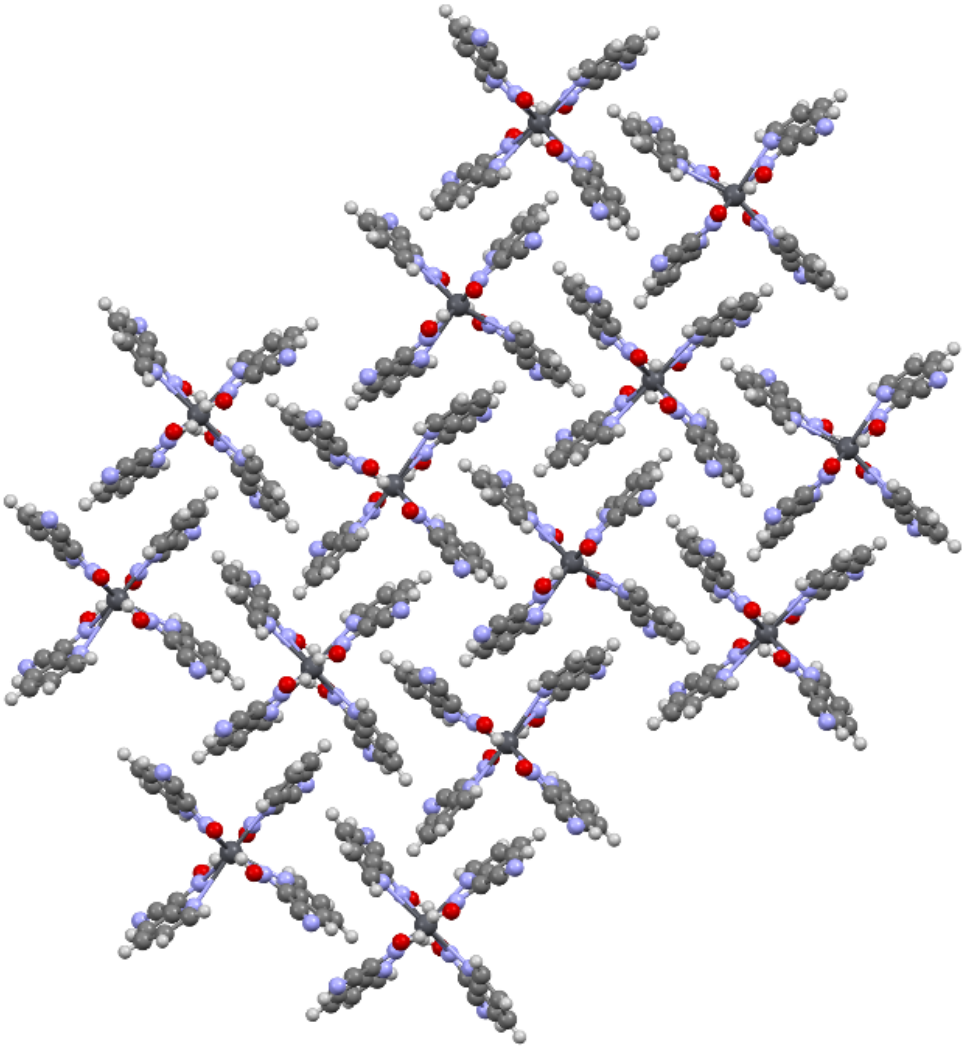

Figure 59. Crystal packing of the molecular compound of Pb{$(H2PCO)_2(2PCO)_2$} viewing down the *b*-axis.

V.6 Vibrational Spectroscopy

The IR spectroscopy was used in effort to characterize all synthesized "PbL_2" products. Key molecular fragments were identified in the bulk products as well as material from plugs removed from the narrow tubes during crystal growth. For comparative purposes, spectra for the pure ligands were obtained to observe shifts of frequencies for key peaks. The key functional groups identified in all products and ligands are (C≡N), ($C=N_{ox}$), and (N-O) and additional peaks such as C-H, OH and C=S vibrations were identified as needed for each compound. Assignment of vibrational frequencies can be seen in Table 24. All of the complexes, except Pb(BCO) and Pb(MCO), show a 30-60 cm^{-1} upward shift in the (N-O) frequency from the ligand to the lead complex. This indicates a change in the bonding with either the N or the O oxygen of the oxime fragment which is due to redistribution of electron density on that fragment. Overall, the identified peaks support proposed composition of products of interactions in the Pb^{2+} cyanoxime systems.

Table 22. IR spectroscopy data identifying frequencies (cm^{-1}) of main fragments in ligands and lead (II) cyanoximates.

Compound	Source	ν(O-H)	ν(C-H)	ν(C≡N)	ν(C=O)	ρ(NH_2)	ν(C=N_{py})	ν(C-O_{ox})	ν(N-O)	ν(C=S)
H(2PCO)		*	3087	2229	*	*	1587	1472	979	*
Pb(2PCO)	1:2 Ac	*	3070	2212	*	*	1585	1459	1019	*
Pb(2PCO)	Rxn 2-2	*	3088	2221	*	*	1588	1461	1022	*
H(MeCO)		*	3200	2234	1723	*	*	1436	1057	*
Pb(MeCO)	Rxn 5-2	*	3185	2204	1696	*	*	1439	1103	*
H(ECO)		*	3114	2232	1721	*	*	1424	1061	*
Pb(ECO)	Rxn 4-2	*	2987	2222	1698	*	*	1445	1098	*
H(PiCO)		*	2978	2231	1667	*	*	1391	928	*
Pb(PiCO)	Rxn 8-1	3325	2974	2212	1644	*	*	1368	962	*
H(BCO)		*	3267	2240	1637	*	*	1415	1145	*
Pb(BCO)	1:2	*	3057	2212	1629	*	*	1401	1140	*
Pb(BCO)	Rxn 3-2	*	3062	2214	1634	*	*	1460	1159	*
H(PiPCO)		*	3051	2183	1615	*	*	1455	1032	*
Pb(PiPCO)	Rxn7-2	*	2935	2209	1592	*	*	1445	1102	*
Pb(PiPCO)	1:2	*	2935	2207	1593	*	*	1442	1096	*
H(DCO)		*	2952	2239	1614	*	*	1401	1037	*
Pb(DCO)	Rxn 9-1	*	2932	2207	1604	*	*	1406	1065	*
H(MCO)		*	2809	2239	1623	*	*	1442	997	*
Pb(MCO)	Rxn 11-1	*	2857	2211	1590	*	*	1435	1018	*
H(PyrCO)		*	2952	2226	1604	*	*	1450	1034	*
Pb(PyrCO)	Rxn 10-1	*	2962	2209	1582	*	*	1436	1092	*
H(TCO)		*	3150	2250	*	1601	*	1415	1058	885
Pb(TCO)	Rxn 6-1	3400	2922	2215	*	1590	*	1462	1147	840
Pb(TCO)	Rxn 14-1	3400	2965	2218	*	1624	*	1462	1149	875

V.7 Thermal Analysis

DSC/TG analyses of all compounds showed lead (II) cyanoximates have different thermodynamic stability. Stepwise decomposition can be seen leading to different products of decomposition. The most interesting and unexpected finding was the discovery of three complexes that exhibited sharp and intense exothermic peaks during decomposition. In total, there are three compounds that can be classified as potentially high-energy compounds.

The "Pb(ECO)" product matches the composition of the crystal structure that was grown and reported for this system which is $K_2[Pb_3(AACO)_4(H_2O)]_2$. However, the decomposition of bulk powder does not indicate any water in the system. The water in the unit cell is most likely is trapped and is occluded from the preparation procedure. It is not a stoichiometric amount of water which may explain the lack of clearly observed water leaving the system. Another consideration is that the water did not have the opportunity to be expelled from the system before the violent decomposition occurred at 172° C. The analysis shows complete decomposition, down to elemental lead, which was left as droplets in the crucible the terminal temperature.

The "Pb(DCO)" product matches the composition of the crystal structure that was grown and reported for this system, $Pb_3(OH)(NO_3)(DCO)_4$, The decomposition traces do not show any water presence in the structure, which is in agreement with the given formula of basic salt. An exothermic event occurs at 184° C then continues to a complete decomposition at 800° C with flakey elemental lead left in the crucible.

Four bulk powdery compounds, $Pb(2PCO)_2$, $Pb(PiCO)_2 \cdot 3\ H_2O$, $Pb(TCO)_2 \cdot 2\ H_2O$, and $Pb(TCO)_2 \cdot 3H_2O$, were analyzed and their thermogravimetric results discussed earlier in the "Desktop Synthesis of PbL_2" section. In $K_2[Pb(AACO)_2](H_2O)$ the presence of water is supported by IR spectroscopy but is not seen/detected leaving the system. A possible

explanation may be similar to the Pb(ECO) system as a violent decomposition occurred in this compound at 185° C. Complete decomposition occurred at 698° C leaving elemental droplets of lead in the crucible. The weight loss analysis showed 46% of the original product remained in the crucible compared to 45% in the proposed structure, which is very good agreement of data. The "Pb(BCO)", "Pb(PiPCO)", "Pb(PyrCO)", and "Pb(MCO)" all have exothermic effects at different temperatures, 168°, 206°, 183°, and 172° respectively with different decomposition products. Respectively, they are lead oxide with presumed carbon residue, mostly elemental lead but small amount of carbon residue, lead oxide with spongy looking carbon residue and a leftover stench of pyrrolidine, and what appears in color to be elemental lead, but looks like a hollow filigree ball. Images can be seen in Figure 60. Instrumentation images can be found in Appendix C.

V.7.1 Potential High-Energy Compounds Thermal Analyses. A very interesting finding during investigation of thermal stability of complexes was the discovery of three compounds that maybe viewed as potential heat-activated explosives or high-energy compounds. For example, high energy compounds, such as lead azide [$Pb(N_3)_2$], are produced in tons as a shock-activated primer for detonators in a variety of ammunition including bullets and artillery shells. A firing pin strikes the primer, which is hypersensitive to shock, causing a very rapid high burst of energy which then ignites the propellant (gunpowder) and causes it to start burning. As the powder quickly burns the buildup of gas and pressure will blow the top off, sending the ammunition downrange.

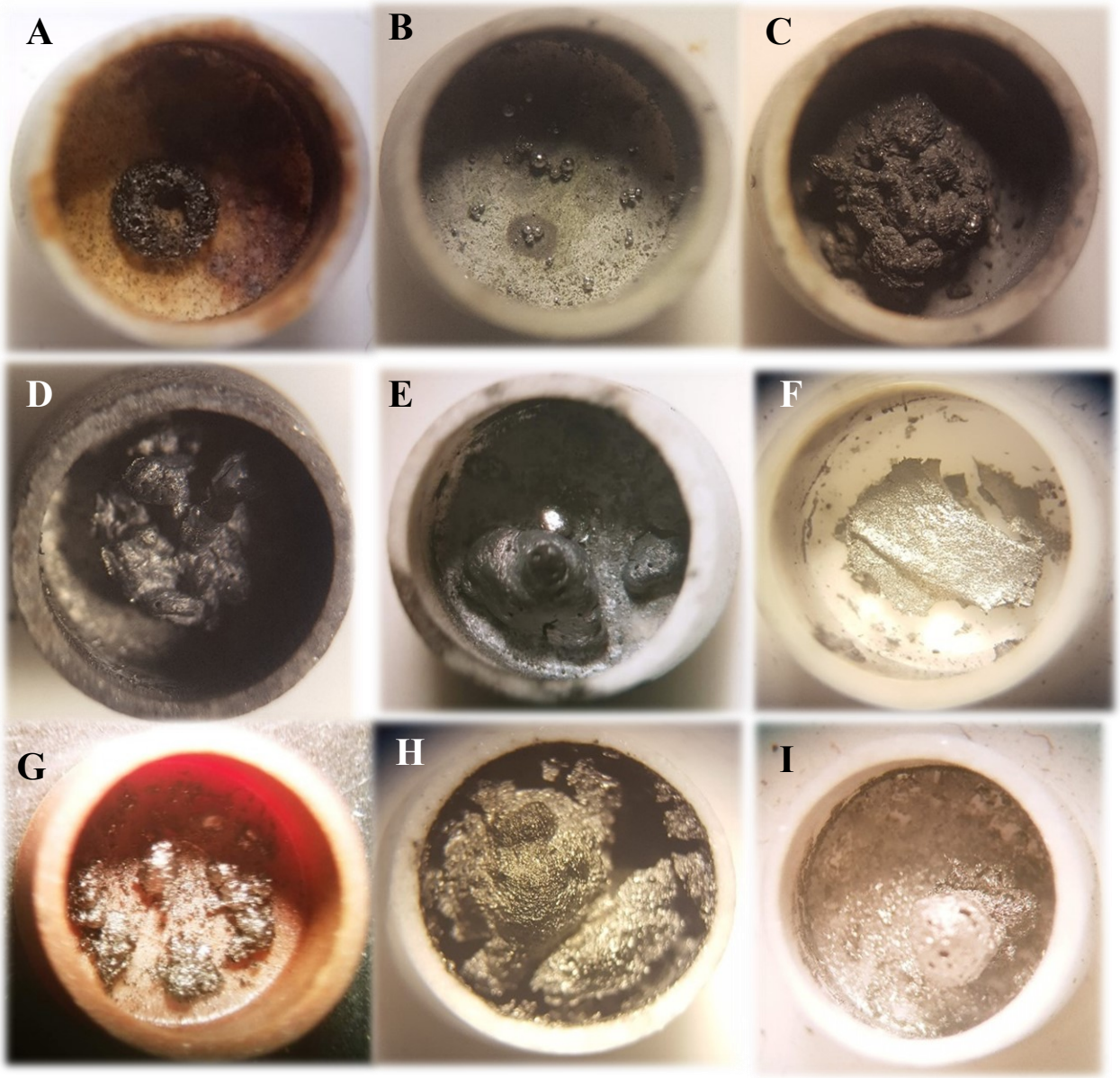

Figure 60. Crucible observations after DSC/TGA analysis. **A -** Pb(2PCO); **B –** Pb(MeCO); **C -** Pb(BCO); **D -** Pb(TCO) from Reaction 6-1; **E -** Pb(TCO) Reaction 14-1; **F -** Pb(MCO); **G -** Pb(PiPCO); **H -** Pb(PyrCO); **I-** Pb(DCO).

We decided that a comparison of heat effects needs to be for our compounds against known high-energy compounds. We selected ionic salts $KMnO_4$, NaN_3, and $NaClO_4$ with the latter two specifically known as heat activated primers. The two ester-cyanoximes, "Pb(ECO)" and "Pb(MeCO)", and the sulfur containing cyanoxime, "Pb(TCO)", when heated at a rate of

10°C/min underwent violent decompositions. The "Pb(ECO)" at 170°, "Pb(MeCO)" at 185° C, "Pb(TCO)" (from Rxn 6-1) at 182°, and "Pb(TCO)" (from Rxn 14-1) at 165°. All decompositions were very fast with a strong exothermic effect. At first, we started by investigating each of the three compounds by recording TG/DSC traces at 5°, 8°, 10°, 15°, and 20°/min. Thus, energy liberated could be calculated from peak integration values (Table 23). The trend showed that as the ramp rate increased the integration value for the exothermic event decreased which was opposite of what was expected assuming a faster heating ramp would cause a more energetic decomposition. We consulted with Dr. Jennifer Schott, Applications Support Engineer from TA Instruments – Waters, LLC. She explained that the heat flow is based on the specific heat and mass, according to the heat flow equation, yet energetic material reactions are additionally dependent on surface area and not just overall mass. Also, decomposition is kinetic in nature and so many other factors are involved. When the temperature is rapidly raised it will cause a higher thermal lag which aligns with the data collected in the "heat stories" (or variable heating rates) of our three compounds. Another consideration was typically instrument calibration is optimized for higher temperatures so more variability may be expected in low temperature raw signals which can lead to instrument variation. Overall, her professional advice was to run all our samples and standards with a constant temperature ramp and very tight tolerance for the sample mass so the only independent variable would be the generated heat.

Based on her suggestions, a series of experiments has been carried out including our three compounds, and a thallium based cyanoxime compound, Tl_2(1,3-BCO) [43]. This salt came from a previous study in the NG research group which also showed potential for being a high-energy compound [43]. Also, at the same conditions three standards that are known to be high energy compounds, NaN_3, $KMnO_4$, and $NaClO_4$, were examined by the TGA/DSC method. Sample

Table 23. "Heat Stories" for high-energy compounds.

Sample	Sample size (mg)	Temp (°C)	Rate (°C/min)	Peak Integ. (J/g)	Peak Integ. (J)	Peak Integ. (KJ/mol)	MM (g/mol)	Exp. Decomp Temp (°C)	Theo Decomp Temp (°C)
Pb(TCO)	12.119	161	5	589	7.14	304.8	517.49	**147**	*
Pb(TCO)	13.058	165	8	530	6.92	274.3	517.49	150	*
Pb(TCO)	15.779	165	10	438	6.91	226.7	517.49	151	*
Pb(TCO)	14.686	166	12	463	6.80	239.6	517.49	150	*
Pb(TCO)	9.724	166	15	421	4.09	217.9	517.49	150	*
Pb(TCO)	10.478	175	20	377	3.95	195.1	517.49	155	*
Pb(TCO)	5.353	168	5	518	2.77	268.2	517.49	151	*
Pb(ECO)	16.114	170	5	126	2.03	289.7	2304.57	165	*
Pb(ECO)	11.012	175	8	127	1.40	292.7	2304.57	170	*
Pb(ECO)	10.203	172	10	110	1.12	253.5	2304.57	165	*
Pb(ECO)	12.223	178	15	61	0.75	140.6	2304.57	165	*
Pb(ECO)	8.991	184	20	48	0.43	110.6	2304.57	174	*
Pb(ECO)	5.353	182	5	116.3	0.62	268.0	2304.57	124	*
Pb(MeCO)	8.593	183	5	376	3.23	1676.6	4459.11	136	*
Pb(MeCO)	14.843	184	8	115	1.71	512.8	4459.11	145	*
Pb(MeCO)	10.636	185	10	129	1.37	575.2	4459.11	156	*
Pb(MeCO)	10.087	187	10	147	1.48	655.5	4459.11	130	*
Pb(MeCO)	11.442	192	15	74	0.85	330.0	4459.11	137	*
Pb(MeCO)	5.411	192	5	248.5	1.34	1108.1	4459.11	156	*

masses were meticulously weighed staying as close to 5.4 mg as was possible to do on the instrument. All scans were conducted under an anerobic atmosphere (N_2) with a ramp rate of 10° C/min. Results show exothermic events occurring simultaneously with a massive weight loss in every sample. Samples of the thermal scans can be seen in Figures 62-66. These

exothermic peaks were integrated (Figure 67) to calculate the amount of energy liberated from the system during that short period of violent decomposition. Once the data was collected, a comparison of peak integration values in KJ/mol was conducted. The standard's values for heat evolution were calculated at 7.04 KJ/mol for $KMnO_4$, 20.47 KJ/mol for NaN_3, and 40.24 KJ/mol for $NaClO_4$ compared to our samples ranging between 268.22 - 1108.09 KJ/mol! The highest performance from our three samples was detected for the "Pb(MeCO)" complex. It must be noted that the calculation is based on a hypothetical structure (hence molecular mass), although supported by literature review, elemental analysis, IR spectroscopy, and thermal analysis. Therefore, it necessitates further investigation on actual crystal structure of the complex for more accurate data. The new potential high-energy compounds appear to release significantly more energy per mole than the known standards and are activated at lower temperatures (as low as 124° C compared to 240° C for the lowest, $KMnO_4$). The experimental decomposition temperatures match almost identically to the published data for two of the standards giving more merit for further investigation for these complexes as potentially being developed and applied as heat-activated temperature primers and initiators. Data for comparison can be seen in Table 24.

Table 24. Thermal analysis comparing standards to potential high-energy cyanoximate compounds.

Sample	Sample size (mg)	Temp (°C)	Rate (°C/min)	Peak Integ. (J/g)	Peak Integ. (J)	Peak Integ. (KJ/mol)	MM (g/mol)	Exp. Decomp Temp (°C)	Theo Decomp Temp (°C)
NaN3	5.522	390	5	314.5	1.74	20.5	65.099	350	275
KMnO4	5.492	278	5	44.53	0.24	7.0	158.034	240	240
NaClO4	5.528	560	5	328.7	1.82	40.2	122.44	457	468
Pb(ECO)	5.353	182	5	116.3	0.62	268.0	2304.57	124	*
Pb(MeCO)	5.411	192	5	248.5	1.34	1108.1	4459.11	156	*
Pb(TCO)	5.356	168	5	518.3	2.78	268.2	517.49	151	*
Tl_2(1,3-BCO)	5.498	271	5	514.2	2.83	319.3	620.93	240	*

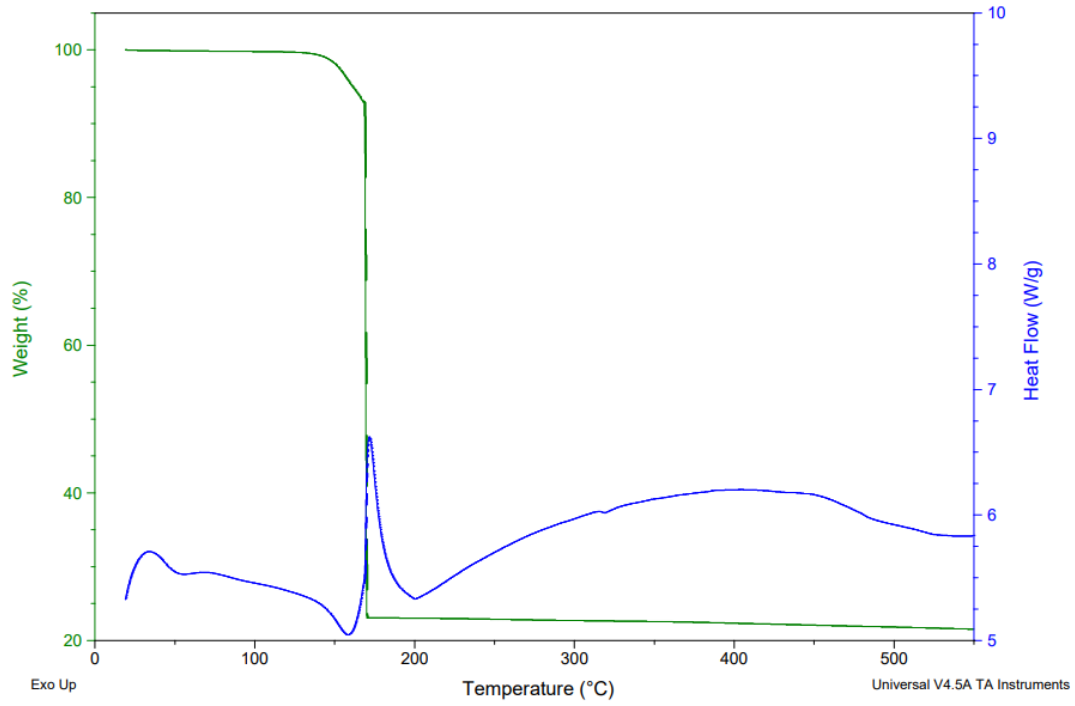

Figure 61. The TG/DSC traces of "Pb(ECO)" compound showing violent decomposition of the complex as sharp exo-peak and weight drop!

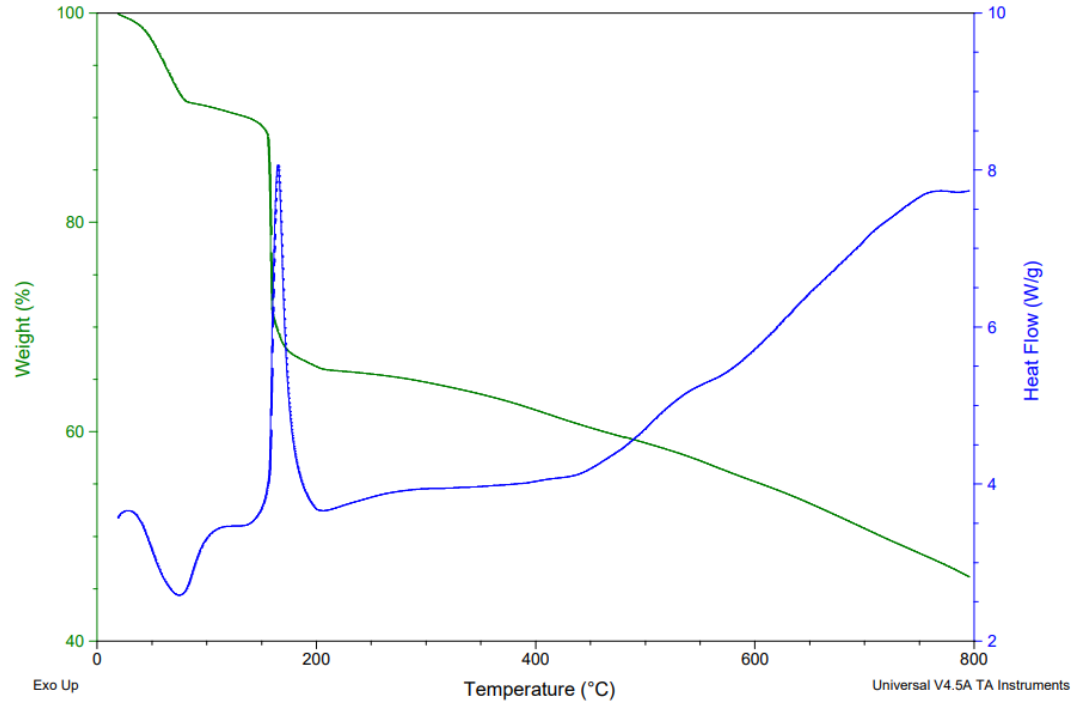

Figure 62. Original and first thermal scan of $Pb(TCO)_2 \cdot 3H_2O$ compound showing the large exothermic peak

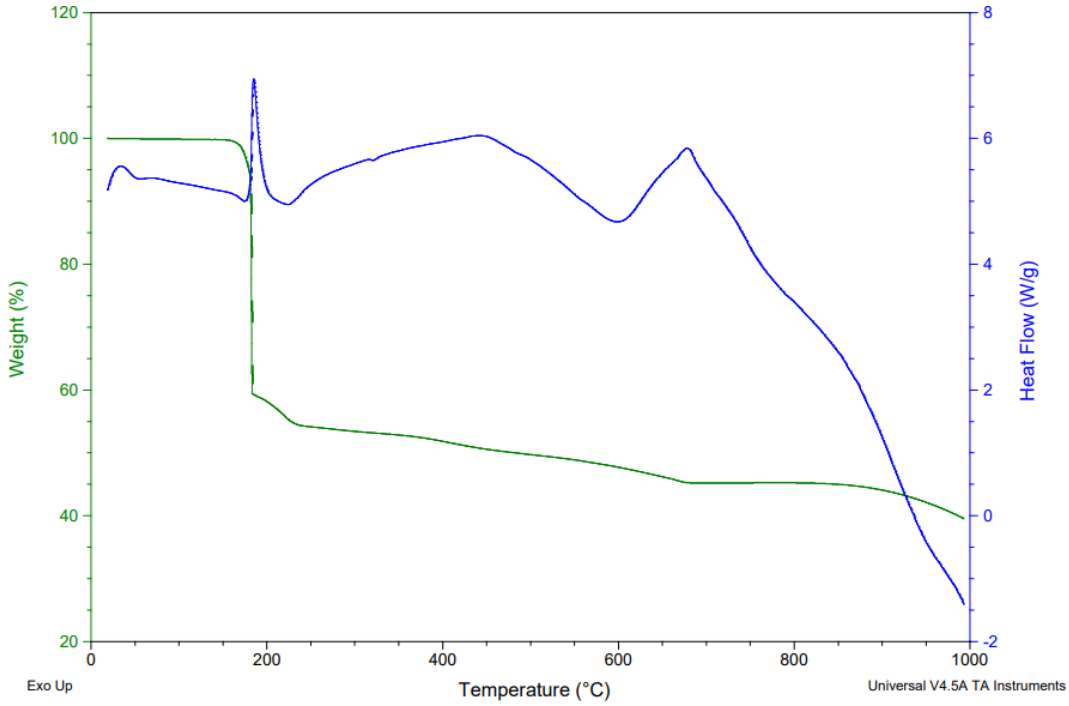

Figure 63. The TG/DSC traces for "Pb(MeCO)" compound.

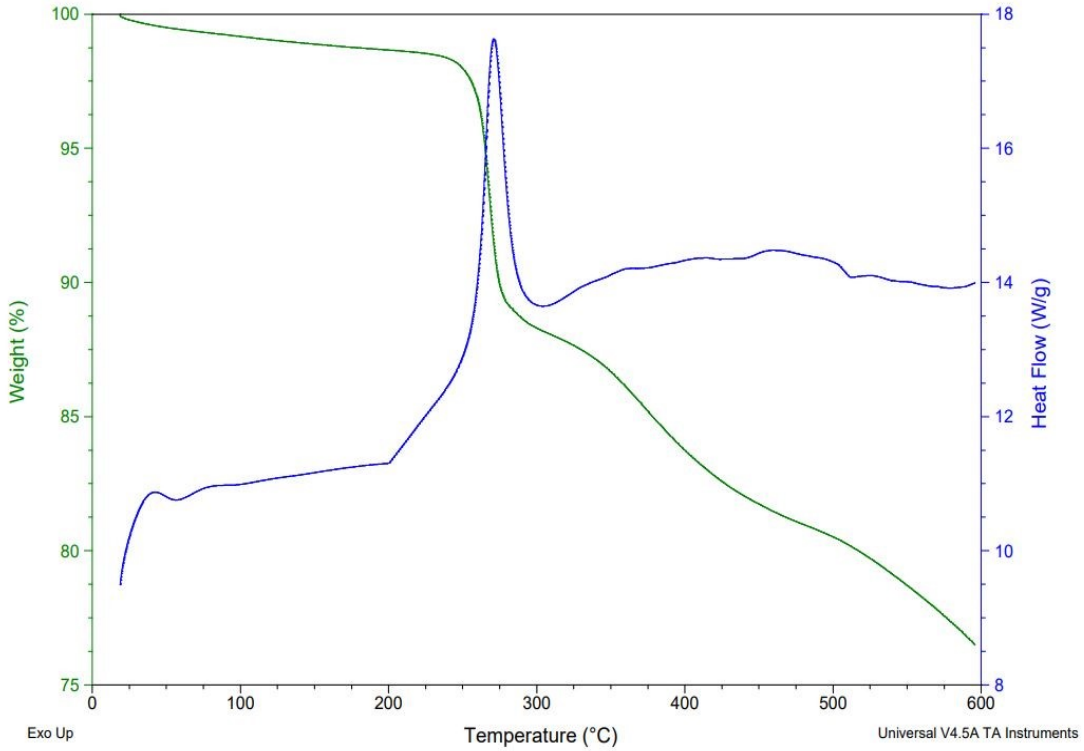

Figure 64. The TG/DSC traces for Tl_2(1,3-BCO) compound that was claimed to be potential high-energy compound [43].

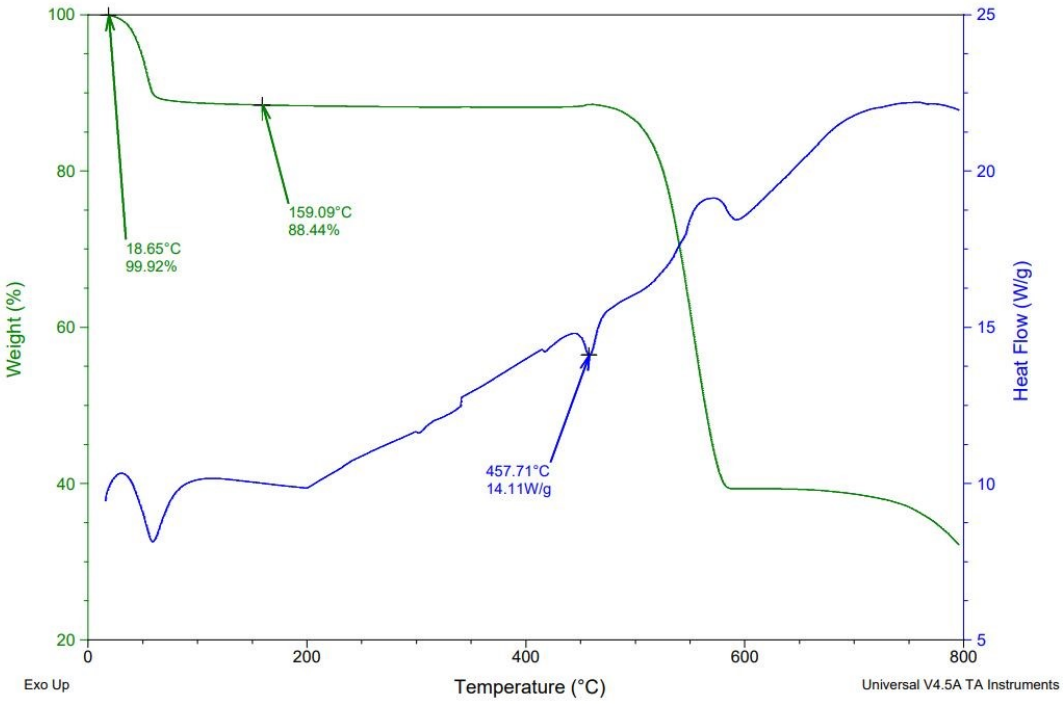

Figure 65. Thermogravimetric data for $NaCLO_4$ that we used as standard compound.

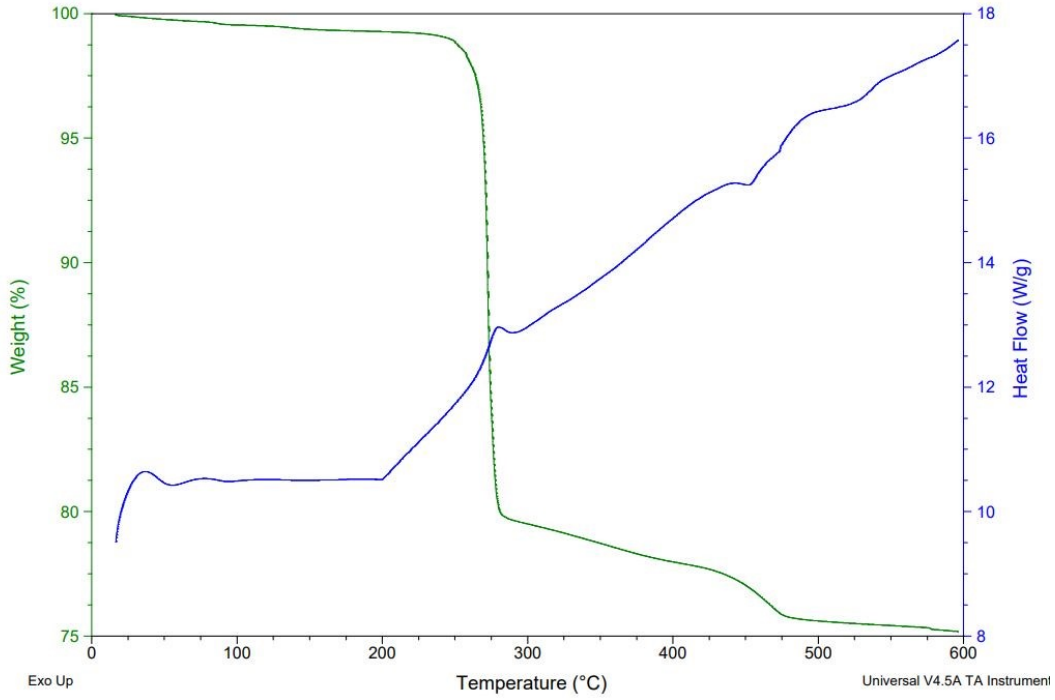

Figure 66. Thermogravimetric data for the $KMnO_4$ that we used as control.

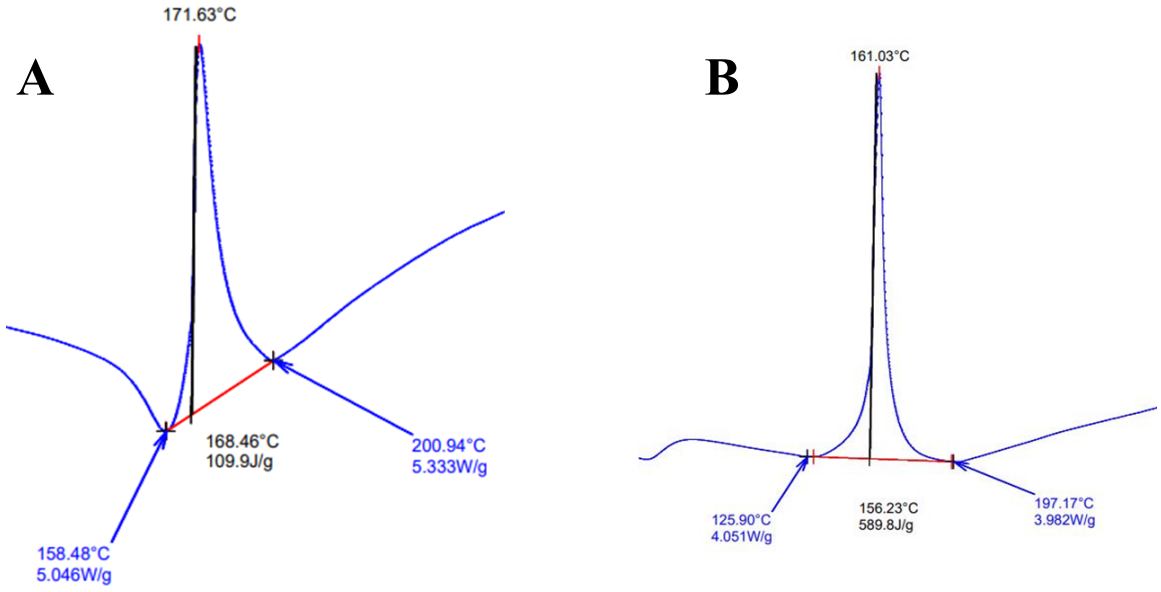

Figure 67. Integration calculations of exo-peaks. **A -** "Pb(ECO)" compound; **B -** $Pb(TCO)_2 \cdot 3H_2O$ compound.

V.8 Hydrolysis and Side Products.

During our investigations we found another obstacle to desired products. The difficulty in obtaining the desired products also lies in the ability for hydrolysis processes that are competing in the system. Thus, the lead(II) cations and the ligand anions, stemming from weak acids, make that delicate balance. (Figure 74) It is knowns that Pb^{2+} produces a slightly acidic solution due to hydrolysis. When the lead nitrate dissociates in water the Pb^{2+} will coordinate with the OH^- ion leaving the H^+ ion in solution which has two consequences: 1) the bond between Pb-OH is formed and 2) solution is acidified. Studies show that there are three distinct phases in the Pb^{2+}--NO_3^---H_2O reaction vessel (which initially produces the $[Pb(OH)_4]^{4+}$ cluster cation) where the product is dependent upon the pH of the system. The first precipitate obtained is $[Pb_4(OH)_4](NO_3)_2$. When the pH increases above 5.25 the NO_3- is replaced with the OH- ion. Other products are found as the pH continues to increase, $[Pb_3(OH)_4]^{2+}$ and $[Pb_6O(OH)_6]^{4+}$ for

pH 7 and 8.5 respectively [44]. The solubility or Ksp value for lead (II) hydroxide varies in literature. One of the higher values found is 1.2×10^{-12}. This is a strong indicator that some form of lead hydroxide or hydrate is prone to precipitate out as a product.

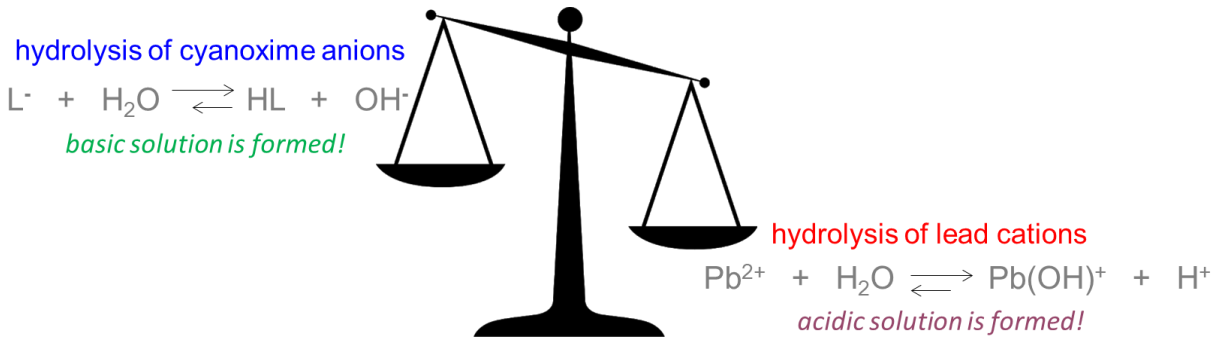

Figure 68. Balancing the hydrolysis between the cyanoxime anions and the lead cations.

On the other side, cyanoximes are weak acids. The ligands chosen for this study have pKa values ranging from 4.29 – 6.77 [25]. The ligands are deprotonated with a stoichiometric amount of base for all reactions in this study because it increases their reactivity. As weak acids in aqueous solutions, the deprotonated ligands will undergo hydrolysis and coordinate with the H^+ ion from the water. This coordination has two consequences: 1) the deprotonated ligand now bonds with the hydrogen atom re-protonating the ligand rendering it almost non-reactive and 2) solution is basified.

Three different side products were identified from various systems. All represent basic salts. All were clear crystals with structures that have been previously characterized: Pb(OH)Cl (also known as Laurionite), [45] $Pb_{16}(OH)_{16}(NO_3)_{16}$ (lead hydroxide nitrate), [46] and $Pb_2Cl_2CO_3$ (Phosgenit) [47]. These side products are a direct result from hydrolysis of the lead (II) ion.

Figure 75 shows the process of hydrolysis of lead (II) cation in aqueous solutions and how the side products were dependent on the presence of the other ions in the system. Two additional "side products", a white crystalline material retrieved from two different systems, turned out to be one of the reactants, the protonated ligand. Now, these "products" are a direct result from the hydrolysis of the ligand. However, judging from the results of the side products and the crystal structures determined through XRD analyses, hydrolysis of Pb(II) is much more overpowering and stronger than the hydrolysis of the ligands and has a greater effect on the outcome.

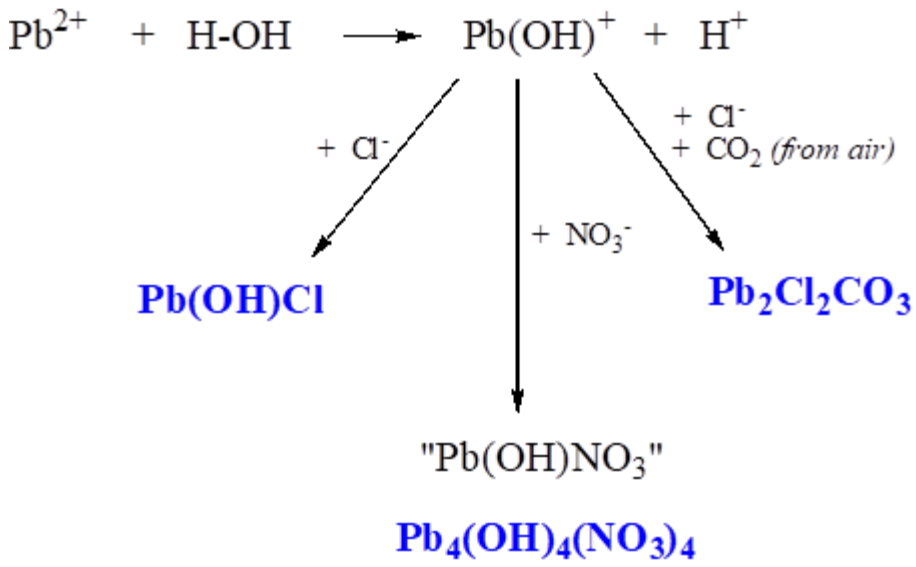

Figure 69. Hydrolysis of lead(II) cations in aqueous solutions that lead to three side products which depended on presence of other ions in the system.

Ironically, the lead hydroxide nitrate (which was found in five of the narrow tube systems) is a monoclinic crystal in the Cc space group—a non-centrosymmetric crystal! A literature search for the crystal structure uncovered in 2014 it was studied and published at the first time as a non-linear optical compound which possesses a large SHG response ~3.5 times that of potassium diphosphate (KDP), [46] one of the oldest used non-linear materials.

VI. SUMMARY AND CONCLUSION

The results and conclusions drawn from this research project are summarized below.

- Synthesized two protonated HL ligands for the purpose of preparing new lead (II) cyanoxime-containing compounds

- Three targeted PbL_2 compounds were synthesized. The composition of the bulk products was supported by elemental analysis, IR Spectroscopy, and DSC/TGA analysis. We were not successful in growing any crystals for structural determination of these compounds.

- Three crystal structures were determined for the H(TCO) cyanoxime and its cesium salt which were used for preparation of new Pb-cyanoxime-containing compounds.

- Considerable efforts were made for crystals growth using a variety of methods.

- Twenty-three narrow tubes were assembled and proved to be the suitable system for obtaining quality single crystals for the XRD analysis. All crystals used for the XRD analysis were retrieved from these tubes in different areas.

- Six new crystal structures containing Pb(II) and cyanoximate anions were determined by the XRD analysis and characterized by elemental analysis, IR Spectroscopy, and DSC/TGA analysis.

- The $Pb_3(OH)(NO_3)(DCO)_4$ structure's finding was that only one of the three lead center's crystallographic data revealed co-crystallized two diastereomers of the ligand. Thus, cis-anti isomer forming a 5-membered chelate ring while the cis-syn forming a 6-membered ring.

- Five of the new structures have active $6s^2$ lone pairs on Pb(II) centers.

- The $2PCO^-$ anion bridges three lead (II) ions in one complex which is not even found in transition metal complexes to which this cyanoxime ligand has great affinity.

- Three lead (II) cyanoximates were found to have properties of high-energy compounds, which violently decompose, with release of significant heat and kinetic energy, leaving only droplets of elemental Pb. Compared to known high-energy compounds these have high potential for use as heat-triggered actuators.

VII. REFERENCES

[1] Gerasimchuk, N. Chemistry and Applications of Cyanoximes and Their Metal Complexes. *Dalton Trans.,* **2019**, *48* (23), 7985–8013. https://doi.org/10.1039/c9dt01057b.

[2] Gerasimchuk, N. N. The Synthesis, IR Spectra, and Structure of Lead(II) Complexes with Amide-Cyanoximate Ion ONC(CN)C(O)NH2-. *Russ. J. Inorg. Chem*., **1993**, *38* (2), 266–271.

[3] Miessler, G. L.; Fischer, P. J.; Tarr, D. A. *Inorganic Chemistry.*, 5th ed.; Pearson: Boston, 2014.

[4] House, J. E.; Kathleen Ann House. *Descriptive Inorganic Chemistry*; Brooks/Cole Publishing Company, 2001.

[5] Britannica. Ligand | Chemistry | Britannica. *Encyclopædia Britannica*; 2020.

[6] chelate | Etymology, origin and meaning of chelate by etymonline https://www.etymonline.com/word/chelate (accessed 2022 -10 -30).

[7] Hsieh, C.-H.; Brothers, S. M.; Reibenspies, J. H.; Hall, M. B.; Popescu, C. V.; Darensbourg, M. Y. Ambidentate Thiocyanate and Cyanate Ligands in Dinitrosyl Iron Complexes. *Inorg. Chem.,* **2013**, *52* (4), 2119–2124. https://doi.org/10.1021/ic3025149.

[8] Pushkin, D.; Serezhkin, V. N.; Davidovich, R. Stereochemical Effect of a Lone Electron Pair in the Structure of Diamine Complexonates of Bismuth(III). *Russ. J. Inorg. Chem*., **2003**, *48* (5), 700–704.

[9] Sidey, V. On the Effective Ionic Radii for the Tin(II) Cation. *J Phys Chem Solids,* **2022**, *171*, 110992. https://doi.org/10.1016/j.jpcs.2022.110992.

[10] Gerasimchuk, N.; Domasevitch, K.; Kapshuk, A.; Chernega, A. Coordination Compounds of N,N-Dimethylthioamidocyanoxime. *Russ. J. Inorg. Chem*., **1993**, *38* (11), 1837–1841.

[11] Trinh, D. Linear Electrooptic Microscopy: Applications to Micro- and Nano-Structured Materials. Ph.D. Thesis, Laboratoire de Photonique Quantique et Moleculaire, **2015**.

[12] Franken, P. A.; Hill, A. E.; Peters, C. W.; Weinreich, G. Generation of Optical Harmonics. *J Phys Chem Solids*, **1961**, *7* (4), 118–119. https://doi.org/10.1103/physrevlett.7.118.

[13] Megaw, H. D. A Note on the Structure of Lithium Niobate, LiNbO3. *Acta Crystallogr A: Crystal Physics, Diffraction, Theoretical and General Crystallography* **1968**, *24* (6), 583–588. https://doi.org/10.1107/s0567739468001282.

[14] Bloembergen, N.; Pershan, P. S. Light Waves at the Boundary of Nonlinear Media. *American Physical Society.* **1962**, *128*, 606. https://doi.org/https://doi.org/10.1103/PhysRev.128.606.

[15] Arivuoli, D. Fundamentals of Nonlinear Optical Materials. *Pramana* **2001**, *57* (5-6), 871–883. https://doi.org/10.1007/s12043-001-0004-1.

[16] Bordui, P. F.; Fejer, M. M. Inorganic Crystals for Nonlinear Optical Frequency Conversion. *Annu. Rev. Mater. Res.,* **1993**, *23* (1), 321–379. https://doi.org/10.1146/annurev.ms.23.080193.001541.

[17] Tordjman, P. I.; Masse, E.; Guitel, J. C. Structure Cristalline Du Monophosphate $KTiPO_5$. *Z KRISTALLOGR.,***1974**, *139* (1-2), 103–115. https://doi.org/10.1524/zkri.1974.139.1-2.103.

[18] Bierlein, J. D.; Vanherzeele, H. Potassium Titanyl Phosphate: Properties and New Applications. *JOSAB*, **1989**, *6* (4), 622. https://doi.org/10.1364/josab.6.000622.

[19] Huband, S.; Keeble, D. S.; Zhang, N.; Glazer, A. M.; Bartasyte, A.; Thomas, P. A. Crystallographic and Optical Study of $LiNb_{1-x}Ta_xO_3$. *Acta Cryst B,* **2017**, *73* (3), 498–506. https://doi.org/10.1107/s2052520617004711.

[20] Uecker, R. The Historical Development of the Czochralski Method. *J. Cryst. Growth,* **2014**, *401*, 7–24. https://doi.org/10.1016/j.jcrysgro.2013.11.095.

[21] Wang, H.; Jin, M. Y.; Jarnagin, R. C.; Bunning, T. J.; Adams, W.; Cull, B.; Shi, Y.; Kumar, S.; Samulski, E. T. Thermally Stable Nonlinear Optical Activity in a Smectic-A Liquid Crystal. *Nature* **1996**, *384* (6606), 244–247. https://doi.org/10.1038/384244a0.

[22] Marder, S. R.; Perry, J. W.; Schaefer, W. P. Synthesis of Organic Salts with Large Second-Order Optical Nonlinearities. *Science* **1989**, *245* (4918), 626–628.

[23] Goud, N. R.; Zhang, X.; Brédas, J.-L.; Coropceanu, V.; Matzger, A. J. Discovery of Non-Linear Optical Materials by Function-Based Screening of Multi-Component Solids. *Chem* **2018**, *4* (1), 150–161. https://doi.org/10.1016/j.chempr.2017.12.010.

[24] Ghoohestani, M.; Arab, A.; Hashemifar, S. J.; Sadeghi, H. *Ab-Initio*Investigation of Rb Substitution in KTP Single Crystal. *J. Appl. Phys.,* **2018**, *123* (1), 015702. https://doi.org/10.1063/1.5000242.

[25] Gerasimchuk, N.; Guzei, I.; Sipos, P. Structural Peculiarities of Cyanoximes and Their Anions: Co-Crystallization of Two Diastereomers and Formation of Acid-Salts. *Curr. Inorg. Chem,.* **2015**, *5* (1), 38–63. https://doi.org/10.2174/1877944105666150417231145.

[26] Norbury, A. H.; Sinha, A. I. P. The Co-Ordination of Ambidentate Ligands. *Chem. Soc. Rev.,* **1970**, *24* (1), 69. https://doi.org/10.1039/qr9702400069.

[27] Fedorenko, D.; Gerasimchuk, N.; Domasevich, K. 2-Oxyiminopivaloylacetonitrile, the First (ALPHA)-Ketocyanoxime: Synthesis and Donor Properties. *Russ. J. Inorg. Chem,* **1993**, *38* (9), 1535–1539.

[28] Vallet, V.; Wahlgren, U.; Grenthe, I. Chelate Effect and Thermodynamics of Metal Complex Formation in Solution: A Quantum Chemical Study. *J. Am. Chem. Soc*., **2003**, *125* (48), 14941–14950. https://doi.org/10.1021/ja036646j.

[29] Gerasimchuk, N.; Barnes, C. L.; Boaz, D. Preparation, Spectroscopic, and Structural Characterization of the First Co(III) Cyanoxime Complex: Two Polymorphs of *Fac*-, *Tris*(Benzoylcyanoximato)Cobalt(III), $Co(BCO)_3$. *J. Coord. Chem, 63* (6), 943–953. https://doi.org/10.1080/00958971003671801.

[30] Domashevskaya, O. A.; Siminov, Yu. A.; Gerasimchuk, N.; Dvorkin, A. A.; Mazus, M. D. Synthesis and Crystal Structure of the Complex of Ni2+ with a Tetraamino Aliphatic Ligand and an ONC(CN)C(S)NH2- Ion. . *Russ. J. Inorg. Chem,* **1990**, *16* (11), 1544–1548.

[31] Gerasimchuk, N.; Zhmurko, O.; Tyukjtenko, S. 2-Pyridylcyanoxime and Related Complex Compounds of Cu(II) and Ni(II). *Russ. J. Inorg. Chem*., **1993**, *38* (2), 238–287.

[32] Domasevich, K.; Lindeman, S.; Struchkov, Y.; Gerasimchuk, N.; Gerasimchuk, O. The Synthesis and Investigation of Copper(II) Complexes with N,N-Dimethylacetamidooximate Ion. *Russ. J. Inorg. Chem*., **1993**, *38* (1), 108–113.

[33] Eddings, D.; Barnes, C.; Gerasimchuk, N.; Durham, P.; Domasevich, K. First Bivalent Palladium and Platinum Cyanoximates: Synthesis, Characterization, and Biological Activity†. *Inorg. Chem,* **2004**, *43* (13), 3894–3909. https://doi.org/10.1021/ic0303439.

[34] Ratcliff, J.; Kuduk-Jaworska, J.; Chojnacki, H.; Nemykin, V.; Gerasimchuk, N. Part 1: Experimental and Theoretical Studies of 2-Cyano-2-Isonitroso-N-Piperidynylacetamide (HPiPCO), 2-Cyano-2-Isonitroso-N-Morpholylacetamide (HMCO) and Their Pt- and Pd-Complexes. *Inorg. Chim. Acta,* **2012**, *385*, 1–11. https://doi.org/10.1016/j.ica.2011.12.005.

[35] Katz, M. J.; Michaelis, V. K.; Aguiar, P. M.; Yson, R.; Lu, H.; Kaluarachchi, H.; Batchelor, R. J.; Schreckenbach, G.; Kroeker, S.; Patterson, H. H.; Leznoff, D. B. Structural and Spectroscopic Impact of Tuning the Stereochemical Activity of the Lone Pair in Lead(II) Cyanoaurate Coordination Polymers via Ancillary Ligands. *Inorg. Chem,* **2008**, *47* (14), 6353–6363. https://doi.org/10.1021/ic800425f.

[36] Dannen, S. D.; Cornelison, L.; Durham, P.; Morley, J. E.; Shahverdi, K.; Du, J.; Zhou, H.; Sudlow, L. C.; Hunter, D.; Wood, M. D.; Berezin, M. Y.; Gerasimchuk, N. New in Vitro Highly Cytotoxic Platinum and Palladium Cyanoximates with Minimal Side Effects in Vivo. *J. Inorg. Biochem.,* **2020**, *208*, 111082. https://doi.org/10.1016/j.jinorgbio.2020.111082.

[37] Charlier, H.; Gerasimchuk, N. Cyanoxime Inhibitors of Carbonyl Reductase and Methods of Using Said Inhibitors in Treatments Involving Antracyclines, US Patent # 7,727,967 B2, June 1, 2010.

[38] Gerasimchuk, N.; Domasevich, K. The Stability of Tris(Cycnoximato)-Ferrates(II) in Aqueous Solution. *Russ. J. Inorg. Chem*, **1992**, *37* (10), 1163–1167.

[39] Henisch, H. K. *Crystal Growth in Gels*; Penn State University Press, 1970.

[40] Opalade, A. A.; Gomez-Garcia, C. J.; Gerasimchuk, N. New Route to Polynuclear Ni(II) and Cu(II) Complexes with Bridging Oxime Groups That Are Inaccessible by Conventional Preparations. *Cryst. Growth Des,* **2019**, *19* (2), 678–693. https://doi.org/10.1021/acs.cgd.8b01262.

[41] Gerasimchuk, N.; Kuzmann, E.; Büki, A.; Vértes, A.; Nagy, L.; Burger, K. Synthesis and Infrared and Mössbauer Studies of Eu(III) Complexes with Cyanoxime Anions. *Inorganica Chim. Acta,* **1991**, *188* (1), 45–50. https://doi.org/10.1016/s0020-1693(00)80915-9.

[42] Marcano, D.; V. Lindeman, S.; Pyrkosz-Bulska, M.; Gumienna-Kontecka, E.; Lengyel, A.; Kuzmann, E.; Rominger, F.; Gerasimchuk, N. The 2-Pyridylcyanoxime and Its Complexes. *Curr. Inorg. Chem,* **2015**, *5* (2), 98–113. https://doi.org/10.2174/1877944105021507021029O5.

[43] Curtis, S.; Lottes, B.; Robertson, D.; Lindeman, S. V.; Gerasimchuk., N. Search for the Shortest Intermetallic Tl---Tl Contacts: Synthesis and Characterization of Thallium(I) Coordination Polymers with Several Mono- and Bis-Cyanoximes. *Inorganica Chim. Acta,* **2020**, *508*, 119597. https://doi.org/10.1016/j.ica.2020.119597.

[44] Grimes, S. M.; Johnston, S. R.; Abrahams, I. Characterisation of the Predominant Low-pH Lead(II)–Hydroxo Cation, $[Pb_4(OH)_4]^{4+}$; Crystal Structure of $[Pb_4(OH)_4][NO_3]_4$and the Implications of Basic Salt Formation on the Transport of Lead in the Aqueous Environment. *J. Chem. Soc., Dalton Trans.* **1995**, No. 12, 2081–2086. https://doi.org/10.1039/dt9950002081.

[45] Venetopoulos, C. Ch.; Rentzeperis, P. J. The Crystal Structure of Laurionite, Pb(OH)Cl. *Z KRIST-NEW CRYST ST,* **1975**, *141* (3-4), 246–259. https://doi.org/10.1524/zkri.1975.141.3-4.246.

[46] Chang, L.; Wang, L.; Su, X.; Pan, S.; Hailili, R.; Yu, H.; Yang, Z. A Nitrate Nonlinear Optical Crystal Pb16(OH)16(NO3)16 with a Large Second-Harmonic Generation Response. *Inorg Chem,* **2014**, *53* (7), 3320–3325. https://doi.org/10.1021/ic402404a.

[47] Giuseppetti, G.; Tadini, C. Reexamination of the Crystal Structure of Phosgenite, Pb2Cl2(CO3). *TMPM,* **1974**, *21* (2), 101–109. https://doi.org/10.1007/bf01081262.

APPENDICES

Appendix A: Crystal Structures of Auxiliary Non-lead Containing Compounds

Appendix A-1 Crystal Structure of Pre-TCO. The molecular structure of thiocyanoacetamide, the precursor for thioamide cyanoxime (HTCO), can be seen in ORTEP representation in Appendix A-1.1. The molecule is non-planar with the two planar fragments in the structure being the *cyano* fragment C1-C2-N1 and the thioamide fragment S1-C3-N2 (Appendix A-1.2). The dihedral angle between these two planes is ~42º. Bond lengths and angles in the *cyano* group (C≡N) and the thioketone (C=S) are consistent with the expected values and summarized in Appendix A-1.2. Molecules are packed into the crystal by means of Van der Waals interactions and hydrogen bonding. Hydrogen bonding occurs between the nitrogen atom N1 from the *cyano* group and the hydrogen atom (H2N2) from the amide group thus forming a layer. Parameters for the H-bonding in the crystal are N2-H2N2---N1 = 2.355 Å and the bond angle is 164º. Another system of hydrogen bonding between the sulfur atom S1 and the hydrogen atom (H1N2) from the amide group binds the layers together to pack the unit

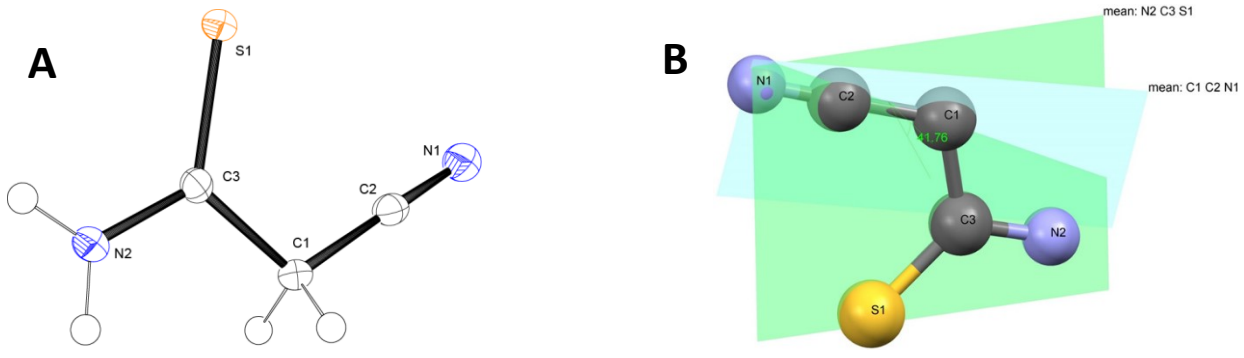

Appendix A-1.1. A - ASU of pre-TCO in ORTEP view at 50% ellipsoids with atomic labeling; **B –** planarity analysis of pre-TCO molecule with H-atoms removed for clarity.

cell as seen in Appendix A-1.3. Bonding parameters for this system are N2-H1N2---S1 = 2.535 Å with an angle of 173º. The crystal and refinement data is shown in Appendix A-1.4.

Appendix A-1.2. Key structural bond lengths and angles in Pre-TCO, H(TCO) and Cs(TCO).

Pre-TCO				**H(TCO)**				**Cs(TCO)**			
Bond	(Å)	Angle	(°)	Bond	(Å)	Angle	(°)	Bond	(Å)	Angle	(°)
C1-C2	1.465	C1-C3-S1	121.8	C1-N1	1.289	C1-C2-N2	177.12	C2-N2	1.127	C1-C2-N2	176.15
C1-N1	1.146	S1-C3-N2	124.05	N1-O1	1.343	N1-C1-C2	123.08	C2-C1	1.413	C2-C1-C3	119.76
C1-C3	1.523	N2-C3-C1	114.14	C2-N2	1.138	C2-C1-C3	119.54	C1-N1	1.333	C3-C1-N1	118.8
C3-S1	1.676	C1-C2-N1	179.09	C3-S1	1.654	C3-C1-N1	117.28	N1-O1	1.266	N1-C1-C2	122.2
C3-N2	1.312			C3-N3	1.313	C1-C3-S1	119.7	C3-S1	1.662	S1-C3-N3	121.48
						S1-C3-N3	124.62	C3-N3	1.303	N3-C3-C1	117.27
						N3-C3-C1	115.66	N3-Cs1	3.573	C1-C3-S1	121.21
								C1-C3	1.433	Cs1-N3-C3	93.78

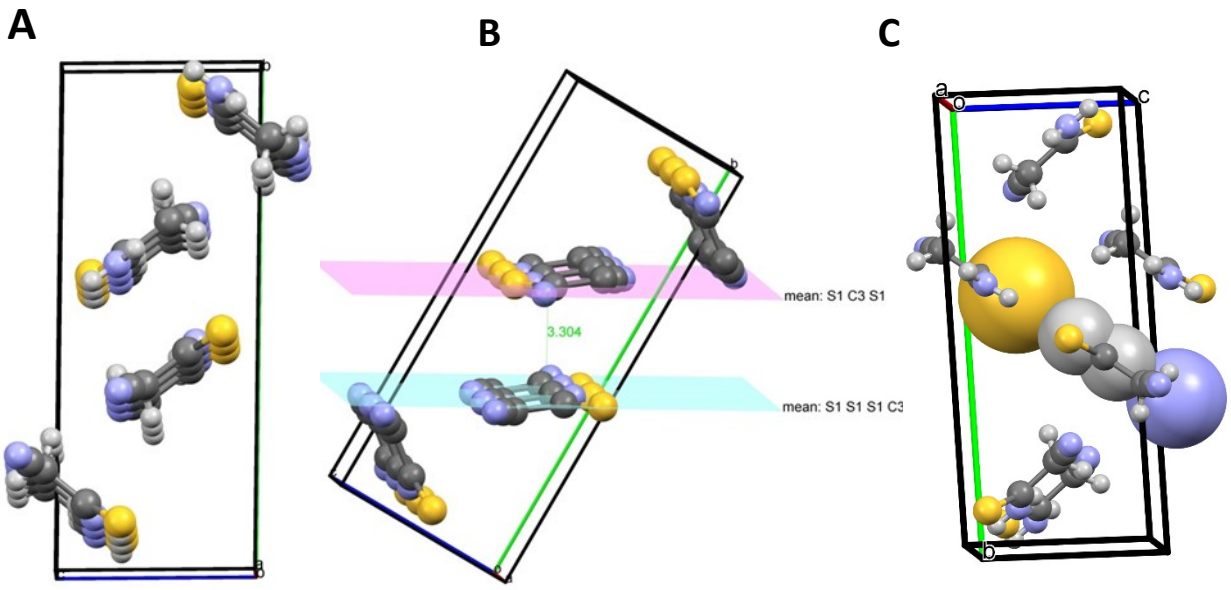

Appendix A-1.3. Analysis of crystal packing in the structure of thiocyanoacetamide. **A –** Prospective view of the unit cell content showing layered structure of compound; **B –** Prospective view showing interlayer distance in the structure; **C –** Hydrogen bonding between neighboring molecules shown in space filled style.

Appendix A-1.4. Crystal and refinement data for Pre-TCO, H(TCO), and Cs(TCO).

Parameter	Pre-TCO	H(TCO)	Cs(TCO)
Formula	$C_3H_4N_2S$	$C_3H_3N_3OS$	$C_3H_2CsN_3OS$
F.W., g/mol	100.14	129.14	261.04
Temperature	100(2)	120(2)	120
Wavelength, Å	0.71073	0.71073	0.71073
Crystal System	Monoclinic	Monoclinic	Monoclinic
Space Group	P 1 21/c 1	P 1 21/n 1	P 1 21/c 1
Unit Cell, Å/ º	*a* = 5.8606(8)	*a* = 7.429(2)	*a* = 5.384(9)
	b = 13.9206(19)	*b* = 6.987(2)	*b* = 7.299(12)
	c = 6.0984(8)	*c* = 10.757(3)	*c* = 17.07(3)
	α = 90	α = 90	α = 90
	β = 116.230(2)	β = 102.766(5)	β = 96.61(3)
	γ = 90	γ = 90	γ = 90
Cell Volume, Å3	446.29(10)	544.6(3)	666.4(19)
Z	4	4	4
D (Calc), g/cm3	1.49	1.575	2.602
Abs. μ (mm-1)	0.545	0.485	5.786
F(000)	208	264	479.7
Cryst. Size, mm	0.077 x 0.214 x 0.295	n/a	n/a
θ Range, º	2.93 to 33.08	3.04 to 25.00	4.8 to 50
Index Ranges	h: -8 to 8	h: -8 to 8	h: -8 to 8
	k: -20 to 20	k: -8 to 8	k: -11 to 10
	l: -9 to 9	l: -12 to 12	l: -24 to 26
Reflections Total	6074	5569	1180
Independent Refl.	1591	952	1160
	[R(int) = 0.0387]	[R(int) = 0.0420]	[R(int) = 0.0184
Completeness, %	94	99.9	100
Absorption Method	Numerical	Multi-scan	Multi-scan
Tmax. And Tmin.	0.9590 / 0.8560	1.000 / 0.93763	1.000 / 0.7442
D / R / P**	1591 / 0 / 71	952 / 0 / 85	1180 / 0 / 90
GOF on F2	1.209	1.034	1.05
Final R values [I>2σ(I)]	R1 = 0.0426,	R1 = 0.0443,	R1 = 0.0175,
	wR2 = 0.1013	wR2 = 0.1168	wR2 = 0.0382
R Indices (all data)	R1 = 0.0551,	R1 = 0.0566,	R1 = 0.0179,
	wR2 = 0.1121	wR2 = 0.1261	wR2 = 0.0384
Largest Peak/Hole, e- Å3	0.599 / -0.547	0.792 / -0.224	0.80 / -0.34
Volume Taken, Å3 (%)	308.9 (69.2)	368.4 (67.6)	496.3 (74.5)
Dimensionality	Molecular	Molecular	3D

*-Refinement Method Full-matric least-sq. on F2 ; **-listing of Data, Restraints and Parameters

Appendix A-2 Crystal Structure of H(TCO). The molecular structure of protonated thioamide cyanoxime (HTCO) can be seen in ORTEP representation in Appendix A-2.1 with the crystal and refinement data shown in Appendix A-1.2. This molecule is nearly planar with the two fragments studied in the structure being the *cyano* fragment N2-C3-N3-C1 and the thioamide fragment S1-C3-N3-C1. The dihedral angle between the two is 6.22º (Appendix A-2.1). Supporting this planarity, trigonal planar geometry is found around the three central atoms of the molecule being C1, C3 and N3 with bond angles ranging from 117.28º to 124.62º. Highly interested in the cyanoxime portion of this molecule, the crystallographic data shows that H(TCO) crystallizes in the trans-anti geometry with regards to the sulfur atom placement. Analyzing the fragments further shows the bond angles and bond lengths in the cyanoxime group are consistent with expected and anticipated values. The molecule displays oxime character as the C1-N1 bond length is 1.289 Å which is shorter than the N1-O1 bond of 1.343 Å while the collected data shows typical bond lengths and angles for the *cyano* group. An analysis of the bonds around central carbon atom C3 does indicate that there is likely some electron sharing occurring as the bond lengths between C3-S1 and C3-N3 are closer in distance to published data for double bonds rather than single bonds, being 1.654 Å and 1.313 Å respectively, therefore resonance structures are probable. Appendix A-1.3 summarizes the key structural bond lengths and angles for H(TCO).

Molecules of H(TCO) are packed into the unit cell and held together through two different groups involved in hydrogen bonding. The first and strongest bond is found between the nitrogen atom N2 and the hydrogen atom (H1O1) from the oxime group. Bonding parameters for this system are O1-H1O1---N2 = 1.739 Å with an angle of 170º. The other system is the sulfur atom S1 from the thioamide group and the hydrogen atom (H2N3) from a

neighboring amide group forming a "zig-zag" pattern in the unit cell as seen in Appendix A-2.2**.** Parameters for the H-bonding in the crystal for this system are N-H2N3---S1 = 2.503 Å with a bond angle of 166º. Actual crystal on the diffractometer can be seen in Appendix A-2.3.

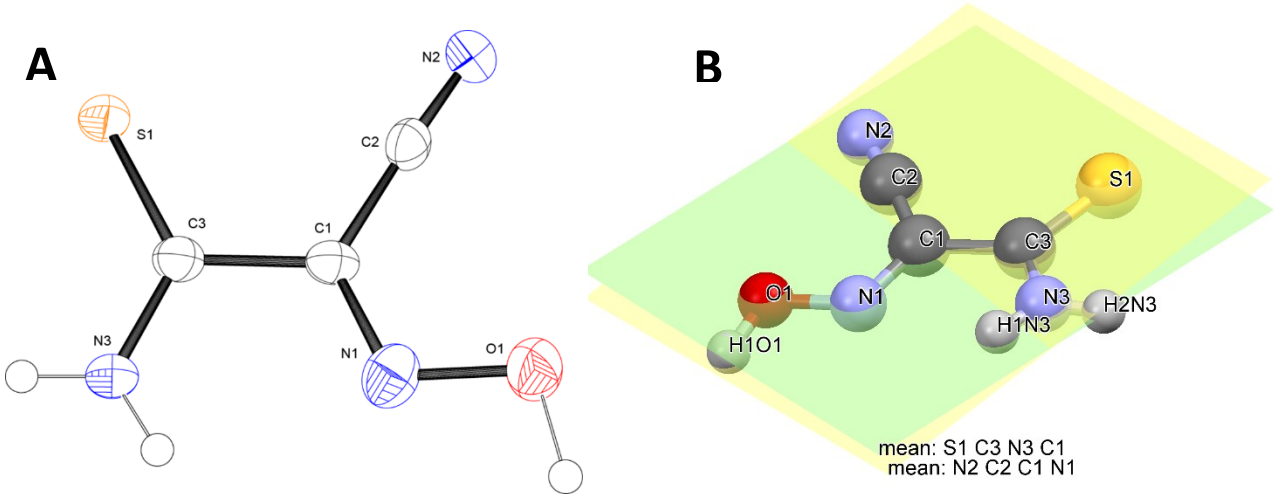

Appendix A-2.1. A - ORTEP view at 50% ellipsoids with atomic labeling of the ASU for H(TCO); **B –** planarity analysis of the H(TCO) molecule.

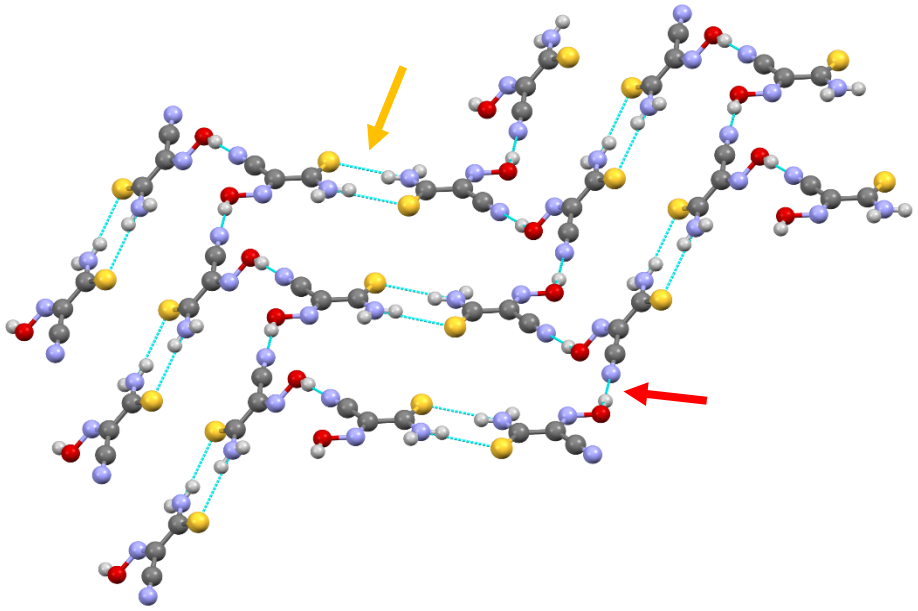

Appendix A-2.2. Crystal packing of H(TCO). Hydrogen bonding with the sulfur atom and hydrogen bonding with the oxygen atom highlighted with blue dashed lines and color coordinated arrows.

Appendix A-3 Crystal Structure of Cs(TCO). The Cs(TCO) complex crystallized out in a monoclinic system and P 1 21/c 1 space group with a formula of $C_3H_2CsN_3OS$. It is highly symmetrical having 27 inversion centers, two gliding planes and six 2-fold screw axes. The ORTEP representation can be seen in Appendix A-2.1 while the crystal and refinement data are presented in Appendix A-1.2.

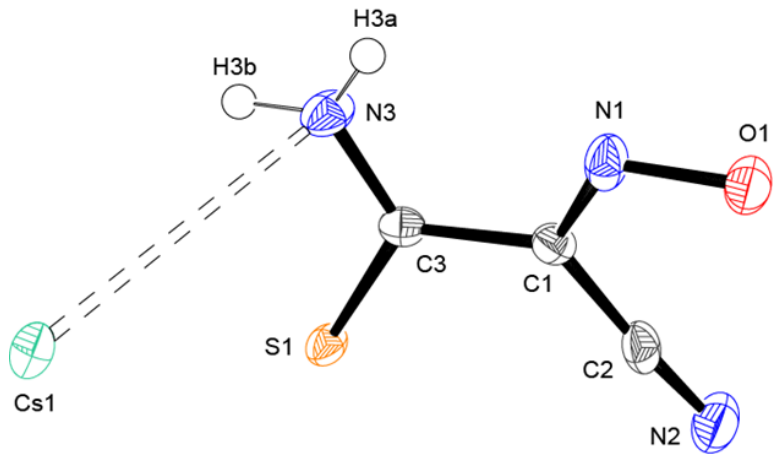

Appendix A-3.1. ORTEP view at 50% ellipsoids with atomic labeling of the ASU for Cs(TCO).

To begin, an overall analysis of the different fragments of this compound was conducted. The *cyano* group was typical with expected bond lengths and bond angles. However, the oxime group shows bond lengths that are typical of *nitroso* character with C1-N1 1.333 Å and N1-O1 1.266 Å. The bond lengths around one of the central carbon atoms C3 indicates a double bond with N3 (1.303 Å). There appears to be some resonance or electron sharing between C3-S1 (1.662 Å) with C3-C1 (1.433 Å) as these listed values in the Cs(TCO) fall between the published typical bond lengths for single and double bonds. Key structural data can be found in Appendix A-1.3.

The ligand portion of this compound has a small dihedral angle between the cyanoxime group N2-C2-C1-N1-O1 and the thioamide group S2-C3-N3 which is 14.11°. (Appendix A-2.2) Additionally, evidence of bond angles typical to trigonal planar geometry are found around the two central carbon atoms, C1 and C3 supporting a planar backbone to the ASU. The cesium atom stands out from the rest of the ASU molecule. A dihedral angle was calculated by comparing a plane including Cs1-N3-C3 with the amide plane (H3a-H3b-N3 C3) and was 63.01° (Appendix A-2.2) revealing how much the Cs1 atom "stands alone".

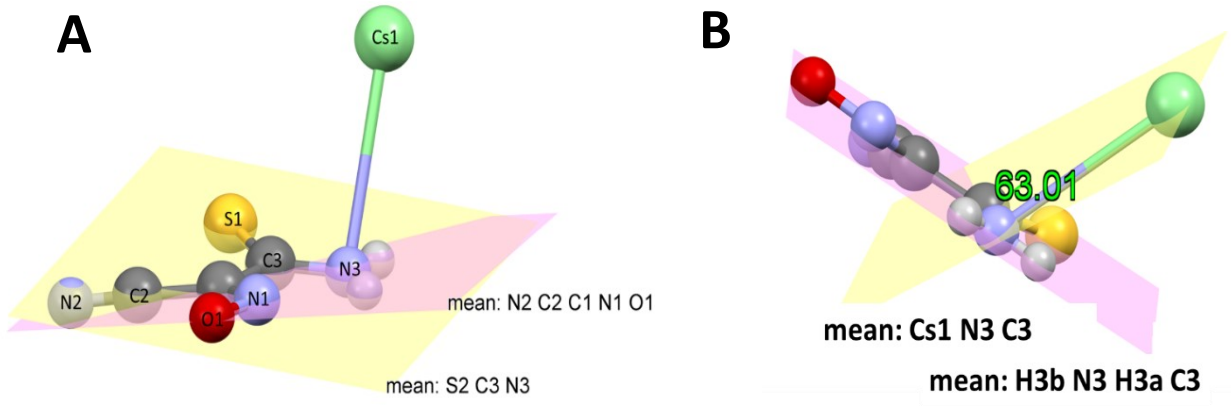

Appendix A-3.2. **A –** dihedral angle between the cyanoxime and the thioamide fragments in Cs(TCO); **B –** dihedral angle between the cesium atom plane and the amide fragment in Cs(TCO).

Isolation of the Cs1 atom removes any steric issues and makes it available for bonding in all directions. This is what happens in the packing of this compound as six different ligands experience long electrostatic interactions with the Cs1 atom giving it a coordination number of 10. (Appendix A-2.3) The TCO ligand is an example of an ampolydentate ligand. Every ligand has different connectivity and with different atoms and can be seen in Appendix A-2.3 where the individual ligands are represented in different colors. **L1** and **L2** acts as a chelator via the O1 and N1 from the oxime group while **L2** additionally has a long bond with C2. The **L5** acts as a

chelator but via the S1 and N2 atoms. The remaining ligands have a single connection to the cesium atom; **L3** via the O1, **L4** via the amide nitrogen atom N3, and the **L6** via the *cyano* nitrogen N2. As these ligands are intricately bound, they are packed into the unit cell as a 3D complex. The integrity of the compound is also held together with hydrogen bonding; N3-H3a---N1 with 2.178 Å bond length and 169.62° angle as well as N3-H3b---S1 with 2.625 Å bond length and 140.41° angle.

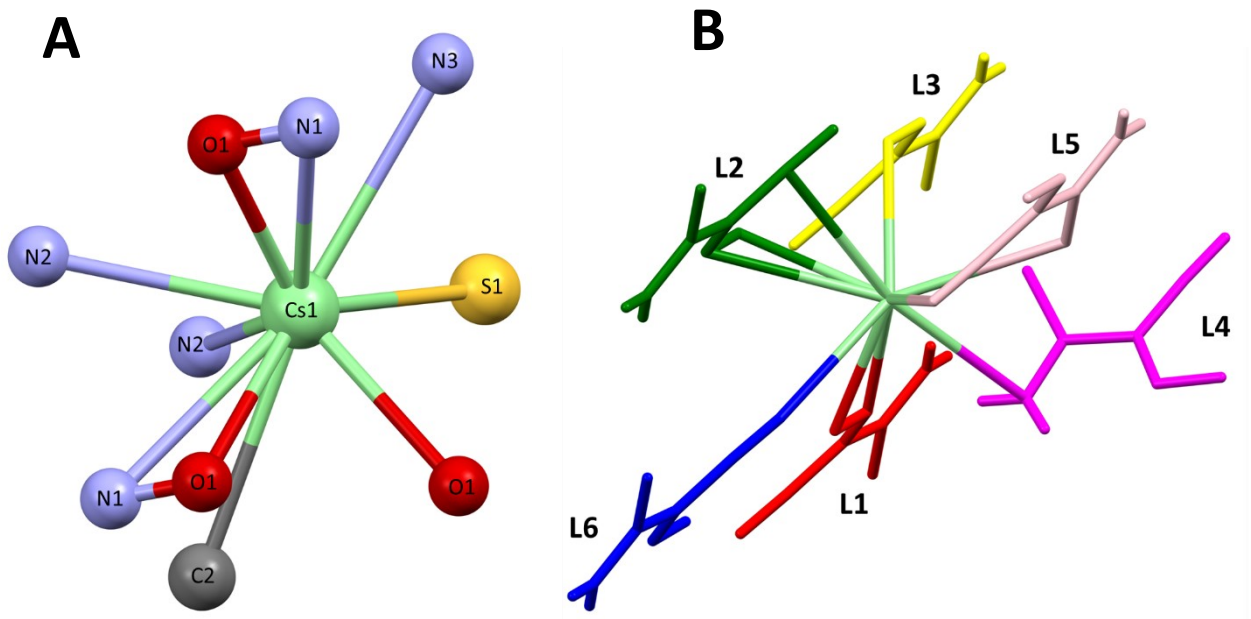

Appendix A-2.3. **A -** Cesium center showing connectivity (CN 10) for the packing of Cs(TCO); **B –** Cesium center showing the six different color coded (TCO) ligands and their varying connectivity for the packing of Cs(TCO).

Appendix B: Crystal checkCIF Reports for Studied Complexes

Appendix B-1. Auxiliary structures of starting compounds: The ligand H(TCO) and its Cs-salt Cs(TCO).

checkCIF/PLATON (basic structural check)

Structure factors have been supplied for datablock(s) HTCO

THIS REPORT IS FOR GUIDANCE ONLY. IF USED AS PART OF A REVIEW PROCEDURE FOR PUBLICATION, IT SHOULD NOT REPLACE THE EXPERTISE OF AN EXPERIENCED CRYSTALLOGRAPHIC REFEREE.

No syntax errors found. CIF dictionary
Please wait while processing .... Interpreting this report
Structure factor report

Datablock: HTCO

```
Bond precision: C-C = 0.0040 A          Wavelength=0.71073
Cell:        a=7.429(2) b=6.987(2)      c=10.757(3)
             alpha=90   beta=102.766(5) gamma=90
Temperature: 120 K
                Calculated                Reported
Volume          544.6(3)                  544.5(3)
Space group     P 21/n                    P 21/n
Hall group      -P 2yn                    -P 2yn
Moiety formula  C3 H3 N3 O S              ?
Sum formula     C3 H3 N3 O S              C3 H3 N3 O S
Mr              129.14                    129.14
Dx,g cm-3       1.575                     1.575
Z               4                         4
Mu (mm-1)       0.485                     0.485
F000            264.0                     264.0
F000'           264.58
h,k,lmax        8,8,12                    8,8,12
Nref            953                       952
Tmin,Tmax       0.948,0.954               0.927,1.000
Tmin'           0.948
Correction method= # Reported T Limits:
Tmin=0.927 Tmax=1.000 AbsCorr = NUMERICAL
Data completeness= 0.999 Theta(max)= 24.997
R(reflections)= 0.0443( 777)          wR2(reflections)=
                                      0.1261( 952)
 S = 1.034         Npar= 85
```

The following ALERTS were generated. Each ALERT has the format
test-name_ALERT_alert-type_alert-level.
Click on the hyperlinks for more details of the test.

Alert level C

PLAT018_ALERT_1_C _diffrn_measured_fraction_theta_max .NE. *_full ! Check
PLAT094_ALERT_2_C Ratio of Maximum / Minimum Residual Density .... 3.54 Report
PLAT355_ALERT_3_C Long O-H (X0.82,N0.98A) O1 - H1O1 . 1.06 Ang.
PLAT975_ALERT_2_C Check Calcd Resid. Dens. 1.02Ang From N1 . 0.76 eA-3

Alert level G

PLAT720_ALERT_4_G Number of Unusual/Non-Standard Labels ..... 3 Note
PLAT883_ALERT_1_G No Info/Value for _atom_sites_solution_primary . Please Do !
PLAT909_ALERT_3_G Percentage of I>2sig(I) Data at Theta(Max) Still 70% Note
PLAT965_ALERT_2_G The SHELXL WEIGHT Optimisation has not Converged Please Check
PLAT967_ALERT_5_G Note: Two-Theta Cutoff Value in Embedded .res .. 50.0 Degree
PLAT978_ALERT_2_G Number C-C Bonds with Positive Residual Density. 1 Info

0 **ALERT level A** = Most likely a serious problem - resolve or explain
0 **ALERT level B** = A potentially serious problem, consider carefully
4 **ALERT level C** = Check. Ensure it is not caused by an omission or oversight
6 **ALERT level G** = General information/check it is not something unexpected

2 ALERT type 1 CIF construction/syntax error, inconsistent or missing data
4 ALERT type 2 Indicator that the structure model may be wrong or deficient
2 ALERT type 3 Indicator that the structure quality may be low
1 ALERT type 4 Improvement, methodology, query or suggestion
1 ALERT type 5 Informative message, check

PLATON version of 12/09/2022; check.def file version of 09/08/2022

Datablock HTCO - ellipsoid plot

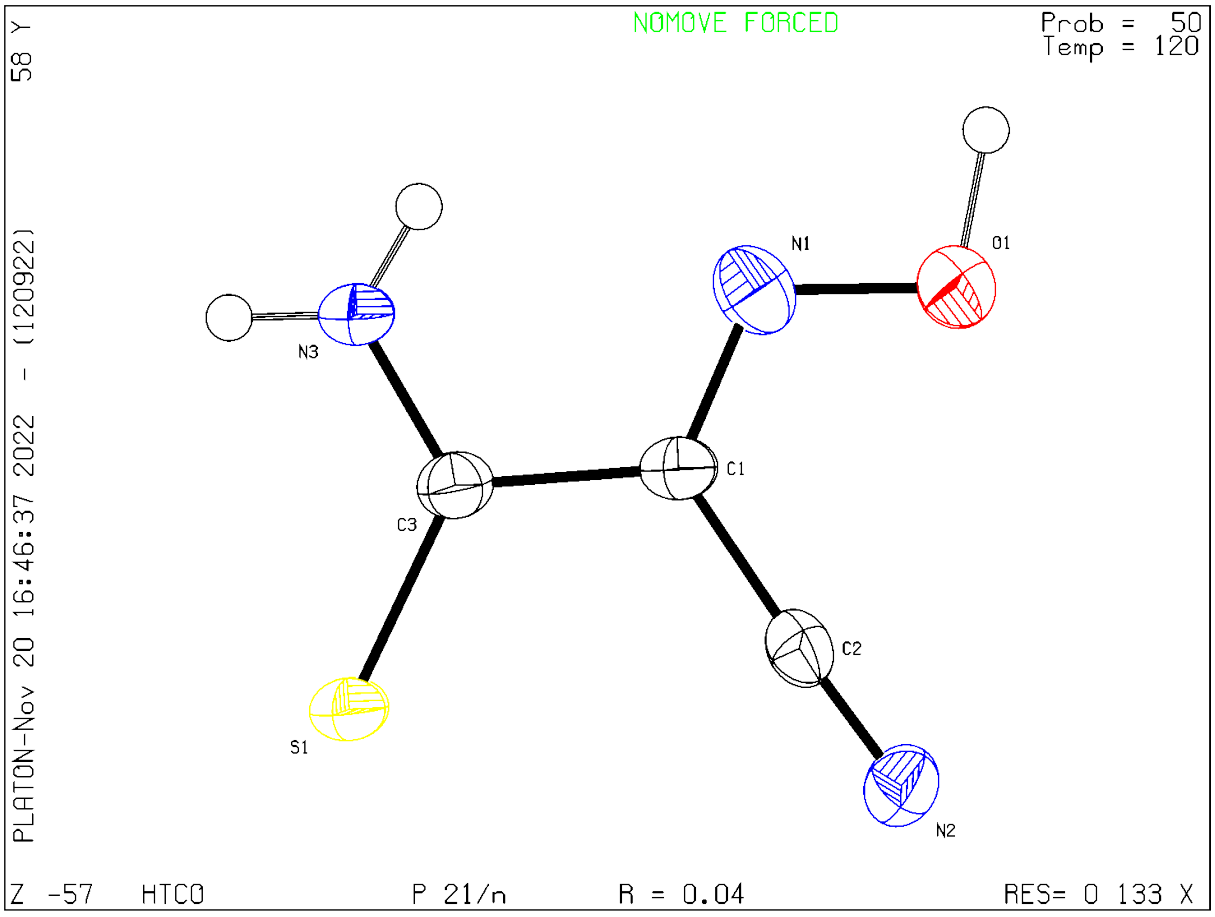

Download CIF editor (publCIF) from the IUCr
Download CIF editor (enCIFer) from the CCDC
Test a new CIF entry

checkCIF/PLATON (basic structural check)

Structure factors have been supplied for datablock(s) CsTCO

THIS REPORT IS FOR GUIDANCE ONLY. IF USED AS PART OF A REVIEW PROCEDURE FOR PUBLICATION, IT SHOULD NOT REPLACE THE EXPERTISE OF AN EXPERIENCED CRYSTALLOGRAPHIC REFEREE.

No syntax errors found. CIF dictionary
Please wait while processing .... Interpreting this report
Structure factor report

Datablock: CsTCO

```
Bond precision:  C-C = 0.0050 A          Wavelength=0.71073
Cell:         a=5.384(9) b=7.299(12)   c=17.07(3)
              alpha=90   beta=96.61(3) gamma=90
Temperature: 100 K
                Calculated                Reported
Volume          666(2)                    666.4(19)
Space group     P 21/c                    P 1 21/c 1
Hall group      -P 2ybc                   -P 2ybc
Moiety formula  C3 H2 Cs N3 O S           C3 H2 Cs N3 O S
Sum formula     C3 H2 Cs N3 O S           C3 H2 Cs N3 O S
Mr              261.05                    261.04
Dx,g cm-3       2.604                     2.602
Z               4                         4
Mu (mm-1)       5.789                     5.786
F000            480.0                     479.7
F000'           479.14
h,k,lmax        6,8,20                    6,8,20
Nref            1180                      1180
Tmin,Tmax                                 0.744,1.000
Tmin'
Correction method= # Reported T Limits:
Tmin=0.744 Tmax=1.000 AbsCorr = MULTI-SCAN
Data completeness= 1.000 Theta(max)= 25.000
R(reflections)= 0.0175( 1160)          wR2(reflections)=
                                       0.0384( 1180)
 S = 1.050          Npar= 90
```

The following ALERTS were generated. Each ALERT has the format
test-name_ALERT_alert-type_alert-level.
Click on the hyperlinks for more details of the test.

Alert level B

PLAT230_ALERT_2_B Hirshfeld Test Diff for N1 --C1 . 8.0 s.u.

Alert level C

PLAT053_ALERT_1_C Minimum Crystal Dimension Missing (or Error) ... Please Check
PLAT054_ALERT_1_C Medium Crystal Dimension Missing (or Error) ... Please Check
PLAT055_ALERT_1_C Maximum Crystal Dimension Missing (or Error) ... Please Check
PLAT094_ALERT_2_C Ratio of Maximum / Minimum Residual Density .... 2.34 Report
PLAT148_ALERT_3_C s.u. on the a - Axis is (Too) Large .... 0.009 Ang.
And 2 other PLAT148 Alerts
More ...

Alert level G

PLAT003_ALERT_2_G Number of Uiso or Uij Restrained non-H Atoms ... 9 Report
PLAT004_ALERT_5_G Polymeric Structure Found with Maximum Dimension 3 Info
PLAT068_ALERT_1_G Reported F000 Differs from Calcd (or Missing)... Please Check
PLAT187_ALERT_4_G The CIF-Embedded .res File Contains RIGU Records 1 Report
PLAT769_ALERT_4_G CIF Embedded explicitly supplied scattering data Please Note
PLAT780_ALERT_1_G Coordinates do not Form a Properly Connected Set Please Do !
PLAT909_ALERT_3_G Percentage of I>2sig(I) Data at Theta(Max) Still 96% Note
PLAT961_ALERT_5_G Dataset Contains no Negative Intensities ..... Please Check
PLAT967_ALERT_5_G Note: Two-Theta Cutoff Value in Embedded .res .. 50.0 Degree
PLAT978_ALERT_2_G Number C-C Bonds with Positive Residual Density. 1 Info
PLAT982_ALERT_1_G The Cs-f'= -0.2534 Deviates from IT-value = -0.3680 Check
PLAT983_ALERT_1_G The Cs-f"= 2.1896 Deviates from IT-Value = 2.1192 Check
PLAT983_ALERT_1_G The S-f"= 0.1244 Deviates from IT-Value = 0.1234 Check

---

0 **ALERT level A** = Most likely a serious problem - resolve or explain
1 **ALERT level B** = A potentially serious problem, consider carefully
7 **ALERT level C** = Check. Ensure it is not caused by an omission or oversight
13 **ALERT level G** = General information/check it is not something unexpected

8 ALERT type 1 CIF construction/syntax error, inconsistent or missing data
4 ALERT type 2 Indicator that the structure model may be wrong or deficient
4 ALERT type 3 Indicator that the structure quality may be low
2 ALERT type 4 Improvement, methodology, query or suggestion
3 ALERT type 5 Informative message, check

PLATON version of 12/09/2022; check.def file version of 09/08/2022

Datablock CsTCO - ellipsoid plot

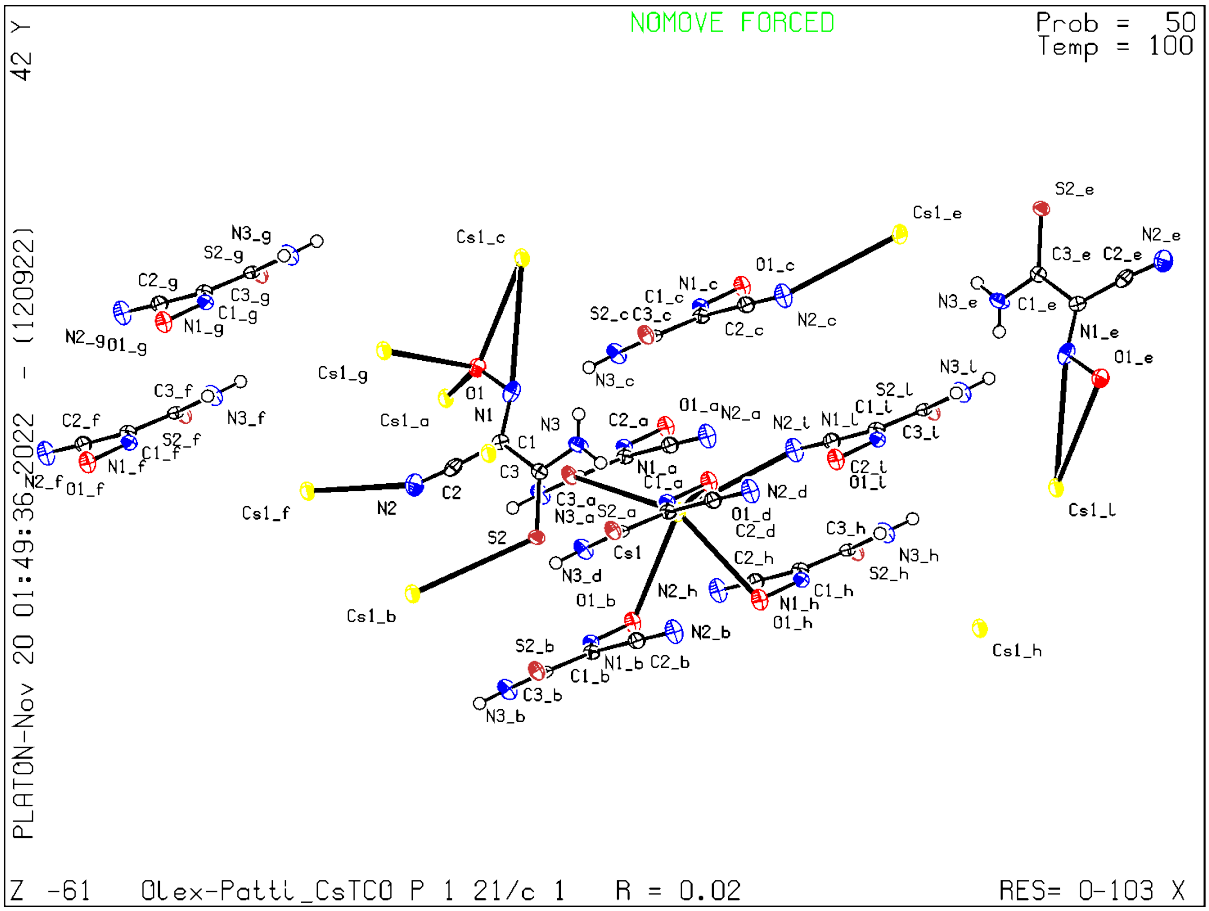

Download CIF editor (publCIF) from the IUCr
Download CIF editor (enCIFer) from the CCDC
Test a new CIF entry

Appendix B-2. Structures of principal compounds obtained in this thesis.

checkCIF/PLATON (basic structural check)

Structure factors have been supplied for datablock(s) Pb4(OH)3(PipCO)3(NO3)2(H2O)

THIS REPORT IS FOR GUIDANCE ONLY. IF USED AS PART OF A REVIEW PROCEDURE FOR PUBLICATION, IT SHOULD NOT REPLACE THE EXPERTISE OF AN EXPERIENCED CRYSTALLOGRAPHIC REFEREE.

No syntax errors found. CIF dictionary
Please wait while processing .... Interpreting this report
Structure factor report

Datablock: Pb4(OH)3(PipCO)3(NO3)2(H2O)

Bond precision: C-C = 0.0158 A Wavelength=1.54184

Cell: a=16.2866(2) b=14.9728(2) c=15.7834(2)
alpha=90 beta=90.8176(13) gamma=90

Temperature: 100 K

	Calculated	Reported
Volume	3848.49(9)	3848.48(10)
Space group	P 21/c	P 21/c
Hall group	-P 2ybc	-P 2ybc
Moiety formula	C24 H35 N11 O16 Pb4	?
Sum formula	C24 H35 N11 O16 Pb4	C24 H35 N11 O16 Pb4
Mr	1562.43	1562.39
Dx,g cm-3	2.697	2.697
Z	4	4
Mu (mm-1)	34.107	34.107
F000	2848.0	2848.0
F000'	2791.38	
h,k,lmax	19,18,19	19,18,19
Nref	7382	7291
Tmin,Tmax		0.489,0.755
Tmin'		

Correction method= # Reported T Limits:
Tmin=0.489 Tmax=0.755 AbsCorr = MULTI-SCAN

Data completeness= 0.988 Theta(max)= 70.574

R(reflections)= 0.0447(6562) wR2(reflections)= 0.1131(7291)

S = 1.060 Npar= 516

The following ALERTS were generated. Each ALERT has the format
test-name_ALERT_alert-type_alert-level.
Click on the hyperlinks for more details of the test.

Alert level A

PLAT971_ALERT_2_A Check Calcd Resid. Dens. 0.90Ang From Pb3 5.48 eA-3
And 7 other PLAT971 Alerts
More ...
PLAT973_ALERT_2_A Check Calcd Positive Resid. Density on Pb3 3.09 eA-3
And 3 other PLAT973 Alerts
More ...

Alert level B

PLAT094_ALERT_2_B Ratio of Maximum / Minimum Residual Density .... 4.28 Report
PLAT780_ALERT_1_B Coordinates do not Form a Properly Connected Set Please Do !

Alert level C

PLAT018_ALERT_1_C _diffrn_measured_fraction_theta_max .NE. *_full ! Check
PLAT053_ALERT_1_C Minimum Crystal Dimension Missing (or Error) ... Please Check
PLAT054_ALERT_1_C Medium Crystal Dimension Missing (or Error) ... Please Check
PLAT055_ALERT_1_C Maximum Crystal Dimension Missing (or Error) ... Please Check
PLAT222_ALERT_3_C NonSolvent Resd 1 H Uiso(max)/Uiso(min) Range 10.0 Ratio
PLAT241_ALERT_2_C High 'MainMol' Ueq as Compared to Neighbors of C14 Check
PLAT242_ALERT_2_C Low 'MainMol' Ueq as Compared to Neighbors of N2AN Check
PLAT245_ALERT_2_C U(iso) H2BR Smaller than U(eq) O2BR by 0.017 Ang**2
PLAT245_ALERT_2_C U(iso) H16C Smaller than U(eq) O1W by 0.039 Ang**2
PLAT342_ALERT_3_C Low Bond Precision on C-C Bonds ..... 0.01578 Ang.
PLAT355_ALERT_3_C Long O-H (X0.82,N0.98A) O1W - H16D . 1.04 Ang.
PLAT911_ALERT_3_C Missing FCF Refl Between Thmin & STh/L= 0.600 3 Report
PLAT971_ALERT_2_C Check Calcd Resid. Dens. 2.96Ang From O6AN 2.01 eA-3
And 4 other PLAT971 Alerts
More ...

Alert level G

PLAT004_ALERT_5_G Polymeric Structure Found with Maximum Dimension 3 Info
PLAT303_ALERT_2_G Full Occupancy Atom H1BR with # Connections 2.00 Check
And 2 other PLAT303 Alerts
More ...
PLAT480_ALERT_4_G Long H...A H-Bond Reported H8A ..O1AN . 2.61 Ang.
And 5 other PLAT480 Alerts
More ...
PLAT720_ALERT_4_G Number of Unusual/Non-Standard Labels ..... 14 Note
PLAT794_ALERT_5_G Tentative Bond Valency for Pb1 (II) . 2.17 Info
And 3 other PLAT794 Alerts
More ...
PLAT883_ALERT_1_G No Info/Value for _atom_sites_solution_primary . Please Do !
PLAT910_ALERT_3_G Missing # of FCF Reflection(s) Below Theta(Min). 1 Note
PLAT912_ALERT_4_G Missing # of FCF Reflections Above STh/L= 0.600 87 Note
PLAT913_ALERT_3_G Missing # of Very Strong Reflections in FCF .... 1 Note
PLAT933_ALERT_2_G Number of HKL-OMIT Records in Embedded .res File 3 Note
PLAT941_ALERT_3_G Average HKL Measurement Multiplicity ..... 4.8 Low
PLAT978_ALERT_2_G Number C-C Bonds with Positive Residual Density. 0 Info

12 **ALERT level A** = Most likely a serious problem - resolve or explain
2 **ALERT level B** = A potentially serious problem, consider carefully
17 **ALERT level C** = Check. Ensure it is not caused by an omission or oversight
22 **ALERT level G** = General information/check it is not something unexpected

6 ALERT type 1 CIF construction/syntax error, inconsistent or missing data
27 ALERT type 2 Indicator that the structure model may be wrong or deficient
7 ALERT type 3 Indicator that the structure quality may be low
8 ALERT type 4 Improvement, methodology, query or suggestion
5 ALERT type 5 Informative message, check

PLATON version of 12/09/2022; check.def file version of 09/08/2022

Datablock Pb4(OH)3(PipCO)3(NO3)2(H2O) - ellipsoid plot

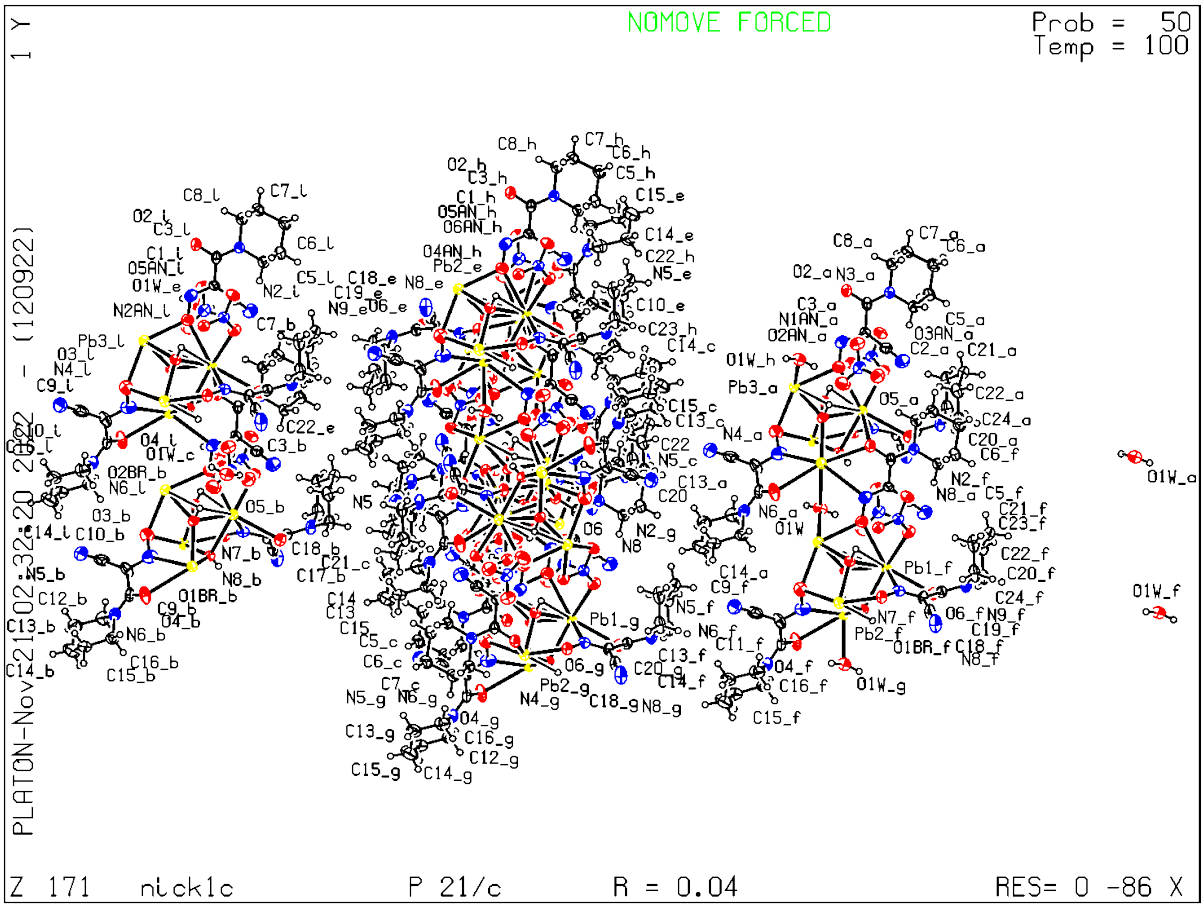

Download CIF editor (publCIF) from the IUCr
Download CIF editor (enCIFer) from the CCDC
Test a new CIF entry

checkCIF/PLATON (basic structural check)

Structure factors have been supplied for datablock(s) Pb3-H2PCO6-2PCO6

THIS REPORT IS FOR GUIDANCE ONLY. IF USED AS PART OF A REVIEW PROCEDURE FOR PUBLICATION, IT SHOULD NOT REPLACE THE EXPERTISE OF AN EXPERIENCED CRYSTALLOGRAPHIC REFEREE.

No syntax errors found. CIF dictionary
Please wait while processing .... Interpreting this report
Structure factor report

Datablock: Pb3-H2PCO6-2PCO6

```
Bond precision:  C-C = 0.0156 A          Wavelength=0.71073
Cell:         a=24.284(5) b=9.2688(19)    c=38.955(8)
              alpha=90    beta=106.587(3) gamma=90
Temperature: 120 K
                Calculated                Reported
Volume          8403(3)                   8403(3)
Space group     C 2/c                     C 2/c
Hall group      -C 2yc                    -C 2yc
Moiety formula  C28 H18 N12 O4 Pb         ?
Sum formula     C28 H18 N12 O4 Pb         C84 H54 N36 O12 Pb3
Mr              793.74                    2381.20
Dx,g cm-3       1.882                     1.882
Z               12                        4
Mu (mm-1)       6.083                     6.083
F000            4608.0                    4608.0
F000'           4569.71
h,k,lmax        34,13,55                  29,13,54
Nref            12617                     5996
Tmin,Tmax       0.343,0.506               0.450,0.746
Tmin'           0.266
Correction method= # Reported T Limits:
Tmin=0.450 Tmax=0.746 AbsCorr = MULTI-SCAN
Data completeness= 0.475 Theta(max)= 30.311
R(reflections)= 0.0790( 3489)          wR2(reflections)=
                                       0.1320( 5996)
 S = 1.034          Npar= 617
```

The following ALERTS were generated. Each ALERT has the format
test-name_ALERT_alert-type_alert-level.
Click on the hyperlinks for more details of the test.

Alert level A

PLAT029_ALERT_3_A _diffrn_measured_fraction_theta_full value Low . 0.635 Why?
PLAT881_ALERT_1_A No Datum for _diffrn_reflns_av_R_equivalents ... Please Do !

Alert level B

PLAT911_ALERT_3_B Missing FCF Refl Between Thmin & STh/L= 0.600 2778 Report
PLAT973_ALERT_2_B Check Calcd Positive Resid. Density on Pb2 1.79 eA-3

Alert level C

PLAT088_ALERT_3_C Poor Data / Parameter Ratio ..... 9.72 Note
PLAT213_ALERT_2_C Atom C10 has ADP max/min Ratio ..... 3.4 oblate
PLAT220_ALERT_2_C NonSolvent Resd 1 C Ueq(max)/Ueq(min) Range 4.1 Ratio
PLAT342_ALERT_3_C Low Bond Precision on C-C Bonds ..... 0.01564 Ang.
PLAT906_ALERT_3_C Large K Value in the Analysis of Variance ..... 34.758 Check
And 3 other PLAT906 Alerts
More ...
PLAT971_ALERT_2_C Check Calcd Resid. Dens. 0.25Ang From Pb1 1.55 eA-3
PLAT971_ALERT_2_C Check Calcd Resid. Dens. 1.07Ang From Pb1 1.54 eA-3
PLAT977_ALERT_2_C Check Negative Difference Density on H6 . -0.34 eA-3
PLAT977_ALERT_2_C Check Negative Difference Density on H20 . -0.37 eA-3

Alert level G

PLAT002_ALERT_2_G Number of Distance or Angle Restraints on AtSite 6 Note
PLAT003_ALERT_2_G Number of Uiso or Uij Restrained non-H Atoms ... 68 Report
PLAT007_ALERT_5_G Number of Unrefined Donor-H Atoms ..... 4 Report
PLAT045_ALERT_1_G Calculated and Reported Z Differ by a Factor ... 3 Check
PLAT083_ALERT_2_G SHELXL Second Parameter in WGHT Unusually Large 78.27 Why ?
PLAT164_ALERT_4_G Nr. of Refined C-H H-Atoms in Heavy-Atom Struct. 1 Note
PLAT172_ALERT_4_G The CIF-Embedded .res File Contains DFIX Records 2 Report
PLAT173_ALERT_4_G The CIF-Embedded .res File Contains DANG Records 2 Report
PLAT186_ALERT_4_G The CIF-Embedded .res File Contains ISOR Records 1 Report
PLAT300_ALERT_4_G Atom Site Occupancy of H6O6 Constrained at 0.5 Check
PLAT300_ALERT_4_G Atom Site Occupancy of H7O7 Constrained at 0.5 Check
PLAT720_ALERT_4_G Number of Unusual/Non-Standard Labels ..... 2 Note
PLAT794_ALERT_5_G Tentative Bond Valency for Pb1 (II) . 2.31 Info
PLAT860_ALERT_3_G Number of Least-Squares Restraints ..... 412 Note
PLAT883_ALERT_1_G No Info/Value for _atom_sites_solution_primary . Please Do !
PLAT910_ALERT_3_G Missing # of FCF Reflection(s) Below Theta(Min). 1 Note
PLAT912_ALERT_4_G Missing # of FCF Reflections Above STh/L= 0.600 3840 Note
PLAT933_ALERT_2_G Number of HKL-OMIT Records in Embedded .res File 20 Note
PLAT941_ALERT_3_G Average HKL Measurement Multiplicity ..... 1.0 Low
PLAT950_ALERT_5_G Calculated (ThMax) and CIF-Reported Hmax Differ 5 Units
PLAT953_ALERT_1_G Reported (CIF) and Actual (FCF) Hmax Differ by . 5 Units
PLAT961_ALERT_5_G Dataset Contains no Negative Intensities ..... Please Check
PLAT965_ALERT_2_G The SHELXL WEIGHT Optimisation has not Converged Please Check
PLAT978_ALERT_2_G Number C-C Bonds with Positive Residual Density. 0 Info

2 **ALERT level A** = Most likely a serious problem - resolve or explain
2 **ALERT level B** = A potentially serious problem, consider carefully
12 **ALERT level C** = Check. Ensure it is not caused by an omission or oversight
24 **ALERT level G** = General information/check it is not something unexpected

4 ALERT type 1 CIF construction/syntax error, inconsistent or missing data
13 ALERT type 2 Indicator that the structure model may be wrong or deficient
11 ALERT type 3 Indicator that the structure quality may be low
8 ALERT type 4 Improvement, methodology, query or suggestion
4 ALERT type 5 Informative message, check

PLATON version of 12/09/2022; check.def file version of 09/08/2022

Datablock Pb3-H2PCO6-2PCO6 - ellipsoid plot

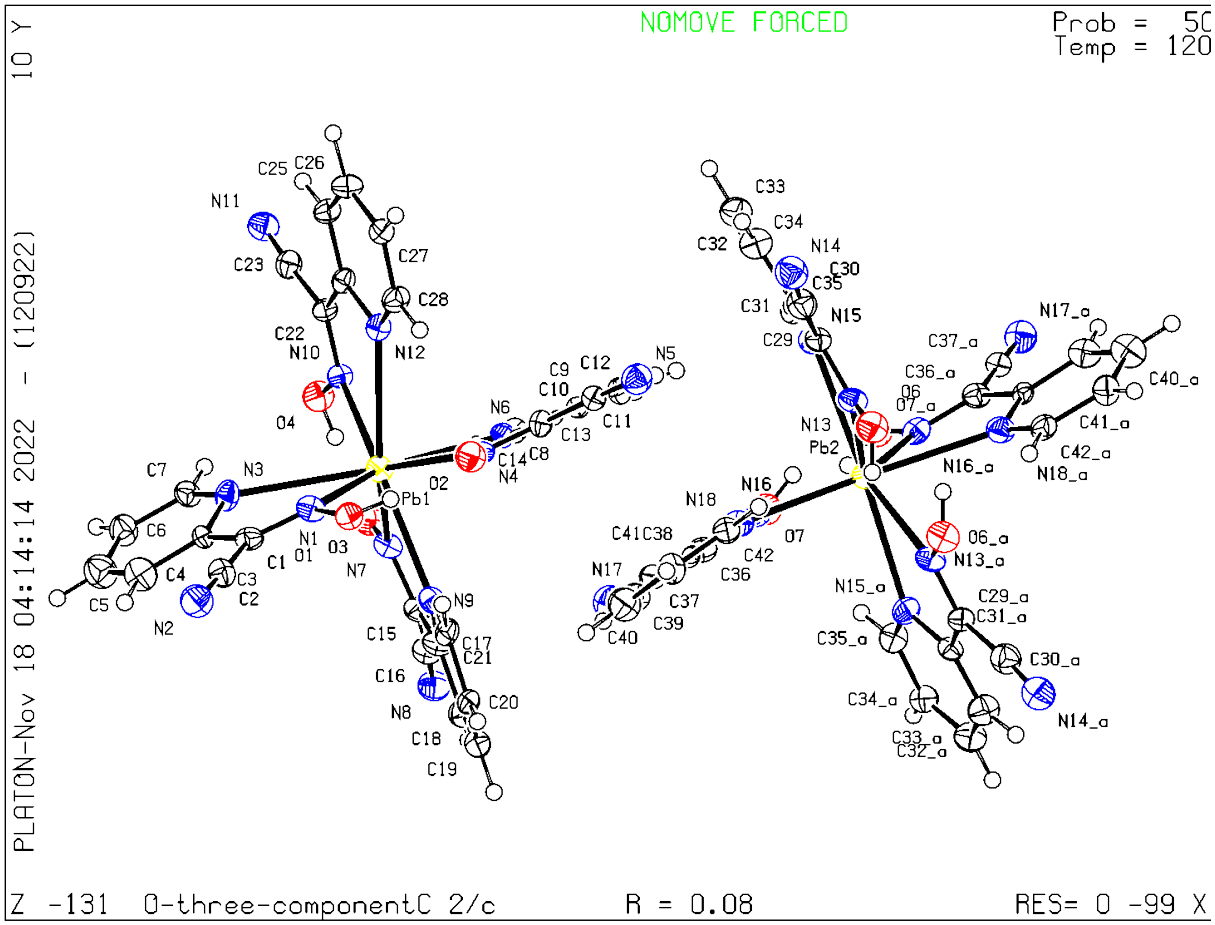

Download CIF editor (publCIF) from the IUCr
Download CIF editor (enCIFer) from the CCDC
Test a new CIF entry

checkCIF/PLATON (basic structural check)

Structure factors have been supplied for datablock(s) Pb_DCO_NO3_system

THIS REPORT IS FOR GUIDANCE ONLY. IF USED AS PART OF A REVIEW PROCEDURE FOR PUBLICATION, IT SHOULD NOT REPLACE THE EXPERTISE OF AN EXPERIENCED CRYSTALLOGRAPHIC REFEREE.

No syntax errors found. CIF dictionary
Please wait while processing .... Interpreting this report
Structure factor report

Datablock: Pb_DCO_NO3_system

```
Bond precision: C-C = 0.0125 A          Wavelength=0.71073
Cell:        a=7.9470(4)     b=13.8353(7)   c=14.6259(8)
             alpha=92.001(2) beta=92.280(2) gamma=100.625(2)
Temperature: 100 K
                Calculated                Reported
Volume          1577.82(14)               1577.82(14)
Space group     P -1                      P -1
Hall group      -P 1                      -P 1
Moiety formula  C20 H25 N13 O12 Pb3       ?
Sum formula     C20 H25 N13 O12 Pb3       C20 H25 N13 O12 Pb3
Mr              1261.13                   1261.10
Dx,g cm-3       2.655                     2.654
Z               2                         2
Mu (mm-1)       16.046                    16.046
F000            1156.0                    1156.0
F000'           1137.32
h,k,lmax        11,19,20                  11,19,20
Nref            8920                      8775
Tmin,Tmax       0.328,0.852               0.462,0.746
Tmin'           0.011
Correction method= # Reported T Limits:
Tmin=0.462 Tmax=0.746 AbsCorr = MULTI-SCAN
Data completeness= 0.984 Theta(max)= 29.655
R(reflections)= 0.0439( 6397)          wR2(reflections)=
                                       0.0830( 8775)
S = 1.031          Npar= 451
```

The following ALERTS were generated. Each ALERT has the format
test-name_ALERT_alert-type_alert-level.
Click on the hyperlinks for more details of the test.

Alert level B

PLAT971_ALERT_2_B Check Calcd Resid. Dens. 0.98Ang From O1 2.58 eA-3

Alert level C

PLAT220_ALERT_2_C NonSolvent Resd 1 N Ueq(max)/Ueq(min) Range 3.2 Ratio
PLAT241_ALERT_2_C High 'MainMol' Ueq as Compared to Neighbors of O5 Check
PLAT342_ALERT_3_C Low Bond Precision on C-C Bonds ..... 0.0125 Ang.
PLAT906_ALERT_3_C Large K Value in the Analysis of Variance ..... 2.513 Check
PLAT910_ALERT_3_C Missing # of FCF Reflection(s) Below Theta(Min). 5 Note
PLAT911_ALERT_3_C Missing FCF Refl Between Thmin & STh/L= 0.600 14 Report
PLAT971_ALERT_2_C Check Calcd Resid. Dens. 0.72Ang From O2 2.49 eA-3
And 9 other PLAT971 Alerts
More ...
PLAT972_ALERT_2_C Check Calcd Resid. Dens. 0.87Ang From Pb3 -1.95 eA-3
And 2 other PLAT972 Alerts
More ...
PLAT977_ALERT_2_C Check Negative Difference Density on H01J . -0.49 eA-3
And 3 other PLAT977 Alerts
More ...

Alert level G

PLAT002_ALERT_2_G Number of Distance or Angle Restraints on AtSite 6 Note
PLAT003_ALERT_2_G Number of Uiso or Uij Restrained non-H Atoms ... 50 Report
PLAT004_ALERT_5_G Polymeric Structure Found with Maximum Dimension 1 Info
PLAT083_ALERT_2_G SHELXL Second Parameter in WGHT Unusually Large 5.43 Why ?
PLAT154_ALERT_1_G The s.u.'s on the Cell Angles are Equal ..(Note) 0.002 Degree
PLAT171_ALERT_4_G The CIF-Embedded .res File Contains EADP Records 2 Report
PLAT172_ALERT_4_G The CIF-Embedded .res File Contains DFIX Records 1 Report
PLAT176_ALERT_4_G The CIF-Embedded .res File Contains SADI Records 1 Report
PLAT186_ALERT_4_G The CIF-Embedded .res File Contains ISOR Records 1 Report
PLAT232_ALERT_2_G Hirshfeld Test Diff (M-X) Pb1 --O1 . 6.7 s.u.
And 6 other PLAT232 Alerts
More ...
PLAT300_ALERT_4_G Atom Site Occupancy of O8A Constrained at 0.55 Check
And 3 other PLAT300 Alerts
More ...
PLAT301_ALERT_3_G Main Residue Disorder .....(Resd 1) 4% Note
PLAT303_ALERT_2_G Full Occupancy Atom H1BR with # Connections 2.00 Check
PLAT720_ALERT_4_G Number of Unusual/Non-Standard Labels ..... 27 Note
PLAT860_ALERT_3_G Number of Least-Squares Restraints ..... 302 Note
PLAT883_ALERT_1_G No Info/Value for _atom_sites_solution_primary . Please Do !
PLAT912_ALERT_4_G Missing # of FCF Reflections Above STh/L= 0.600 126 Note
PLAT933_ALERT_2_G Number of HKL-OMIT Records in Embedded .res File 6 Note
PLAT941_ALERT_3_G Average HKL Measurement Multiplicity ..... 2.8 Low
PLAT965_ALERT_2_G The SHELXL WEIGHT Optimisation has not Converged Please Check
PLAT978_ALERT_2_G Number C-C Bonds with Positive Residual Density. 1 Info

---

0 **ALERT level A** = Most likely a serious problem - resolve or explain
1 **ALERT level B** = A potentially serious problem, consider carefully
23 **ALERT level C** = Check. Ensure it is not caused by an omission or oversight
30 **ALERT level G** = General information/check it is not something unexpected

2 ALERT type 1 CIF construction/syntax error, inconsistent or missing data
34 ALERT type 2 Indicator that the structure model may be wrong or deficient
7 ALERT type 3 Indicator that the structure quality may be low
10 ALERT type 4 Improvement, methodology, query or suggestion
1 ALERT type 5 Informative message, check

PLATON version of 12/09/2022; check.def file version of 09/08/2022

Datablock Pb_DCO_NO3_system - ellipsoid plot

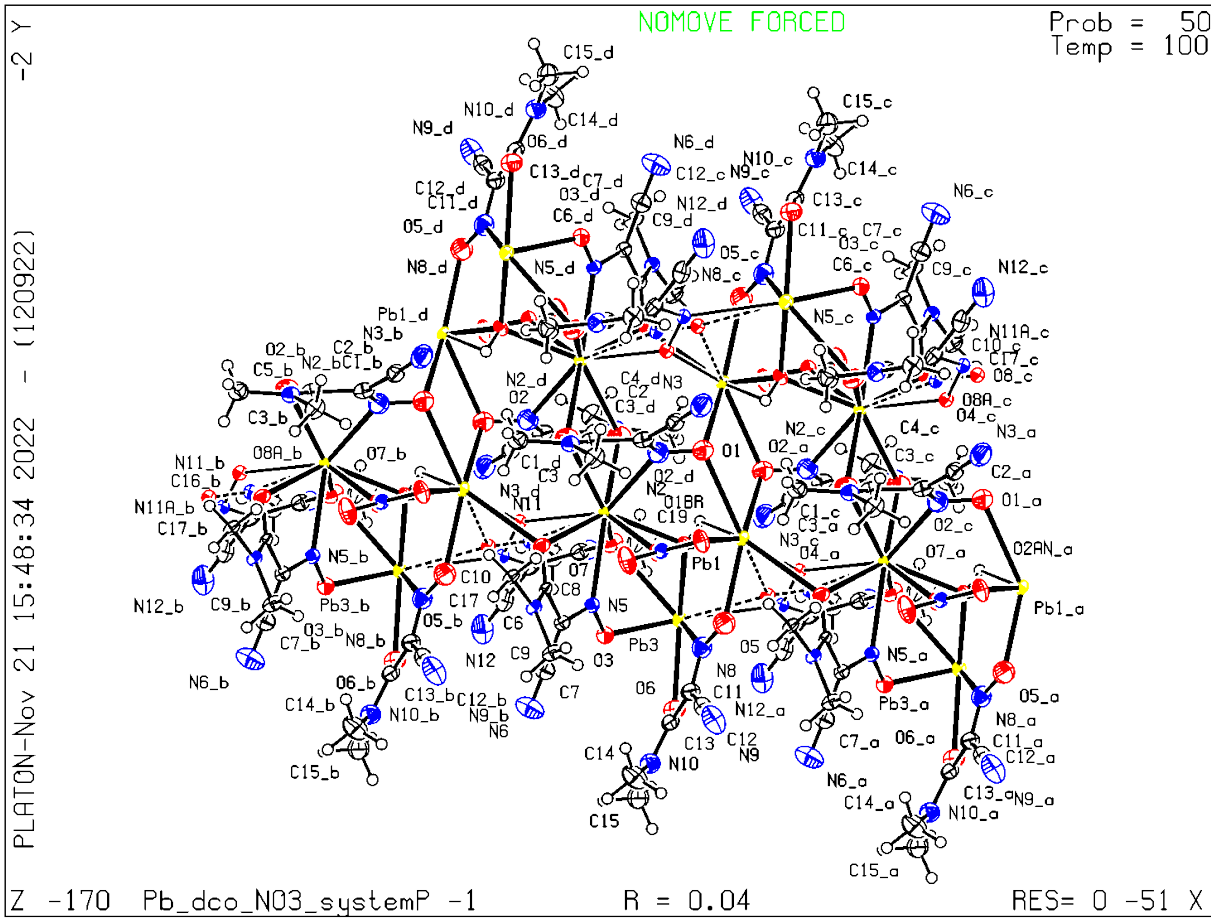

Download CIF editor (publCIF) from the IUCr
Download CIF editor (enCIFer) from the CCDC
Test a new CIF entry

checkCIF/PLATON (basic structural check)

Structure factors have been supplied for datablock(s) Pb3(2PCO)4(NO3)2

THIS REPORT IS FOR GUIDANCE ONLY. IF USED AS PART OF A REVIEW PROCEDURE FOR PUBLICATION, IT SHOULD NOT REPLACE THE EXPERTISE OF AN EXPERIENCED CRYSTALLOGRAPHIC REFEREE.

No syntax errors found. CIF dictionary
Please wait while processing .... Interpreting this report
Structure factor report

Datablock: Pb3(2PCO)4(NO3)2

Bond precision: C-C = 0.0203 A Wavelength=0.71073

Cell: a=9.3579(13) b=14.038(2) c=14.627(2)
alpha=99.849(2) beta=101.511(2) gamma=107.829(2)

Temperature: 100 K

	Calculated	Reported
Volume	1736.0(4)	1736.0(4)
Space group	P -1	P -1
Hall group	-P 1	-P 1
Moiety formula	C28 H16 N14 O10 Pb3	?
Sum formula	C28 H16 N14 O10 Pb3	C14 H8 N7 O5 Pb1.50
Mr	1330.15	665.06
Dx,g cm-3	2.545	2.545
Z	2	4
Mu (mm-1)	14.589	14.588
F000	1216.0	1216.0
F000'	1197.24	
h,k,lmax	11,17,18	11,17,18
Nref	7115	7099
Tmin,Tmax	0.048,0.335	0.516,0.745
Tmin'	0.021	

Correction method= # Reported T Limits:
Tmin=0.516 Tmax=0.745 AbsCorr = MULTI-SCAN

Data completeness= 0.998 Theta(max)= 26.377

R(reflections)= 0.0497(4476) wR2(reflections)= 0.1210(7099)

S = 0.966 Npar= 496

The following ALERTS were generated. Each ALERT has the format
test-name_ALERT_alert-type_alert-level.
Click on the hyperlinks for more details of the test.

Alert level A

PLAT973_ALERT_2_A Check Calcd Positive Resid. Density on Pb1 2.36 eA-3
PLAT973_ALERT_2_A Check Calcd Positive Resid. Density on Pb3 2.29 eA-3

Alert level B

PLAT213_ALERT_2_B Atom C28 has ADP max/min Ratio ..... 4.6 oblate
PLAT342_ALERT_3_B Low Bond Precision on C-C Bonds ..... 0.02033 Ang.
PLAT971_ALERT_2_B Check Calcd Resid. Dens. 1.17Ang From O4AN 3.07 eA-3
PLAT973_ALERT_2_B Check Calcd Positive Resid. Density on Pb2 1.93 eA-3

Alert level C

PLAT234_ALERT_4_C Large Hirshfeld Difference Pb1 --O5AN_a . 0.19 Ang.
And 5 other PLAT234 Alerts
More ...
PLAT241_ALERT_2_C High 'MainMol' Ueq as Compared to Neighbors of O3 Check
And 2 other PLAT241 Alerts
More ...
PLAT911_ALERT_3_C Missing FCF Refl Between Thmin & STh/L= 0.600 5 Report
PLAT925_ALERT_1_C The Reported and Calculated Rho(max) Differ by . 1.17 eA-3
PLAT971_ALERT_2_C Check Calcd Resid. Dens. 1.59Ang From C18 2.27 eA-3
And 5 other PLAT971 Alerts
More ...
PLAT972_ALERT_2_C Check Calcd Resid. Dens. 0.77Ang From Pb3 -2.24 eA-3
And 2 other PLAT972 Alerts
More ...
PLAT975_ALERT_2_C Check Calcd Resid. Dens. 1.00Ang From O2 . 1.07 eA-3

Alert level G

PLAT004_ALERT_5_G Polymeric Structure Found with Maximum Dimension 1 Info
PLAT045_ALERT_1_G Calculated and Reported Z Differ by a Factor ... 0.500 Check
PLAT154_ALERT_1_G The s.u.'s on the Cell Angles are Equal ..(Note) 0.002 Degree
PLAT432_ALERT_2_G Short Inter X...Y Contact C12 ..C12 . 3.20 Ang.
1-x,1-y,1-z = 2_666 Check
PLAT720_ALERT_4_G Number of Unusual/Non-Standard Labels ..... 8 Note
PLAT794_ALERT_5_G Tentative Bond Valency for Pb1 (II) . 2.24 Info
And 2 other PLAT794 Alerts
More ...
PLAT883_ALERT_1_G No Info/Value for _atom_sites_solution_primary . Please Do !
PLAT910_ALERT_3_G Missing # of FCF Reflection(s) Below Theta(Min). 1 Note
PLAT912_ALERT_4_G Missing # of FCF Reflections Above STh/L= 0.600 11 Note
PLAT933_ALERT_2_G Number of HKL-OMIT Records in Embedded .res File 5 Note
PLAT941_ALERT_3_G Average HKL Measurement Multiplicity ..... 2.9 Low
PLAT978_ALERT_2_G Number C-C Bonds with Positive Residual Density. 0 Info

---

2 **ALERT level A** = Most likely a serious problem - resolve or explain
4 **ALERT level B** = A potentially serious problem, consider carefully
21 **ALERT level C** = Check. Ensure it is not caused by an omission or oversight
14 **ALERT level G** = General information/check it is not something unexpected

4 ALERT type 1 CIF construction/syntax error, inconsistent or missing data
21 ALERT type 2 Indicator that the structure model may be wrong or deficient
4 ALERT type 3 Indicator that the structure quality may be low

8 ALERT type 4 Improvement, methodology, query or suggestion
4 ALERT type 5 Informative message, check

PLATON version of 12/09/2022; check.def file version of 09/08/2022

Datablock Pb3(2PCO)4(NO3)2 - ellipsoid plot

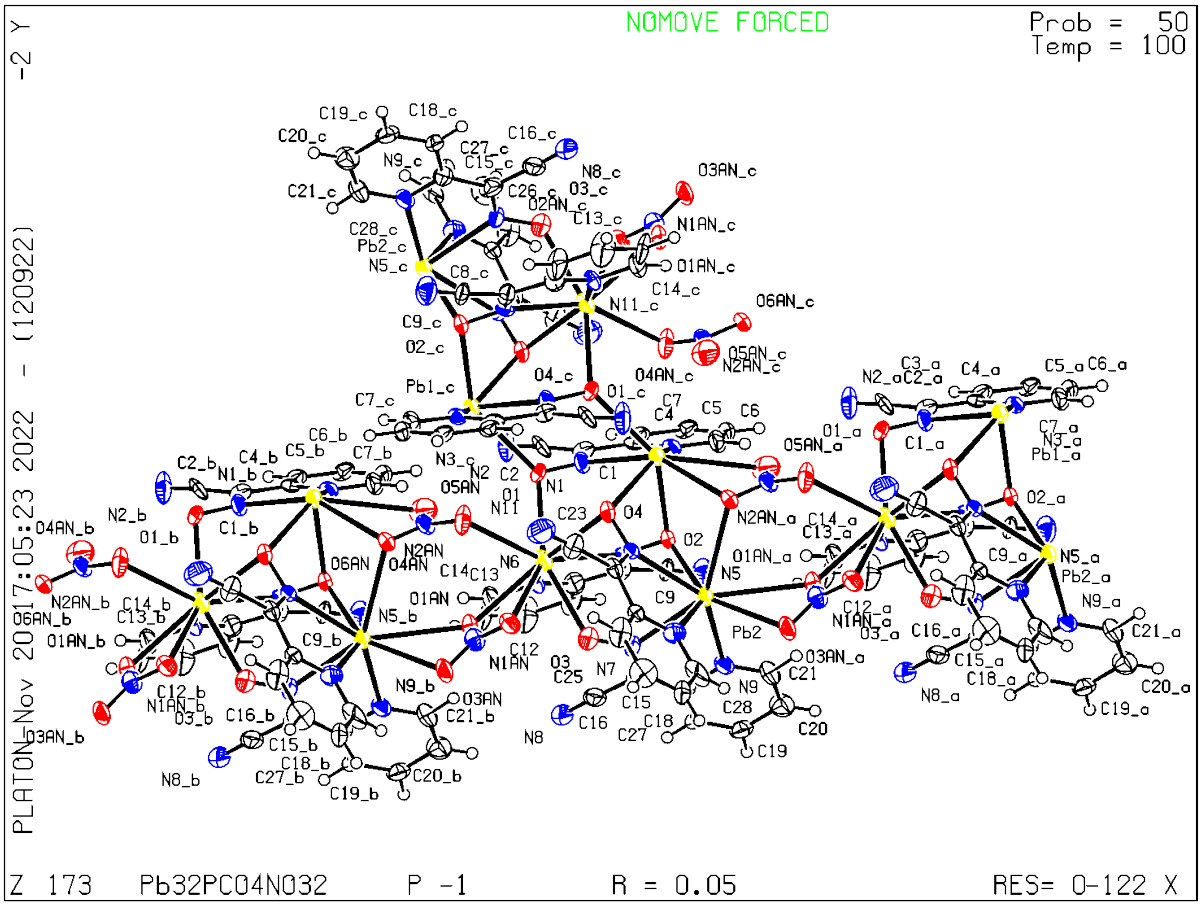

Download CIF editor (publCIF) from the IUCr
Download CIF editor (enCIFer) from the CCDC
Test a new CIF entry

checkCIF/PLATON (basic structural check)

Structure factors have been supplied for datablock(s) Pb(H2PCO)(2PCO)2(H2O)

THIS REPORT IS FOR GUIDANCE ONLY. IF USED AS PART OF A REVIEW PROCEDURE FOR PUBLICATION, IT SHOULD NOT REPLACE THE EXPERTISE OF AN EXPERIENCED CRYSTALLOGRAPHIC REFEREE.

No syntax errors found. CIF dictionary
Please wait while processing .... Interpreting this report
Structure factor report

Datablock: Pb(H2PCO)(2PCO)2(H2O)

Bond precision: C-C = 0.0081 A Wavelength=0.71073

Cell: a=14.1677(8) b=9.2091(5) c=16.9054(9)
alpha=90 beta=101.861(2) gamma=90

Temperature: 150 K

	Calculated	Reported
Volume	2158.6(2)	2158.6(2)
Space group	P 21/n	P 21/n
Hall group	-P 2yn	-P 2yn
Moiety formula	C42 H26 N18 O6.53 Pb2, 0.616(O)	?
Sum formula	C42 H26 N18 O7.15 Pb2	C21 H13 N9 O Pb
Mr	1311.58	614.59
Dx,g cm-3	2.018	1.891
Z	2	4
Mu (mm-1)	7.865	7.849
F000	1250.4	1168.0
F000'	1237.63	
h,k,lmax	18,12,22	18,12,22
Nref	5385	5378
Tmin,Tmax	0.508,0.772	0.589,0.794
Tmin'	0.389	

Correction method= # Reported T Limits:
Tmin=0.589 Tmax=0.794 AbsCorr = MULTI-SCAN

Data completeness= 0.999 Theta(max)= 28.325

R(reflections)= 0.0369(4508) wR2(reflections)= 0.0639(5378)

S = 1.105 Npar= 362

The following ALERTS were generated. Each ALERT has the format
test-name_ALERT_alert-type_alert-level.
Click on the hyperlinks for more details of the test.

Alert level A

PLAT375_ALERT_2_A Strange C-O-H Geometry (C-O > 1.45 Ang) ..... O2W Check
PLAT430_ALERT_2_A Short Inter D...A Contact N5 ..O1W . 2.03 Ang.
x,1+y,z = 1_565 Check

Alert level B

PLAT043_ALERT_1_B Calculated and Reported Mol. Weight Differ by .. 82.40 Check
PLAT420_ALERT_2_B D-H Bond Without Acceptor O2W --H13 . Please Check
PLAT430_ALERT_2_B Short Inter D...A Contact N5 ..O2W . 2.78 Ang.
x,1+y,z = 1_565 Check

Alert level C

PLAT041_ALERT_1_C Calc. and Reported SumFormula Strings Differ Please Check
PLAT068_ALERT_1_C Reported F000 Differs from Calcd (or Missing)... Please Check
PLAT077_ALERT_4_C Unitcell Contains Non-integer Number of Atoms .. Please Check
PLAT220_ALERT_2_C NonSolvent Resd 1 O Ueq(max)/Ueq(min) Range 3.5 Ratio
PLAT230_ALERT_2_C Hirshfeld Test Diff for N7 --C15 . 6.5 s.u.
PLAT245_ALERT_2_C U(iso) H4 Smaller than U(eq) C4 by 0.014 Ang**2
PLAT245_ALERT_2_C U(iso) H20 Smaller than U(eq) C20 by 0.015 Ang**2
PLAT303_ALERT_2_C Full Occupancy Atom H13 with # Connections 1.27 Check
PLAT342_ALERT_3_C Low Bond Precision on C-C Bonds ..... 0.00806 Ang.
PLAT350_ALERT_3_C Short C-H (X0.96,N1.08A) C5 - H5 . 0.82 Ang.
And 3 other PLAT350 Alerts
More ...
PLAT430_ALERT_2_C Short Inter D...A Contact O1 ..N7 . 2.88 Ang.
x,1+y,z = 1_565 Check
PLAT906_ALERT_3_C Large K Value in the Analysis of Variance ..... 4.664 Check
PLAT911_ALERT_3_C Missing FCF Refl Between Thmin & STh/L= 0.600 2 Report
PLAT971_ALERT_2_C Check Calcd Resid. Dens. 0.63Ang From Pb1 1.95 eA-3
And 2 other PLAT971 Alerts
More ...
PLAT972_ALERT_2_C Check Calcd Resid. Dens. 0.50Ang From Pb1 -1.57 eA-3
PLAT975_ALERT_2_C Check Calcd Resid. Dens. 0.98Ang From N7 . 0.79 eA-3
And 2 other PLAT975 Alerts
More ...
PLAT976_ALERT_2_C Check Calcd Resid. Dens. 0.67Ang From O3 . -0.47 eA-3

Alert level G

FORMU01_ALERT_2_G There is a discrepancy between the atom counts in the
_chemical_formula_sum and the formula from the _atom_site* data.
Atom count from _chemical_formula_sum:C21 H13 N9 O1 Pb1
Atom count from the _atom_site data: C21 H13 N9 O3.574 Pb1
CELLZ01_ALERT_1_G Difference between formula and atom_site contents detected.
CELLZ01_ALERT_1_G ALERT: Large difference may be due to a
symmetry error - see SYMMG tests
From the CIF: _cell_formula_units_Z 4
From the CIF: _chemical_formula_sum C21 H13 N9 O Pb
TEST: Compare cell contents of formula and atom_site data

atom Z*formula cif sites diff
C 84.00 84.00 0.00

H	52.00	52.00	0.00
N	36.00	36.00	0.00
O	4.00	14.30	-10.30
Pb	4.00	4.00	0.00

PLAT007_ALERT_5_G Number of Unrefined Donor-H Atoms ..... 1 Report
PLAT045_ALERT_1_G Calculated and Reported Z Differ by a Factor ... 0.500 Check
PLAT083_ALERT_2_G SHELXL Second Parameter in WGHT Unusually Large 13.92 Why ?
PLAT164_ALERT_4_G Nr. of Refined C-H H-Atoms in Heavy-Atom Struct. 11 Note
PLAT232_ALERT_2_G Hirshfeld Test Diff (M-X) Pb1 --O3 . 5.5 s.u.
PLAT301_ALERT_3_G Main Residue Disorder .....(Resd 1) 1% Note
PLAT302_ALERT_4_G Anion/Solvent/Minor-Residue Disorder (Resd 2) 100% Note
PLAT304_ALERT_4_G Non-Integer Number of Atoms in ..... (Resd 1) 94.53 Check
PLAT304_ALERT_4_G Non-Integer Number of Atoms in ..... (Resd 2) 0.31 Check
PLAT311_ALERT_2_G Isolated Disordered Oxygen Atom (No H's ?) ..... O1W Check
PLAT432_ALERT_2_G Short Inter X...Y Contact O1W ..C11 . 2.02 Ang.
1/2-x,-1/2+y,1/2-z = 2_545 Check
And 3 other PLAT432 Alerts
More ...
1/2-x,-1/2+y,1/2-z = 2_545 Check
PLAT432_ALERT_2_G Short Inter X...Y Contact O1W ..C12 . 2.62 Ang.
1/2-x,-1/2+y,1/2-z = 2_545 Check
PLAT432_ALERT_2_G Short Inter X...Y Contact O2W ..C11 . 2.75 Ang.
1/2-x,-1/2+y,1/2-z = 2_545 Check
PLAT480_ALERT_4_G Long H...A H-Bond Reported H21 ..N1 . 2.66 Ang.
And 8 other PLAT480 Alerts
More ...
PLAT793_ALERT_4_G Model has Chirality at C13 (Centro SPGR) R Verify
PLAT794_ALERT_5_G Tentative Bond Valency for Pb1 (II) . 2.14 Info
PLAT883_ALERT_1_G No Info/Value for _atom_sites_solution_primary . Please Do !
PLAT910_ALERT_3_G Missing # of FCF Reflection(s) Below Theta(Min). 1 Note
PLAT912_ALERT_4_G Missing # of FCF Reflections Above STh/L= 0.600 4 Note
PLAT933_ALERT_2_G Number of HKL-OMIT Records in Embedded .res File 3 Note
PLAT965_ALERT_2_G The SHELXL WEIGHT Optimisation has not Converged Please Check
PLAT978_ALERT_2_G Number C-C Bonds with Positive Residual Density. 0 Info

---

2 **ALERT level A** = Most likely a serious problem - resolve or explain
3 **ALERT level B** = A potentially serious problem, consider carefully
24 **ALERT level C** = Check. Ensure it is not caused by an omission or oversight
36 **ALERT level G** = General information/check it is not something unexpected

7 ALERT type 1 CIF construction/syntax error, inconsistent or missing data
31 ALERT type 2 Indicator that the structure model may be wrong or deficient
9 ALERT type 3 Indicator that the structure quality may be low
16 ALERT type 4 Improvement, methodology, query or suggestion
2 ALERT type 5 Informative message, check

PLATON version of 12/09/2022; check.def file version of 09/08/2022

Datablock Pb(H2PCO)(2PCO)2(H2O)- ellipsoid plot

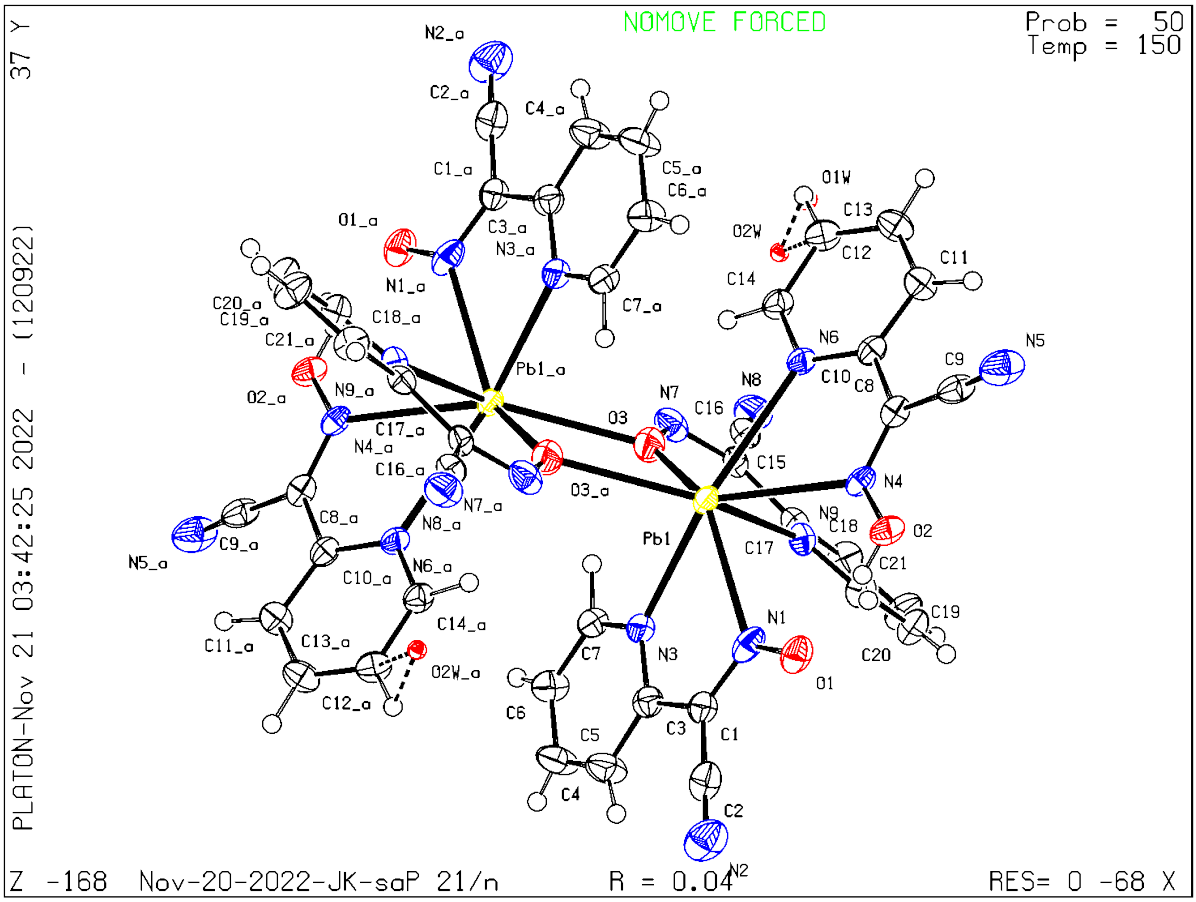

Download CIF editor (publCIF) from the IUCr
Download CIF editor (enCIFer) from the CCDC
Test a new CIF entry

checkCIF/PLATON (basic structural check)

Structure factors have been supplied for datablock(s) K4_Pb6_AACO8

THIS REPORT IS FOR GUIDANCE ONLY. IF USED AS PART OF A REVIEW PROCEDURE FOR PUBLICATION, IT SHOULD NOT REPLACE THE EXPERTISE OF AN EXPERIENCED CRYSTALLOGRAPHIC REFEREE.

No syntax errors found. CIF dictionary
Please wait while processing .... Interpreting this report
Structure factor report

Datablock: K4_Pb6_AACO8

Bond precision: C-C = 0.0085 A Wavelength=0.71073

Cell: a=10.7097(15) b=10.7097(15) c=21.490(3)
alpha=90 beta=90 gamma=90

Temperature: 120 K

	Calculated	Reported
Volume	2464.9(8)	2464.9(6)
Space group	P 4/m n c	P 4/m n c
Hall group	-P 4 2n	-P 4 2n
Moiety formula	C24 N16 O24 Pb6, 0.53(O), 4(K)	0.5(C48 K8 N32 O49.06 Pb12)
Sum formula	C24 K4 N16 O24.53 Pb6	C24 K4 N16 O24.532 Pb6
Mr	2304.48	2304.57
Dx,g cm-3	3.105	3.105
Z	2	2
Mu (mm-1)	20.852	20.857
F000	2040.5	2007.6
F000'	2005.19	
h,k,lmax	13,13,26	13,9,26
Nref	1298	1300
Tmin,Tmax		
Tmin'		

Correction method= Not given

Data completeness= 1.002 Theta(max)= 26.330

R(reflections)= 0.0221(1101) wR2(reflections)= 0.0556(1300)

S = 1.011 Npar= 90

The following ALERTS were generated. Each ALERT has the format
test-name_ALERT_alert-type_alert-level.
Click on the hyperlinks for more details of the test.

Alert level A

PLAT971_ALERT_2_A Check Calcd Resid. Dens. 1.75Ang From Pb2 3.81 eA-3
PLAT973_ALERT_2_A Check Calcd Positive Resid. Density on Pb1 3.80 eA-3
PLAT973_ALERT_2_A Check Calcd Positive Resid. Density on Pb2 3.07 eA-3

Alert level B

PLAT601_ALERT_2_B Unit Cell Contains Solvent Accessible VOIDS of . 112 Ang**3
PLAT975_ALERT_2_B Check Calcd Resid. Dens. 1.02Ang From O1 . 1.93 eA-3

Alert level C

PLAT042_ALERT_1_C Calc. and Reported MoietyFormula Strings Differ Please Check
PLAT053_ALERT_1_C Minimum Crystal Dimension Missing (or Error) ... Please Check
PLAT054_ALERT_1_C Medium Crystal Dimension Missing (or Error) ... Please Check
PLAT055_ALERT_1_C Maximum Crystal Dimension Missing (or Error) ... Please Check
PLAT068_ALERT_1_C Reported F000 Differs from Calcd (or Missing)... Please Check
PLAT094_ALERT_2_C Ratio of Maximum / Minimum Residual Density .... 3.23 Report
PLAT342_ALERT_3_C Low Bond Precision on C-C Bonds ..... 0.0085 Ang.
PLAT971_ALERT_2_C Check Calcd Resid. Dens. 1.02Ang From O1 1.93 eA-3
And 2 other PLAT971 Alerts
More ...
PLAT976_ALERT_2_C Check Calcd Resid. Dens. 0.90Ang From O1 . -0.63 eA-3

Alert level G

PLAT004_ALERT_5_G Polymeric Structure Found with Maximum Dimension 2 Info
PLAT040_ALERT_1_G No H-atoms in this Carbon Containing Compound .. Please Check
PLAT083_ALERT_2_G SHELXL Second Parameter in WGHT Unusually Large 11.38 Why ?
PLAT152_ALERT_1_G The Supplied and Calc. Volume s.u. Differ by ... 2 Units
PLAT302_ALERT_4_G Anion/Solvent/Minor-Residue Disorder (Resd 2) 100% Note
PLAT311_ALERT_2_G Isolated Disordered Oxygen Atom (No H's ?) ..... O1W Check
PLAT769_ALERT_4_G CIF Embedded explicitly supplied scattering data Please Note
PLAT794_ALERT_5_G Tentative Bond Valency for Pb1 (II) . 2.24 Info
PLAT794_ALERT_5_G Tentative Bond Valency for Pb2 (II) . 2.06 Info
PLAT883_ALERT_1_G No Info/Value for _atom_sites_solution_primary . Please Do !
PLAT982_ALERT_1_G The K-f'= 0.2117 Deviates from IT-value = 0.2009 Check
PLAT982_ALERT_1_G The Pb-f'= -3.2085 Deviates from IT-value = -3.3944 Check
PLAT983_ALERT_1_G The K-f"= 0.2656 Deviates from IT-Value = 0.2494 Check
PLAT983_ALERT_1_G The Pb-f"= 10.1539 Deviates from IT-Value = 10.1111 Check

3 **ALERT level A** = Most likely a serious problem - resolve or explain
2 **ALERT level B** = A potentially serious problem, consider carefully
11 **ALERT level C** = Check. Ensure it is not caused by an omission or oversight
14 **ALERT level G** = General information/check it is not something unexpected

12 ALERT type 1 CIF construction/syntax error, inconsistent or missing data
12 ALERT type 2 Indicator that the structure model may be wrong or deficient
1 ALERT type 3 Indicator that the structure quality may be low
2 ALERT type 4 Improvement, methodology, query or suggestion
3 ALERT type 5 Informative message, check

PLATON version of 12/09/2022; check.def file version of 09/08/2022

Datablock K4_Pb6_AACO8 - ellipsoid plot

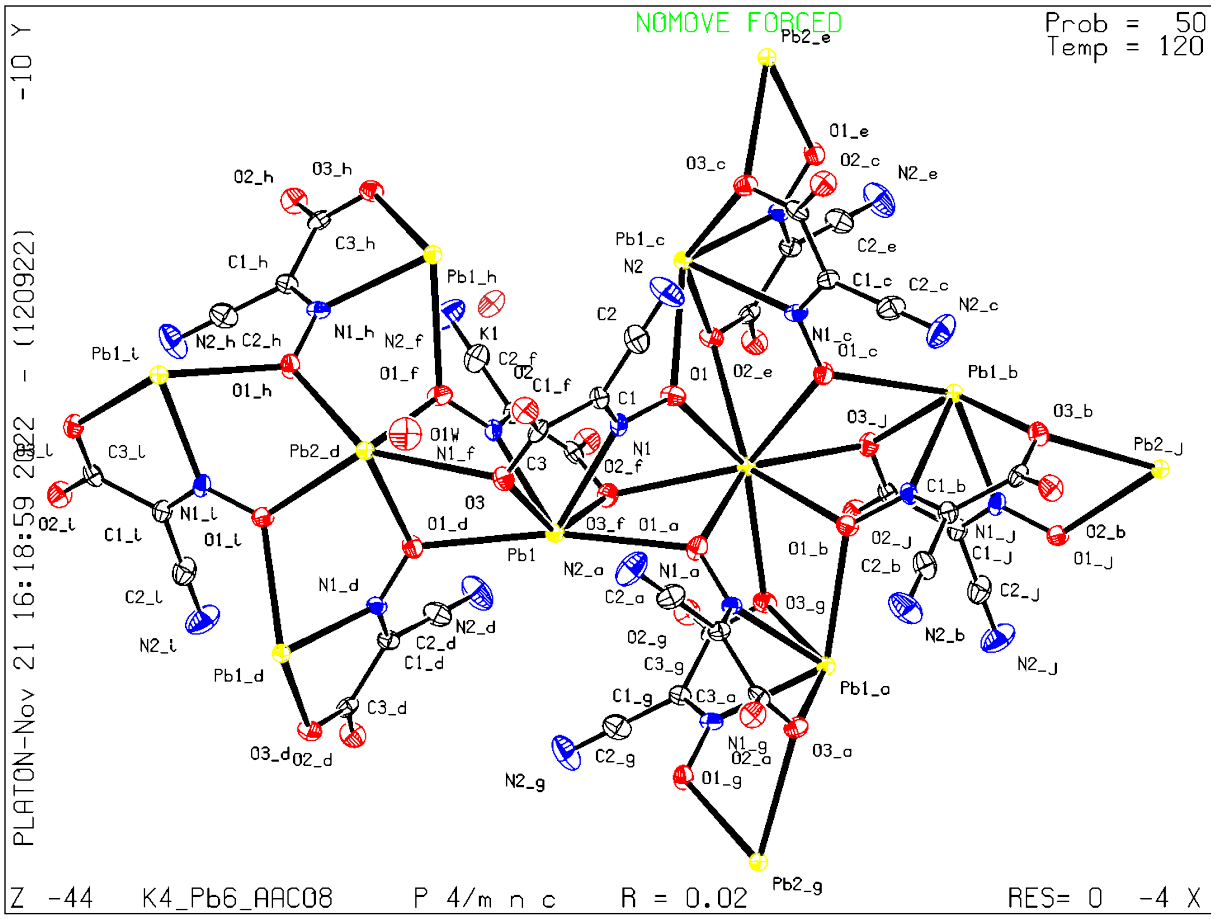

Download CIF editor (publCIF) from the IUCr
Download CIF editor (enCIFer) from the CCDC
Test a new CIF entry

Appendix C. Instrumentation of TG/DSC Analysis

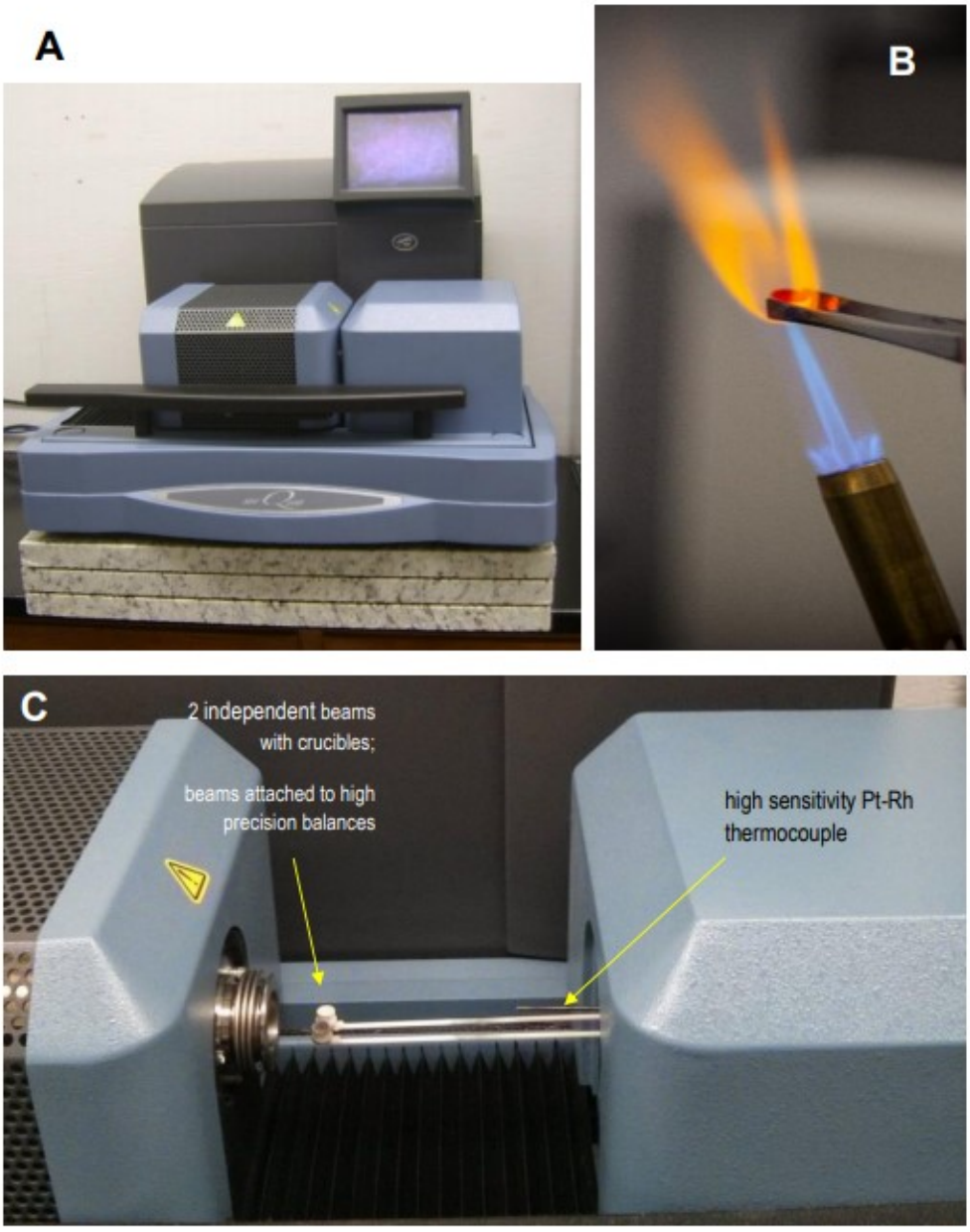

Appendix C-1. A - General view of the thermal analyzer; **B -** cleaning of alumina crucible with flame; **C -** opened furnace view showing two beams with alumina crucibles for differential analysis.